Faculty of Engineering and Science

Department of Chemical Engineering

Energy Efficient Process, Dynamic Modelling and Control of Boric Acid Promoted Potassium Carbonate Based CO_2 Capture System

Foster Kofi Ayittey

This thesis is presented for the Degree of

Doctor of Philosophy

of

Curtin University

May 2020

DECLARATION

To the best of my knowledge and belief, this thesis contains no material previously published by any other person except where due acknowledgment has been made. This thesis contains no material which has been accepted for the award of any other degree or diploma in any university.

Signature: ……

Date: 18th May 2020

ABSTRACT

As the deliberation over global warming persists, it is unarguable that many nations are beginning to adopt strategies aimed at reducing greenhouse gas (GHG) emissions. It is widely recognized that increasing the emission of these GHGs, particularly CO_2, to our atmosphere is the primary contributor to global climate change. In this regard, CO_2 capture system at major emitters such as coal-fired power plants plays a vital role in decreasing the effects of climate change. While the carbon dioxide capture and sequestration technology is not new, it is considered expensive in its current state. Numerous methods for capturing CO_2 have been proposed, however, the most developed technology is post-combustion capture using monoethanolamine (MEA) solvent. Despite its popularity, it has been acknowledged that the implementation of MEA-based capture system is associated with high cost and some operational issues such as corrosion, solvent loss and degradation, resulting in toxic waste products and unwanted side reactions with SO_2 and NO_x. For these reasons, potassium carbonate promoted with boric acid has been extensively studied as a low cost and more effective and environmentally friendly solvent. To date, however, most of these studies are related to lab-scale experimental works and kinetics studies. None of the works have been dedicated to materialise this technology into a power plant scale through process design and simulation. Process design and simulation are essential to evaluate the techno-economic performances of the plant with an integrated CO_2 capture system and it is few steps closer to the commercialization of this improved solvent in large scales. Moreover, dynamic models (for the purpose of control system design) and process control strategies directed towards minimising the cost of integrated capture systems are very scarce in the literature.

Using the ELECNRTL property method, a rigorous rate-based simulation was performed and validated for MEA, MEA/PZ, K_2CO_3 and H_3BO_3/K_2CO_3 post-combustion carbon capture systems. Various modified process configurations were also investigated to discover their full impacts on the carbon capture processes. Furthermore, parametric analyses were performed for the hot potassium carbonate (HPC) capture process for optimisation purposes. It was observed that the HPC-based carbon capture technology is a more energy-efficient technology than the conventional amine-based carbon capture process. Whereas the reboiler duty and total energy usage

in the amine-based capture process were 3.98 MJ/kgCO_2 and 8.61 MJ/kgCO_2 respectively, and the respective requirements in the HPC process were only 2.76 MJ/kgCO_2 and 5.15 MJ/kgCO_2. After the successful implementation of optimisation strategies, these figures were further reduced to 2.35 MJ/kgCO_2 and 4.53 MJ/kgCO_2 respectively. This is a demonstration that the K_2CO_3 capture process is able to scale down the reboiler duty and total energy usage in the MEA-based capture process by 40.95% and 47.39% respectively. Modified process configurations were also investigated to ascertain their influences on the MEA-based and HPC-based capture systems. It was discovered that absorber intercooling yields the highest carbon capture level in the MEA system whereas the flue gas precooling appears to be the most capable modification in improving the decarbonisation level in the HPC process. With regard to energy-saving configurations, the lean vapour compression was discovered to function as the best energy-saving modification for both systems.

Aside these observations, the dynamic simulations performed for the HPC process prove that agitations in the lean solvent concentration and the CO_2 concentration in the flue gas stream could cause high instabilities in the HPC capture plant. For both variables, long settling times were required to reach new setpoints for the carbon capture efficiency and stripper reboiler temperature. Single input single-output (SISO) and multiple-input multiple-output (MIMO) control systems were equally designed and applied to study the controllability of the HPC process. Whereas it takes a much shorter time to reach the steady state values for the reboiler temperature, the capture plants take longer time to attain the carbon capture level setpoints. Additionally, no significant negative interaction effects were observed in the MIMO control system. This signifies that the SISO controller tuning parameters can perform adequately well in a MIMO scenario.

It is believed that the findings of this research project would set the foundation for a better understanding of the hot potassium carbonate capture process, including the controllability of this post-combustion carbon capture technology. Ultimately, it is envisaged that the application of this technology could offer a more energy-efficient means of decarbonising the flue gas from coal-fired power plants as compared to its counterpart amine-based capture technology.

ACKNOWLEDGEMENT

This research was funded by Curtin Malaysia Research Institute (CMRI) under CMRI Academic Research Grant Project No. 6019. My first gratitude goes to my thesis committee for their expert guidance, especially my main supervisor, Associate Professor Dr. Agus Saptoro. I equally acknowledge the inputs of my Thesis Committee Chairperson, Professor Chua Hang Bing, and my co-supervisors, Associate Professor Dr. Perumal Kumar and Dr. Mee Kee Wong. I also wish to express my sincere thanks to the Faculty of Engineering and Science, Curtin University Malaysia for providing partial Ph.D. study support. Finally, I acknowledge my colleagues who have supported me in one way or the other, and the whole HDR administration, especially Miss Florence, Miss Daisy and Miss Jacqueline for their guidance with respect to all paper works that needed to be done to make this project successful.

TABLE OF CONTENTS

LIST OF FIGURES

LIST OF TABLES

NOMENCLATURES

Abbreviations

ACM – Aspen Plus Custom Modeller

AEP – American Electric Power

ASU – Air Separation Unit

BASF – Badische Anilin Und Soda Fabrik (German) Or Baden Aniline and Soda Factory (English)

BMI – Battelle Memorial Institute

CA – Carbonic Anhydrase

CAC – Carbon Avoidance Cost

CAP – Chilled Ammonia Process

CCS – CO_2 Capture and Storage

CHP – Combined Heat and Power Plant

CMRI – Curtin Malaysia Research Institute

CO2CRC – Cooperative Research Centre for Greenhouse Gas Technologies

CSIRO – Commonwealth Scientific and Industrial Research Organisation

CV – Controlled Variable

DCC – Direct Contact Cooler

DOE – Department of Energy

DEA – Diethanolamine

DRPC – Disturbance Rejection Predictive Controller

DV – Disturbance Variable

EIA – Energy Information Administration

ELECNRTL – Electrolyte Non-Random Two Liquid Property Method

EO – Ethylene Oxide

EPRI – Electric Power Research Institute

ESA – Electric Swing Adsorption

FCCU – Fluid Catalytic Cracking Unit

FGD – Flue Gas Desulphurisation

FOPDT - First Order Plus Dead Time

GDP – Gross Domestic Product

GHG – Greenhouse Gas

GISS – Goddard Institute for Space Studies

GRACE – Gravity Recovery and Climate Experiment

HDR – Higher Degree by Research

HPC – Hot Potassium Carbonate

HSSS – Heat-Stable Salts

IEA – International Energy Agency

IPCC – Intergovernmental Panel on Climate Change

IGCC – Integrated Gasification Combined Cycle Power Plants

IMTP – Intalox Metal Tower Packing

ITAE – Integral Time Absolute Error

LCOE – Levelised Cost of Electricity

MEA – Monoethanolamine

MIMO – Multiple-Input Multiple-Output Control System

MPC – Model Predictive Controller

MV – Manipulated Variable

NASA – National Aeronautics and Space Administration

NCCC – National Carbon Capture Centre

NOAA – National Oceanic and Atmospheric Administration

PCC – Post Combustion Capture

PI – Process Intensification

PID – Proportional Integral Derivative Control System

Pm – Picometre

Ppmv – Parts Per Million in Volume

PSA – Pressure Swing Adsorption

PTC – Parabolic Trough Collector

PVF – Product Validation Facility

PZ – Piperazine

RGA – Relative Gain Array

RPB – Rotating Packed Bed

SISO – Single-Input Single-Output Control System

SRI – Stanford Research Institute

TCM – Test Centre Mongstad

TEA – Triethanolamine

TSA – Temperature Swing Adsorption

UNFCCC – United Nations Framework Convention On Climate Change

UOP – Universal Oil Products

VT – Vacuum Tube

WGS – Water-Gas-Shift

Symbols

$B(OH)_4^-$ – Tetrahydroxyborate

C_2H_4 – Ethylene

CH_4 – Methane

C_2H_4 – Ethylene

C_2H_4O – Ethylene Oxide

CO – Carbon Monoxide

CO_2 – Carbon Dioxide

H_2O – Water

H_2O_2 – Hydrogen Peroxide

H_2S – Hydrogen Sulphide

H_3BO_3 – Boric Acid

K_2CO_3 – Potassium Carbonate

$K_2CO_3.1.5H_2O$ – Sesquihydrate Potassium Carbonate Crystal

$KHCO_3$ – Potassium Bicarbonate

KOH – Potassium Hydroxide

K_p – Steady-State Process Gain

Na_2SO_3 – Sodium Sulphite

$NaHSO_3$ – Sodium Bisulphite

NaOH – Sodium Hydroxide

NH_3 – Ammonia

NOx – Nitrous Oxides

$(NH_4)_2CO_3$ – Ammonium Carbonate

$(NH_4)H_2NCO_2$ – Ammonium Carbamate

$(NH_4)HCO_3$ – Ammonium Bicarbonate

SO_2 – Sulphur Dioxide

V_2O_5 – Vanadium Pentoxide

θ_p – Apparent Dead Time (min)

τ_p – Process Time Constant (min)

Q_{reb} – Specific Reboiler Duty ($MJ/kgCO_2$)

Q_{sen} – Sensible Heat ($MJ/kgCO_2$)

Q_{des} – Desorption Energy ($MJ/kgCO_2$)

Q_{vap} – Latent Heat of Vapourisation ($MJ/kgCO_2$)

C_p – Heat Capacity (MJ/kg.K)

CHAPTER 1

INTRODUCTION

The mitigation of greenhouse gases (GHGs), particularly carbon dioxide (CO_2), is necessary to combat the looming issue of global warming and its related climatic changes. Policymakers and researchers have considered various means of decreasing the quantity of CO_2 produced through diverse anthropogenic activities. Among others, the use of renewable sources for power generation, and carbon capture and storage (CCS) appear to be the most effective clean-energy technologies capable of reducing the amount of CO_2 emitted into the environment. Whereas the use of renewables to generate sufficient power to feed the increasing global population needs time and research to fully dominate the energy sector, power generation from the combustion of fossil fuel is still going to be the primary source of electricity for quite a number of years to come. This necessitates carbon capture and storage from major emission points such as the coal-fired power plants to be implemented within the shortest possible time to tackle the large emission of the dangerous GHG into the atmosphere.

1.1 CLIMATE CHANGE AND CARBON DIOXIDE MITIGATION

In the last 40 years, there have been mounting concerns over the significant changes in the earth's climatic conditions, especially the steady warming of the globe. According to reports of independent analyses released by the National Oceanic and Atmospheric Administration (NOAA) and the National Aeronautics and Space Administration (NASA) on February 6th, 2019, the earth's surface temperatures recorded in 2018 were the fourth warmest for the past 140 years. On the average, the earth was observed in 2018 by NASA's Goddard Institute for Space Studies (GISS) in New York, to have experienced a global temperature rise of almost 0.83 ^{o}C (1.5 ^{o}F) over the mean value within the duration of 1951–1980. The current value (updated by NASA on May 28th, 2019) however stands at 0.9 ^{o}C (1.62 ^{o}F) increase in the mean surface temperature of the planet since the late 19th century. This increasing pattern of the global average surface temperature as shown in Figure 1.1, has led to many evident changes in the climate situation worldwide. For instance, the oceans' surface temperature (about 700 meters deep) is detected to have experienced warming of

roughly 0.4 ^{o}F since 1969. This phenomenon is believed to result from the gradual absorbance of the increased heat in the planet's atmosphere by the ocean (Levitus et al. 2017; Cheng et al. 2017).

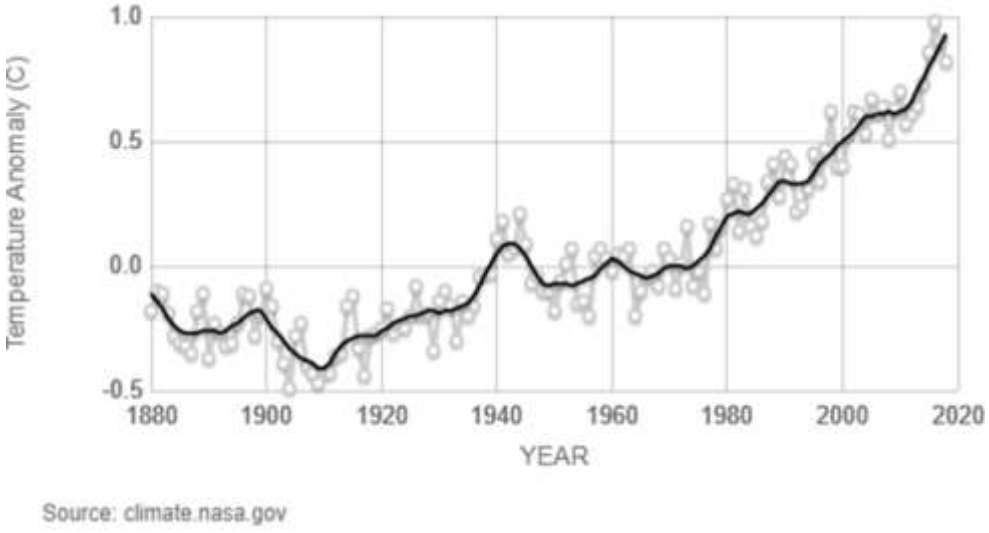

Figure 1.1. Changes in global surface temperature relative to 1951-1980 average temperatures (climate.nasa.gov).

According to satellite observations by NASA's Gravity Recovery and Climate Experiment (GRACE), the mass ice sheets in Greenland and Antarctica have respectively lost on the average 286 Gt and 127 Gt of ice annually between the years 1993 and 2016, with Antarctica undergoing almost triple ice mass loss rate within the past decade. These projections, presented in Figures 1.2 and 1.3, are strongly believed to be the shreds of evidence highlighting the aggravation of global warming.

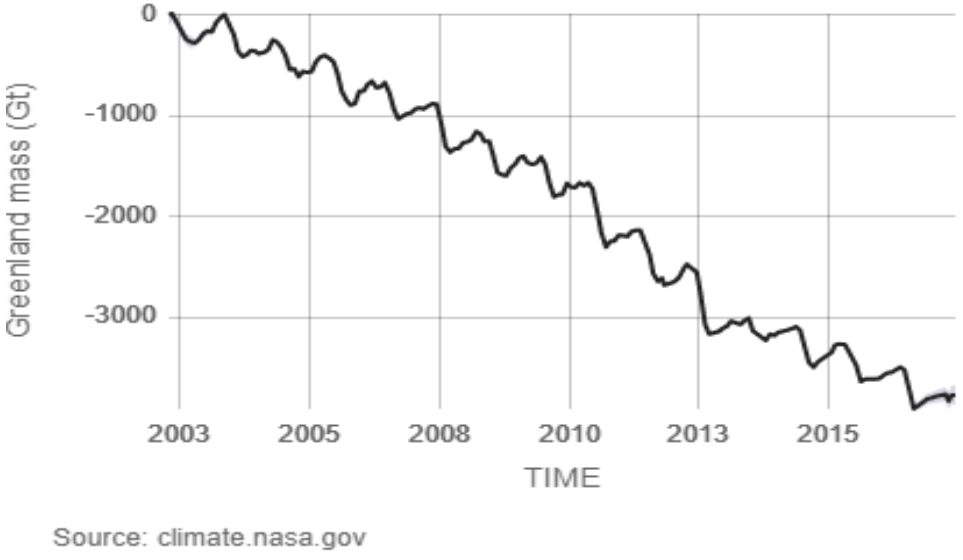

Figure 1.2. Greenland mass variation since 2002 (climate.nasa.gov).

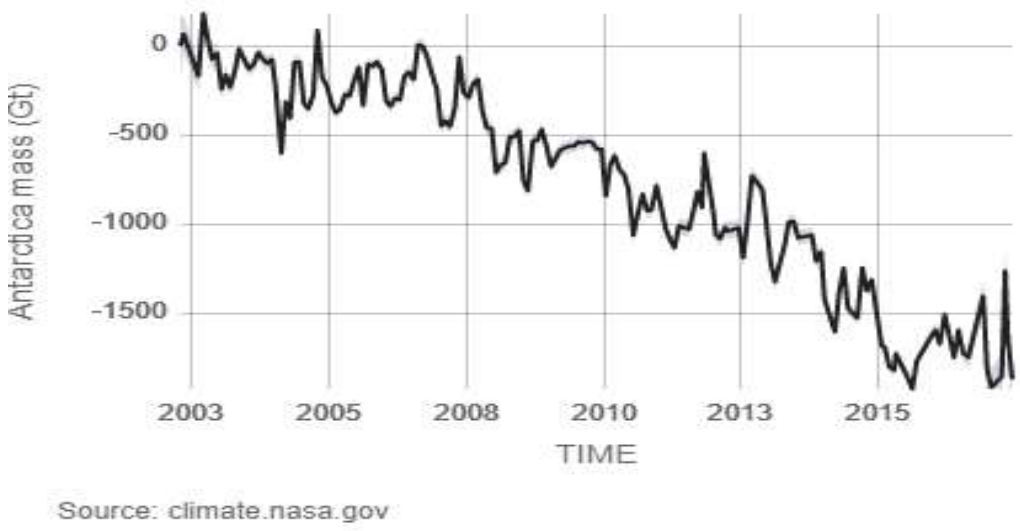

Figure 1.3. Antarctica mass variation since 2002 (climate.nasa.gov).

Documented evidence by Nerem et al. 2018 also showed that the global sea level has risen to about 0.2 meters within the last hundred years, with the last two decades demonstrating the most rapidly increasing rate. If the current trends of global warming and ice melting persist, scientists believe that sea levels could rise to as high as 1.2 m in 2100, posing serious danger to vulnerable islands across the globe, including the Republic of Maldives (Nerem et al. 2018). The current heatwaves across Europe and bush fires across Asia, including the Sarawak state of Malaysia, are also indications of what imminent scenarios are about to take over the globe if actions are not taken to tackle global warming within the shortest possible time.

The chief contributing gases to the greenhouse effect are noted to be water vapour (H_2O), methane (CH_4), nitrous oxide (N_2O) and carbon dioxide (CO_2). The human expansion of the greenhouse effect is due to continual activities that have resulted in the increased production of these gases over the years. However, it is important to note that some of these gases alleviate the greenhouse effect and are often referred to as "feedbacks", while gases that exacerbate the greenhouse effect are described as "forcing" climate change. The long-lasting gases which exist semi-permanently in the planet's atmosphere and hardly respond chemically or physically to temperature changes turn to be the most heat-trapping gases which usually force changes in the climate. Water vapour, for instance, is named among the feedback gases because it undergoes physical and chemical changes as a result of temperature variations in the atmosphere. Thus, although water vapour is the most abundant GHG, its actions are

much needed for the formation of clouds and precipitation, making it a chief contributor of the most important feedback mechanisms to the greenhouse effect.

Methane and Nitrous oxide on the other hand, despite being counted among the negative drivers of climate change, are much less abundant in the atmosphere. Carbon dioxide, however, has been investigated to be the most important long-lived greenhouse gas in the atmosphere (Bi et al. 2012; Omidfar et al. 2015). Over the years, this gas has accumulated in the atmosphere through natural sources such as respiration and volcanic eruptions, and via anthropogenic activities such as land-use changes, deforestation, and combustion of fossil fuel. Since the beginning of the industrial revolution, human activities have caused a significant increase in the atmospheric carbon dioxide concentration.

On average, the global level of CO_2 concentration is recorded to have ascended from 280 ppm to 404 ppm in May 2016, the optimum observed in the previous 650 millennia (Nogalska et al. 2018). According to the NOAA, the current value, however, stood at 409.36 ppm as of December 2018, which showed an increase of 2.83 ppm over the level in December 2017. These observations are depicted in Figure 1.4.

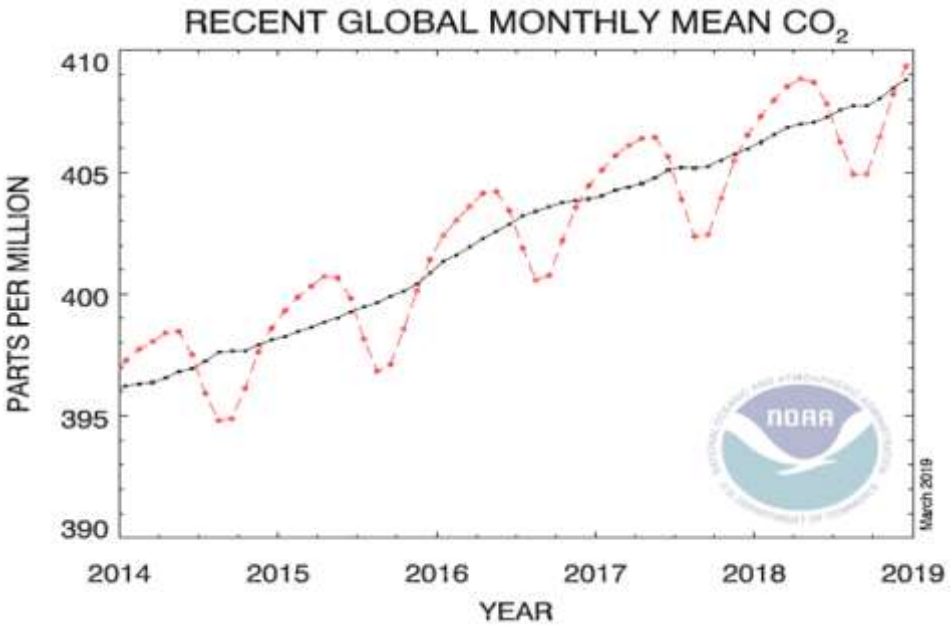

Figure 1.4. Global Monthly Average atmospheric CO_2 concentration (www.noaa.gov)

A research conducted by Song et al. 2019 acknowledged that power plants serve as the predominant sources of CO_2 emission worldwide. It was reported that nearly 2 billion tonnes of CO_2 are emitted into the atmosphere from power plants annually. Relative

to power generation sources, other sources such as the cement factory, oil refineries, iron and steel industry as well as the petrochemical industries are believed to contribute to the increased carbon emission in minimal proportions. The breakdown of the magnitude to which each sector contributes to global carbon emission is summarised in Figure 1.5. Based on the breakdown, it could be concluded that global warming cannot be effectively curbed without heavy reliance on renewable energy sources and setting up measures of mitigating carbon dioxide emissions from the power stations.

Over the past decades, renewable energy sources have been closely researched and adopted in many nations to supply considerable amounts of power. According to the projections from the US Energy Information Administration (EIA) on international energy outlook in 2013, as shown in Figure 1.6, the worldwide hydropower renewable energy is predicted to account for about 9.6 trillion kWh net electricity supply by the year 2040.

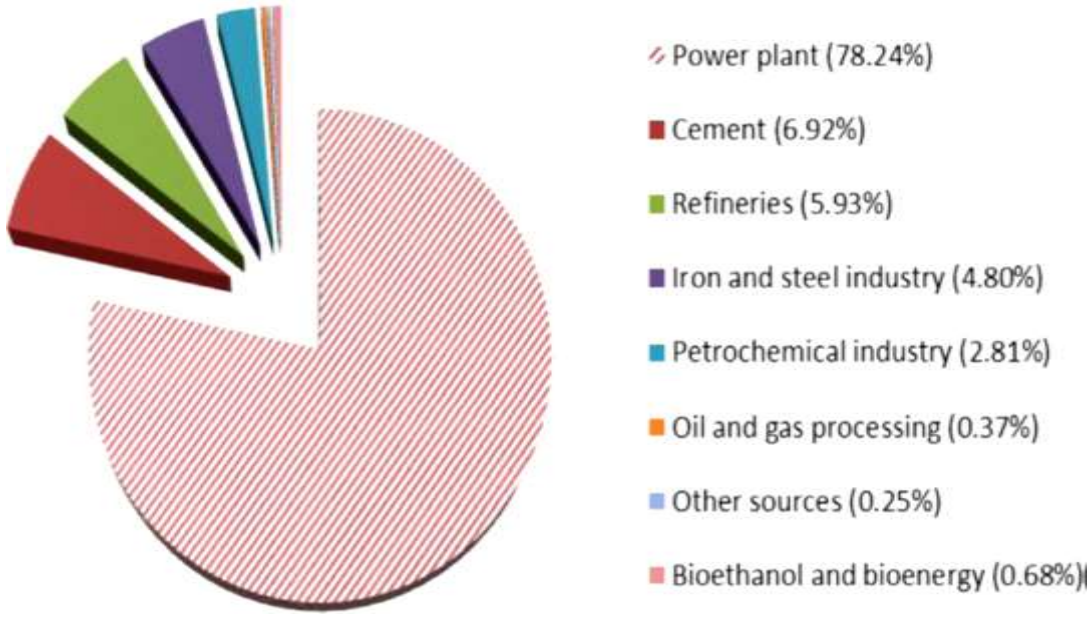

Figure 1.5. Breakdown of the dominant CO_2 emission sources (Song et al. 2019)

The global electricity generation from non-hydropower renewable energy sources such as wind, biofuel and solar energy, are estimated to account for a total of 3.4 trillion kWh energy supply in 2040. Despite similar fast-growing trends observed in natural gas and nuclear power generation, coal remains the dominant energy production source, and it is a well-known fact that the current global infrastructure is not ready to shut down coal-fired power plants. As a matter of fact, the number of coal-fired power plants is projected to grow at an annual rate of 2.3% through 2030, insinuating that

coal is still expected to continue as the largest source of global energy production for a long time to come (Sieminski 2013, Parker et al. 2010).

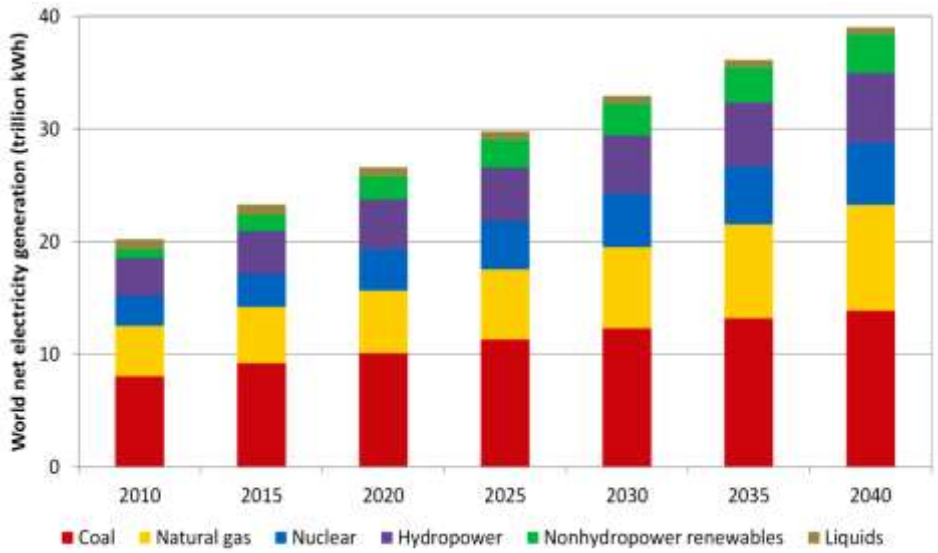

Figure 1.6. World net electricity generation by energy sources, 2010 – 2040 (www.eia.gov)

Global carbon emissions are driven by dissimilar regional dynamics. Specifically, until the year 2000, the growth in emissions was mainly driven by the United Nations Framework Convention on Climate Change (UNFCCC) Annex I nations and the United States in particular. However, these countries have generally cut down their emissions over the years while emerging economies have generally realized increases in carbon emissions. As a result of this shift in regional emission rates, Asia is currently leading the carbon dioxide emissions worldwide, with China alone contributing to about 50%. These data are available in Figures 1.7 and 1.8.

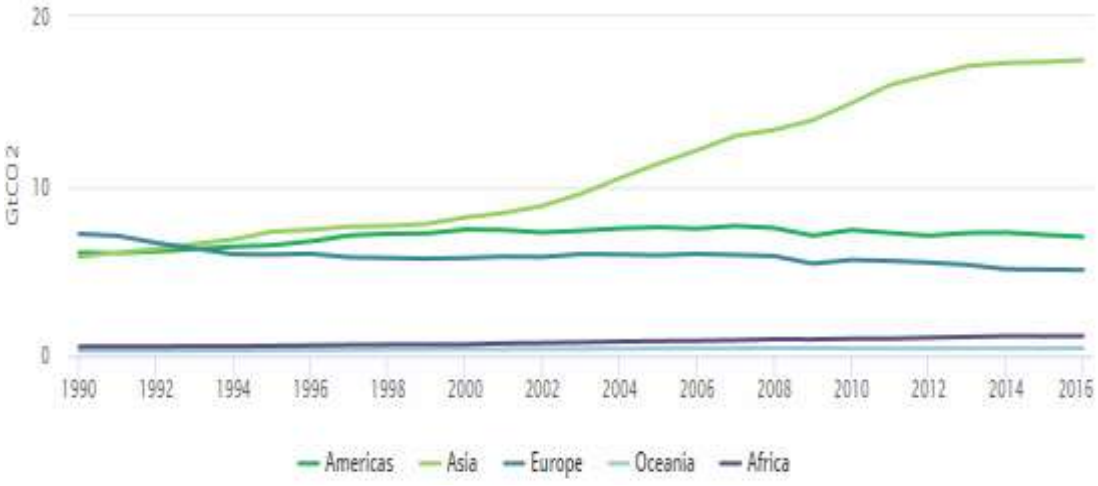

Figure 1.7. CO_2 emissions from fuel combustion by region (www.iea.org)

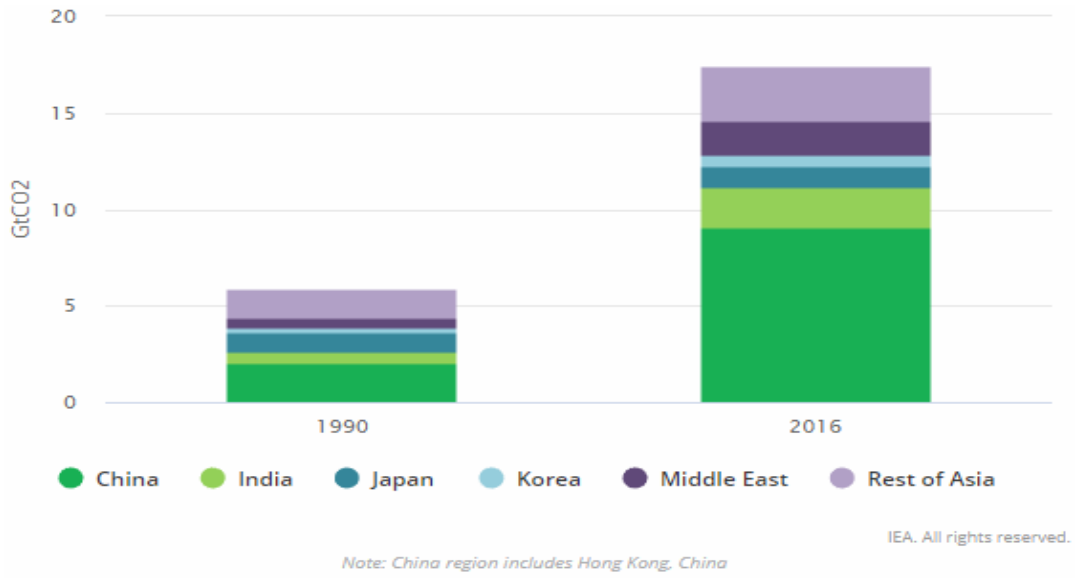

Figure 1.8. CO_2 emissions from fuel combustion in Asia (www.iea.org)

In the context of Malaysia, which forms part of the rest of Asia as shown in Figure 1.8, the national electricity demand is expected to grow around 4.7% per year spurred by annual gross domestic product (GDP) growth of 6.2% and population growth of 2.5% (Shekarchian et al. 2011). To ensure the provision of adequate electricity for the fast-growing population, Malaysia's power generation relies heavily on fossil fuel where natural gas and coal contribute to nearly 90.8% (Othman et al. 2009). While the share of natural gas in electricity generation is expected to decrease steadily over the years, coal is likely to remain as the primary source of energy production where its contribution is anticipated to increase to 42% or 17,600 MW by the year 2020 (Oh et al. 2010).

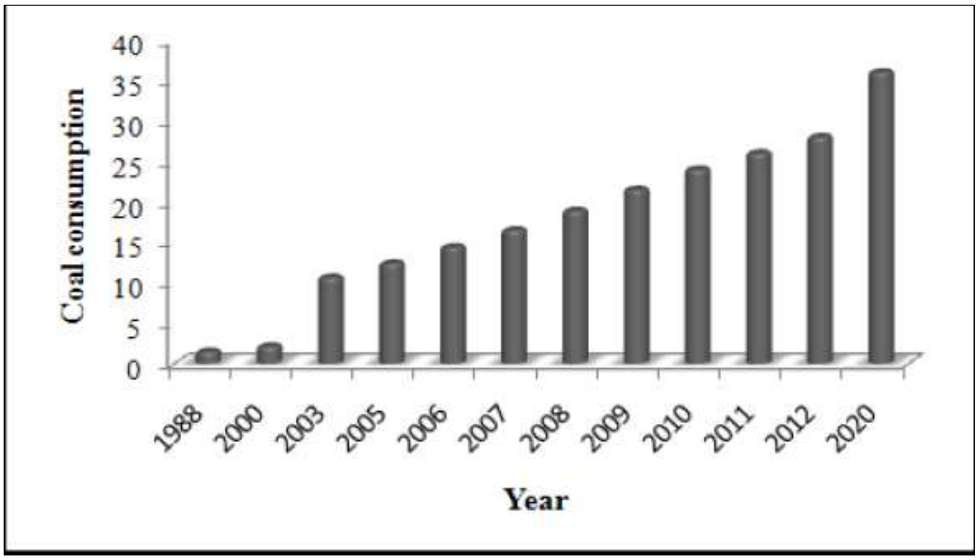

Figure 1.9. Coal consumption (million tonnes) for electricity generation in Malaysia (Oh et al. 2010).

This forecast is presented in Figure 1.9. Along with this increase, the concomitant total carbon dioxide emission from coal-fired power plants in Malaysia is foreseen to grow at a rate of 4.1% annually (Othman et al. 2009). Figure 1.10 indicates that CO_2 emission is estimated to be 98 million tonnes in 2020. This trend is likely to increase with the maximising capacity of the existing power plants and the construction of new ones.

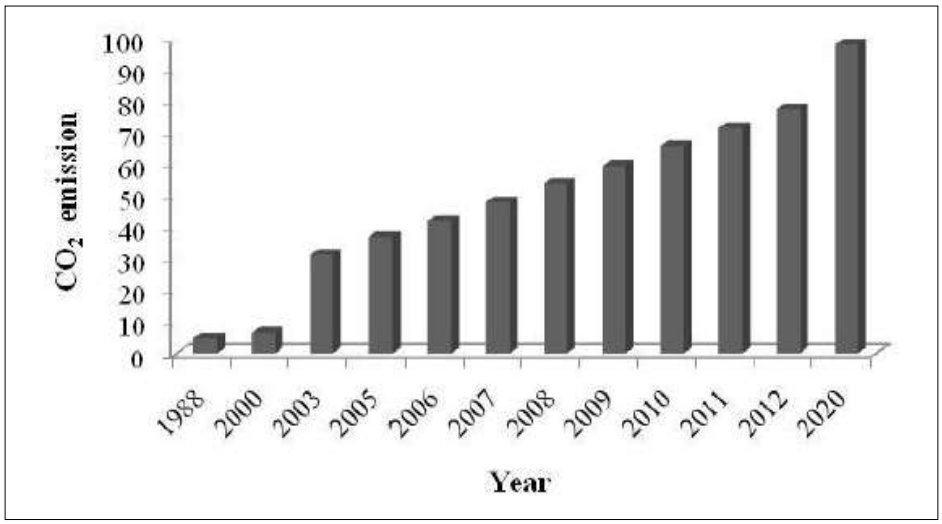

Figure 1.10. Carbon dioxide emissions from the coal-fired power plant in Malaysia (Othman et al. 2009).

Malaysia, as one of the countries that endorsed the Kyoto Protocol, has formulated the National Green Technology Policy in April 2009 which shows the nation's seriousness in driving clean and green energy towards sustainable development. The nation also equally formulated the National Biofuel Policy with the primary agenda of decreasing the reliance on fossil fuel for power generation. In December 2009 at the Copenhagen Climate Change conference, former Prime Minister Najib Razak announced Malaysia's commitment to reduce its carbon emissions up to 40% by 2020 (Shafie et al. 2011). Thus, an effort in combating global warming by reducing greenhouse gas emissions from coal-based power generation is one of the current primary agenda of the Malaysian government.

1.2 CO_2 CAPTURE PATHWAYS AND RESEARCH MOTIVATION

The three major pathways which are currently investigated for capturing CO_2 from the coal-fired power plants are the oxy-fuel combustion carbon capture, pre-combustion carbon capture, and post-combustion carbon capture. Oxy-fuel combustion capture

involves the combustion of the fuel in a pure oxygen gas instead of a mixture of oxygen and nitrogen (air). This yields a CO_2 concentrated flue gas which can easily be treated. The enormous amount of energy required to separate the oxygen from nitrogen in an air separation unit (ASU) however makes this carbon capture pathway currently unappealing. The pre-combustion carbon capture involves pre-processing the fuel to remove the carbon dioxide before combusting the remaining fuel, which is almost a pure hydrogen stream. The post-combustion carbon capture aims at carbon extraction from the gas flue which is produced after the fuel is combusted. This is the preferred technology to be retrofitted into existing power plants. Among other separation methods, the CO_2 is mostly removed using the chemical absorption method. Although monoethanolamine (MEA) has shown a very high efficiency in achieving the desired capture level, the operational issues related to its use and its energy intensiveness have necessitated researches into other capable chemical solvents including ammonia (NH_3) and potassium carbonate (K_2CO_3). The issue of high solvent slip, which requires expensive refrigeration systems, and carbon footprint associated with NH_3 has however led to the suggestion that K_2CO_3 might be the current sustainable and economical solvent to be considered in carbon capture technologies.

Despite this discovery, it is also a known fact that the CO_2 removal efficacy of K_2CO_3 is low as compared to the popular amine solvent. This led to several research works investigating promoters to be included in the K_2CO_3-based capture system, with the purpose of enhancing the performance of this solvent. Among several additives, boric acid has been proposed as the most-friendly promoter to the environment. That notwithstanding, current works on post-combustion CO_2 capture using unpromoted and H_3BO_3 promoted K_2CO_3 are limited to experimental and kinetic studies at the laboratory scale. To date, efforts to materialise this technology into commercial-scale have not been reported in the literature as highlighted by Hu et al. 2016. This research gap needs to be addressed to accelerate the practical implementation of post-combustion CO_2 capture using unpromoted and H_3BO_3 promoted K_2CO_3. Consequently, to tap the potential application of this improved solvent in the real scale, a detailed analysis of a commercial post-combustion CO_2 capture based on unpromoted and H_3BO_3 promoted K_2CO_3 is required. These stages are essential to evaluate and optimise the techno-economic feasibility of the capture plant with regards to operating conditions and costs. Thus, process design and optimisation of this

technology via simulation are necessary since existing studies in these areas are only dedicated to MEA-based and NH_3-based CO_2 capture. On the other hand, only a few are found for unpromoted and H_3BO_3 promoted K_2CO_3-based systems (Quyn et al. 2013; Molina et al. 2015). This project, therefore, seeks to conduct detailed investigations on post-combustion carbon capture for coal-fired power plants using unpromoted and H_3BO_3 promoted K_2CO_3 as capture solvents. This process is believed to offer a more energy-efficient and environmentally benign carbon capture system over the conventional amine process.

1.3 RESEARCH QUESTIONS

There are three research questions considered for this study:

a) At the lab-scale absorption process, K_2CO_3 and H_3BO_3/K_2CO_3 have shown to be promising alternatives to traditional MEA. However, there is still a question on how the performance of the real scale plant implementing this improved technology compares to traditional MEA-based technology. Through process design, simulation, optimisation, and control system analyses, what insights could be obtained on the energy-efficiency of this novel technology?
b) Process modifications had been proposed and tested for MEA and NH_3-based CO_2 capture systems to reduce energy usage. What impacts could these process modifications have on the energy consumption level of the K_2CO_3-based capture system?
c) To further promote the application of this improved solvent, how will process dynamic modelling and control contribute towards making this technology more flexible and attractive?

1.4 RESEARCH OBJECTIVES

This project aims to carry out process design, dynamic modelling, and control analyses of K_2CO_3-based CO_2 capture system with the following objectives:

a. To perform process design and simulation for evaluation of the performances of K_2CO_3-based CO_2 capture plants for conventional and modified process configurations.

b. To develop and simulate dynamic models of CO_2 capture plant for H_3BO_3 promoted and unpromoted K_2CO_3 systems.
c. To propose and design preliminary PID control systems for the base case CO_2 capture plants for H_3BO_3 promoted and unpromoted K_2CO_3 systems.

1.5 SIGNIFICANCES

The theoretical and practical novel contributions of this project are as follows:

a. Theoretical contributions
    1. Adding knowledge and literature on the analyses of conventional and modified configurations of H_3BO_3 promoted and unpromoted K_2CO_3-based CO_2 capture systems.
    2. The dynamic models developed in this project serve as the basis for future dynamic studies on this novel solvent.
    3. The proposed PID control strategies in this project also serve as novel contributions in the field.
b. Practical implementations

    The results and findings from this project will provide a solid foundation for the real scale implementations of the low-cost post-combustion CO_2 capture system based on H_3BO_3 promoted and unpromoted K_2CO_3 technology either in designing new plants or retrofitting into existing plants.

1.6 SUMMARY OF CHAPTER 1

This chapter introduces the current status of climate change and the need for the implementation of carbon capture from coal-fired power plants as a means of curbing global warming. The issues regarding the use of traditional carbon capture technologies have been highlighted, indicating the necessity of intensive research works into K_2CO_3-based capture systems as promising alternatives to the conventional processes. The question of why H_3BO_3 is considered as the promoter for the K_2CO_3-based capture process has also been answered in this chapter. Finally, the research questions, objectives and the novel contributions envisaged for the current study have been covered into details in this chapter.

CHAPTER 2

CO_2 MITIGATION AND CAPTURE ROUTES

This chapter discusses the various options for mitigating carbon dioxide in the atmosphere and continues to expound on available options for carbon capture and separation technologies.

2.1 CO_2 MITIGATION ROUTES

There are six possible strategies to mitigate CO_2 emission. As shown in Figure 2.1, these strategies are: (1) efficient use of electricity; (2) use of renewable energy; (3) enhancement of power generation efficiency and fuel switching; (4) electricity generation from nuclear power plant; (5) end-use fuel switching; (6) CO_2 capture and storage. While the above strategies offer great potentials to curb CO_2 emission, due to the rapid increase in global population and the increasing demand for electricity per inhabitant, implementation of these strategies, even in massive scale, will not suffice without CO_2 removal and storage. Consistent with the International Energy Agency (IEA) modelling, carbon capture and storage (CCS) is able to deliver 13% of the cumulative emissions reductions needed by 2050 to restrict the global temperature increase to 2 degrees Celsius. This represents the capture and storage of about 6 Gigatonnes (Gt) of CO_2 emissions on an annual basis in 2050, nearly the current carbon emission rate from China's energy sector (IEA, 2015). Moreover, in many countries including Malaysia, nuclear power generation is still not a viable option since it is viewed as a high-risk technology, and requires further research to prove it friendly to humans and the environment. Consequently, CO_2 capture appears to be a very promising solution to limit CO_2 emission alongside the implementation of other strategies such as renewable energy usage and efficient energy usage.

Broadly speaking, the CO_2 removal systems can be implemented through three routes: pre-combustion, oxy-combustion and post-combustion technologies as shown in Figure 2.2. Among these classifications, post-combustion and oxy-combustion are the current leading technologies which are heavily researched to control CO_2 emissions. Post-combustion has the advantage of being either applied to retrofit existing plants or

integrated with new power plants. This is generally not the case for the pre-combustion process where it can only be applied to new plants.

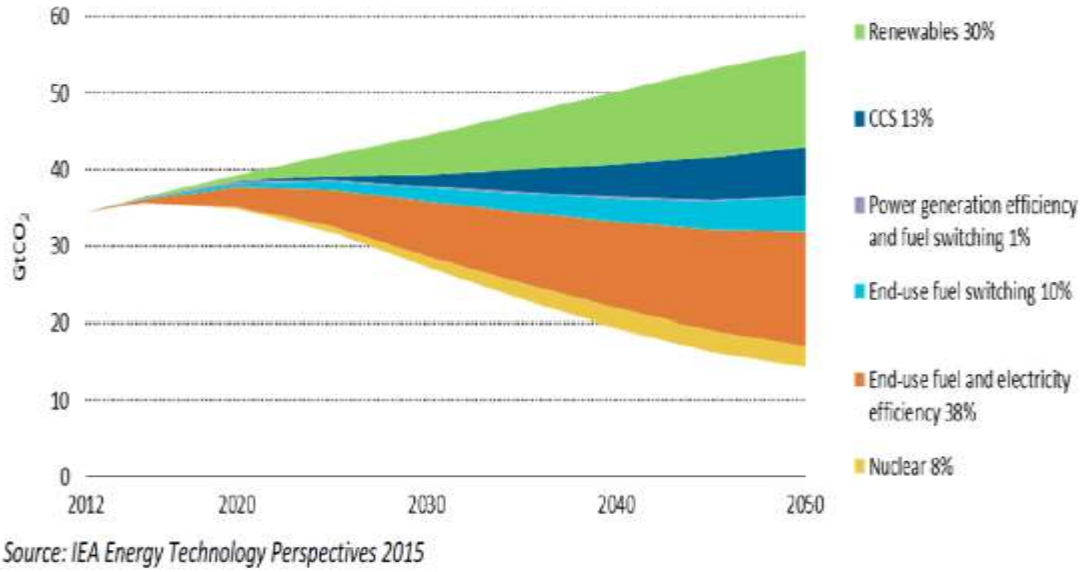

Source: IEA Energy Technology Perspectives 2015

Figure 2.1. Contribution of technologies and sectors to global cumulative CO_2 reductions IEA, 2015

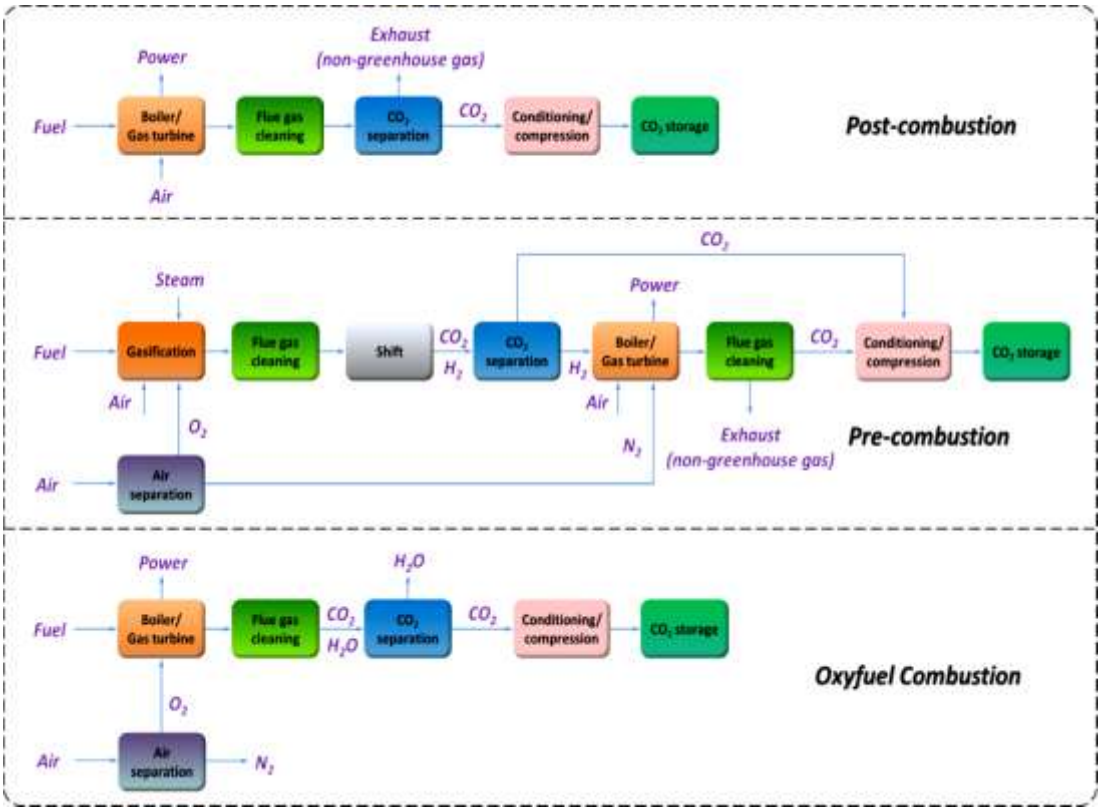

Figure 2.2. Schematic representation of main carbon dioxide capture routes (Song et al. 2019)

2.1.1 Pre-Combustion Capture Route

The pre-combustion carbon capture route is employed to decarbonise the fuel prior to combustion so that upon combustion, a stream of nearly pure H_2O is produced with minimal hydrogen peroxide (H_2O_2) and nitrogen oxides (NOx). Pre-combustion decarbonisation can be used to produce hydrogen, generate electricity or both. Figure 2.3 represents a schematic diagram of pre-combustion decarbonisation, adapted from Jansen et al. 2015. Generally, the process can be separated into five main stages. During the first stage which is the syngas island, the primary fuel is converted into a synthetic gas in the presence of steam, oxygen or both. In either case, the resulting products are usually carbon dioxide, carbon monoxide (CO) and hydrogen gas. If steam is employed in the reaction, the process is referred to as "steam reforming." On the other hand, if oxygen is used, the process is usually called "partial oxidation" when the primary fuel is liquid (e.g. crude oil) or gaseous (e.g. natural gas).

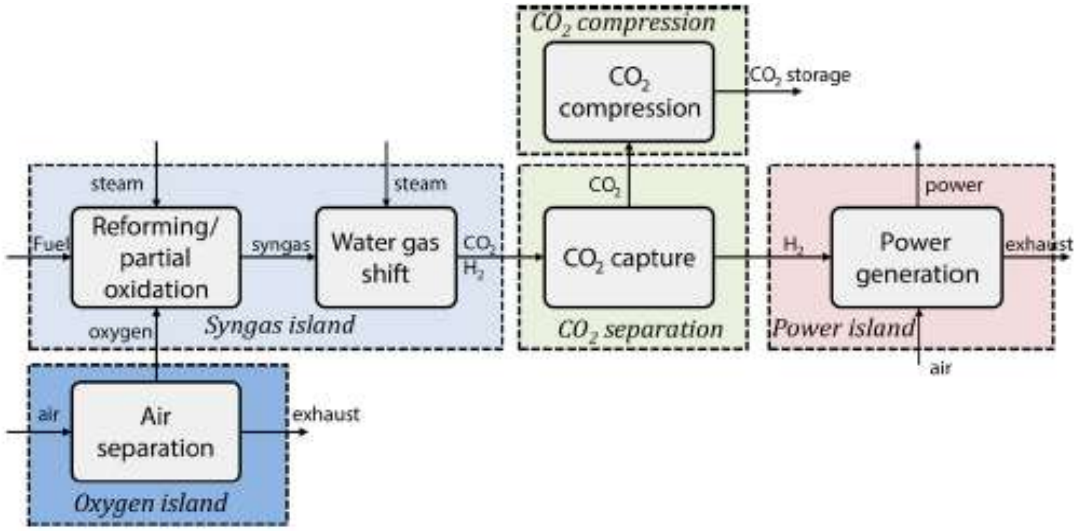

Figure 2.3. Schematic representation of pre-combustion capture (Jansen et al. 2015)

When the primary fuel is solid (e.g. pulverised coal) however, the process is termed "gasification". The principles in all these processes are the same. Basically, the primary fuel is reacted with steam and/or oxygen in the presence of intense heat to yield CO_2, CO, and H_2. If oxygen is used in the process, then an air separation unit will be used (as shown on the oxygen island) to separate oxygen and nitrogen to produce the required pure oxygen. The nitrogen produced from this process can be used as a coolant in the power plant as it is normally the case in an integrated gasification combined cycle power plants (IGCC). Since the syngas produced has a

high concentration of CO in most cases, the syngas is shifted in a water-gas-shift (WGS) reaction to convert the CO to CO_2. This is done in order to facilitate carbon capture and simultaneously increase the hydrogen production. If the syngas stream contains impurities such as sulphur and other solid particles, the gas stream is usually purified prior to the carbon capture process. During the carbon capture process, H_2 and CO_2 are separated using adsorption, absorption, membrane separation or cryogenic separation. These technologies will be further discussed later in this chapter. After the carbon separation process, the CO_2 gas stream is compressed and channelled to storage. The pure hydrogen gas is then used for combustion in the power island to generate electricity.

The pre-combustion capture route is similar in principle for coal, oil and natural gas. More stages are however required if coal or oil is the primary fuel, and the stages are to purify the syngas and remove ash particles, sulphur compounds and other impurities that might be present. It is worth mentioning that this carbon capture route has been in existence for nearly a century. Its commercial applications are however used in the industries that produce hydrogen and other chemicals, where CO_2 is viewed as a by-product and is usually removed. In this regard, pre-combustion capture can be considered as a mature technology that serves as the basis for carbon capture in general (Jansen et al. 2015; Song et al. 2019; Rackley 2010).

2.1.2 Oxy-fuel Combustion Capture Route

This capture route also referred to as oxy-firing, requires the use of nearly pure oxygen instead of air to combust the fuel in the combustion chamber. Pure oxygen may be delivered either as a gas stream produced by the separation of O_2 from air in an air separation unit (ASU) or as a solid oxide via a chemical looping process. Although pure oxygen is used in the combustion, a key feature of the oxy-fuel combustion system is that during start-up, air firing may be essential so that sufficient recycle of the flue gas is established before oxygen firing is introduced. This demands the equipment needed for air firing and the required additional controls. A diagrammatic representation of this process is shown in Figure 2.4.

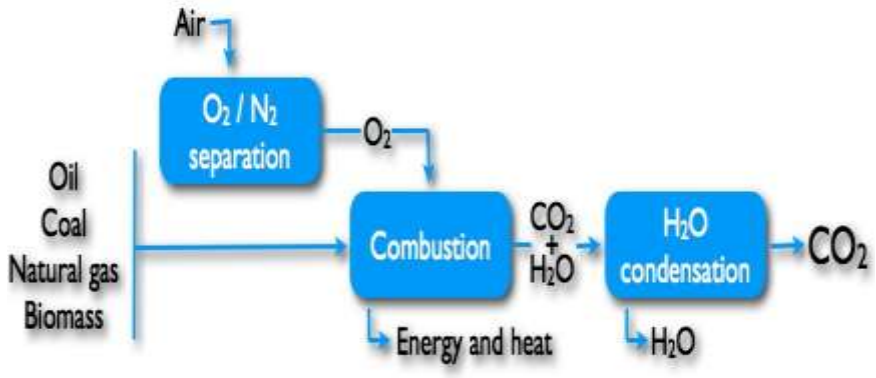

Figure 2.4. Schematic representation of Oxy-fuel combustion capture

The flue gas produced during this process is highly concentrated with CO_2, which constitutes almost 80%, and water vapour. The separation of these two gases is far easier than it is the case when nitrogen and other constituents are present in the flue gas. Thus, this capture method is mainly used to avoid the high volume of nitrogen gas which is usually present in the flue gas when air is used in the combustion process. This huge reduction in the flowrate of flue gas produced allows oxy-fuel combustion capture to use smaller absorber and regenerator columns during the carbon separation process, cutting down on equipment costs. If the flue gas composition happens to be only CO_2 and H_2O, separation is normally achieved by condensation of water. Due to the combustion process that took place in pure O_2, the flue gas produced is often associated with extremely high temperatures. This high-temperature flue gas stream is recycled to the combustor to recover waste heat. That notwithstanding, oxy-fuel combustion technology is regarded as energy-intensive due to high energy demand in the air separation unit, which is usually operated under cryogenic conditions to obtain an oxygen stream close to 95% purity. At this purity level, only the separation of nitrogen is required and the energy demand is typically about 0.2 kWh/kgO_2, although some recent enhancements are capable of lessening the energy demand to 0.16 kWh/kgO_2. (Habib et al. 2019; Kothandaraman 2010; Toftegaard et al. 2010; Tranier et al. 2011; Darde et al. 2009).

2.1.3 Post-Combustion Capture Route

The post-combustion carbon capture method is a downstream process that involves decarbonisation of the flue gas that is emitted from the power plant after the combustion of the fuel in air. It includes all the operations that extract diluted CO_2 from emissions produced by combusting biomass and fossil fuels, namely natural gas, coal

and crude oil. Usually, the flue gas produced is a mixture of a number of major gases including oxygen, nitrogen, water vapour, carbon dioxide and some other minor gases such as argon, and oxides of nitrogen and sulphur. The typical partial pressure of the carbon dioxide content of the flue gas is highly dependent on the type of fuel combusted. Table 2.1 represents the typical CO_2 concentrations in the flue gases emitted by different power plants, adapted from Kothandaraman 2010, and a diagram depicting the post-combustion capture method is shown in Figure 2.5.

Table 2.1: CO_2 concentration in flue gases of different combustion systems (Kothandaraman 2010)

Flue gas source	CO_2 concentration, % vol (dry)	Pressure of gas stream, MPa	CO_2 partial pressure, MPa
Natural gas fired boilers	7-10	0.1	0.007-0.01
Gas turbines	3-4	0.1	0.003-0.004
Oil fired boilers	11-13	0.1	0.011-0.013
Coal fired boilers	12-14	0.1	0.012-0.014
IGCC after combustion	12-14	0.1	0.012-0.014
IGCC synthesis gas after gasification	8-20	2-7	0.16-1.4 (before shift)

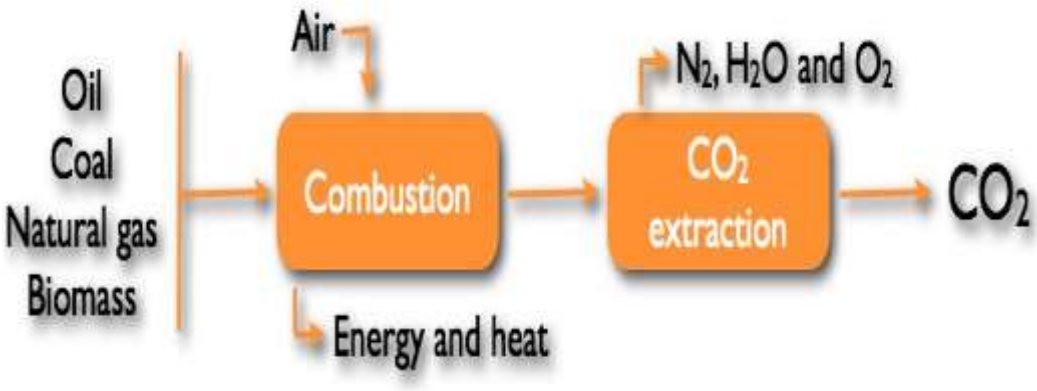

Figure 2.5. Schematic representation of post-combustion capture

Depending on the carbon separation method that is adopted, the flue gas stream may have to be cooled down in a direct contact cooler (DCC) and if impurities such as sulphur oxides are present, then there is usually a desulphurisation process before the main carbon separation stage. The separation of CO_2 can be achieved via chemical

absorption, physical absorption, adsorption, membrane separation, and cryogenic separation. These separation techniques will be further discussed in this chapter.

Table 2.2: Advantages and disadvantages of the three different carbon capture options

	Advantages	Disadvantages	References
Post-combustion	Easy to retrofit into an existing plant. Fully developed for commercial use.	High solvent regeneration energy usage. High capital and operating costs for current absorption systems. Applicable to low CO_2 concentration (5–15 vol%) in flue gas.	(Rackley 2010; Song et al. 2019; Hedin et al. 2013; Leung et al. 2014)
Pre-combustion	Applicable to high CO_2 concentration (~45 vol%) in flue gas. Commercially applicable in some industries. Lower energy requirements for CO_2 capture and compression	Severe operating conditions (15–20 bar and 190–210 °C). Temperature and efficiency issues associated with hydrogen-rich gas turbine fuel.	(Rackley 2010; Song et al. 2019; Dai et al. 2016; Nandi et al. 2015)
Oxy-fuel combustion	Yields high CO_2 concentration (80–98 vol%). Mature air separation technologies available	Significant plant impact makes retrofit less attractive. High energy penalty due to air separation unit (ASU)	(Rackley 2010; Song et al. 2019; Tonziello et al. 2011)

Unlike oxy-fuel combustion and pre-combustion technologies, post-combustion carbon capture systems can be added directly to existing power plants with little retrofitting (Mukherjee et al. 2019; Kothandaraman 2010; Song et al. 2019). This makes post-combustion carbon capture the preferred choice for many capture cases. That notwithstanding, the selection of any of these routes depends on many other factors, which are summarised into the advantages and disadvantages of the three different capture routes in Table 2.2.

2.2 CO_2 SEPARATION TECHNIQUES

Several CO_2 removal techniques potentially suitable for post-combustion and pre-combustion capture technologies are currently available. These processes include

membrane separation, removal by adsorption, cryogenic separation, and absorption. Each of these techniques operates by different separation principles. Owing to these variations in operating principles, the adoption of an appropriate separation method for various industrial emission points is vital in order to attain high efficiencies, which in turn depends on different parameters. Examples of these parameters include stream conditions, economics, flue gas composition and target products. While the majority of these techniques require further technological development to become commercialized, a few of them are well established and commercially used. Among these established techniques, chemical and physical absorption by solvents are by far the most advanced and numerous developments of these techniques are in progress.

2.2.1 Separation by Adsorption

Adsorption is a physical or chemical process that involves mass transfer of gas or liquid to a solid surface. In this carbon separation process, the selective removal of carbon dioxide from the flue gas is achieved via solid adsorbents with high surface area and, regenerated through a desorption process. The mechanism is called physical adsorption when it is physically induced by either ion-quadrupole interaction or van der Waals force, as it is the case in the microporous materials of zeolites, molecular sieves, activated carbons and microporous polymers. On the other hand, if the adsorption is chemically induced by adopting solid chemicals such as carbon-supported amine materials or amine-grafted silica materials which reactively interact with the carbon dioxide molecules, then the process is termed chemical adsorption. In the case of physical adsorption, the efficiency is dependent on factors such as the porosity of the adsorbent, its specific surface area size and active site counts. For a more effective adsorption, it is recommended that the adsorbent should have a high specific surface area, numerous active sites and a well-developed micro-pores. The efficiency of a chemical adsorbent is however dependent on the interfacial mass transfer rate between the adsorbent and adsorbate, as well as the overall mass transfer rate in the adsorption and desorption process. This requires that chemical adsorbents with large pore size and pore volume for high loading and swift diffusion of carbon dioxide molecules are to be used to achieve higher capture efficiency (Wang et al. 2019; Kaur et al. 2019; Li et al. 2019; Choi et al. 2019; Jang et al. 2018).

Regardless of whether the adsorption is physically induced or chemically induced, the desorption process differs based on whether the adsorption procedure is a temperature swing adsorption (TSA), a pressure swing adsorption (PSA), or an electric swing adsorption (ESA). In a TSA, the regeneration of the adsorbent is achieved by simply increasing the temperature in the desorption column at a constant pressure. This forces the adsorbent to release the entrapped carbon dioxide molecules due to mild expansion in the pores of the adsorbent or chemical dissociation induced by the temperature rise. A relatively high adsorbate could be forced out of the adsorbent with a moderate increase in temperature. This implies a higher temperature is required to efficiently drive out the adsorbate molecules from the pores of the adsorbent. However, the temperature rise must be controlled to ensure that no irreversible degradation is caused in the adsorbent. To effectively utilise this process, a change in temperature alone is not usually employed in the industry. Rather, the passage of steam or hot purge gases through the adsorber bed is used to sweep out the desorbed molecules in conjunction with the temperature increase (Plaza et al. 2019; Zhao et al. 2019; Mondino et al. 2019). ESA operates with similar principles as in TSA. The only difference is that heating in ESA is achieved by employing a low voltage electric current to heat up the adsorbent by the direct joule effect. The main advantage of ESA over TSA is that the heating process is faster, thus increasing the overall speed and efficiency of the process. Also, in cases where waste energy is not enough to heat up the adsorbent in a TSA process, an ESA could be adopted to meet the high-temperature requirement. Since ESA uses direct electric current for the heating process, the cost associated with this method of adsorption could sometimes be very high (Grande et al. 2008; Keller et al. 2019).

Unlike TSA and ESA, a PSA is carried out at near atmospheric temperatures but with a huge pressure swing between the adsorption stage and the desorption stage. The target gas is adsorbed at very high pressures in the adsorption stage and regeneration is achieved at very low pressures during the desorption stage. PSA mechanism utilises the fact that under very high pressures, gas molecules tend to be attracted to solid surfaces and detach at lower pressure. Thus, the higher the temperature, the more target gas is adsorbed. Although this is generally the case, the pressure has to be controlled to selectively adsorb the target gas only. When the pressure control is not efficiently managed, many other gases in the flue gas stream could be adsorbed in the process,

which will minimise the efficiency of the whole process (Tao et al. 2019; Khanna et al. 2019).

Some of the solid adsorbents investigated so far include synthetic or natural zeolites, molecular sieves, activated carbon, polymers, and alumina. Even though few of these adsorbents have been successfully tested to capture CO_2 (Li et al. 2011; Zhao et al. 2007), current adsorption systems may not be applicable in large scale capacity of flue gas from power plants. A diagrammatic presentation of the adsorption process is shown in Figures 2.6 and 2.7.

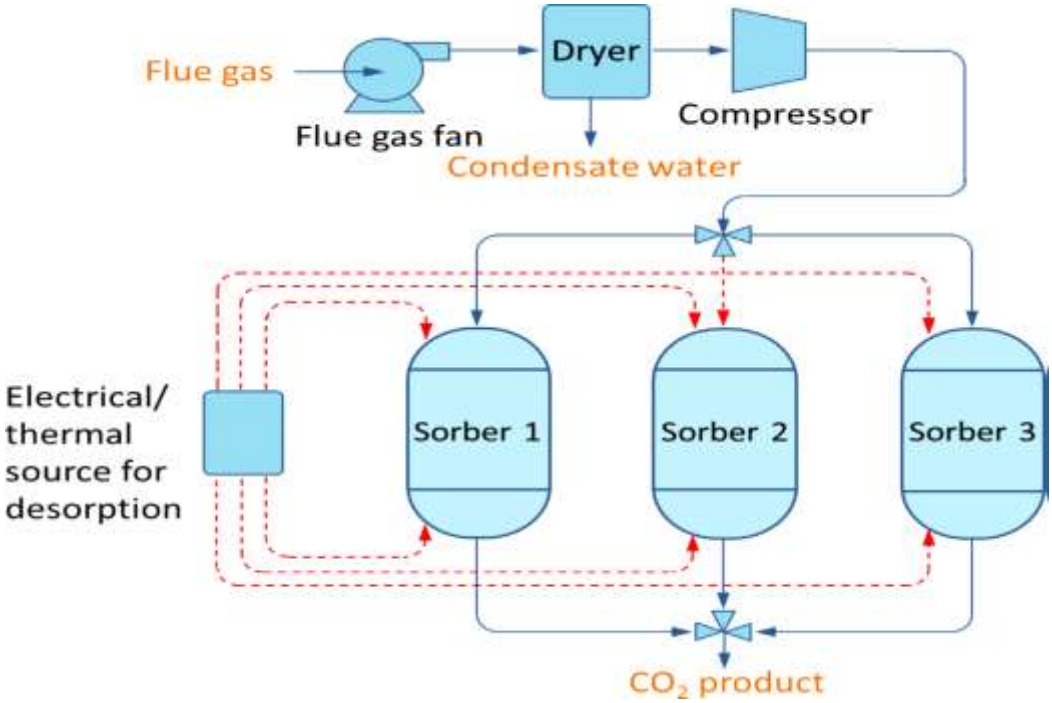

Figure 2.6. Process flow diagram for carbon capture by adsorption process (Song et al. 2019).

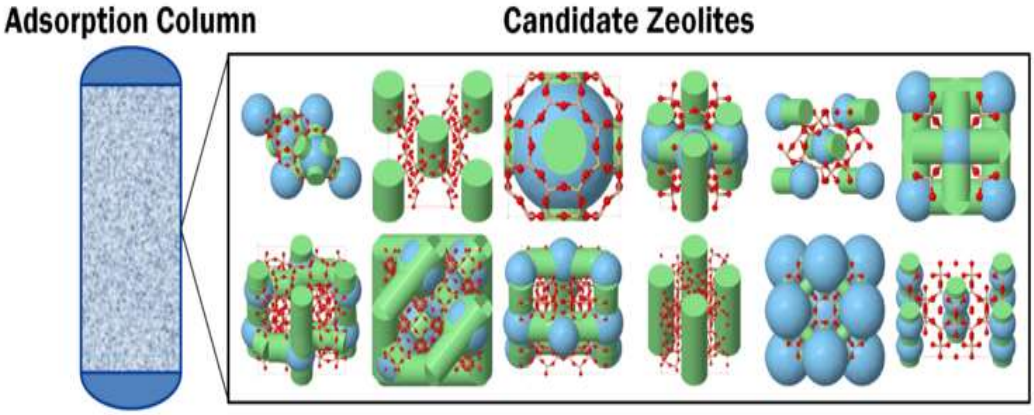

Figure 2.7. The anatomy of an adsorption column with a zeolite candidate (Hasan et al. 2013).

2.2.2 Cryogenic Separation

Cryogenic-based carbon capture technology is a low-temperature capture process which employs the principles of condensation and sublimation to separate carbon dioxide from other gases in the flue gas stream. Despite variations in the applications of this technology, the cryogenic separation method typically involves cooling, condensation, compression, desublimation, and finally distillation to yield liquid carbon dioxide.

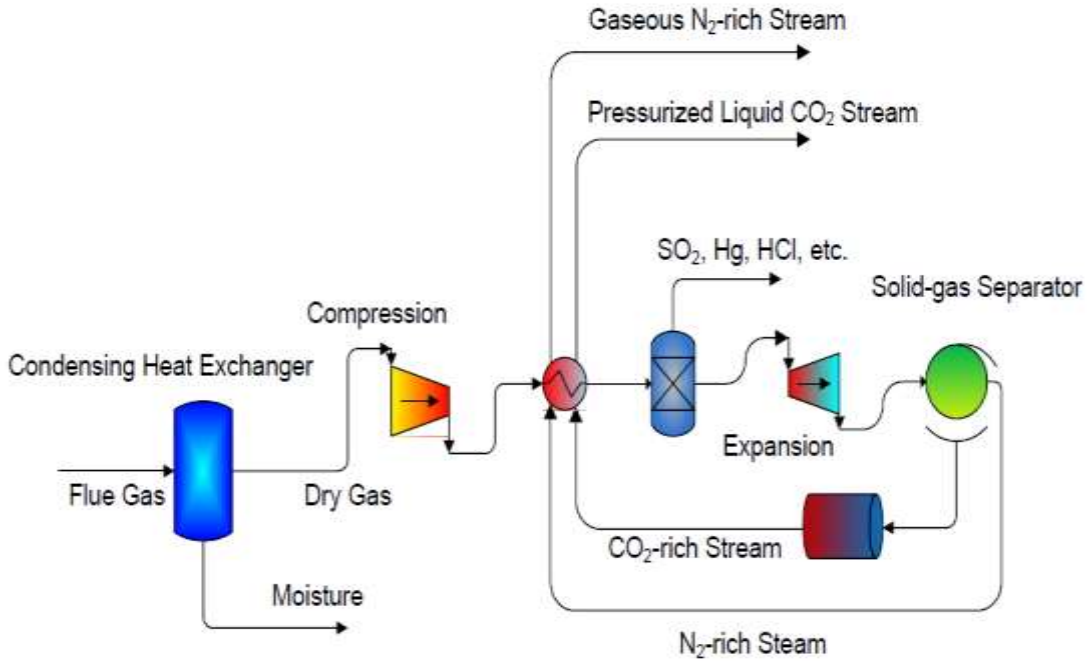

Figure 2.8. Schematic diagram of a cryogenic carbon separation system (Baxter et al. 2009).

As depicted in Figure 2.8, the process begins with flue gas drying and moisture removal via a condensing heat exchanger. This is required to separate water vapour from the flue gas stream. The dry flue gas stream is then compressed and cooled further in a cross heat exchanger to a temperature just slightly higher than the solid deposition point of carbon dioxide (-78.5 °C at atmospheric pressure). The next stage involves the separation of other gases such as SOx using series of fractionating and distillation columns to attain the required purity of carbon dioxide. The CO_2 rich stream then undergoes expansion to further cool the gas to form solid particles. A solid-gas separator is then used to separate the solid carbon dioxide from the nitrogen gas still present. The carbon dioxide stream and nitrogen streams are then used to cool the next dry flue gas stream in the cross heat exchanger. A pressurised liquid carbon dioxide

stream is produced in the process and ready for storage (Baxter et al. 2009; Song et al. 2019; Surovtseva 2010; Surovtseva et al. 2011).

Although this process appears to be one of the most effective methods of producing pure CO_2 for industrial uses, the cost associated with the several refrigeration processes involved makes it unattractive for dilute CO_2 streams in post-combustion capture technologies. This makes the cryogenic separation process typically attractive in oxy-fuel combustion and pre-combustion carbon capture technologies.

2.2.3 Membrane Separation

Selective gas separation using membranes is achieved by diffusing individual gas components across thin semi-permeable membrane barriers that are able to filter the gas stream. This method is applicable in all three carbon capture routes namely pre-combustion, oxy-fuel combustion and post-combustion capture routes. The working principle is the difference between the sizes between the CO_2 molecules and the other gas components. CO_2 is a very small gas species with a kinetic diameter of 330 pm. This value is much smaller than other common component gases such as sulphur dioxide (360 pm), argon (340 pm), nitrogen (364 pm) and oxygen (346 pm). Water, however, has a smaller kinetic diameter (265 pm) than CO_2 and requires to be condensed from the gas stream prior to membrane separation. If that is not done, the purity of the carbon dioxide product gas stream would be compromised. Therefore, traditional membrane separation is the most suitable in cases where a very high purity of the product gas stream is not mandatory. Apart from that, membranes are more often than not, affected by some chemicals in the gas stream and requires to be replaced frequently, thus increasing the operational cost of this process. There are also reported cases of membrane degradation under high temperature, requiring the influent gas stream to be cooled to a reasonably lower temperature than the membrane material withstand. Current membrane materials are made from molecular sieves, rubbery and glassy polymers, and many other inorganic materials (Ebner et al. 2009; Brunetti et al. 2010; Mohanty et al. 2011; Prasad et al. 2019).

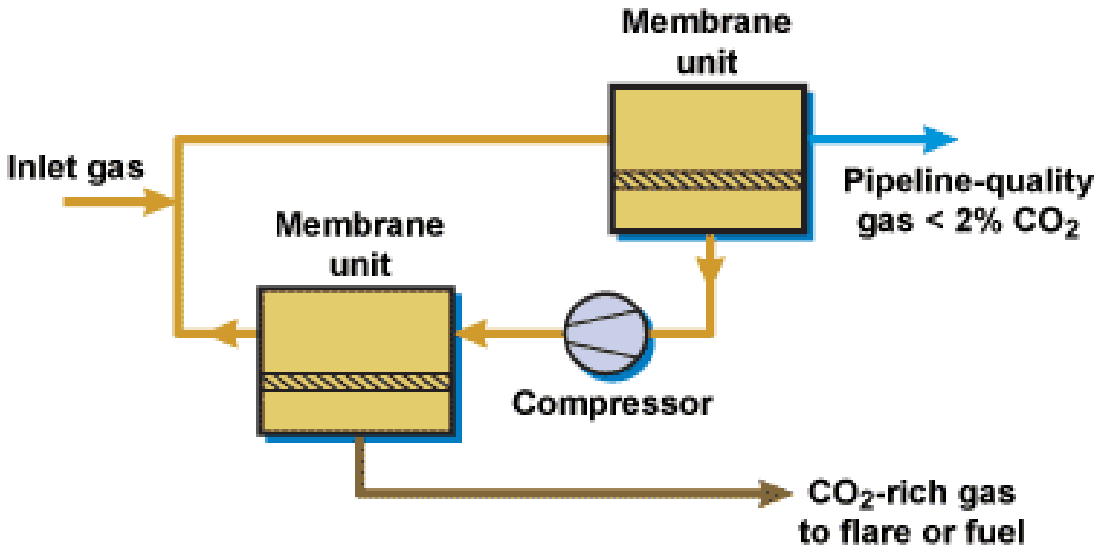

Figure 2.9. Process diagram of the membrane separation applied to carbon capture

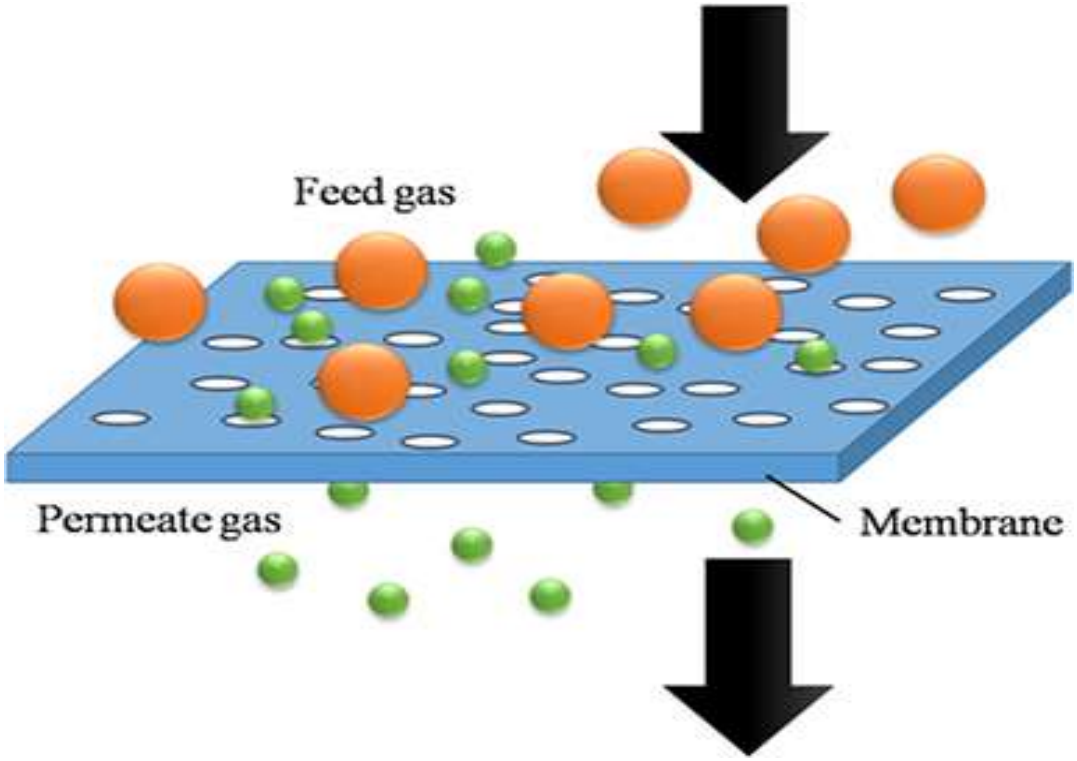

Figure 2.10. Anatomy of a membrane material (Ji et al. 2017)

In general, this carbon separation method possesses some advantages such as small footprint, modularity, no moving parts, and besides no desorption energy is required. Nevertheless, there is still the need to advance membrane permeability, selectivity, and durability at high temperatures for carbon capture. Moreover, membrane separation incurs extra capital and operating costs since multistage separations are required due to the low selectivity of the separation (Gielen et al. 2004). Figure 2.9 shows a process

diagram of the membrane separation applied to carbon capture, and Figure 2.10 displays the anatomy of a membrane material, adapted from Ji et al. 2017.

2.2.4 Physical Absorption

Physical absorption involves the use of non-reactive solvents which dissolves the target gas component without necessarily reacting with it. When applied in CO_2 separation from a gas stream, the physical solvent selectively absorbs the carbon dioxide molecules without chemical reacting with it. Thus, physical absorption relies on the particular solubility associated with CO_2 in the solvent rather than on the chemical reaction using the solvent, and the solvent can be reused just by changing the temperature or pressure of the solution in the desorber column. This type of absorption is often referred to as heterogeneous enhancement and is achieved by the presence of finely dispersed second phase in the carrier liquid. This second phase solvent can either be solid or liquid and has a feature of being immiscible with the continuous liquid phase, coupled with a high specific capacity to dissolve the target gas, which is CO_2 in this case. Because of the immiscible nature of this system, the mixture is normally called an emulsion. Physical absorption has received attention in recent years because of its main advantage of offering lower regeneration energy usage than the conventional chemical absorption (Chiesa et al. 1999; Littel et al. 1994; Tantikhajorngosol et al. 2019).

Physical absorption techniques are the preferred carbon removal methods for pre-combustion technology because it is only economical for relatively concentrated streams of carbon dioxide at partial pressures higher than 15 vol%. This process is commercially applied in removing CO_2 and H_2S from natural gas (acid gas treating) and for removal of carbon dioxide from synthesis gas in methanol, hydrogen, and ammonia production. Some of the solvents employed in this process are polyethylene glycol, cold methanol and dimethyl ether. These solvents have been applied in processes such as the Purisol process which uses n-methyl-2-pyrrolidone; the Rectisol process which uses methanol; the Fluorsolv process which uses propylene carbonate; and the Selexol process which uses polyethylene glycol dimethyl ether (Luis 2016). Recent researches have however investigated several ionic liquid solvents suitable for the physical absorption process. These liquids mostly contain anions such as dicyanamide, trifluoromethanesulfonate, tetrafluoroborate, hexafluorophosphate and

cation-based ion liquids containing imidazolium, ammonium and phosphonium salts (Palomar et al. 2011; Makino et al. 2019).

2.2.5 Chemical Absorption

Chemical absorption, on the other hand, involves the reaction of CO_2 and a chemical solvent to form a weakly bounded intermediate compound, which can be regenerated in a stripper column. This type of absorption is suitable for a typical flue gas from coal-fired power plants where CO_2 composition is in the range of 10% to 15% by volume. Figure 2.11 shows a typical chemical absorption process. The system typically includes an absorber column and a desorber or regenerator column.

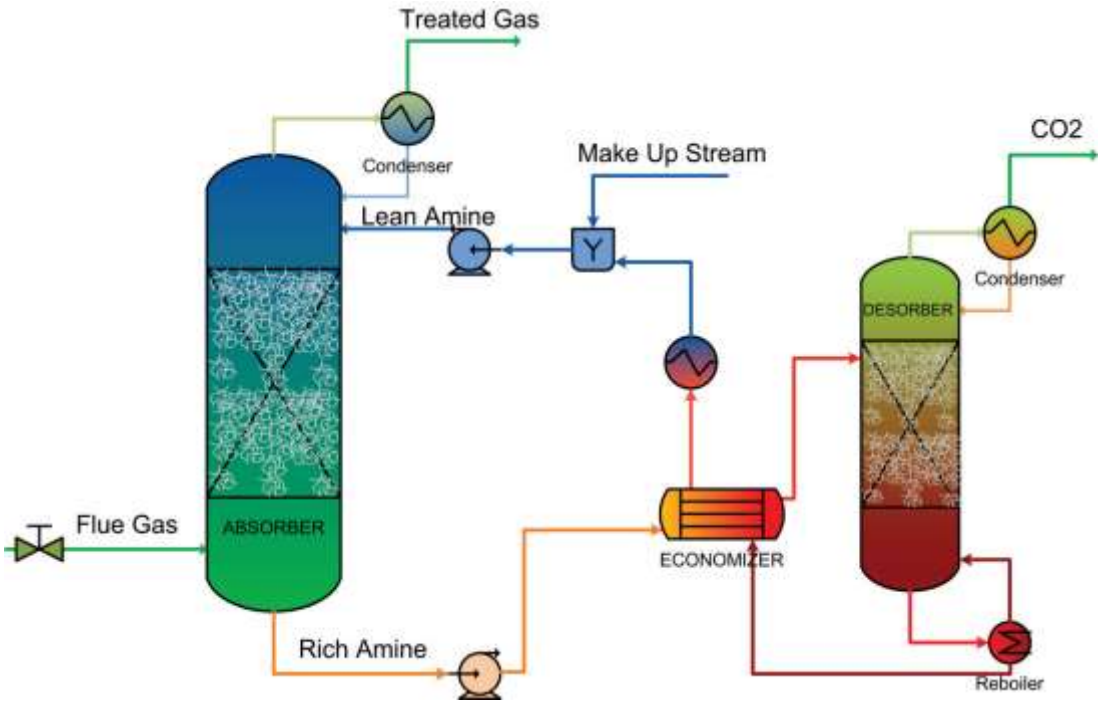

Figure 2.11. Process diagram of chemical absorption applied to carbon separation (Gaspar et al. 2016)

The flue gas is mostly cooled in a direct contact cooler before it is blown into the absorber column. The chemical absorbent is introduced into the absorber column to react with the CO_2 in the flue gas stream. The treated gas is then flared into the atmosphere while the CO_2 rich solvent stream is heated up the desorber column to regenerate the chemical absorbent and release the captured CO_2 for compression and storage (Gaspar et al. 2016; Nwokedi et al. 2019; Chen et al. 2018). The use of chemical absorption for the removal of CO_2 from exhaust gas streams has benefits of high selectivity of separation and producing a relatively pure CO_2 stream. Although

the efficiency of the system largely depends on the type of chemical absorbent used, this separation method is largely considered as the most advanced and most suited for CO_2 mitigation from industrial flue gases.

For many reasons, amine-based chemical absorption processes are the most preferable for capturing CO_2 from power plants (Lecomte et al. 2010; Rao et al. 2002) since this technology is relatively mature and commercially available. To date, aqueous monoethanolamine (MEA) is a widely used solvent for CO_2 removal system from flue gas streams. MEA-based CO_2 absorption process can be operated at room temperature and atmospheric pressure and it has been proven in commercial demonstrations in the Fluor Daniel Econamine FG^{TM} process which uses 30% w/w MEA solution (Sander et al. 1992), Kerr-McGee/ABB-Lummus Crest technology which uses 15% - 20% w/w MEA solution (Barchas et al. 1992) and Prosernat HiCapt process (Lemaire et al. 2014) which uses 30% - 40% w/w MEA solution (Lecomte et al. 2010).

Post-combustion CO_2 capture using MEA offers the opportunity of reducing CO_2 emissions to the atmosphere. However, its implementation results in energy penalties as it could reduce the efficiency of the power plant up to 30% (Yu et al. 2012; Goto et al. 2013). The separation processes (absorption and solvent regeneration) are energy-intensive and they represent about 75-80% of the total cost of the entire carbon capture and storage process (Wang et al. 2011; Zahra et al. 2011). The solvent regeneration normally uses steam from the power plant cycle, affecting the performance of the plant and reducing the plant efficiency which results in the rising of cost per kWh. Lower output of the plant may also interrupt the stability and sufficiency of the power supplied to the grid. Capture cost can be approximately 40-60 Euros per tonne of CO_2 avoided and this could result in soaring electricity production cost up to 60% more for a coal-fired power plant (Lecomte et al. 2010). Moreover, apart from being energy-intensive and costly, the use of MEA incurs many operational concerns associated with solvent degradation at high temperature and/or in the presence of oxygen, solvent-loss to evaporation due to its high vapour pressure, equipment corrosion, toxic products and amine waste discharge (Ghosh et al. 2009; Shen et al. 2013). Upstream pre-treatment processes for sulphur dioxide (SO_2) and NO_x removal are also required for more effective CO_2 capture since MEA irreversibly reacts with these gas components forming heat-stable corrosive salts which lead to solvent degradation and foaming (Smith et al. 2009; Thee et al. 2012). For the above reasons, a significant amount of

research is being directed towards two aspects: (1) developing lower cost, more effective and environment-friendly solvents; (2) inventing modified and intensified processes to minimise the energy penalties.

An alternative solvent that may potentially overcome issues associated with the MEA solvent is potassium carbonate (K_2CO_3). Compared to MEA, potassium carbonate offers many benefits including low cost, less energy requirement for solvent regeneration, less toxicity and solvent losses, less prone to degradation (no thermal and oxidative degradation), no-formation of heat-stable salts, better resistance to the presences of SO_2 and NO_x and ability to run the absorption process at high temperature. Despite these better performances, the use of potassium carbonate is limited by its slow reaction rate with CO_2 resulting in a poor absorption rate of CO_2. Moreover, when it is implemented for capturing CO_2 from the power plant flue gas, its reaction rate will be much slower due to its operations at normal pressure and relatively low temperature. To address this constraint and enhance the performance of potassium carbonate for CO_2 absorption, many experimental studies have suggested the addition of promoters such as piperazine (PZ), amino acids, arsenious acid, amine derivatives, carbonic anhydrase (CA) and boric acid (Thee 2013; Borhani et al. 2015). Nevertheless, they also indicated that there are few issues related to these promoters especially piperazine, arsenious acid and amine derivatives. Traditional promoters such as piperazine, diethanolamine and arsenic trioxide are known to be very toxic and hazardous to the environment, raising safety and environmental concerns. Carbonic anhydrase, despite its ability in increasing the reaction rate, its stability and effectiveness of the regeneration cycle is questionable and have not been well-investigated. Its activity is also lowered after immobilization. Amino acid-based promoters such as glycine, sarcosine, proline and arginine have also recently gained interest since they are green chemicals and have low volatility. Nevertheless, literature and data on amino acid-based promoters are very scarce and more basic research is still required (Hu et al. 2016; Thee et al. 2014). On the other hand, boric acid is very promising because it is not only more environmentally friendly but also relatively cheaper, readily available for mass production and does not interact with flue gas impurities such as SO_x and NO_x (Shen et al. 2014). Moreover, considering overall performance, toxicity, stability, volatility and corrosivity, boric acid has been hypothesized as "the best" compared to arsenic acid, MEA, DEA, PZ, amino acids and

CA. Therefore, potassium carbonate promoted with boric acid has been viewed as a better alternative to traditional commercial MEA-based CO_2 capture systems.

2.3 SUMMARY OF CHAPTER 2

This chapter reviews the possible strategies of mitigating CO_2 emission, zooming in on the contribution of carbon capture and storage as one of the most effective strategies. The three main carbon capture routes namely, oxy-fuel combustion, pre-combustion and post-combustion capture routes, have been explained into details, concluding on the latter as the most convenient option to retrofit into existing power plants. Various CO_2 separation methods were also reviewed. Among these separation techniques, chemical absorption was realised to be the most popular and efficient. MEA, NH_3 and K_2CO_3 were briefly discussed as the most common solvents used in the chemical absorption process. The justification for using K_2CO_3 in this project is also introduced here, and the need for promoters in the K_2CO_3-based capture technology was also presented. The chapter concluded with an overview of various additives currently being studied as possible promoters, pointing out why H_3BO_3 is considered to be among the most promising options.

CHAPTER 3

CO_2 CAPTURE USING CHEMICAL SOLVENTS

As mentioned earlier in chapter 2, chemical absorption is by far the most advanced method suitable to be employed in post-combustion carbon capture technology. The main solvents widely researched and adopted for CO_2 separation by chemical absorption are amines, ammonia and potassium carbonate. This section reviews the background and relevant research works that exist in literature on these solvents.

3.1 AMINE SCRUBBING

Amines are the most investigated chemical solvents for the absorption separation of carbon dioxide in the post-combustion capture technology. Aqueous amine solvents react with carbon dioxide and produce water-soluble amine-CO_2 complexes, which allows for the amine solvent to absorb CO_2 at low partial pressures and result in a high carbon capture efficiency. In customary amine scrubbing, CO_2 is absorbed at low temperatures (~40°C) and regenerated at high temperatures (120°C~150°C). Typically, primary amines such as MEA and secondary amines such as diethanolamine (DEA) are used in this technology. The two most important kinetic reaction equations of amines with CO_2 during the capture process are as follows:

$$REA + CO_2 + H_2O \rightleftharpoons REACOO^- + H_3O^+ \quad \ldots\ldots\ldots\ldots 3.1$$

$$REACOO^- + H_3O^+ \rightleftharpoons REA + CO_2 + H_2O \quad \ldots\ldots\ldots\ldots 3.2$$

The primary and secondary amines tend to form stable carbamates ($REACOO^-$) in their reaction with carbon dioxide (reaction 3.1). For this reason, the primary and secondary amines demand higher heat duties in the regeneration column for the desorption process in reaction 3.2 compared to the tertiary amines (Chowdhury et al. 2013). MEA is however considered the benchmarking amine solvent in carbon capture technologies because of its commercial availability and application in various industrial areas. Detailed description of the MEA-based process is discussed below in the Kerr-McGee/ABB Lummus Crest technology, the Fluor Daniel ECONAMINE FG technology, and the HiCapt process.

3.1.1 Kerr-McGee/ABB Lummus Crest Technology (Barchas et al. 1992)

This technology is a commercially proven process developed by Kerr-McGee Chemical Corporation (an American energy company founded in 1929) at their Argus Soda Ash facility in California, designed to recover CO_2 from the Oklahoma coal-fired power plant. The technology is currently licensed jointly by Kerr-McGee and the ABB Lummus Crest Incorporation (a foreign UK-based company founded in 1996). This technology was originally invented to manufacture chemical-grade and food-grade carbon dioxide from coal-fired flue gas but is equally applicable to engine exhausts, natural gas or oil-fired flue gases, and any other waste gases containing oxygen. Figure 3.1 shows a schematic representation of the Kerr McGee/ABB Lummus Crest carbon capture technology.

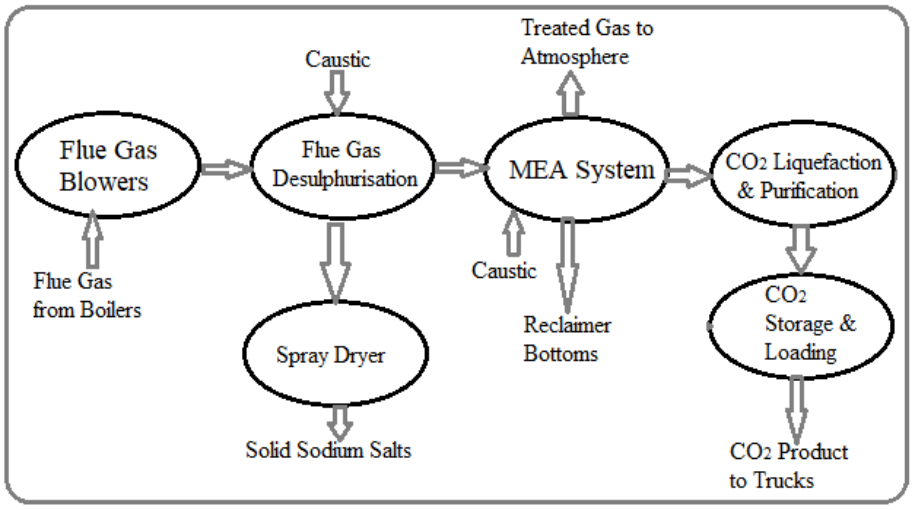

Figure 3.1. Kerr-McGee/ABB Lummus Crest Carbon Capture Technology

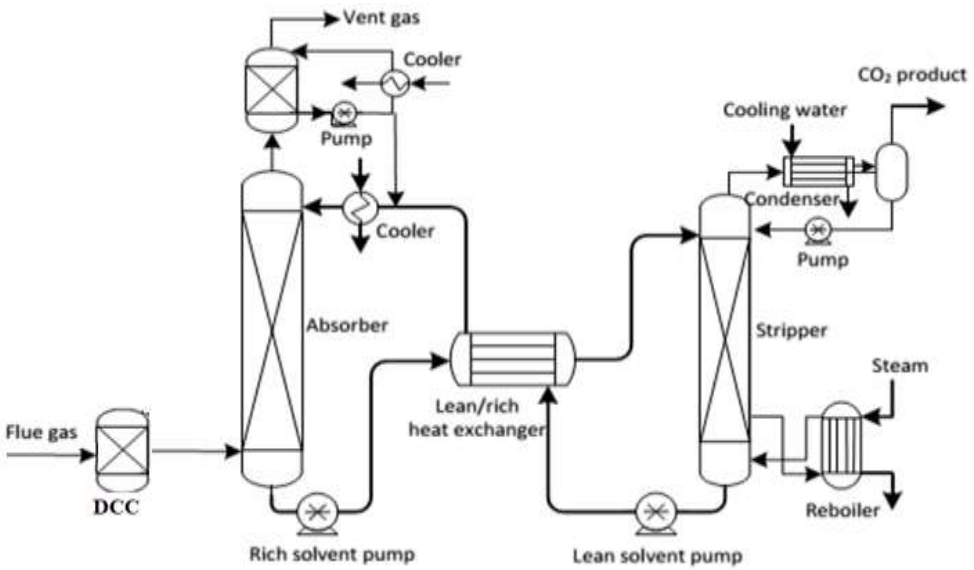

Figure 3.2. Schematic flow sheet of amine scrubbing process

The flue gas from the power plant is blown in the desulphurisation plant using centrifugal blowers at the pressure of 2 psig (1.136 atm). The desulphurisation system uses sodium hydroxide (NaOH) to mitigate the concentration of sulphur dioxide (SO_2) from as high as >100 ppm to <10 ppm on a volume basis. The NaOH reacts with the SO_2 to yield sodium bisulphite ($NaHSO_3$) which is then converted into sodium sulphite (Na_2SO_3) upon addition of extra NaOH (also called caustic soda or lye). The wet Na_2SO_3 is then dried in a spray dryer to yield solid sodium salts.

The essence of removing the SO_2 from the flue gas stream is to inhibit the irreversible reaction with MEA to produce MEA sulphite. If that occurs, caustic soda has to be added to the MEA system in a reclaiming process to produce Na_2SO_3 and liberate the MEA for reuse. The MEA system in this technology is a simple absorber/stripper system as shown in Figure 3.2.

The typical concentration of aqueous MEA solution used is in the range of 15-20% by weight. The desulphurised flue gas stream is then ducted into the MEA system after cooling in a direct contact cooler (DCC). The absorber column treats the gas stream to scrub off almost 90% of the carbon content. The treated gas stream is then released into the atmosphere after washing to minimise the loss of the volatile MEA. The rich CO_2 solvent stream is preheated in the heat exchanger in Figure 3.2 prior to the regeneration process in the stripper column. The recovered MEA from the stripper stream is recycled to the absorber column while the CO_2 recovered at the overhead is liquefied and purified for storage. The liquefaction is achieved using an ammonia refrigeration system while the purification process is completed using various adsorbents as well as extra stripper columns to remove contaminants such as nitrous oxides, non-condensable gases, oil, sulphur compounds and any available trace metals.

3.1.2 Fluor Daniel ECONAMINE FG Technology (Sander et al. 1992)

This technology was initially invented by the Dow Chemical Company in the 1980s but later acquired by Fluor Daniel Incorporation in the year 1989. Similar to the Kerr-McGee technology, this process is also used to produce pure CO_2 for chemical and food industries. Its application is however employed in Enhanced Oil Recovery (EOR) as well, and capture efficiencies of 85 – 95% were reported. The chemicals used are 30 wt% MEA and proprietary inhibitors. These inhibitors, coupled with special

solution maintenance techniques allow this technology to run with concentrated MEA solutions without heavily corroding ordinary metal alloys. One major drawback of the process, however, is that the corrosion inhibitor is less functional in the presence of reducing gases such as carbon monoxide and hydrogen sulphide. It also loses its efficacy in the absence of an adequate amount of oxygen in the flue gas. Since there is usually no desulphurisation process included in this technology, it is usually suitable for flue gases with ≤10 ppmv of SO_2. Any amount higher than this will create a convenient environment for the irreversible reactions between MEA and SO_2.

3.1.3 The HiCapt Process (Lemaire et al. 2014)

The HiCapt carbon capture process was developed by IFPEN and PROSERNAT to utilise high concentrations of MEA, typically within the ranges of 30 to 40 wt%, and oxidative inhibitors to limit the oxidative degradation of the solvent and also permit the use of high concentrations of the solvent. The process description of this technology is not much different from that of the Kerr-McGee process and the Fluor Daniel technology. To validate this process on an industrial scale, IFPEN came into agreement with ENEL in 2009 to use this technology in the CO_2 pilot capture plant operated by ENEL in Italy. The capacity of the capture plant was 2.25 tonnes per hour of CO_2 captured from 12 tonnes per hour of flue gas from a 4 x 660 MWe industrial coal-fired power plant located in Brindisi. The pilot runs were tested for 20 wt%, 30 wt% and 40 wt% MEA to study various operational parameters and the reliability of the HiCapt process. The results from the experiments and later works at another project referred to as the Castor project were convincing enough for IFPEN to conclude that the use of carbon steel is not possible for all MEA based processes. Materials such as stainless steel and duplex steel were however found to have shown minimal corrosion, with stainless steel recording ≤10 μm per year for all concentrations of MEA and duplex steel recording ≤10 μm per year for a typical HiCapt process and ≤5 μm per year for processes utilising less than 40 wt% MEA. Hence, stainless steel and duplex steel were concluded by IFPEN and PROSERNAT to be the suitable materials in designing the absorber column, stripper column and other process equipment for MEA-based carbon capture processes.

Since the invention of the above technologies, many other companies have developed their own amine scrubbing process with the purpose of improving upon the entire

process and inhibitors to control corrosion in process equipment and also to minimise the energy consumption of the plant. Some of these companies include the Mitsubishi Heavy Industries, Kansai Electric Power, Shell, Aker Clean Carbon, Alston Power, Powerspan, Siemens, etc. Despite minimal variations in the technologies developed by these companies, the fundamental working principles of the scrubbing process remains the same (Oko et al. 2017).

3.1.4 State of The Art Review of MEA Capture Process

Adopting the ELECNRTL thermodynamic property package in a rigorous rate-based studies by Li[c] et al. 2016, using Aspen Plus Modeller, the authors conducted a systematic study of an aqueous MEA-based carbon capture process to investigate the energy consumption associated with the whole process and offer suggestions on process improvements. The results from these studies indicated that the regeneration energy requirements for the conventional absorber/stripper capture process are in the range of 4.01 to 5.20 MJ/kg CO_2. The findings of this research closely compared to those recorded from the pilot plant trials conducted at the Tarong Power Station in Queensland for a coal-fired power plant. These trials indicated solvent regeneration energy consumptions within the range of 3.86 to 4.60 MJ/kg CO_2. Both the pilot plant studies and the simulation studies yielded carbon capture efficiencies above 90%. Combined parametric optimisations and process improvements investigated by the authors, however, showed that the stripper reboiler energy usage could be reduced to as low as 3.1 MJ/kg CO_2 (Li[c] et al. 2016).

Nakagaki et al. 2017 also conducted a lab-scale experimental work and simulation studies for a 30 wt% MEA-based post-combustion capture process to quantify the heat of CO_2 dissociation (Q_R), the sensible heat of amine solution (Q_H), latent heat of condensation (Q_V) and heat leakage from the stripper system (Q_L). The results of these experimental studies, as shown in Figure 3.3, indicated that the Aspen Plus simulation work undermines the Q_R value by -3.2 kJ/mol-CO_2. The results also showed that Q_R and Q_H represent the major energy consumptions in the system, signifying that, process improvements seeking to reduce energy consumption need to consider ways of reducing these values. The energy leakage from the experimental work, which was also undermined in the simulation by a factor of -1.6 kJ/mol-CO_2, was quite significant. This implies that advanced process developments that could reduce energy

loss in the capture process can equally render the MEA-based capture process a cheaper technology (Nakagaki et al. 2017).

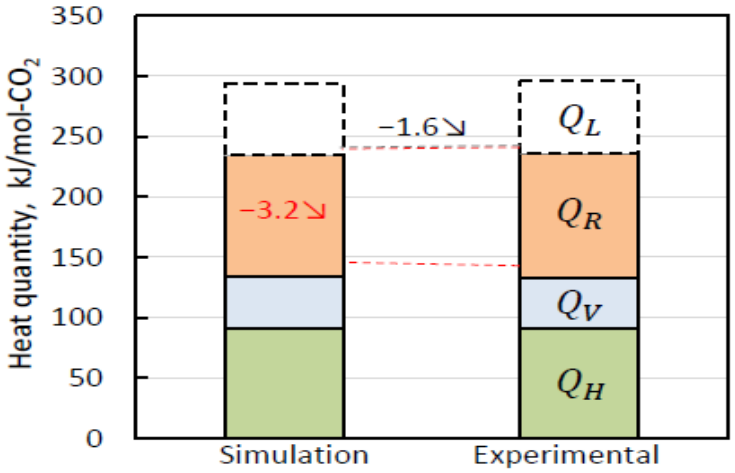

Figure 3.3. Comparison of experimental and simulation studies from Nakagaki et al. 2017.

In a recent experimental and simulation works undertaken by Ling et al. 2019, the effects of heat-stable salts (HSSs) on the performance of a 30 wt% aqueous MEA-based capture process were comprehensively studied. This research was motivated by the fact that MEA undergoes oxidation degradations to produce carboxylic acids which tend to form HSSs with MEA. To facilitate the formation of these HSSs in the experimental system, the researchers introduced nine different carboxylic acids into the absorber system in varying quantities. A major conclusion from their work was that the initial pH values, equilibrium solubility of CO_2 and overall absorption rate decreases upon addition of the carboxylic acids. The impact was also observed to increase with an increasing amount of the carboxylic acids. These phenomena were explained to be a result of introducing more H^+ into the system which lowers the pH of the system. Also, upon reaction of these acids with MEA, the active number of the amine chemical decreases, reducing the CO_2 solubility rate in the solvent and ultimately affecting the overall absorption rate negatively. Despite these adverse findings, admittedly, the introduction of carboxylic acids into the system appeared to have decreased the regeneration energy requirement and advance the overall desorption rate. This impact was also observed to increase with increasing quantities of carboxylic acids. The explanation given for this scenario was that the extra H^+ ions introduced into the system upon the addition of carboxylic acids tend to enhance the decomposition reaction of carbamate, which is the key step in the desorption process. Thus, the enhancement in carbamate decomposition propagates into the desorption

process, promoting the regeneration process and lessening the total heat duty requirement in the regenerator.

The researchers recommended that since the production of carboxylic acids and heat stable salts in the MEA-based capture process have shown to negatively influence the performance of the absorber but positively impact the regeneration process, it would be wise to remove these acidic degradation products from the recycled MEA lean stream before introducing it into the absorber. These acids can, however, be left in the stripper column to enhance the desorption process (Ling et al. 2019).

Considering process intensifications (PI), many researchers have studied and proposed varied intensifications for the MEA-based post-combustion carbon capture process. A summary of the conclusions could be found in Borhani et al. 2018 and Wang et al. 2015. The study by Borhani et al. 2019 at the University of Hull, UK, concluded that the use of a rotating packed bed (RPB) absorber has the advantage of yielding higher mass transfer capabilities over the conventional absorber. The critical review on intensified processes, which was completed by Wang et al. 2015, also concluded that the spinning disc technology could help to intensify heat transfer in the reboiler system of the stripper. The same authors also observed that the printed circuit heat exchanger might offer preferable heat transfer performances over the traditional cross heat exchanger. The authors, however, mentioned that there is a need for further research to identify the most suitable solvents for the intensified post-combustion carbon capture process (Wang et al. 2015).

3.2 AMMONIA-BASED CAPTURE TECHNOLOGY

Another solvent that researchers have investigated for the last decade is NH_3. The dissolution and absorption of CO_2 into aqueous NH_3 involves a series of physical and chemical processes. Figure 3.4 describes the chemical species and vapour-liquid-solid phase equilibrium in the NH_3-CO_2-H_2O system. Some pilot plants have been constructed and operated to assess the economic and technical feasibility of this solvent's application in post-combustion capture processes. The most common process employed for these pilot demonstrations is the Alstom's Chilled Ammonia Process (CAP). The detailed description of this process is discussed below.

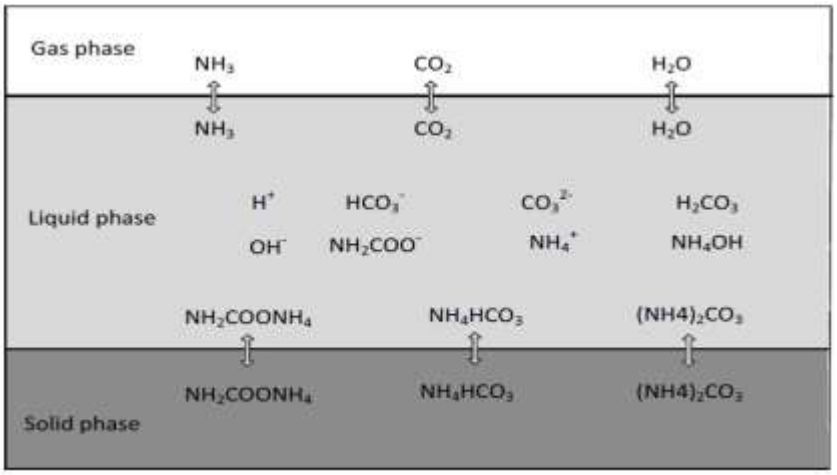

Figure 3.4. Chemical species and vapour-liquid-solid phase equilibrium in the NH_3–CO_2–H_2O system (Li[a] 2016)

3.2.1 Alstom Chilled Ammonia Process (CAP)

This NH_3-based carbon capture process was developed by the French multinational company Alstom SA, and licensed in 2006. A bench-scale testing of the process was carried out at the Alstom Research Laboratory in Vaxjo, Sweden. Figure 3.5 represents the 4 main systems involved in the CAP process shown in Figure 3.6.

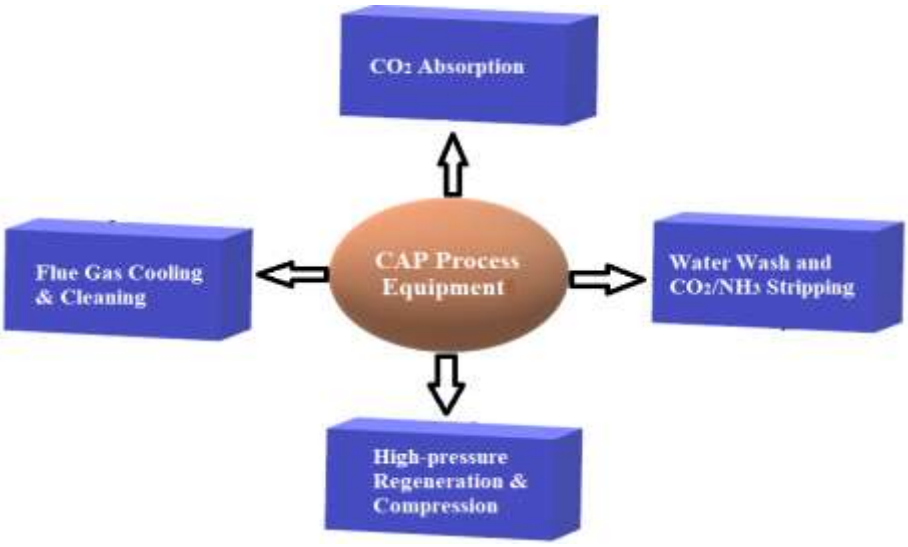

Figure 3.5. Systems of CAP process equipment

The downstream flue gas slipstream is cooled in a direct contact cooler (DCC) before it is fanned using a booster fan into the absorber. The cooling process is necessary to operate the system at low temperatures that reduce the slip of ammonia from the absorber column. The low temperature also enhances the formation of ammonium

bicarbonate solids, which improves the carbon capture efficiency of the system significantly.

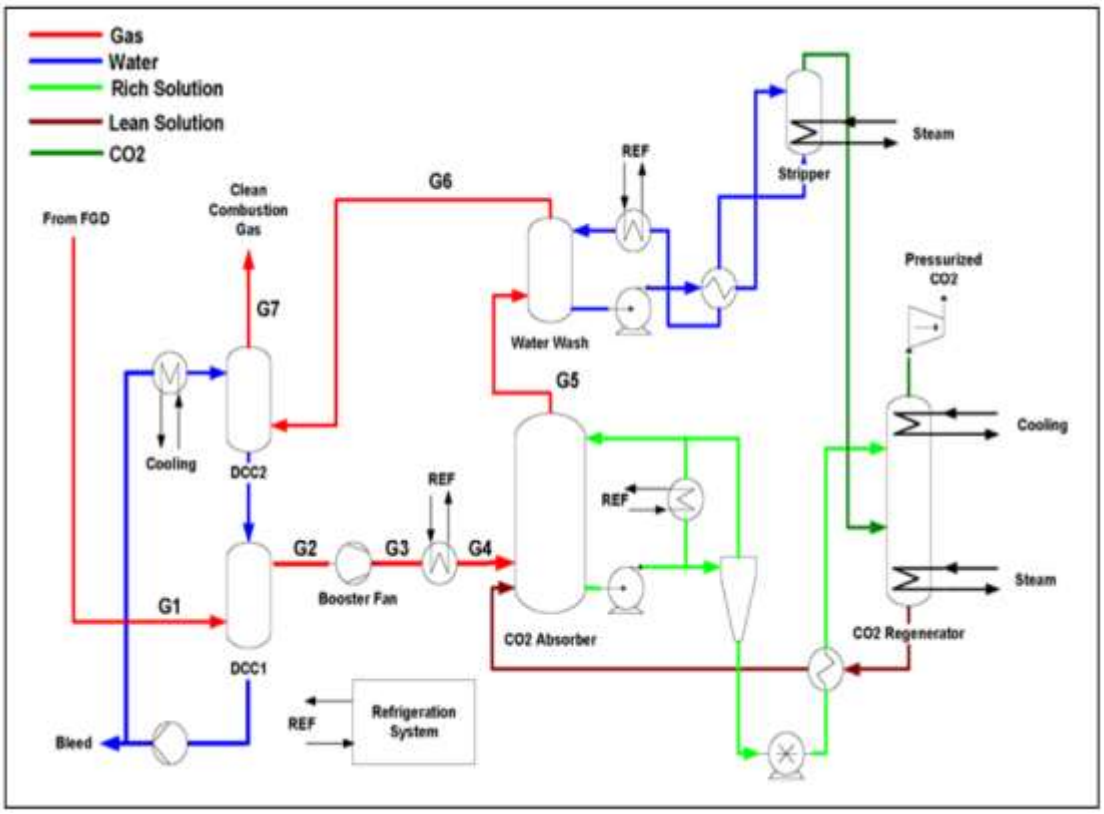

Figure 3.6. Process flow diagram of the CAP process (Sherrick et al. 2008)

Another benefit of the cooling process is that it condenses any moisture in the flue gas slipstream, thereby reducing the volumetric gas flowrate, increasing the carbon concentration and reducing the absorber vessel size. The cooling process also has an added advantage of cleaning the flue gas stream of residual pollutants such as SO_2, SO_3, hydrogen chloride and hydrogen fluoride gases which are washed away by the cooling water sprayed into the column. The treated gas exiting the absorber column is also cooled to purify the stream of any remaining pollutants before it is released into the atmosphere. The bleed stream from the DCC1, primarily containing ammonium sulphate, is purged off for disposal or possible commercial use as fertiliser. The clean flue gas stream is then channelled through cooling coils to further decrease the temperature before entering the absorber column. The absorption process follows the chemical reactions below:

$$2NH_3(g) + H_2O(l) + CO_2(g) \rightleftharpoons (NH_4)_2CO_3(aq) \dots\dots\dots\dots\dots\dots 3.3$$

$$NH_3(aq) + H_2O(l) + CO_2(g) \rightleftharpoons (NH_4)HCO_3(aq) \dots\dots\dots\dots\dots\dots 3.4$$

$$(NH_4)_2CO_3(aq) + H_2O(l) + CO_2(g) \rightleftharpoons 2(NH_4)HCO_3(aq) \dots\dots\dots\dots\dots\dots 3.5$$

$$(NH_4)HCO_3(s) \rightleftharpoons NH_3(aq) + H_2O(l) + CO_2(g) \ldots\ldots\ldots\ldots\ldots\ldots 3.6$$

$$2NH_3(aq) + CO_2(g) \rightleftharpoons NH_4(H_2NCO_2)(s) \ldots\ldots\ldots\ldots\ldots\ldots 3.7$$

The flue gas reacts with the aqueous ammonia solvent to form ammonium bicarbonate ($(NH_4)HCO_3$), ammonium carbonate ($(NH_4)_2CO_3$), and ammonium carbamate ($NH_4(H_2NCO_2)$) salts. The reactions are reversible, so increasing the temperature and pressure in the regenerator system releases the CO_2 and recovers the chemical solvent for recycle. It is worth noting that all the reactions are exothermic with the exception of reaction 3.6. So while the other reactions need pumparound cooling system to control ammonia slip in the absorber, reaction 3.6 needs energy input in the stripper column for the solvent regeneration. A small amount of fresh ammonium carbonate is added to the lean solvent stream to replenish the lost ammonia from the system. The pure carbon dioxide stream is compressed to a pressure of about 103 bars and piped to storage. To minimise the slip of ammonia vapour from the system, the treated gas from the absorber column is directed to a water wash system that absorbs the ammonia vapour. The ammoniated water is then sent to the stripper column where the ammonia is stripped off and returned to the process as reagent. The CAP process used a refrigeration system to chill the process. The chilling removes heat from the direct contact coolers, the absorber recirculation streams and the water wash recirculation streams. The refrigerants employed mostly are ammonia and hydrofluorocarbons (www.alstom.com; Sherrick et al. 2008; Sherrick et al. 2009; Styring et al. 2014).

The American General Electric Energy Infrastructure Company, commonly known as GE Power, has currently developed a proprietary CAP process capable of attaining 90% carbon capture efficiency with over 99.9% purity. The developers claimed that this process can be applied to mitigate carbon from power plants that burn coal, natural gas, oil and biomass, as well as a vast array of industrial processes emitting carbon including urea production, methanol production, petroleum refineries, and soda ash production The process is equally designed for applications in the oxyfuel combustion carbon capture technologies and in membrane separation technologies (www.ge.com; Augustsson et al. 2017). The detailed description of this process is not covered in this report.

3.2.2 State of The Art Review of Alstom's CAP

Various Alstom's CAP trials have been completed in several different pilot-scale test runs in the USA, France, Poland, Germany, Sweden, Norway and Canada (Black et al. 2009). The initial pilot testing carried out at the We Energies facility, Wisconsin, was engineered, installed and operated as a co-operative effort between Alstom, Electric Power Research Institute (EPRI), We Energies Statoil Hydro and Stanford Research Institute (SRI) International. The facility was designed to capture 15 million tonnes per annum (1,600 kgCO_2/hr) of CO_2 from the We Energies' Pleasant Prairie 5 MW coal-fired power plant and was operated from June 2008 to October 2009 (for a total of 7,700 hours). The results from this project proved that the Alstom CAP process is capable of attaining 90% capture efficiency in a continuous commercial operation. The purity of the captured CO_2 was reported to be greater than 99.5%. The plant was able to run 66% through full-time run, and only minimal solvent degradation was observed with residual flue gas NH_3 slip less than 10 ppmv. The steam consumption of this test was reported to be 1.2 GJ per tonne of CO_2 captured. The total refrigeration energy requirement of the process was however not reported although the regenerator condensation duty was recorded as 0.0465 GJ per tonne of CO_2 captured (Black et al. 2009; Telikapalli et al. 2011; Darde et al. 2011; Kozak et al. 2009).

A similar US$ 15 million pilot-scale experiment was carried out in Southern Sweden by Alstom and E.ON to capture 15,000 tonnes/year of carbon emitted at the 5 MW E.ON's Karlshamn Oil/Gas-fired Power Plant. The plant was commissioned in April 2009 and was operated based on the Alstom CAP technology. Similar results to those obtained at the We Energies facility demonstration were realised. Additional improvements were also recorded. The major improvement was that this capture plant was able to run on anhydrous ammonia, which is much cheaper than aqueous ammonia, reducing the excess water introduced into the CAP process (Telikapalli et al. 2011).

A larger-scale carbon capture Product Validation Facility (PVF) was undertaken by Alstom, American Electric Power (AEP) and the Battelle Memorial Institute (BMI). This facility has a capture capacity of 100 million per year and was designed to remove carbon from AEP's 30 MW Mountaineer coal-fired power plant at New Haven, USA. The BMI was in charge of developing the geologic storage system for the captured CO_2. The facility began operation in September 2009 and started the dedicated

geological storage in October 2009. The facility employed two absorber systems which were able to operate at 75% capture efficiency. The ammonia slip from the system was reported to be less than 50 ppmv, and the moisture content in the captured CO_2 stream was less than 600 ppmv. The main achievement of this project demonstration is a satisfactory operation of a complete CCS using CAP technology. Although it was designed to perform at 75% capture efficiency, the process was able to attain 75-90% efficiency during the demonstration. The purity of the captured carbon stream was also reported to be higher than 99.9%. Approximately 50 million CO_2 per year was removed during the initial trials, and 37 million were injected into dedicated geological storage. The captured CO_2 stream was successfully compressed and piped to the Rose Run Sandstone storage system, approximately 2380 meters underground; and the Copper Ridge B-Zone storage system, approximately 2500 meters underground. (Telikapalli et al. 2011; Augustsson et al. 2017).

The world's largest PVF with carbon capture capacity of 104 million per year, was built at the Test Centre Mongstad (TCM), adjacent to the Statoil Refinery in Mongstad, Norway. The TCM is owned by Gassnova, Statoil, Shell, and Sasol. The plant was commissioned in October 2012 to employ Alstom's CAP technology to capture carbon dioxide from flue gas generated by a Fluid Catalytic Cracking Unit (FCCU) and the exhaust from a gas turbine-based combined heat and power plant (CHP). 82 million per year of CO_2 is captured from the FCCU and 22 million per year is removed from the exhaust of the CHP. The preliminary results from the demonstrations on this plant yielded a carbon capture efficiency of 75% to 87%, with purity greater than 99.9%. The ammonia emission from this plant was reported to be very low, approximately 2 ppmv, with minimal solvent degradation. At the end of the test campaign and operation in August 2014, the plant had performed successfully for more than 6000 hours. Approximately 39,500 tonnes of carbon were safely captured. The performance of this plant boosted confidence in Alstom's CAP technology for commercial carbon mitigation solutions (Lombardo et al. 2014; Augustsson et al. 2017).

3.2.3 Review of Other Research Findings for Ammonia-based Capture Technology

Many other research works have investigated the use of ammonia in the CCS technology. The majority of these works have investigated the energy analysis of this

technology, various optimisation strategies and the application of this process in the cement industry. Some of the latest findings from these research projects are reviewed in this section.

In a comparative review executed by Shakerian et al. 2015, the authors presented the advantages and disadvantages of ammonia and amines as sorption media for post-combustion carbon capture. Their findings concluded that the ammonia-based capture process requires lesser regeneration energy duty than amine-based capture processes. The authors also found out that increasing both amine and ammonia solvent concentrations increases the carbon capture efficiency. But in the case of the former solvent, corrosion of process equipment is the risk, whereas the high slip of solvent is the major issue with the latter. Another conclusion from this work was that amines turn to be more stable than ammonia as they can withstand higher temperatures. With regard to solvent degradation, the authors did mention that ammonia shows a lesser degradation rate than amines. This is because ammonia reacts reversibly with the sulphur oxides in the flue gas stream to yield ammonium sulphate, which can be used as fertiliser. Amines, however, react irreversibly with these oxides to produce heat stable salts that interfere with the absorption rate of the process. A blend of amines and ammonia also shows a higher capture efficiency than either of the single solvents (Shakerian et al. 2015).

Another profound study completed by Bak et al. 2015 in a lab-scale experiment investigated the effect of temperature variations on the system performance of CAP, using a 7 wt% aqueous ammonia solution. The authors varied the temperatures of the feed gas and lean solvent from 2 to 20 Celcius degrees. Their results showed that increasing the feed gas temperature slightly improves the absorption efficiency of the process. Increasing the lean solvent temperature however displayed a more profound effect on the absorption rate, causing a significant increase in the carbon capture efficiency. The ammonia slip was also found to increase with increasing temperature of either the feed gas or lean solvent. The authors obtained the best result for the system at a lean solvent temperature of 7 °C and feed gas temperature of 10 °C. At this absorber operation conditions, the authors reported carbon capture efficiency higher than 85% and minimised ammonia slip from the system (Bak et al. 2015).

In an equilibrium-based simulation, Zhang et al. 2017 analysed the regeneration energy requirement for ammonia-based capture technology. The authors also compared the performance of the equilibrium-based simulation to a rate-based simulation. Their conclusions revealed that increasing the stripper stage number from 5 to 20 caused the regeneration energy requirement to decrease from about 5.53 to about 5.35 MJ/kgCO_2. Any further increase of the stripper height and stage number beyond 20 was observed to have no significant effect on the regeneration energy usage. The rate-based studies, however, displayed no significant impact on the regeneration energy need. Increasing the solvent stream flowrate was also observed to increase the carbon capture efficiency in both the equilibrium and rate-based simulations. The average carbon capture efficiency in the rate-based model was however noticed to be lower than that obtained in the equilibrium-based model. The authors attributed this finding to the fact that the rate-based model considers the actual heat and mass transfer rates in the system, which is a lot more simplified in the equilibrium model (Zhang et al. 2017).

A more recent simulation research considering the energy analysis for ammonia-based capture in a power plant was conducted at the Chinese Hudian Electric Power Research Institute by Zheng et al. 2019. The capture plant which was modelled in Aspen Plus was designed for a 350 MW coal-fired power plant. The authors proposed a new capture technology which uses a reinforced crystallisation method to regenerate the chemical solvent rather than employing a stripper column as it is the case in a traditional process. The findings from this research showed that the new technology has a higher capture efficiency than the traditional method. The authors claimed that the regeneration energy requirement in the crystallisation process is only 42.6% of the requirements in a typical traditional stripping process (Zheng et al. 2019).

3.3 CARBON FOOTPRINT ASSOCIATED WITH NH_3 AND AMINES

As discussed above, amines and ammonia have received a wide range of attention as benchmarking solvents for the post-combustion carbon mitigation process in the energy sector. Several researchers have conducted experimental and simulation projects using these two solvents in attempts to improve upon the process performance. Nonetheless, it is important to understand the environmental sustainability issues associated with the use of these chemicals. One of the profound researchers who

considered the global sustainability issues regarding the use of these solvents is Luis Patricia. In her work entitled "Use of Monoethanolamine (MEA) for CO_2 capture in a global scenario: consequences and alternatives", Luis proved that emission of CO_2 is inherent in the production process of ammonia and amines. This is an important issue which has to be considered in the use of these chemicals on a large scale to decarbonise the energy sector. A critical review of this paper is presented in this section.

The synthesis of ammonia is by the reaction between hydrogen and nitrogen as shown in reaction 3.8 below:

$$3H_2 + N_2 \rightarrow 2NH_3 \ldots\ldots\ldots\ldots\ldots 3.8$$

The required nitrogen is obtained from atmospheric air while 80% of the hydrogen gas is produced from methane (CH_4) through the steam reforming process as shown in reaction 3.9. The remaining 20% is usually obtained from other fossil fuel feedstocks through partial oxidation reactions.

$$CH_4 + H_2O \rightarrow CO + 3H_2 \ldots\ldots\ldots\ldots\ldots 3.9$$

Since reaction 3.9 is highly endothermic, a high amount of energy is required in the primary reformer to achieve even a 60% conversion rate. Natural gas or other fossil fuel is usually combusted to obtain the huge amount of heat required for this process. After the reaction is completed the CO in the synthetic gas is converted to CO_2 and more H_2 in a water gas shift reaction as shown in reaction 3.10.

$$CO + H_2O \rightarrow CO_2 + H_2 \ldots\ldots\ldots\ldots\ldots 3.10$$

Prior to the secondary reforming process, which involves the reaction between hydrogen and nitrogen to yield the desired ammonia product, the large quantity of CO_2 in the system is removed using physical or chemical absorption technologies.

Looking at the complete cycle of the ammonia-based carbon capture technology in a bigger picture can lead to the conclusion that majority of the ammonia chemical solvent is only produced to capture the CO_2 by-product from the ammonia production process, and to capture the CO_2 produced during the fossil fuel combustion to generate enough heat for the primary reforming process in reaction 3.9. Hence, a complete cycle of the carbon capture process using ammonia only results in intensive energy consumption, which will only necessitate the burning of more fossil fuels. The economic and environmental sustainability of large-scale adoption of ammonia-based carbon capture is therefore very questionable. A more rigorous economic and

environmental impact assessment of this technology is therefore required before it is advanced into a large-scale commercialisation.

Amines are traditionally produced via a non-catalytic exothermic reaction between aqueous NH_3 and ethylene oxide (EO). In order to keep the NH_3 in the liquid state, the reaction is normally carried out at a pressure of 50 to 70 bars. To produce a primary amine; monoethanolamine (MEA), there must be more NH_3 reactants than EO to favour the reaction of one molecule of NH_3 with one molecule of EO. If NH_3 reacts with two molecules of EO, then a secondary amine diethanolamine (DEA) is produced. In an event that the NH_3 molecules react with the EO molecules in the ratio 1:3, then tertiary amine triethanolamine (TEA) is produced. Thus, to favour the production of MEA, it is advisable to have more NH_3 reactants in the system than EO reactants in order to ensure a 1:1 reaction since NH_3 can react with one, two or three molecules of EO. The excess NH_3 can then be stripped off after the reaction and the amines can be separated in a series in distillation units. An illustration of this process is shown in Figure 3.7.

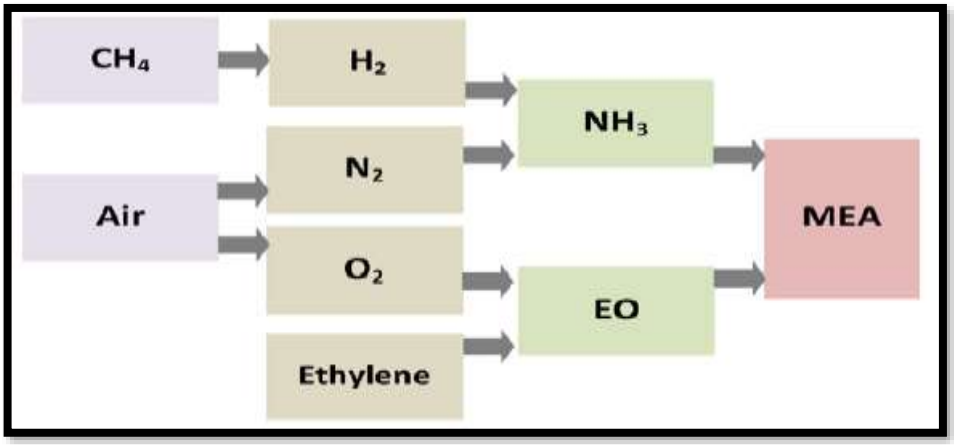

Figure 3.7. Schematic process flowsheet of MEA production (Luis 2016)

The ethylene oxide required for this reaction is produced by an oxidation reaction between ethylene (C_2H_4) and oxygen. The oxygen is usually obtained from atmospheric air. The partial oxidation process which occurs at about 15 bars and 250 °C, as shown in reaction 3.11, yields ethylene oxide (C_2H_4O). The total oxidation reaction presented in reaction 3.12, however, also occurs during the ethylene production process, resulting in the production of carbon dioxide and water.

$$C_2H_4 + \frac{1}{2}O_2 \rightarrow C_2H_4O \ldots\ldots\ldots\ldots\ldots\ldots\ldots 3.11$$

$$C_2H_4 + 3O_2 \rightarrow 2CO_2 + 2H_2O \ldots\ldots\ldots\ldots\ldots\ldots\ldots 3.12$$

Considering that MEA is manufactured from ammonia and ethylene oxide, the carbon footprint associated with the production of these chemicals is a matter of concern. As previously discussed in the case of ammonia-based carbon capture, a large-scale implementation of MEA based carbon capture also poses environmental concerns. There is, therefore, the need to comprehensively analyse the environmental impacts of MEA to ascertain is sustainability before its usage for carbon capture can be professed on commercial scale (Luis 2016). These facts necessitate the need to discover other chemical solvents that have less or no associated carbon footprints in their production and usage in a large-scale carbon capture technology. One of such sustainable solvents is potassium carbonate. A review of potassium carbonate-based capture technology is discussed in the next section.

3.4 K_2CO_3-BASED CAPTURE TECHNOLOGY

Owing to the carbon footprint, operational challenges, high volatility and high energy consumption associated with the use of amines and chilled ammonia in the post-combustion carbon capture system, recent research works have delved into the use of potassium carbonate (K_2CO_3) as an alternative solvent.

The potassium carbonate-based absorption method was first established in the 1950s by Benson and Field and was consequently called the Benfield Process (Benson et al. 1954). The capture of carbon dioxide in the Benfield process takes place at a high temperature of about 120 °C and pressure of 3000 kPag. This offers improved absorption efficiency due to the faster reaction rate and the high-pressure driving force. Moreover, due to the high operating temperature in the absorber column, it is not required to heat the solution further before the regeneration process, which results in a lower process energy consumption. Additionally, operations at this high temperature increase the solubility capacities of the bicarbonate species, and this enables the process to operate with highly concentrated carbonate solutions. A typical Benfield process that was developed by the Honeywell Universal Oil Products (UOP) is described below.

3.4.1 UOP Benfield™ Process (www.uop.com; www.apett.net; Echt 2013)

The Hot Potassium Carbonate (HPC) capture process was originally developed by Benson and Field at the United States' Bureau of Mines in the early 1950s as part of a programme to manufacture liquid fuels from coal.

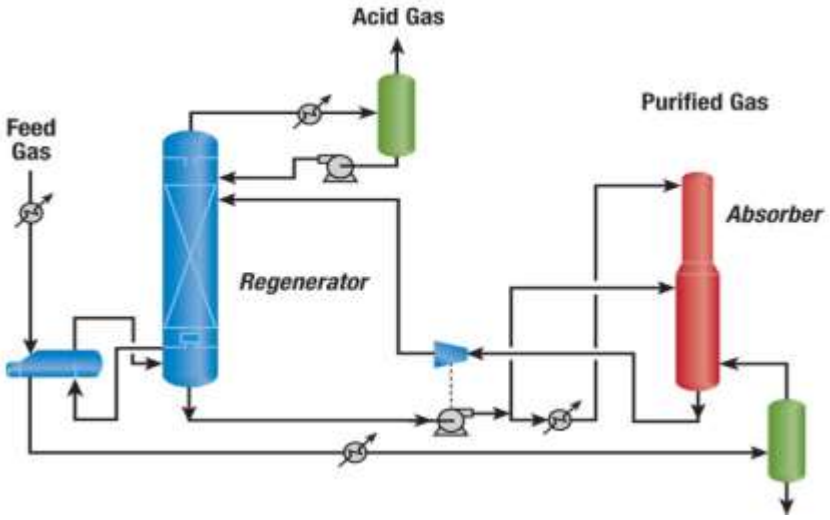

Figure 3.8. UOP Conventional Benfield Process

The process was subsequently modified by Universal Oil Products (UOP), Honeywell. The UOP HPC or Benfield Process is a thermally regenerated cyclical solvent process that uses an activated, inhibited HPC solution to mitigate CO_2, hydrogen sulphide (H_2S) and other acid gas contents of a gas stream. The flow scheme of a conventional UOP Benfield process is presented in Figure 3.8.

The system typically consists of a direct contact cooler (DCC), an absorber column and a regenerator column. The concentration of aqueous K_2CO_3 employed is usually 20–40 wt%. A 1–3 wt% of proprietary organic activator (ACT-1) is used to enhance the carbon capture efficiency and minimise energy consumption during the regeneration process. It also doubles as an antifoaming reagent. To combat corrosion in the process equipment, a 4–7 wt% vanadium pentoxide (V_2O_5) is used to inhibit corrosion and to control foaming as well. The overall absorption step entails chemical reactions between the HPC solution and CO_2 as shown in reaction equation 3.13. The feed gas is introduced at the bottom of the absorber column and flows countercurrent to the lean Benfield solvent which is introduced at the top section of the column.

$$K_2CO_3(aq) + H_2O(l) + CO_2(g) \rightleftharpoons 2KHCO_3(aq) \dots\dots\dots\dots\dots\dots 3.13$$

The reaction can easily be reversed in the regenerator column by a pressure swing desorption or temperature swing desorption. The H_2S contaminant in the feed gas stream is also absorbed as shown in the equation reaction 3.14.

$$K_2CO_3(aq) + H_2S(g) \rightleftharpoons K_2S(s) + H_2CO_3(aq) \ldots\ldots\ldots\ldots\ldots\ldots 3.14$$

Since the colourless potassium sulphide salt readily reacts with water to yield potassium hydrosulphide and potassium hydroxide, reaction 3.14 proceeds to reaction 3.15 as follows:

$$K_2S(s) + H_2O(aq) \rightleftharpoons KSH(s) + KOH(aq) \ldots\ldots\ldots\ldots\ldots\ldots 3.15$$

Since K_2CO_3 and $KHCO_3$ are strong electrolytes, they dissociate completely to yield cations of potassium and anions of carbonate and bicarbonate as shown in equations 3.16 and 3.17.

$$K_2CO_3(aq) \rightleftharpoons 2K^+ + {CO_3}^{2-} \ldots\ldots\ldots\ldots\ldots\ldots 3.16$$

$$KHCO_3(aq) \rightleftharpoons K^+ + {HCO_3}^- \ldots\ldots\ldots\ldots\ldots\ldots 3.17$$

So, in a practical potassium carbonate absorption process, the overall reaction of K_2CO_3 with CO_2 proceeds in the ionic medium as follows:

$${CO_3}^{2-}(aq) + H_2O(l) + CO_2(g) \rightleftharpoons 2{HCO_3}^-(aq) \ldots\ldots\ldots\ldots\ldots\ldots 3.18$$

But since there is no direct reaction between the carbonate ions and the CO_2 molecules, reaction 3.18 results through the following elementary mechanisms:

$${CO_3}^{2-}(aq) + H_2O(l) \rightleftharpoons OH^- + {HCO_3}^- \ldots\ldots\ldots\ldots\ldots\ldots 3.19$$

$$CO_2 + OH^- \rightleftharpoons {HCO_3}^- \ldots\ldots\ldots\ldots\ldots\ldots 3.20$$

There is also the possibility of hydrolysis reactions between water and CO_2 molecules to produce carbonic acid as shown in reaction 3.21.

$$H_2O(l) + CO_2(g) \rightleftharpoons H_2CO_3(aq) \ldots\ldots\ldots\ldots\ldots\ldots 3.21$$

This reaction, however, only proceeds in the acidic medium and requires the pH of the system to be lower than 8. But at pH greater than 8, which is typical of industrial processes (mostly carried out at pH range of 9 to 11), the reaction of CO_2 with hydroxyl ions in equation 3.20 dominates the HPC capture system and is termed as the rate-determining step. The slow nature of this reaction is what necessitates the addition of catalysts in the potassium carbonate-based capture process. It is, however, worth noting that the absorption of H_2S by the bicarbonate ions as shown in reaction 3.22, is much faster than the absorption of CO_2 in the HPC capture process.

$$H_2S + {HCO_3}^- \rightleftharpoons CO_2 + H_2O + HS^- \ldots\ldots\ldots\ldots\ldots\ldots 3.22$$

After the absorption reaction, the treated gas from the absorber column is vented into the atmosphere from the top while the CO_2 saturated solvent stream is channelled to the regenerator column to recover the chemical solvent. If the process operates at a low absorber temperature, then the rich CO_2 solvent stream is preheated before it is

introduced into the regenerator column. Otherwise, if the absorption is carried out in a hot potassium solution which is typical of the Benfield process, then the rich stream is directly introduced into the regenerator without preheating, and the solvent recovery is achieved by a pressure swing between the absorber and the regenerator. The recovered lean solvent stream is reused in the absorption process while the pure CO_2 stream is compressed for storage.

UOP has recently improved upon the conventional Benfield process and named it the UOP Benfield LoHeat™ technology as shown in Figure 3.9. The improved process has an added lean solution filtration system, a lean solution flash vessel, and a condensate reboiler system.

The lean solution filter is used to remove impurities from a split portion of the lean solvent stream before it is recycled into the absorber column. The lean solvent from the carbonate reboiler system and the heated condensate from the condensate reboiler system are flashed in the lean solution flash vessel to recover heat. The vapour recovered in the flashing process is recycled back into the regenerator column while the liquid recovered at the bottom of the flash vessel is pumped into the absorber.

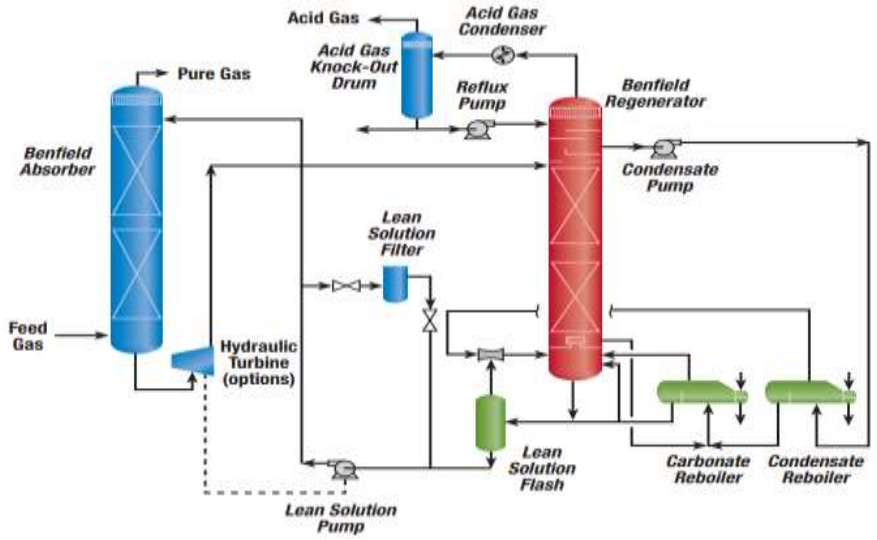

Figure 3.9. UOP Benfield LoHeat Process

UOP also claims that they have three revamp options which can be adopted in addition to the use of a high capacity proprietary column packing developed for them by Raschig, to significantly improve the overall performance of the Benfield process. In particular, the proprietary LoHeat technology was announced to attain energy savings of 15-40% over the conventional process (Furukawa et al. 1997; Benson et al. 1994; Staton 1985; www.uop.com; www.apett.net).

Currently, several variations of the potassium carbonate capture process exist including the Vetrocoke process (licensed by Davy McKee Corporation) which employs potassium carbonate promoted with glycine and arsenic trioxide; the Catacarb process (licensed by Eickmeyer and Associates) which uses 25 – 30 wt% potassium carbonate solution and undisclosed additives; the Lurgi process which uses 25 – 30 wt% potassium carbonate solution and proprietary additives; the Carsol process which uses potassium carbonate solution and other additives; and the Flexsorb HP process which uses amine promoted potassium carbonate solution (Luis 2016). These processes have been developed by competing companies that use proprietary chemicals to improve HPC-based capture technology.

3.4.2 State of The Art Review of HPC Capture Process

Many researchers have studied the solubility and reaction rate of carbon dioxide in un-promoted aqueous potassium carbonate solutions. The Australian Cooperative Research Centre for Greenhouse Gas Technologies (CO2CRC) has patented an alternative precipitating potassium carbonate process called the UNO MK 3. The CO2CRC's process is similar to the Benfield Process but operates at higher temperatures than 120 degrees Celsius. In order to test the performance of the process, a pilot plant facility was built and commissioned in 2012 at the Parkville campus of the University of Melbourne. In addition to testing the hydraulic aspects of the UNO MK 3, the plant results were also meant to be used in validating Aspen Plus simulation models. The capture plant was designed to remove 4-10 kg/hr of carbon from a 30-55 kg/hr of an air-CO_2 mixture, using different packing materials in the experimental columns. A range of solvent concentrations have been studied in several trials, ranging from 20 wt% to 30 wt%. Their results proved that the dynamic holdup of the system increases linearly with the liquid flow rate. The temperature profile and carbon loading in the rich solvent from the rate-based simulation was also found to compare very well with the experimental results. These results served as the validity of the project and provided fundamental data for further research by the team (Quyn et al. 2013). In the following pilot plant demonstration at the Hazelwood Coal-fired Power Station in Victoria, the same research team reported a solvent regeneration heat duty of 2–2.5 MJ/kgCO_2 for the UNO MK 3 process (Smith et al. 2013).

Using a stirred cell reactor and Danckwert Peter's theory for result interpretations, Ye et al. 2014 conducted a lab-scale experiment to study the kinetics of carbon absorption into uncatalysed K_2CO_3-$KHCO_3$ solutions. Their analysis was directed towards the effects of carbon loading and solution ionic strengths on the activation energy of the system. The range of lean solvent concentration used was 5 – 40 wt%, with varied levels of carbon loading for a 25 – 80 °C temperature range. The partial pressure of CO_2 in the feed gas was also controlled from 3.4 kPa to 50.2 kPa. Their conclusion identified that the activation energy of the system was highly affected by the CO_2 loading in the solution. Increasing the carbon loading was seen to cause a significant decline in the activation energy value. The ionic strength of the solution was however found not to have any significant effects on the activation energy (Ye et al. 2014).

In an earlier research completed by Harkin et al. 2012, the authors analysed the energy requirement for retrofitting a potassium carbonate-based carbon capture plant into an existing coal-fired power plant. The work was a simulation-based studies using Aspen Plus. The steam temperature used in this simulation was 162 °C, with a stripper pressure of 250 kPa. Their findings showed that a total electricity loss of 1.02 megajoules would be encountered in the power plant for every kg of CO_2 captured. An optimisation and heat integration was however proposed by the authors to minimise this energy penalty by 0.4 MJ/kgCO_2. This study also revealed that the regeneration energy requirement in a typical K_2CO_3-based post-combustion capture plant could be 5.3 MJ/kgCO_2. The findings of this study give a rough overview of the energy requirements for an HPC capture process (Harkin et al. 2012).

A later experimental study which was undertaken by Bohloul et al. 2017 examined the solubility of CO_2 in aqueous solutions of K_2CO_3. The authors used a pressure-decay method at different solvent concentrations of 15 wt%, 20 wt%, and 30 wt%. The temperature was also varied from 40 °C, to 50 °C and 60 °C, at different pressures up to 1.2 MPa. To anticipate the CO_2 solubility in the aqueous solvent solution, two equations of state were utilised. The Peng-Robinson equation of state (PR-EOS) was used for the fugacity coefficient in the vapour phase, and the Pitzer equation was used to present the activity coefficient in the liquid phase. The equilibrium time for the different solvent concentrations was observed to vary. For the 15 wt% lean solvent concentration, the system took about 110 minutes to reach equilibrium, while the time taken to attain equilibrium in the 20 wt% and 30 wt% concentrations were 130 minutes

and 170 minutes respectively. The authors linked the equilibrium time differences to the increasing absorption capacity which was associated with an increased solvent concentration. Another profound finding from this paper was that for all the different solvent concentrations at constant pressure, the solution loading was seen to decline with temperature rise. But when the temperature was held constant, the solution loading was seen to increase with pressure increase. When both the temperature and pressure were maintained, a rise in solvent concentration resulted in a rise in the solution loading. The results from this paper ascertain how CO_2 solubility in potassium carbonate capture technology depends on temperature, pressure and lean solvent concentration (Bohloul et al. 2017).

Adopting the Electrolyte Non-Random Two Liquid (ENRTL) thermodynamic model and various packing correlations, Wu et al. 2018 also undertook a modelling study of carbon capture in an HPC process using Aspen Plus Custom Modeller (ACM). The study involved an equilibrium modelling and a rate-based modelling for an absorber column for the purpose of parametric and sensitivity analyses. A major discovery made by the authors was that the rigorous rate-based simulation offered better predictions than the equilibrium simulation.

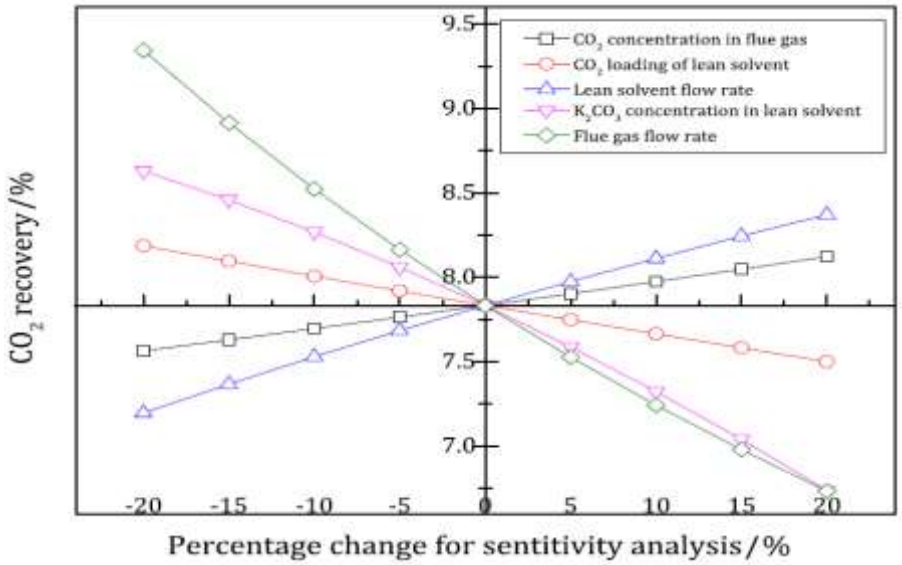

Figure 3.10. Results from parametric and sensitivity analyses in Wu et al. 2018

Also, the authors mentioned that the potassium carbonate concentration in the lean solvent and the inlet flue gas flowrate significantly impacted the CO_2 recovery level of the absorber system. A summary of the results from their sensitivity analysis is presented in Figure 3.10. As shown in the figure, the authors observed that an increase

in the lean solvent flowrate and CO_2 concentration in the flue gas improves the carbon recovery of the system. Increasing the flue gas flowrate, CO_2 loading of the lean solvent and the K_2CO_3 concentration in the lean solvent were noted to have a negative influence on the carbon recovery of the system (Wu et al. 2018). It is worth noting that the findings of this paper disagree with some other literature findings which proved that increasing the solvent concentration contributes to higher CO_2 recovery.

3.4.3 State of The Art Review of Promoted HPC Capture Process

Potassium carbonate has several advantages over amine solvents, the most important being that the absorption process can proceed at high temperatures leading to reduced parasitic load on the power plant. Additionally, K_2CO_3 is relatively cheaper, less corrosive, and less harmful to the environment. It is equally less prone to degradation properties that are usually encountered with amines at high temperatures in the presence of oxygen and other minor flue gas components. It also possesses an added advantage of demonstrating high stability and low volatility. The chemical solvent is equally easier to regenerate, leading to lower regeneration duty demand on the stripper reboiler (Borhani et al. 2015).

The absorption of carbon dioxide into aqueous potassium carbonate is however inhibited by the slow reaction of CO_2 in the liquid phase, causing low mass transfer rates (Ghosh et al. 2009). To improve upon this limiting reaction kinetics, several promoters have been researched for application in the potassium carbonate-based capture system. The key promoters that have been broadly considered for usage in the potassium carbonate-based capture system are amines (Behr et al. 2011), amino acids (Li et al. 2019) and boric acid (Ghosh et al. 2009; Guo et al. 2011).

When added to potassium carbonate solution, cyclic secondary amines such as piperazine, have shown good enhancement qualities in the overall reaction rate to a comparable level with an amine-based system, but with a heat of absorption up to about 50% lesser than that of the conventional MEA (Grimekis et al. 2019; Rochelle et al. 2002). Despite these positive promoting qualities of piperazine, its toxicity level, high volatility and side reactions with other gas components rendered it unsuitable for its application in the HPC process. Amino acids have also been reported to be highly sensitive to the pH of the reaction system (Hu et al. 2017).

Boric acid (H_3BO_3), deemed as a novel catalyst, has caught the attention of researchers for the past few years. Because of its relatively low cost and environmentally benign qualities, this new additive has been proven to be preferable over other promoters. That notwithstanding, it's promoting capabilities have been investigated to be well astounding. Adding 3 wt% boric acid to 30 wt% potassium carbonate solution has been reported to double the overall carbon dioxide absorption rate (Shen et al. 2014). In another study by Ahmadi et al. 2008, borate promoted potassium carbonate solution was observed to improve the carbon capture efficiency by nearly 40%.

The mechanism by which boric acid enhances the rate of carbon dioxide absorption is similar to the carbonic anhydrase mechanism in the human body. According to Guo et al. 2011, the tetrahydroxyborate ion ($B(OH)_4^-$) is the species which reacts with carbon dioxide to speed up the formation of bicarbonate according to the series of reactions described below:

$$B(OH)_3.H_2O \rightleftharpoons B(OH)_4^- + H^+ \ldots\ldots\ldots\ldots\ldots\ldots\ldots\ldots 3.23$$

$$B(OH)_4^- + CO_2 \rightleftharpoons B(OH)_4CO_2^- \ldots\ldots\ldots\ldots\ldots\ldots\ldots\ldots 3.24$$

$$B(OH)_4CO_2^- + H_2O \rightleftharpoons B(OH)_3.H_2O + HCO_3^- \ldots\ldots 3.25$$

The overall reaction is presented in equation 3.26 below:

$$CO_2 + H_2O \rightleftharpoons HCO_3^- + H^+ \ldots\ldots\ldots\ldots\ldots\ldots\ldots\ldots\ldots 3.26$$

Gosh et al. 2009 has performed a lab-scale analysis of carbon dioxide absorption in a wetted-wall column using un-promoted and boric acid promoted potassium carbonate, under conditions in which the reaction of carbon dioxide was of pseudo-first-order. The equilibrium partial pressure and the rate of carbon dioxide absorption were measured in 30wt% K_2CO_3 and 1-5wt% H_3BO_3 at 50-80 °C. He observed that the addition of minimal quantities of boric acid to potassium carbonate resulted in a substantial enhancement of carbon dioxide absorption rates. Hu et al. 2016 have also reviewed the various promoters that researchers have studied so far and concluded with the table of comparison in Table 3.1 (Hu et al. 2016).

It could be observed from Table 3.1 that the more stable, non-toxic, less volatile and less corrosive promoter with good promoting performance is boric acid. Despite this observation, it is obvious that no work has so far concretely reported the exergy performance of boric acid promoting the HPC capture process. This is required to

understand the energy needs of this blended solvent. This research gap is closed in the current study.

Table 3.1: Comparison of different inorganic promoters (Hu et al. 2016)

Promoter	Promoting performance	Toxicity	Stability	Volatility	Corrosivity	Pilot plant performance
Arsenic acid	Very good	Very poor	Very good	Very good	Good	Good
Boric acid	Good	Very good	Good	Very good	Good	Poor
Vanadate	Good	Good	Very poor	Very good	Very good	?
MEA	Very good	Good	Poor	Poor	Poor	Good
DEA	Very good	Good	Poor	Poor	Poor	Good
PZ	Very good	Good	Good	Good	Good	Good
Glycine	Very good	Very good	Poor	Very good	Poor	Good
Sarcosine	Very good	Very good	Good	Very good	?	?
Carbonic anhydrase	Very good	Very good	Very poor	Very good	?	?

3.5 PROCESS MODIFICATIONS

Several research works and reviews of process modifications are available in literature. Most of these works focus on amines (Ho et al. 2019; Hatmi et al. 2018; Sharma et al. 2015; Stec et al. 2017) and ammonia (Obek et al. 2019; Jiang et al. 2019), and have similar goals of improving system capture performance, and reducing overall energy consumption for the capture process. Some of these widely studied process modifications are discussed in this section.

3.5.1 Intercooled Absorber

As displayed in Figure 3.11, absorber intercooling is a widely researched modification (Hemmati et al. 2019). Since carbon dioxide absorption is an exothermic process, it results in temperature rise in the absorber column during a continuous process. This rise in temperature negatively impacts the thermodynamic driving forces for absorption, which leads to lower solvent absorption capacity. To reduce this negative impact, part of the liquid flow is withdrawn from the side of the absorber, cooled down in a heat exchanger and injected back into the absorber. This modification brings dual benefits to the capture process: it reduces the stripper duty by elevating the CO_2 carrying capacity of the solvent and reduces the absorber column height by

maintaining a similar carbon dioxide absorption capacity. For the same height of the absorber column, this modification offers improvements in the overall absorption capacity of the absorbent.

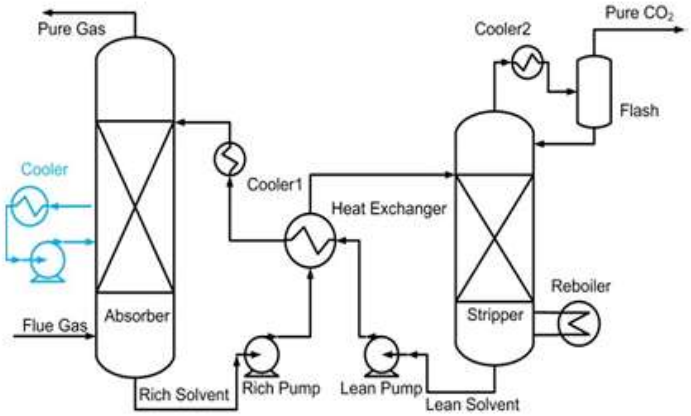

Figure 3.11. Intercooled absorber (Xue et al. 2017)

In a work done on the techno-economic assessment of the MEA process and its improvements, Li[b] et al. 2016 reported that the absorber intercooling is able to reduce regeneration duty from 3.6 to 3.55 MJ/kg CO_2. From the viewpoint of column size reduction, the authors reported that the packed height of the absorber decreased by 25% after applying the intercooling process. In a similar work performed by Xue et al. 2017, the authors observed that absorber intercooling is capable of reducing reboiler duty by 7.1% in the MEA process and by 2.8% in DEA based capture process.

3.5.2 Flue Gas Pre-cooling

The flue gas pre-cooling process is a simple modification investigated in the work of Le et al. 2014. As illustrated in Figure 3.12, the flue gas is cooled to a lower temperature before it is introduced into the absorber column. The principle of this modification is not much different from the intercooled absorber. Basically, it also works by lowering the temperature of vapour-liquid mixture in the absorber and improves carbon dioxide absorption in thermodynamic perspectives. This results in higher CO_2 rich solvent loading, and ultimately less reboiler duty. In a recent work done by Xue et al. 2017, it was observed that cooling the flue gas to about 30 °C is capable of reducing reboiler duty by 5% in MEA-based capture process and by 2% in DEA-based capture process (Xue et al. 2017).

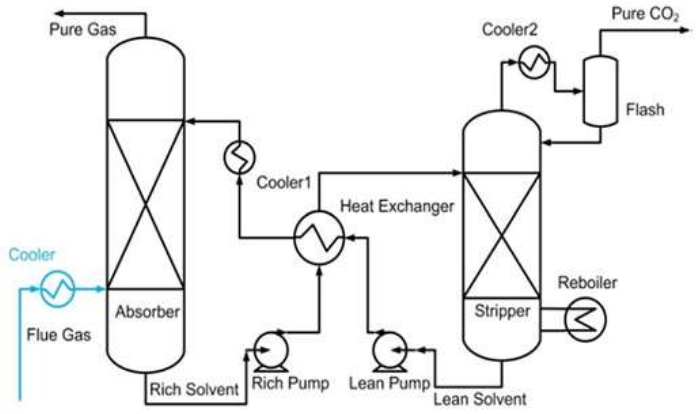

Figure 3.12. Flue Gas Pre-cooling (Xue et al. 2017)

3.5.3 Rich Solvent Splitting

This process modification dates back to the days of Eisenberg and Johnson in 1979 (Eisenberg et al. 1979). As shown in Figure 3.13, the cold rich solvent stream is split into two separate flow streams. One was injected directly into the top stage of the stripper without heating while the other is heated up in the lean/rich heat exchanger, and injected at the lower section of the stripper. The rich split modification is beneficial in two ways; it reduces reboiler duty and enhances the desorption efficiency of the stripper.

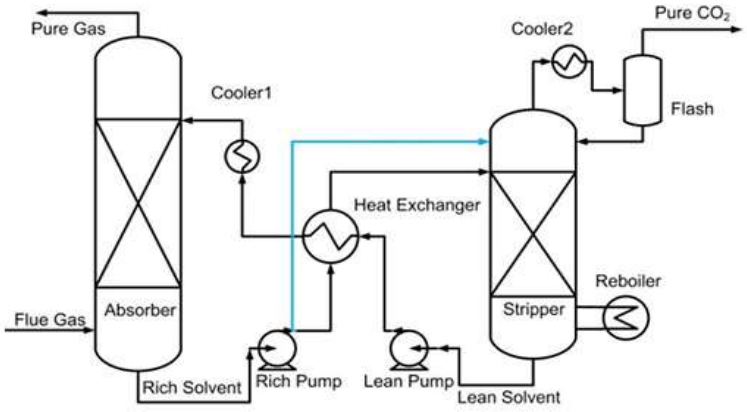

Figure 3.13. Rich Solvent Splitting (Xue et al. 2017)

The cold solvent injected at the top section of the stripper absorbs the would-have-been-wasted heat from the steam generated from the bottom section of the stripper, thereby reducing the reboiler heat duty of the stripper column. Meanwhile, the rich solvent vapour rising up in the stripper column contacts and strip off more carbon dioxide from the cold split dripping down from the top of the stripper column, leading

to an enhanced carbon dioxide capture efficiency. According to Xue et al. 2017, splitting 10% of the rich solvent could result in 7.7% reboiler heat duty savings in MEA-based capture process and 7% in DEA-based capture process. Li[b] et al, 2016 also investigated the effects of the rich solvent split for MEA-based capture process and observed a significant reboiler heat duty saving of 8.3% over the conventional process.

3.5.4 Rich Solvent Pre-heating

This modification was proposed in 1989 by Herrin (Herrin et al. 1989). As shown in Figure 3.14 the cold rich solvent is heated by the hot vapour effluent from the stripper, making use of the latent heat and simultaneously reducing the cooling water requirement in the stripper condenser. When Li[b] et al. 2016 combined this modification with a rich solvent split configuration, it was discovered to reduce reboiler heat duty by 10%.

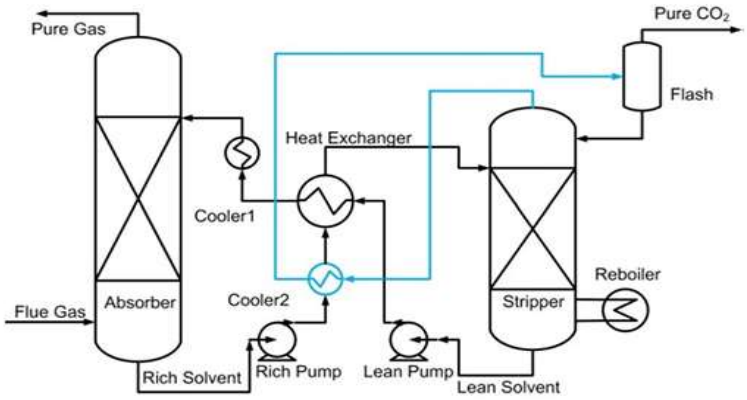

Figure 3.14. Rich Solvent Pre-heating (Xue et al. 2017)

3.5.5 Lean Vapour Compression

Another modified configuration for post-combustion carbon capture which has been widely suggested in literature is lean vapour compression. This configuration works by converting mechanical energy into thermal energy. As displayed in Figure 3.15, the principle is to flash the hot lean solvent at a lower pressure, compress the hot vapour generated and re-inject it into the bottom of the stripper. As the vapour gains from the sensible heat of the hot lean solvent as well as the recompression, it could reach a very

high temperature and pressure, which provides additional steam and heat in the stripping column for desorption.

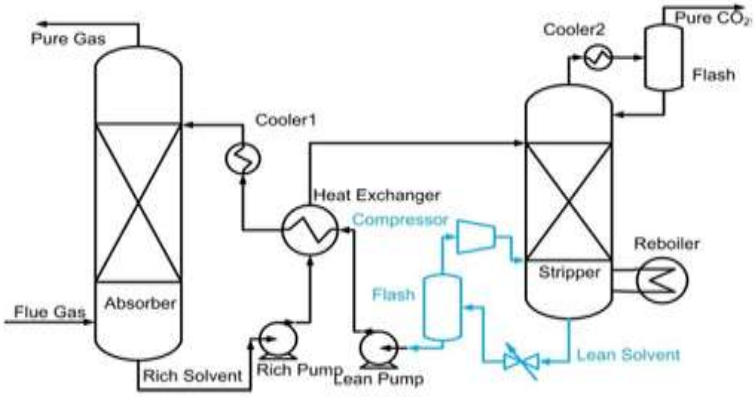

Figure 3.15. Lean Vapour Compression (Xue et al. 2017)

When this modification was applied in Reddy et al. 2009, the authors claimed 11% decrease in the reboiler steam requirement, 16% reduction in cooling water consumption, and 6% decrease in column diameter, where this resulted in 5% saving in the overall operating cost. In a work done by Xue et al. 2017, the hot lean solvent was flashed at atmospheric pressure with the adiabatic efficiency of the compressor set to 80%. The authors observed this modification shows good savings in reboiler duty; with MEA, 12.8% reduction was obtained over the conventional process, and 11.9% for DEA.

3.5.6 Inter-heated Stripper

Stripper inter-heating is equivalent to absorber inter-cooling in its configuration and operation principle. The idea, as shown in Figure 3.16, is to extract a portion of the solvent from one or two intermediate stages of the stripper, heat it up with flue gas and recycle it back to the stripper at a lower stage. This approach is believed to reduce the steam requirement and consequently reduces the reboiler heat duty of the stripper. Several researchers have reported the benefits of this novel configuration. When Mimura et al. 2006 applied this modification in their research work, steam consumption by the stripper column was observed to decrease by 39%. Kamijo et al. 2006 also investigated the benefits of this configuration and reported a 6.77% reduction in reboiler heat duty. Li[b] et al, 2016 equally reported reboiler heat duty reduction of 6.7% and 6.9 MW reduction in energy consumption by applying the stripper inter-heating configuration.

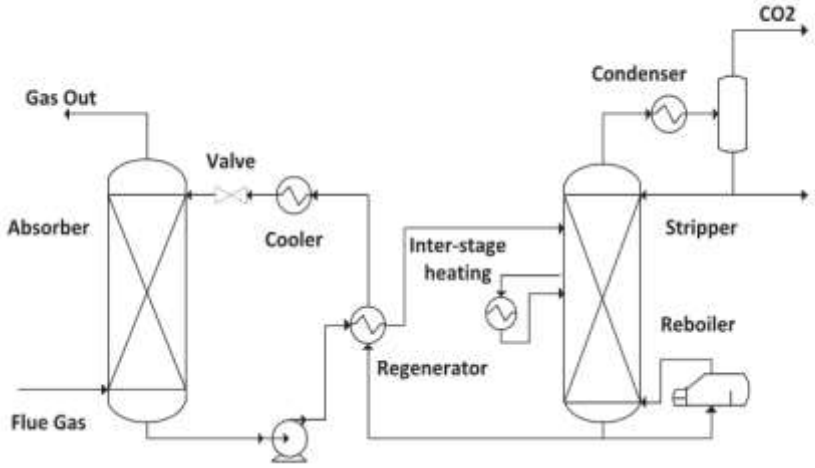

Figure 3.16. Stripper Inter-heating (Sharma et al. 2015)

3.5.7 Summary of Process configurations and Benefits

Several other research works in literature have extensively studied varying process configurations capable of improving the technical and economic performances of chemical absorption in the post-combustion capture process. Their discoveries are summarized in Table 3.2.

The discussions on process modifications and the information in Table 3.2 show that articles on modified process configurations for the hot potassium carbonate absorption process are rare in literature. Part of the objectives of this study, therefore, focuses on modified process configurations that are capable of improving upon the performance of the HPC post-combustion carbon capture process.

Table 3.2: Summary of intensified and modified processes and their techno-economic findings

Power plant	Solvent used	Process Modification	%CO_2 removal	Main findings	Ref
500 MW Coal-fired	30wt% MEA	Vapour recompression, multi pressure stripping and multi pressure stripping with vapour recompression	70, 90 and 95	Multi pressure stripping with vapour recompression performed better than the other process modifications	Jassim et al. 2006
-	30wt% MEA+ PZ	Multi pressure stripping and vacuum stripping	90	Vacuum stripping and 30wt% MEA + PZ solvent are the most favourable	Oyenekan et al. 2006
500 MW	K_2CO_3/PZ MEA/PZ MDEA/PZ	Matrix stripping, internal exchange stripper, multi pressure with split feed stripper and flashing feed stripper	90	The best energy saving of 22% obtained using matrix stripping and MDEA+ PZ	Oyenekan et al. 2007
Coal-fired	30 wt% MEA	Absorber intercooling; matrix stripper; two stripper	90	4-7% of savings in total power required; intercooling gave lowest CAC*	Schach et al. 2010
Coal-fired		Rich split, multi pressure stripping, vapour recompression and compressor integration		Vapour recompression is the best configuration	Karimi et al. 2011
600 MW Coal-fired	30 wt% MEA	Bi-pressure desorber with side compressor which maintains 280kPa and 190kPa at the rectification and stripping sections respectively	90	Reboiler duty reduced from 3.9 to 3.43 MJ/kg CO_2	Liang et al. 2011
Coal-fired	MEA	Solar power to supply energy for solvent regeneration (reboiler)	90	Not economically promising	Qadir et al. 2015
Gas-fired	32.5 wt% MEA	Increased column height from 20 to 30m, increased regenerator pressure from 185 to 210kPa	90	Reboiler duty reduced to 4.1 GJ/tonne CO_2	Canepa et al. 2015
555MW Gas-fired	30 wt% MEA	Recycling part of exhaust gas from the gas turbine to increase CO_2 concentration in flue gas, mixing a portion of condensate water from reboiler with the extracted steam to utilize the superheat degree of the extracted steam	90	By adequately utilising the surplus heat of the extracted steam, the total amount of the extracted steam for CO_2 capture can be reduced by 13.05kg/s, which means 0.93% improvement of the net efficiency	Hu[a] et al. 2017
Coal-fired	30 wt% MEA	High-pressure gasifier	90	Relative efficiency penalty associated with the deployment is 27%	Majoumerd et al. 2014
Gas-fired	30 wt% MEA	High-pressure gasifier	90	Relative efficiency penalty associated with the deployment is 16%	Majoumerd et al. 2014
Coal-fired	30 wt% MEA	Integrated Gasification Combined Cycle (IGCC)	90	Efficiency penalty associated with the deployment is 24%	Majoumerd et al. 2014
Natural gas-fired	29 wt% MEA	Incorporation of lean split with vapour compression	85	Lower energy cost compared to standard absorber-desorber system and system with vapour recompression only	Birkelund et al. 2013
Coal-fired	33 wt% NH_3	Vacuum Tube (VT) solar-assisted post-combustion CO_2 capture	90	Not economically promising	Liu et al. 2016
Coal-fired	33 wt% NH_3	Parabolic Trough Collector (PTC) solar-assisted post-combustion CO_2 capture	90	Not economically promising	Liu et al. 2016
650 MW Coal-fired	35 wt% MEA	Absorber inter-cooling, traditional rich split, modified rich split, stripper inter-heating and combined absorber inter-cooling, traditional rich split, and stripper inter-heating	85	Energy consumption reduced by 13.5% (combined approach)	Li[b] et al. 2016
650 MW Coal-fired	NH_3	Two-stage absorption, traditional rich-split, inter-heating stripper and combined traditional rich-split, inter-heating stripper	85	Energy consumption reduced by 20.2% (combined approach)	Li[a] et al. 2016
Gas-fired	30 wt% MEA	Exhaust gas recirculation	90	Lower energy consumption (not quantified)	Ali et al. 2016
Coal-fired	MEA	Vapour recompression	-	Energy-saving of 8.4%	Jeong et al. 2015
	MEA	Absorber inter-cooling, flue gas splitting, split stream/semi-lean solvent, multiple solvent feeds and combined approach (all)	90	Reductions of energy costs: 5.7% (multiple solvent feeds), 7.4% (flue-gas split), 4.3% (absorber inter-cooling), 3.7% (semi-lean) and 7.8% (combined approach)	Oh et al. 2016
	MEA	Absorber inter-cooling, flue gas pre-cooling, rich solvent split, rich solvent pre-heating, solvent split flow, rich solvent flashing, stripper condensate bypass, stripper condensate heating, lean vapour compression	90	The best four of energy savings (%): 4.61% (rich solvent split), 4.54% (solvent split flow), 4.20% (absorber inter-cooling) and 3.87% (lean vapour compression)	Xue et al. 2017
	DEA	Absorber inter-cooling, flue gas pre-cooling, rich solvent split, rich solvent pre-heating, solvent split flow, rich solvent flashing, stripper condensate bypass, stripper condensate heating, lean vapour compression	90	The best two of energy savings: 4.50% (solvent split flow) and 4.06% (rich solvent split)	Xue et al. 2017

*CAC – carbon avoidance cost.

3.6 DYNAMIC SIMULATIONS AND CONTROL STUDIES

Some researchers have studied the dynamic behaviour of the carbon capture plant and basic control strategies mostly for MEA-based processes. These studies are important to understand the smooth retrofitting strategies of the capture plant into the power plant, and to understand how stability could be achieved in both the capture plant and the power plant. Dynamic studies also reveal how changes in certain system parameters affect the overall power plant and capture plant performances. The behaviour of manipulated variables (MV), controlled variables (CV) and disturbances could also be understood. An understanding of the behaviour of these variables could help to design control strategies necessary to reject disturbances that could fatally impact the flexible and smooth operations of the capture plant. A critical review of some of the literature works that have considered the dynamic and control studies of CCS is presented in this section.

Harun et al. 2012 performed a simulation-based study for MEA absorption capture technique to predict the dynamic behaviour of the process. The resulting gPROMS and Aspen Plus dynamic models were used to understand the transient response of the MEA-based capture process to step changes in the stripper reboiler duty and sinusoidal oscillatory changes in the flue gas flowrate. The results indicated that the changes between the reboiler heat duty and the carbon capture efficiency obeys an approximate ratio of 1:1.4. The transient response of the system to sinusoidal changes in the flue gas flowrate is displayed in Figure 3.17. As shown in the figure, the carbon capture efficiency attained its minimum of 83% when the flue gas flowrate attained its maximum. When the flue gas flowrate reached its minimum value, the capture efficiency was observed to achieve its maximum level of 99%. The authors observed that the lean solvent loading plays a major role in the performance of the capture process. It was also noted that although it is possible to attain higher capture efficiency by increasing the stripper reboiler duty, the act will result in increased operating costs and reduced plant efficiency.

The authors, therefore, recommended that an optimisation analysis is necessary to ascertain the optimal conditions that can result in minimum cost of operation and maximum carbon removal. The results from this study set the foundation for the design of a control system for an amine-based capture process (Harun et al. 2012).

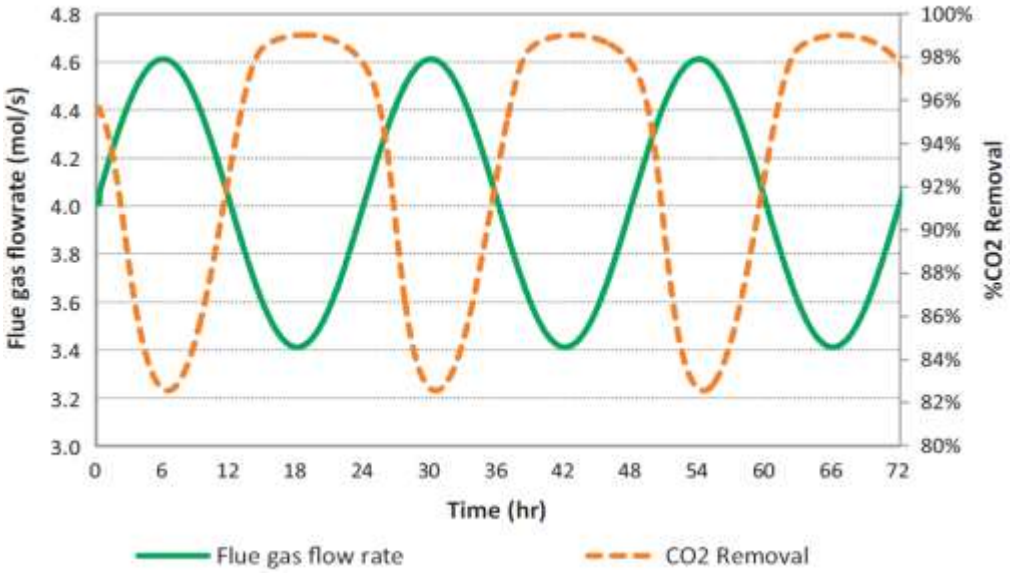

Figure 3.17. CO_2 removal response to sinusoidal changes in flue gas flowrate (Harun et al. 2012)

In another early work carried out by Lawal et al. 2012, the authors demonstrated a commercial scale post-combustion MEA-based carbon capture for a 500 MWe coal-fired power plant through dynamic modelling and simulation using gPROMS modeller. Their studies focused on two dynamic cases. The first considers power plant output reduction and the second looked at increasing capture level set point from 90% to 95%. Figure 3.18 shows the controllers for the design process.

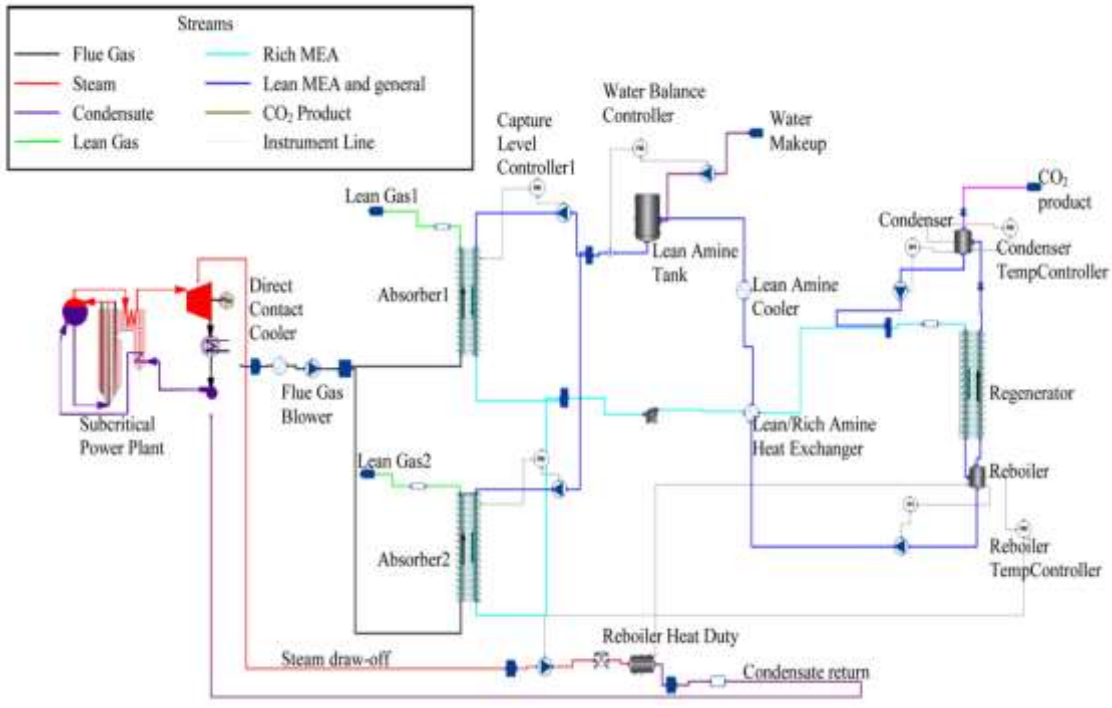

Figure 3.18. Plant-wide control system topology (Lawal et al. 2012)

To study the effect of decreasing the power plant target electricity output on the capture plant, the plant output capacity was lowered from 440 MW to 415 MW over a period of 10 minutes. To achieve this power output drop, the fuel flowrate fed to the combustion chamber was reduced. The capture plant efficiency was held constant at 90% and the base case simulation was run for 4 hours before the disturbance was introduced. Afterward, the simulation was run for 10 hours before the results were analysed. The authors observed that a reduction in the fuel burn rate, in turn, reduced the flue gas produced from the power plant. Hence, less solvent was required to attain a fixed capture efficiency of 90%. There was also a corresponding decrease in the regeneration energy requirement and the steam draw off demand from the power plant as well. The authors, however, observed that the power plant response to the change in fuel flowrate was much faster than the capture plant response to the change in the feed gas to the absorber. This means that the time taken for the power plant to reduce its electricity generation from 440 MW to 415 MW was much shorter than the time taken for the amine capture plant to reduce the lean solvent flowrate and subsequently the steam flowrate fed to the regenerator reboiler system. This proves that the process dynamics of the amine capture plant was relatively slow when compared to the process dynamics of the power plant.

In the second dynamic study case where the capture plant efficiency was increased from 90% to 95%, the power plant base case target power output was maintained. The authors observed that an increase in the capture efficiency of the amine capture plant forced the power plant electricity production to drop by roughly 1.8%. There was also an increasing demand for the fuel flowrate, which oscillated to 34% higher than the base case value before finally settling at 16%. Considering that the capture efficiency was only increased by 5%, the corresponding increase in the fuel flowrate could be said to be high. The authors concluded that the decrease in the power plant output efficiency and the increase in the fuel burn rate were as a result of the higher demand of steam from the power plant to attain the new capture efficiency. It is therefore evident from this study that attaining a 100% capture efficiency could result in a dramatic reduction in the electricity out efficiency of the power plant and cause an enormous upsurge in the fuel requirement of the power plant (Lawal et al. 2012).

A dynamic modelling and control studies recently completed in gCCS modeller by Sharifzadeh et al. 2019, using a single-input single-output (SISO) proportional-

integral-derivative (PID) controllers, examines sensitivity analyses that impact the controllability and operability of an MEA-based capture plant integrated into a natural gas combined cycle plant and pulverised coal power plants.

Table 3.3 presents a summary of the pairing for controlled variables (CV) and manipulated variables MV) and the control objectives of this study. The results from this study show that the flowrate of the steam supplied to the desorber system is a critical MV since it controls the reboiler temperature and the reboiler duty while propagating disturbance to the power plant at the same time. This implies that stabilising this variable is very necessary to stabilise the overall integrated process. The observations from the study concluded that the power plant tends to demonstrate a prolonged stabilisation if it experiences a sharp load reduction as a result of the capture plant integration. On the other hand, if the load reduction is slow, the dynamics of the capture plant tends to be faster than the power plant, enabling the two systems to integrate seamlessly. Although similar observations were made for the gas-fired process and the coal-fired process, the analysis conducted for the coal-fired process in this regard shows a significant overshoot, requiring detuning of the controllers.

Table 3.3: Summary of control structure selection and pairing between controlled variables (CVs) and manipulated variables (MVs) (Sharifzadeh et al. 2019).

Controlled variable	Manipulated variable	Inventory controlled
Absorber pressure	Flowrate of flue gas	Absorber vapour
Absorber sump liquid level	Flowrate of rich solvent	Absorber liquid
Desorber pressure	Flowrate of CO_2 captured	Desorber vapour
Desorber sump liquid level	Flowrate of lean solvent leaving desorber	Desorber liquid
Condenser separator liquid level	Flowrate of liquid leaving condenser separator	Condenser separator liquid
Reboiler liquid level	Flowrate of liquid leaving reboiler	Reboiler liquid
Reboiler pressure	Flowrate of vapour leaving reboiler	Reboiler vapour
Water content of lean solvent stream	Flowrate of water make-up stream	Water in solvent cycle
MEA concentration	Flowrate of water make-up stream	MEA in solvent cycle
Carbon capture rate	Flowrate of lean solvent	Quality of captured CO_2
Reboiler temperature	Flowrate of steam to reboiler	CO_2 desorption rate
Lean solvent temperature	Flowrate of cooling water to lean solvent cooler	CO_2 absorption rate

This observation was attributed to the higher CO_2 content of the coal-fired flue gas, which imposes higher loads on the solvent regeneration process. The authors further indicated that extreme scenarios such as 50% load reduction in a quarter of an hour represent abnormal operations which may require emergency partial shutdown. Hence, they recommended that such scenarios should be avoided since it could induce thermal shocks and other technical difficulties in the process.

Included in the same research, the authors proposed that a good strategy of keeping the power plant process and the capture process in stable conditions is to reduce the carbon capture efficiency in instances that the power load is high. Their analysis however recognised that a sharp reduction of the capture efficiency from 90% to 45% within 15 minutes could cause the capture process to be unstable for a minimum of 2 hours 12.6 minutes. They, therefore, suggested that although the capture setpoint tracking is a feasible operational strategy, it needs to be carried out in a slow manner in order to decouple it from the dynamics of the capture process.

The effects of solvent concentrations and stripper reboiler temperature were however found not to have a significant impact on the dynamics of flexible operation. Nonetheless, the control of stripper reboiler temperature was discovered to be a bit complex as it did not only depend on the steam flowrate, but also on stripper pressure, solvent concentration and CO_2 loading (Sharifzadeh et al. 2019).

In a more comprehensive simulation study done by Wu et al. 2019, the authors explored the dynamic behaviour and disturbance rejection predictive control for a 30 wt% MEA-based post-combustion carbon capture technology. The simulations were completed in gCCS™ and MATLAB™. The studies focused on the dynamic impacts of carbon capture rate change, flue gas flowrate change, and reboiler temperature change.

To examine the dynamic behaviour of the capture process for different capture efficiencies, step response tests were carried out at 50%, 60%, 70%, 80%, 90% and 95% capture levels. While doing this, the flue gas flowrate was held constant at 0.13 kg/s and the reboiler temperature was maintained at 386 K. To control the capture efficiency, step signals in magnitude of +5% of the steady-state values were gradually added to the lean solvent flowrate at time interval 1000 seconds. At the initial stages of the step changes, it was observed that the capture level promptly increased in

response to the lean solvent rise. However, as the reboiler steam flowrate remained constant, the reboiler temperature gradually decreased, resulting in decreasing the regeneration rate and ultimately lowering of the carbon capture level to the new steady state. The authors, however, noted that the capture system took more than 10,000 seconds to attain the new steady-state value. The dynamic response of the system was also observed to be similar for capture levels of 50% to 90%. When the capture level attained 90% to 95%, the authors observed that the peak value of the step response dropped as it becomes more difficult to capture more CO_2 from the flue gas. Nonetheless, there was a corresponding decrease in the steady-state gains of the step responses, and the response speed demonstrated some increases as the capture level increases. The reboiler temperature was also observed to respond faster to the lean solvent disturbances than the carbon capture rate.

To understand the dynamic behaviour of the capture process under varied flue gas flowrates, step response tests were executed at flue gas flowrates of 0.07, 0.10, 0.13 and 0.15 kg/s. For these simulations, the stripper reboiler temperature was kept at 386 K and the carbon capture level was maintained at an initial value of 80%. The authors observed that a rise in flue gas flowrate cause a quick rise in capture level. This is because increasing the flue gas flowrate increases the CO_2 content in the absorber system, which influences a higher mass transfer rate, yielding higher loadings in the rich solvent and resulting in a higher capture rate. The influence of the flue gas flowrate changes on the reboiler temperature was however found to be negligible.

To study the dynamic behaviour of the capture plant under various reboiler temperature, the authors carried out step response tests at stripper reboiler temperatures of 383 K, 384 K, 385 K, 386 K, 387 K and 388 K. The flue gas flowrate and the carbon capture level were maintained at initial values of 0.13 kg/s and 80% respectively. To control the reboiler temperature, the steam flowrate fed to the reboiler was increased gradually. The observations showed that increasing the reboiler temperature resulted in higher carbon capture efficiency, especially within the temperature ranges of 385 K to 387 K. It was therefore concluded that the optimum reboiler temperature is 386 K.

The slow dynamic response of the capture system and the multi-variable coupling effect of the process led the authors to design a model predictive control system for the amine-based capture process, as shown in Figure 3.19. To adapt the MPC more

accurately to the dynamic behaviour of the capture process, the authors proposed a disturbance rejection predictive controller (DRPC) which was composed of a steady-state target calculator, a quasi-infinite horizon MPC and an extended state observer.

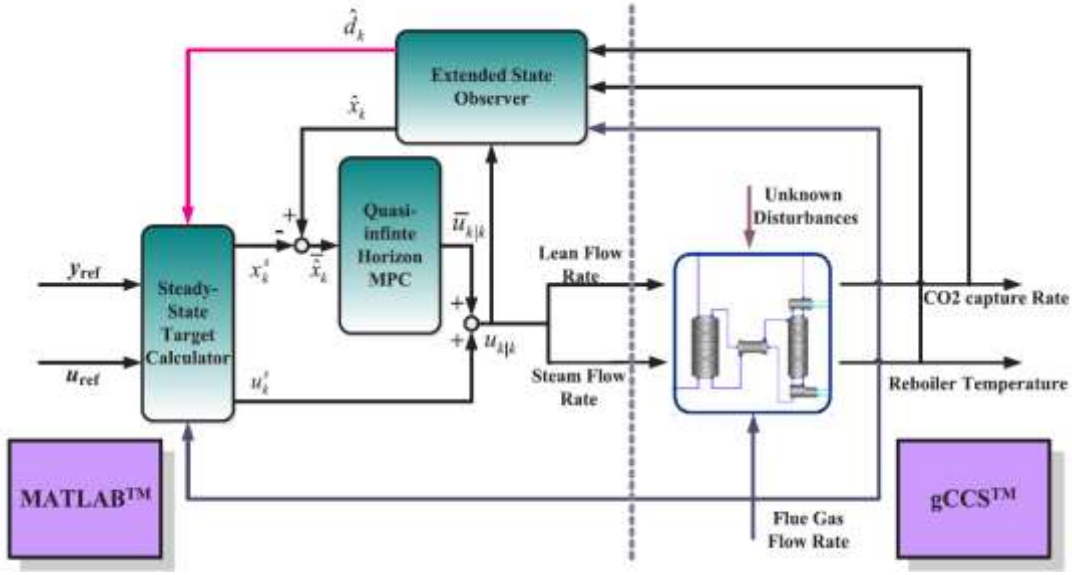

Figure 3.19. Schematic diagram of the DRPC proposed by Wu et al. 2019.

According to the authors, the proposed DRPC is able to quickly adapt to changes in the flue gas flowrate, eradicate the effect of varied behaviours of the plant when unknown disturbances occur, and accomplish a wide range of capture level variations using small prediction steps (Wu et al. 2019).

Recently, in West Virginia University, Chinen et al. 2019 performed a dynamic modelling and validated with a pilot plant data for an MEA-based capture unit. The dynamic simulation was completed in Aspen Plus and the results were validated with pilot plant data from the National Carbon Capture Centre in Wilsonville, Alabama. The dynamic response of the capture unit was studied for changes in the steam flowrate, flue gas flowrate, and the lean solvent flowrate. A transient study was also carried out to evaluate the process time constant and gain for similar changes in the above parameters. Changes in the flue gas flowrate are considered disturbances in this study, whereas changes in the steam flowrate and lean solvent flowrate are taken as manipulated variables.

Their results showed that the carbon capture level follows the same direction of the step changes in the lean solvent flowrate and the steam flowrate. It, however, follows the reverse direction to the changes in the flue gas flowrate. The complete results of their transient studies are summarised in Figure 3.20 and Table 3.4. The results show

that the time constants and the process gains demonstrate considerable changes based on the direction of the disturbance introduced. This indicates nonlinearities in the dynamic behaviour of the capture process.

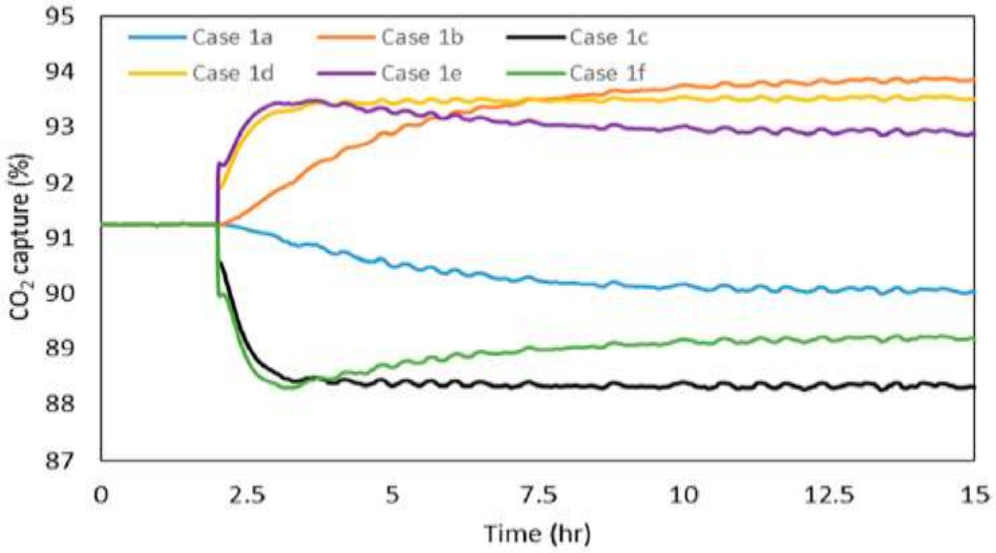

Figure 3.20. Results from transient studies in Chinen et al. 2019

Table 3.4: Time constants and gains obtained for transient studies (Chinen et al. 2019)

Case	Gain	τ_p (min)	Description
Case 1a	0.24	179	Absorber-stripper configuration under a +5% steam flowrate
Case 1b	0.52	164	Absorber-stripper configuration under a -5% steam flowrate
Case 1c	-0.45	19	Absorber-stripper configuration under a +5% flue gas flowrate
Case 1d	-0.59	16	Absorber-stripper configuration under a -5% flue gas flowrate
Case 1e	0.41	19	Absorber-stripper configuration under a +5% lean solvent flowrate
Case 1f	0.33	16	Absorber-stripper configuration under a -5% lean solvent flowrate
+5% solvent	0.49	17	Absorber-only configuration under a +5% lean solvent flowrate
-5% solvent	0.65	18	Absorber-only configuration under a -5% lean solvent flowrate
+5% flue gas	-0.57	15	Absorber-only configuration under a +5% flue gas flowrate
-5% flue gas	-0.43	17	Absorber-only configuration under a -5% flue gas flowrate
+5% steam	0.20	167	Stripper-only configuration under a +5% steam flowrate
-5% steam	0.24	178	Stripper-only configuration under a -5% steam flowrate

Some other research works which have conducted dynamic simulation and control analysis for amine-based capture processes are presented in Table 3.5.

Table 3.5: Summary of dynamic modelling and control studies in the literature

Power Plant	Solvent used	Capture system units	%CO_2 removal	Control System Type	Ref
550 MW Coal-fired	MEA	Traditional absorber and advanced flash stripper	90	Closed-loop Cascade Control system	Walters[a] et al. 2016
Coal-fired	MEA	Traditional absorber-stripper system	75-90	MIMO Feedback PID control system	Manaf et al. 2016
Coal-fired	PZ	Intercooled absorber column and standard stripper	90	Combined feedback and feedforward control system	Walters[b] et al. 2016
Coal-fired	MEA	Traditional absorber-stripper system	90	PID control	Gaspar et al. 2015
750 MW Coal-fired	MEA	Traditional absorber-stripper system	87	PID control	Nittaya et al. 2014
779 MW Coal-fired	MEA	Traditional absorber-stripper system		PID control	Mechleri et al. 2017

Based on the reviews on process dynamic studies and control system analyses discussed above, it is obvious that no research work has yet considered dynamic simulation and control analysis of the HPC capture process. In order to advance this novel technology into a full-scale commercial level for applications in post-combustion capture, it is necessary to study the dynamic behaviour of the HPC process and investigate control strategies for the said process. The dynamic simulation and preliminary control analyses for unpromoted and H_3BO_3 assisted K_2CO_3-based post-combustion capture process are completed in this study.

3.7 SUMMARY OF CHAPTER 3

In this chapter, amine scrubbing, CAP and HPC-based capture technologies are described in detail. State-of-the-art review of the literature information regarding the application of these technologies are thoroughly discussed. Some of the major findings regarding energy usage, carbon capture rates, and drawbacks of MEA-based and NH_3-based capture processes are also covered in this chapter. The carbon footprint associated with the application of these two processes is reviewed to further understand why K_2CO_3 is relatively considered the sustainable solvent for carbon capture. Current literature data on the HPC-based capture technologies are reviewed to demonstrate the potentials of this solvent in post-combustion carbon capture applications. It is also proven in this chapter that modified process modifications, dynamic simulations and

process control analyses for the HPC capture method have not been found in the literature. This highlights some of the major research gaps tackled in this study and delineates the significance and novelties of this thesis.

CHAPTER 4

SIMULATION MODEL DESCRIPTION AND BASE CASE CAPTURE PROCESSES

This work is fully simulation-based and no experimental works were carried out. The software packages involved in the simulations are Aspen Plus® V10, MATLAB R2017b and Loop-Pro Trainer 5. The simulation models are divided into four main categories: equilibrium-based modelling, rate-based modelling, dynamic modelling and control system design. The equilibrium-based, rate-based and dynamic models were designed and simulated in Aspen Plus, while MATLAB and Loop-Pro were engaged in the control system design. This section describes thoroughly how the various models were designed and their applications in the post-combustion capture systems involving MEA, PZ promoted MEA, K_2CO_3 and H_3BO_3 promoted K_2CO_3. Although the focus of this work is to complete simulations for the K_2CO_3 and H_3BO_3 promoted K_2CO_3 capture processes, there was the need to simulate the MEA-based capture system for the basis of comparison. The comparison mainly includes the carbon capture efficiencies and the total energy requirements for solvent regeneration, cooling in stripper condenser and heating in heat exchangers. But since most of the literature works do not include information on the heating and cooling requirements, especially the energy usage in the cross heat exchanger and stripper condenser for the MEA capture process, it was decided to complete the simulation for this benchmarking solvent as well in order to execute a more comprehensive comparison between the performances of the two solvents. Details about mass and energy balance calculations are discussed in the Appendix.

4.1 EQUILIBRIUM-BASED MODELLING

The equilibrium-based modelling approach in Aspen Plus assumes that the liquid phase and the vapour phase in the system are well mixed on each stage of the absorber and stripper columns, implying that equilibrium is attained in the bulk phases of the mixtures. Despite the simplicity of this model approach and inaccurate assumptions, as real systems usually do not attain equilibrium between the liquid and vapour phases, this steady-state model is required for the dynamic simulations.

The equilibrium-based model was executed in a steady-state input mode for the K_2CO_3 and H_3BO_3 promoted K_2CO_3, for which dynamic simulation was later carried out. The model was applied to a traditional absorber/stripper system in an open loop. The RadFrac separator in the column section of the model palettes was used to model the absorber and stripper. Since the simulation calculation type was set to equilibrium, no specifications for the column internals were required in this approach. No kinetic equations were required as well, but the necessary equilibrium and salt dissociation equations and constants, presented in Chapter 5 were inputted under the chemistry properties. The base property employed is the electrolyte non-random two-liquid (ELECNRTL) thermodynamic property method, with the electrolyte calculations option for the simulation approach set to true components rather than apparent components. This is the property model adopted to represent the carbon capture system in most of the literature works reviewed. The activity coefficient basis for Henry components was set to mixed-solvent which is based on the infinite dilution activity coefficient of Henry component in the actual solvent mixture present in the system. No condenser and reboiler were used for the absorber system but in the stripper system, partial condenser with vapour distillate only, and kettle reboiler were applied.

4.2 RATE-BASED MODELLING

The majority of the steady-state modelling was accomplished in the rate-based simulation. This is required to predict the performance of the capture system more accurately. All the steady-state simulations for MEA, PZ promoted MEA, K_2CO_3 and H_3BO_3 promoted K_2CO_3 were completed using the rate-based simulation approach. As an added feature to the equilibrium-based modelling, the absorber/stripper system for the rate-based model was designed in a closed-loop, using pumps, heat exchangers, splitters and mixers where necessary. Kinetic equations and constants were also applied for the rate-based model. The details of these parameters for the different chemical solvents are presented in the chapters that follow.

Several correlations for heat and mass transfer, interfacial areas and liquid holdup are also required in the rate-based modelling. Except otherwise stated, the mixed flow model on intermediate feed stages were adopted along with Bravo-Fair82 and Bravo-Fair85 mass transfer correlations. The same correlation methods were also used to calculate the interfacial area for the columns. The correlation method used to calculate

the heat transfer coefficients for all the systems was the Chilton and Colburn analogy. The film non-ideality correction was applied to both the liquid and vapour phases. The film resistance in the vapour phase was also considered, with the resistance in the liquid phase discretised into 5 points for the MEA system, and 10 points for a more accurate design in the K_2CO_3 system. The liquid holdup was calculated using the Bravo-Fair92 correlation for the MEA system, while the Billet-93 correlation method was applied in the K_2CO_3 system. The Wallis correlation was also involved in calculating the pressure drop in the systems. To design the column internals, relevant literature data was used. The details of these parameters including the packing types and column heights are discussed in chapters 4 and 5 for the different chemical solvents. Structured packing in all the models was left at the default corrugation angle of 60° and the default value of 1 °K minimum temperature approach for the lean/rich solvent cross heat exchanger was adopted for the MEA system. No cross heat exchanger was used in the K_2CO_3 system since the absorption process was carried out at a higher temperature and the rich solvent stream required no preheating before regeneration.

4.3 DYNAMIC MODELLING

As part of the novel studies of this project, dynamic simulations were completed for K_2CO_3 and H_3BO_3 promoted K_2CO_3 systems to understand the transient behaviour of these processes. Changes in various process parameters were examined to evaluate how they affect the carbon capture efficiency and the regeneration energy requirement of the system over time. The data obtained from the dynamic modelling were used in the design of proportional integral and derivative (PID) control systems in Loop-Pro Trainer 5 and MATLAB for the promoted and unpromoted HPC processes.

The equilibrium-based modelling was used to perform the dynamic modelling for the K_2CO_3 and H_3BO_3 promoted K_2CO_3 since the dynamic modelling platform in Aspen Plus does not support the rate-based simulation. To convert the equilibrium-based modelling into a dynamic model, the input mode for the simulation setup was changed from steady-state mode to dynamic mode. Once this change was executed, the model required detail sizing of the reflux drums and sump for the absorber and stripper columns. According to William et al. 2010, the sizing of the reflux drums at the top of the columns and the sump at the base provides liquid surge capacity, and aids in

filtering disturbances in both the flow and compositions to downstream units. As an added benefit, accurate sizing of these units also allows the column to withstand large process disturbances without upsetting the column to the level where flooding and weeping are encountered. The hydraulics information for the columns are also required. The system also requires pressure controllers in the form of valves, pumps, and compressors on the feed streams and effluent streams. The sizing for the various column features were computed using the formulae and heuristics in William et al. 2010. To control the pressure in all inlet and outlet streams, control valves were used.

To size the reflux drums and the sumps, information on the total liquid entering or leaving these units are required since distillation control heuristic requires that these surge volumes should be large enough to provide 5 minutes of liquid holdup when half-filled. The required liquid flowrates were obtained in the hydraulic section of the column profile results after running the equilibrium-based simulation in a steady-state model. The following equation was then used to compute the appropriate design parameters. During this calculation, it was assumed that the reflux drums and sumps have aspen ratio of 2, implying the length (L) is twice as long as the diameter.

$$Length\ (L) \Big/ Diameter\ (D) = 2 \ldots\ldots\ldots\ldots\ldots\ldots\ldots 4.1$$

$$\frac{\pi D^3}{2} = Total\ Volumetric\ Flowrate \ldots\ldots\ldots\ldots\ldots\ldots\ldots 4.2$$

Once the total volumetric liquid flowrates entering or exiting the units were obtained in profile results for the columns, the required diameters for the reflux drums and the sumps were computed using equation 4.2. The length (which is referred to as height in the Aspen Plus model) is then computed using equation 4.1. After all the equipment was sized and pressure controllers were successfully added, the model was exported to the Aspen Plus Dynamic platform. This dynamic model was then used to generate data on the control variables and manipulated variables which were required for the control system design.

4.4 CONTROL SYSTEM DESIGN

A first-order linear control system design was accomplished in MATLAB Simulink and Loop-Pro Trainer 5 for K_2CO_3 and H_3BO_3 promoted K_2CO_3 processes. The dynamic data obtained from Aspen Plus Dynamics simulations were used to generate

the gain (K_p), time constant (τ_p) and dead time (θ_p) in Loop-Pro Trainer 5 using the First Order Plus Dead Time (FOPDT) model. The Laplace equation for the FOPDT model is shown in equation 4.3.

$G_p(s) = \frac{Y_{(s)}}{U_{(s)}} = \frac{K_p e^{-\theta_p s}}{1+\tau_p s}$ ……..4.3 , where Y is the measured process variable, U is the controller output, K_p is the steady-state process gain, θ_p apparent dead time, and τ_p is the process time constant. Equation 4.3 can be written in the time domain as shown in Equation 4.4 below:

$\tau_p \frac{dy(t)}{dt} + y(t) = K_p u(t - \theta_p)$ ……..4.4, where t refers to time.

The values obtained for these process parameters were used to design single input single output (SISO) and multiple-input multiple-output (MIMO) step response control systems in MATLAB Simulink. The carbon capture efficiency and the stripper reboiler temperature were set as the control variables (CV), while the lean solvent flowrate and stripper reboiler duty were set as the manipulated variables (MV). The CO_2 concentration in the flue gas, the flue gas flowrate, the lean solvent concentration and the concentration of boric acid were used as disturbances. The relative gain array (RGA) analyses were performed in MATLAB to determine the appropriate pairing of the control variables and the manipulated variables. Additionally, the selections were confirmed to be at par with information in the dynamic and control works performed by Gaspar 2016 and Zhang 2016. The controllers used were proportional integral derivative (PID) controllers.

4.5 PID CONTROL SYSTEM

The proportional integral derivative controllers are most widely used in industrial control applications. The time-domain representation of the PID controller is shown in Equation 4.5.

$$u(t) = K_p e(t) + K_I \int_0^t e(t)dt + K_D \frac{de(t)}{dt} \text{ ……..4.5}$$

where t is time, u is control variable, e is error value, K_p is a coefficient of the proportional term, K_I is a coefficient of the integral term and K_D is the coefficient of the derivative term. Where the proportional term ($K_p e(t)$) gives an output value in

proportion to the current error value, the integral term ($K_I \int_0^t e(t)dt$) produces an output value in proportion to the current error and the accumulated errors from the past. Using information from the current rate of changes, the derivative term ($K_D \frac{de(t)}{dt}$) functions as a predictor of the future error. This generic feedback control loop mechanism functions well to yield satisfactory results without the need for a process model. In this study, PID controllers are employed in tuning the HPC capture processes.

4.6 DESIGN ASSUMPTIONS, CONSTRAINTS AND SIMULATION OBJECTIVES FOR BASE CASE MODELLING

The major design assumptions, constraints and simulation objectives for the base case MEA-based and K_2CO_3-based capture systems are outlined below:

4.6.1 Design Assumptions

1. The bulk gas and liquid phases in the absorber and stripper columns were assumed to be well-mixed.
2. For the above assumption to hold, the fluid flow is considered turbulent.
3. The pressure drop in the two columns was assumed to be linear.
4. Heat losses from the capture plant to the surrounding is negligible.

The above assumptions are consistent with literature information in Decardi-Nelson et al. 2018 and Harun et al. 2012.

4.6.2 Design Constraints

1. The CO_2 loading of the MEA rich solution was constrained to a maximum of 0.4 by mole to closely resemble the condition in commercial settings (Warudkar et al. 2013).
2. In the K_2CO_3-based capture process, the absorber was constrained to operate at 109–215 ^oC and 10–20 bar to boost the formation of $K_2CO_3.1.5H_2O$ crystals, which are believed to account for the energy-efficient performance of the hot potassium carbonate-based process (Zhao et al. 2013; Kothandaraman 2010).
3. At least 85% carbon capture efficiency must be attained in the MEA-based capture system to demonstrate the high CO_2 absorption efficiency of MEA.

4. The minimum and maximum decarbonisation efficiencies of the hot K_2CO_3-based capture system were set to 76.5% and 93.5% respectively to limit their deviations from the reference data to 10%.

4.6.3 Simulation Objectives

1. To validate base case post-combustion carbon capture technology using MEA and hot K_2CO_3 as absorbents.
2. To establish the average total duty requirements for amine-based and HPC-based capture processes.
3. To demonstrate parametric analyses in the HPC-based capture system, as basis for optimisation.
4. To model an optimised carbon removal process for a hot potassium carbonate-based capture technology.

4.7 MEA-BASED CAPTURE PROCESS

As mentioned in the previous chapters, chemical absorption using monoethanolamine (MEA) is by far the most researched post-combustion carbon capture technology. For the purpose of comparing the total energy requirement of this process to that of the potassium carbonate process, this study considered the amine-based absorption process as the base case scenario. Various simulations for this chemical solvent were performed and validated against literature data. This chapter covers the research methodology for MEA-based post-combustion carbon capture technology. The research methodology, which entails information about the methods and materials involved in the simulation model development, is subdivided into the model reactions used, relations for equilibrium and kinetic constants, model flowsheet and model design. The validation of research findings, modified process simulations and related discussions on this technology are also presented in this section.

4.8 MEA-BASED MODEL DEVELOPMENT

The CSIRO in 2010 collaborated with Tarong Energy, currently known as the Stanwell Corporation Limited, to construct an amine-based post-combustion carbon capture pilot plant in Australia. This capture plant is attached to the black coal-fired Tarong

Power Station sited near Kingaroy, southern Queensland. The pilot plant which is designed to operate at approximately 100 kg/h CO_2 capture rate using aqueous MEA runs on real flue gas (containing 10-14% CO_2, 4-8% H_2O, 72-76% N_2, ~6% O_2) from the Tarong Power Station (Cousins[a] et al. 2011; Cousins[b] et al. 2011). This same flue gas condition and the experimental results from the aforementioned pilot plant and the works of Li[b] et al. 2016 and Li[c] et al. 2016 were adopted as the reference case for the current study.

The electrolyte non-random two-liquid (ELECNRTL) property method for liquid and Redlich-Kwong (RK) equation of state for vapour, the most widely used property methods for chemical absorption carbon capture simulations (Plus[a] et al. 2008; Nagakaki et al. 2017; Li et al. 2014; Razi et al. 2013), were used in a rigorous rate-based model in Aspen Plus V10 for the MEA-CO_2-H_2O system. The following reaction equations, equilibrium constants (Keq) and kinetic constants (r) were included in the model development:

4.8.1 Model Reaction Equations (Plus[a] et al. 2008)

The following equilibrium and kinetic reactions were included in the model development, as adapted from Plus[a] et al. 2008.

1. Equilibrium	$2H_2O \rightleftharpoons H_3O^+ + OH^-$
2. Equilibrium	$CO_2 + 2H_2O \rightleftharpoons H_3O^+ + HCO_3^-$
3. Equilibrium	$HCO_3^- + H_2O \rightleftharpoons H_3O^+ + CO_3^{2-}$
4. Equilibrium	$MEAH^+ + H_2O \rightleftharpoons MEA + H_3O^+$
5. Equilibrium	$MEACOO^- + H_2O \rightleftharpoons MEA + HCO_3^-$
6. Kinetic	$CO_2 + OH^- \rightarrow HCO_3^-$
7. Kinetic	$HCO_3^- \rightarrow CO_2 + OH^-$
8. Kinetic	$MEA + H_2O + CO_2 \rightarrow MEACOO^- + H_3O^+$
9. Kinetic	$MEACOO^- + H_3O^+ \rightarrow MEA + H_2O + CO_2$

4.8.2 Relations for Equilibrium and Kinetic Constants (Plus[a] et al. 2008)

The equilibrium constants for reactions 1-5 were determined using the Aspen Plus built-in equation:

$In(Keq) = A + \frac{B}{T} + C * In(T) + D * T$, where A, B, C and D are temperature-dependent coefficients and T is the temperature in Kelvin units.

The kinetic constants for reactions 6-9 were obtained using the Aspen Plus built-in reduced power-law expression: $r = k\exp\left(-\frac{E}{RT}\right)$, where k is a pre-exponential factor, E is activation energy, R is universal gas constant and T is temperature in Kelvin units.

Table 4.1: Equilibrium constants for MEA-CO_2-H_2O system (Plus[a] et al. 2008; Li et al. 2014; Razi et al. 2013)

Reaction No.	A	B	C	D
1	132.899	-13445.9	0	-22.4773
2	231.465	-12092.1	-36.7816	0
3	216.049	-12431.7	-35.4819	0
4	-3.038325	-7008.357	0	-0.00313489
5	-0.52135	-2545.53	0	0

Table 4.2: Kinetic constants for MEA-CO_2-H_2O system (Plus[a] et al. 2008; Li et al. 2014; Razi et al. 2013)

Reaction No.	k	E (cal/mol)
6	4.32×10^{13}	13249
7	2.38×10^{17}	29451
8	9.77×10^{10}	9855.8
9	3.23×10^{19}	15655

4.8.3 Model Flowsheet

Figure 4.1 shows the flowsheet used in the model simulation. The flue gas (FLUEGAS) which was fed at the bottom stage (stage 20) of the packed absorber column (ABSORBER, operating at atmospheric condition) at 597.8 kg/h, 57.9 ^oC and 1 atm, was contacted with the lean aqueous MEA solution (LEANIN) with ~28.5 wt% concentration, which was fed at the top stage (stage 1) of the column, at the rate of 23.3 L/min, 39.5 ^oC and 1 atm. The lean gas (LEANGAS) after absorption is released into the atmosphere at the top of the absorber column while the rich-solvent (RICHOUT1) from the bottom of the column is pumped through the cross heat exchanger (HX) into the packed stripper column (STRIPPER, operating at 1.7 atm). The CO_2 product stream (CO2PROD) is condensed and compressed for storage whereas the lean-solvent regenerated (LEANOUT) is recycled through HX to heat up

RICHOUT2. For convergence purposes, a portion of the recycle stream is purged in the SPLITTER in other to control the rate of lean-solvent entering the MIXER. The fresh H2O-MEA serves as the makeup block to replenish the lost water and MEA in the system.

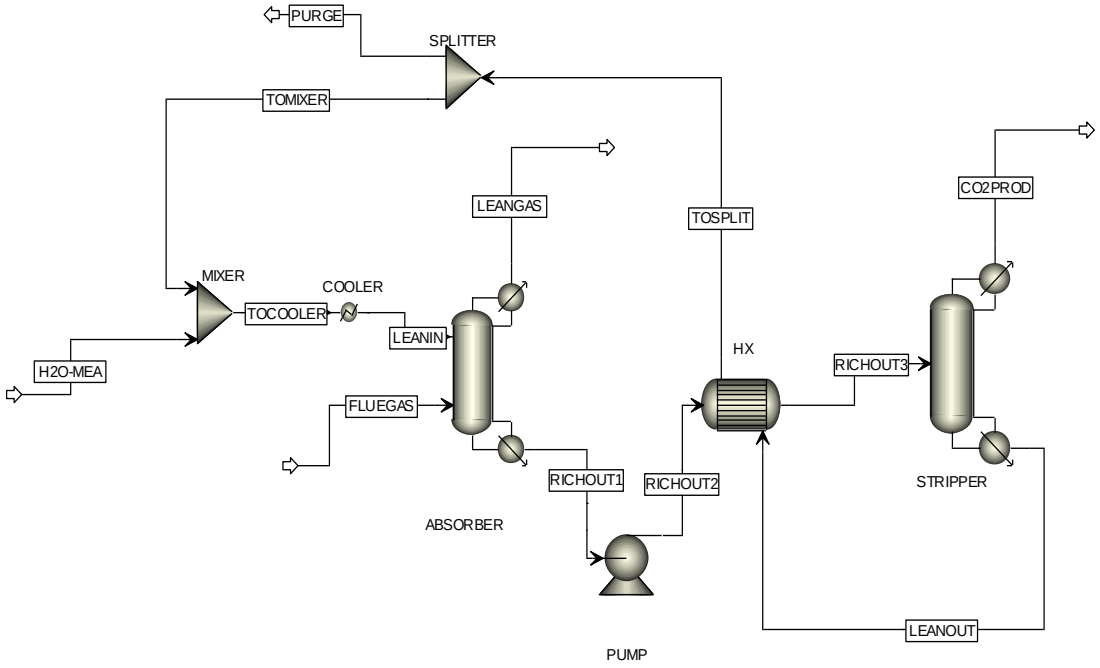

Figure 4.1. Steady-State Model flowsheet for MEA simulation

4.8.4 Model Design

The absorber and stripper columns were designed in detail using the RadFrac column model with the following specifications as obtained from Li[c] et al. 2016:

Table 4.3. RadFrac Specifications for MEA-CO_2-H_2O system (Li[c] et al. 2016)

RadFrac Properties	Absorber	Stripper
Number of stages	20	20
Packing material	Mellapak M250X	Mellapak M350X
Total packed height	7.136m	7.168m
Column diameter	0.35m	0.25m
Flow model	Mixed model	Mixed model
Interfacial area factor	1.8	1.8
Initial liquid hold up	0.03 L	0.03 L
Film resistance	Discrxn for liquid; Film for vapour	Discrxn for liquid; Film for vapour
Discretization points for liquid film	5	5

4.8.5 Model Validation

The converged base case simulation results from this study were validated against the experimental and simulation records in Li[c] et al. 2016.

Table 4.4. Validation of Results for MEA-CO_2-H_2O system

Design specifications	Values
Inlet flue gas flowrate, kg/h	597.8
Inlet flue gas CO_2, vol%	11.1
Lean flowrate, L/min	27.0
Lean MEA conc., wt%	28.5

Base case performance	Current Study	Experiment (Li[c] et al. 2016)	Deviation (%)	Simulation (Li[c] et al. 2016)	Deviation (%)
CO_2 capture level, %	85.96	85.0 ± 1.4	1.1	80.9	6.3
CO_2 product purity, vol%	99.99	99.5	0.5	99.0	1
Reboiler temp, ^oC	121.2	121.6 ± 0.2	0.3	122.3	0.9
Reboiler duty, MJ/kgCO_2	3.98	4.11	3.16	4.22	5.69
Condenser duty, MJ/kgCO_2	0.815	-	-	-	-
Cooling duty, MJ/kgCO_2	1.495	-	-	-	-
Heat Exchanger duty, MJ/kgCO_2	2.32	-	-	-	-
Total duty, MJ/kgCO_2	8.61	-	-	-	-

As presented in Table 4.4, the results from the base case simulation are closely agreeable with the experimental and simulation results from Li[c] et al. 2016. The inlet flue gas flowrate, lean flowrate, lean MEA concentration by weight, and CO_2 concentration were the same as that of Li[c] et al 2016. The current work predicted a slightly higher carbon capture efficiency (6.3%) over the simulation data from the reference paper but in very close agreement with the results from the experimental data. The reboiler temperature and CO_2 product purity are also seen to compare closely with the literature data, with a maximum deviation of 1%, which was recorded as an improvement in the product purity of the current study over the reference simulation result. Reboiler duty savings of 3.16% and 5.69% were, however, observed over the experimental and simulation data respectively. This improvement is a result of the optimisation applied to the stripper reflux ratio. Preliminary studies showed that decreasing the stripper reflux ratio is capable of reducing the reboiler duty at the

expense of capture level and product purity. An optimisation analysis was therefore performed to find the optimum reflux ratio in the current study.

4.9 K_2CO_3-BASED CAPTURE PROCESS

This chapter covers the rate-based Aspen Plus simulation for 40 wt% aqueous K_2CO_3 and boric acid promoted K_2CO_3 carbon capture process for a 1600 MW coal-fired power plant. The CO_2 capture capacity of the plant is roughly 7,000 tonnes (7680 US tons) per annum (about 795 kg/hr). Various parametric studies were performed for the unpromoted and promoted systems to examine the sensitivity of the system performance to changes in some key system parameters. In the subsections that follow, the details of the simulation model development, validation of results, modified process configurations and associated discussions are presented.

4.10 K_2CO_3-BASED MODEL DEVELOPMENT

Post-combustion carbon capture with K_2CO_3 solvent was demonstrated in the works of Mumford et al. 2011. The flue gas used in the pilot plant trials was obtained from a 1600 MW brown-coal-fired power station located at the International Power's Hazelwood power station in Victoria's Latrobe Valley, Australia. The pilot plant, which was built to capture up to 25 tons/day of CO_2 (expandable to 50 tons/day of CO_2), was originally designed based on a proprietary solvent, BASF PuraTreat F. The plant was however operated using 30 wt% K_2CO_3 to demonstrate its performance in a post-combustion CO_2 capture process. Although the pilot plant trials only yielded CO_2 absorption of about 20-25% from the flue gas when using K_2CO_3, valuable operating data were collected, which enabled process modelling and simulations to be compared to real plant data. The flue gas composition as obtained from the Hazelwood power station, the pilot plant and simulation details for the flue gas flowrate and lean solvent flowrate as used in Mumford et al. 2011 were adopted in the current study. The conditions of the flue gas, lean solvent conditions and the design of absorber and stripper internals were taken from the works of Kothandaraman 2010. The operating conditions of the absorber and stripper columns were also obtained from the same source. This decision followed on from some important discoveries made from reviewing the work of Zhao et al. 2013. The authors of this publication mentioned that the formation of sesquihydrate potassium carbonate crystal ($K_2CO_3.1.5H_2O$) in the

K_2CO_3 carbon capture system is the possible reason for low energy consumption in the regenerator. The lower enthalpy of reaction between this crystal and CO_2 molecules and the heat released during its breakdown in the stripper is believed to significantly reduce the reboiler duty. The formation of this crystal, however, occurs only when the absorber is operated at high pressure (10–20 bar) and high temperature (109–215 ^oC). These conditions were not met in Mumford et al. 2011 and could possibly contribute to the high energy consumption and less carbon capture efficiency in the pilot plant. Since these conditions were met in the works of Kothandaraman 2010, it was decided to adopt the operating conditions from this work in the design of the base case K_2CO_3 capture system for the current study. 40 wt% aqueous K_2CO_3 was used in the lean solvent stream, which is at par with the concentration employed in the same publication.

The electrolyte non-random two-liquid (ELECNRTL) thermodynamic property method for liquid and Redlich-Kwong (RK) equation of state for vapour, which are the most widely used property methods for chemical absorption carbon capture simulations, were used in a rigorous rate-based model in Aspen Plus® V10 for the K_2CO_3-CO_2-H_2O system. The reaction equations, equilibrium constants (Keq), kinetic constants (r), model flowsheet and column designs are elaborated on in the following subsections.

4.10.1 Model Reaction Equations (Plus[c] et al. 2008)

The following equilibrium, dissociation and kinetic reaction equations (1-8) were included in the K_2CO_3 simulation model development, as adapted from Plus[c] et al. 2008.

1. Equilibrium: $CO_2 + 2H_2O \rightleftharpoons H_3O^+ + HCO_3^-$
2. Equilibrium: $HCO_3^- + H_2O \rightleftharpoons H_3O^+ + CO_3^{2-}$
3. Equilibrium: $2H_2O \rightleftharpoons H_3O^+ + OH^-$
4. Dissociation: $KOH \rightarrow K^+ + OH^-$
5. Dissociation: $K_2CO_3 \rightarrow 2K^+ + CO_3^{2-}$
6. Dissociation: $KHCO_3 \rightarrow K^+ + HCO_3^-$
7. Kinetic: $CO_2 + OH^- \rightarrow HCO_3^-$
8. Kinetic: $HCO_3^- \rightarrow CO_2 + OH^-$

4.10.2 Relations for Equilibrium and Kinetic Constants (Plus[c] et al. 2008)

The equilibrium constants for reactions 1-3 were determined using the Aspen Plus built-in equation:

$In(Keq) = A + \frac{B}{T} + C * In(T) + D * T$, where A, B, C and D are temperature-dependent coefficients and T is the temperature in Kelvin units.

The kinetic constants for reactions 7 and 8 were obtained using the Aspen Plus built-in reduced power-law expression: $r = k\exp\left(-\frac{E}{RT}\right)$, where k is a pre-exponential factor, E is activation energy, R is universal gas constant and T is the temperature in Kelvin units.

Table 4.5: Equilibrium constants for K_2CO_3-CO_2-H_2O system (Plus[c] et al. 2008; Wu et al. 2018)

Reaction No.	A	B	C	D
1	231.465	-12092.1	-36.7816	0
2	216.05	-12431.7	-35.4819	0
3	132.899	-13445.9	-22.4773	0

Table 4.6: Kinetic constants for K_2CO_3-CO_2-H_2O system (Plus[c] et al. 2008; Wu et al. 2018)

Reaction No.	k	E (cal/mol)
6	4.32×10^{13}	13249
7	2.38×10^{17}	29451

4.10.3 Model Flowsheet

Figure 4.2 shows a schematic flowsheet for the simulation model. The flue gas (FLUEGAS, 110 °C, 15 atm) which was fed at the bottom stage (stage 12) of the packed absorber column (ABSORBER, operating at 15 atm), was contacted with the lean aqueous K_2CO_3 solution (LEANIN, 80 °C, 15 atm) with ~40 wt% concentration, which was fed at the top stage (stage 1) of the column, at the rate of 8250 kg/hr (11,170 kg/hr with makeup), 80 °C and 15 atm. The lean gas (CLEANGAS) after absorption is released into the atmosphere at the top of the absorber column while the rich-solvent (RICHIN) from the bottom of the column is fed to stage 2 of the packed stripper column (STRIPPER, operating at atmospheric condition).

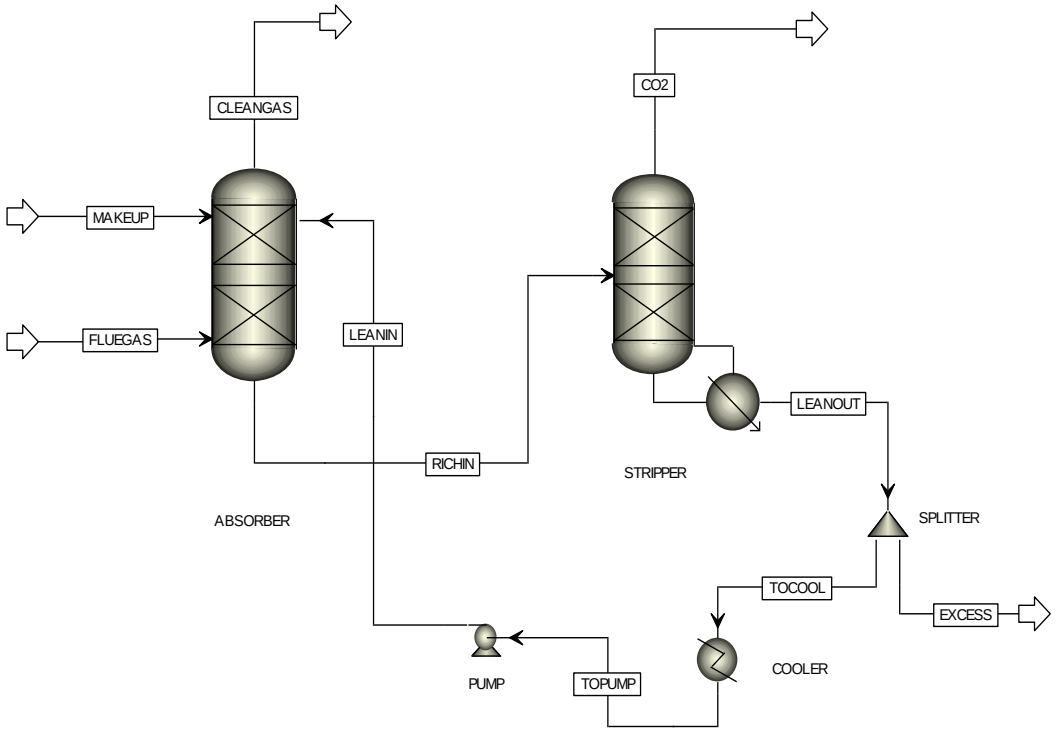

Figure 4.2. Steady-State Model Flowsheet for K_2CO_3 base case capture process

The CO_2 product stream (CO_2) is condensed and compressed for storage whereas the lean-solvent regenerated (LEANOUT) is cooled and recycled to the ABSORBER as LEANIN. For convergence purposes and as a means of discarding some impurities which would otherwise accumulate in the system, a portion of the recycle stream is purged in the SPLITTER to control the rate of lean-solvent entering the ABSORBER. The 2920 kg/hr MAKEUP (80 ^oC, 15 atm) stream serves as the makeup block to replenish the lost water and K_2CO_3 in the system.

4.10.4 Model Design

The absorber and stripper columns were designed in detail using the RadFrac column model with the following specifications as obtained from Mumford et al. 2011 and Kothandaraman 2010:

Table 4.7: RadFrac Specifications for K_2CO_3-CO_2-H_2O system (Mumford et al. 2011 and Kothandaraman 2010)

RadFrac Properties	Absorber	Stripper
Number of stages	12	8
Packing material	Raschig Norton Metal 10 mm	Raschig Norton Metal 6 mm
Total packed height	14 m	12 m
Column diameter	1.5m	1.4m
Flow model	Mixed model	Mixed model
Interfacial area factor	1.8	1.8
Initial liquid hold up	0.03 L	0.03 L
Film resistance	Discrxn for liquid; Film for vapour	Discrxn for liquid; Film for vapour
Discretization points for liquid film	10	10

4.10.5 Model Validation

The converged base case simulation results from this study were validated against the simulation records in Kothandaraman 2010, and compared to the base case results from the MEA process simulation. These are displayed in Table 4.8.

Table 4.8: Validation of Results for K_2CO_3-CO_2-H_2O system

Design specifications	Values
Inlet flue gas flowrate, kg/h	4740
Inlet flue gas CO_2, vol%	13
Lean flowrate, kg/hr	11,170
Lean K_2CO_3 conc., wt%	40

Base case performance	K_2CO_3 Base Case	MEA Base Case	Deviation (%)	Kothandaraman 2010	Deviation (%)
CO_2 capture level, %	78.17	85.96	9.06	85	8.04
Reboiler duty, MJ/kgCO_2	2.76	3.98	30.65	3.20	13.75
Condenser duty, MJ/kgCO_2	1.22	0.815	49.69	-	-
Cooling duty, MJ/kgCO_2	1.17	1.495	21.74	-	-
Heat Exchanger duty, MJ/kgCO_2	-	2.32	-	-	-
Total duty, MJ/kgCO_2	5.15	8.61	40.19	-	-

The results from the HPC capture process, as validated and compared to the MEA based absorption process in Table 4.8, proves that the K_2CO_3 process is a more energy-efficient technology. The high energy savings of 30.65% in reboiler duty and 40.19% in total energy usage over the values in an MEA capture process shows that the regeneration process in hot potassium carbonate capture system requires far less energy than is needed in the amine desorption scenario. The desorption efficiency and overall capture level of the MEA based capture level, however, proves that the amine system has a higher carbon removal efficiency than the K_2CO_3 system. This is shown in the 9.06% lower carbon capture efficiency in the K_2CO_3 process. Preliminary analysis of the K_2CO_3 capture simulation reveals that desiring higher capture efficiency comes with a steep upsurge in the energy usage of the system. This could be observed in the higher capture level in the reference paper, Kothandaraman 2010, which incurred a higher desorption energy duty of 3.20 MJ/kgCO_2. The 8.04% lower CO_2 removal in the current simulation over the results in Kothandaraman 2010 could, therefore, be linked to the 13.75% lower reboiler duty attained in the current simulation. Nevertheless, the results from the current study compare closely with those from the reference paper, indicating the full validity of the current work.

4.11 PARAMETRIC STUDY OF K_2CO_3 CAPTURE SYSTEM

The significance of parametric analysis is to find out the optimal operating conditions of the carbonate absorption process and suggest optimisation strategies accordingly. To test the sensitivity of the performance of the K_2CO_3 carbon capture system to various process parameters, a wide range of parametric analyses were performed. These analyses evaluate the sensitivity of the carbon capture level and stripper reboiler energy consumption to changes in the flue gas flowrate, lean solvent flowrate, lean solvent concentration, reflux ratio, system operating temperatures and pressures, as well as different packing types adopted in both the absorber and stripper columns.

4.11.1 Effect of Column Packing Type

The different packing types investigated were the IMTP Norton Metal, Sulzer Nutter Ring, Super-Pak Metal, Mellapak, Flexipac Koch Metal, and Raschig Norton Metal-32. These packing types were chosen because of their popularity in literature publications. The results from the analysis, as displayed in Table 4.9, indicate that the

system performance generally improves with increasing surface area of packing material. Although the specific reboiler duty does not seem to vary much with different packing types, the capture efficiency appears to improve quite significantly for packing materials with surface area higher than 300 m^2/m^3. There seems to be a discontinuity in the improvement of CO_2 removal efficiency between the Flexipac Koch Metal 1Y and Raschig Norton Metal-32. Even though the former has a lower surface area than the latter, the system performance shows better results in the former than in the latter. The improvement in system performance, however, resumes the general pattern between the two Raschig Norton Metal packing types, with the 814.5 m^2/m^3 surface area demonstrating superior carbon capture level than the material with 543 m^2/m^3.

Table 4.9: Results for Different Column Packing Types

Packing Type	Surface Area, m^2/m^3	CO_2 Capture Rate, %	Reboiler Duty, MJ/kg CO_2
IMTP Norton Metal 50mm	102	77.37	2.79
Sulzer Nutter Ring	226	77.71	2.77
Super-Pak Metal 300	300	77.75	2.77
Mellapak 350Y	353	78.50	2.76
Flexipac Koch Metal 1Y	420	78.60	2.75
Raschig Norton Metal-32	543	78.04	2.76
Raschig Norton Metal-32	814.5	78.24	2.76

Judging from the results in this analysis, it could be concluded that the Flexipac Koch Metal 1Y is the best packing type recommended for the hot potassium carbonate absorption process. Despite having an average surface area, this packing material recorded the highest carbon removal capacity along with the lowest specific reboiler duty.

4.11.2 Effect of Reflux Ratio

To understand how the reflux ratio influences the stripper performance in the desorption process and ultimately on the reboiler duty requirement, the value was varied from 0.25 to 1.25 on a mass basis. Figure 4.3 displays the results obtained from this analysis. The reflux ratio is computed at the overhead of the stripper column. It reflects the ratio between the flowrate of the liquid stream which is returned to the top

section of the stripping column and the CO_2 vapour stream which is recovered for storage. The CO_2 recovery level and the specific reboiler duty increase with an increasing reflux ratio. This is because increasing the reflux rate increases the overall liquid/vapour contact in the stripper column, thereby enhancing the carbon capture efficiency. That notwithstanding, the higher reflux ratio increases the boil-up rate in the base of the column and decreases the overall stripping rate, thereby increasing the stripper energy consumption as observed in Figure 4.3.

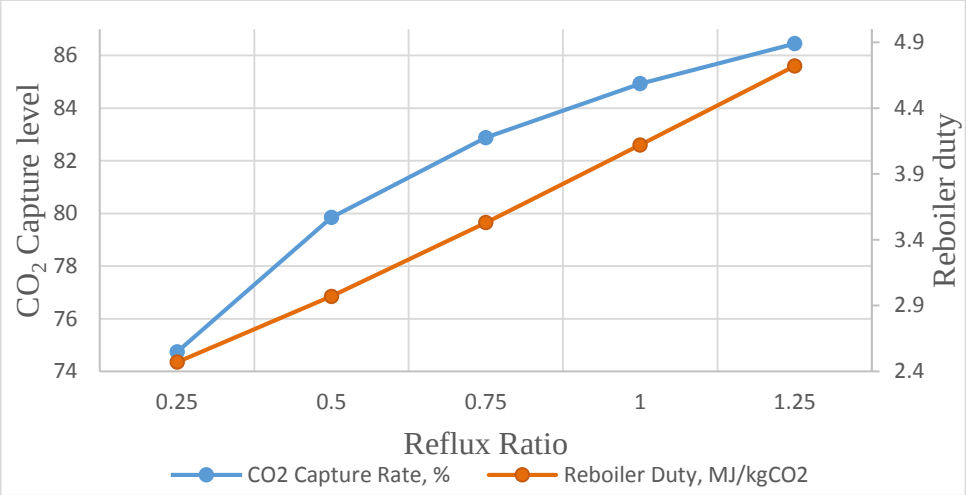

Figure 4.3. Effects of Reflux Ratio on CO_2 Capture level & Reboiler duty

The highest reflux ratio yielded the highest carbon removal efficiency of 86.45% but at the expense of reboiler duty, which attained its greatest value of 4.72 MJ/kgCO_2. The lowest reflux ratio of 0.25 was also observed to produce the lowest carbon recovery level of 74.74% and the lowest specific reboiler duty of 2.47 MJ/kgCO_2. Thus, to recover as much CO_2 as possible at the lowest stripper energy usage, optimisation and economic analyses are required to select the optimum value of the reflux ratio.

4.11.3 Effect of Lean Solvent Flowrate

In an attempt to understand how the lean solvent flowrate impacts the system performance of the hot potassium carbonate process, the solvent flowrate was varied over the range of 11,070 kg/hr to 11,270 kg/hr. This was achieved by varying the flowrate of the makeup solvent stream in steps of 50 kg/hr. The results obtained are shown in Figure 4.4.

The effect of the lean solvent flowrate on the decarbonisation level appears to follow the same pattern as the reflux ratio. Increasing the flowrate increases the decarbonisation efficiency of the system. Interestingly, the increasing carbon capture level had corresponding decreases in the reboiler duty. This is probably due to the higher absorption capacity and CO_2 mass transfer rate which is caused by the higher amount of lean solvent introduced into the absorber column.

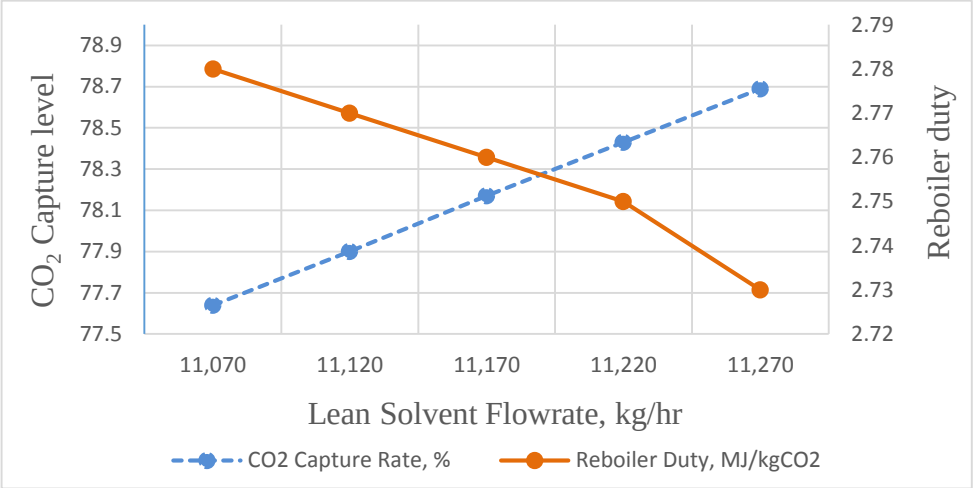

Figure 4.4. Effects of Lean solvent flowrate on CO_2 Capture level & Reboiler duty

This increases the rich solvent loading and decreases the desorption energy requirement in the stripper column. This ultimately minimises the heat demand from the reboiler system. The steep decrease of the reboiler duty at the highest lean solvent flowrate to as low as 2.73 MJ/kgCO_2, which also corresponds to the highest capture rate of 78.69%, suggests that the best flowrate among the five points tested is probably 11,270 kg/hr.

4.11.4 Effect of Flue Gas Flowrate

Similar to the variations in the lean solvent flowrate, the flue gas flowrate was varied over the range of 4640 kg/hr to 4840 kg/hr in steps of 50 kg/hr. The influence of these changes on the decarbonisation efficiency and stripper reboiler duty of the K_2CO_3 capture process is presented in Figure 4.5. As depicted in the Figure, despite significant changes in the carbon capture level as a result of the variations in the flowrate of flue gas, the specific reboiler duty remains constant at 2.76 MJ/kgCO_2. This could be as a result of equal changes that occur both in the amount of carbon dioxide mitigated and the reboiler heat duty whenever the flue gas flowrate changes. The effect of the

changes in both parameters, therefore, cancels out when the specific reboiler duty is computed since the specific reboiler duty is the ratio of the reboiler duty and the amount of CO_2 removed. If the same amount of change is experienced in both value upon changing the flowrate of the flue gas, then the impact of the changes in the two parameters will be nullified once the ratio is calculated.

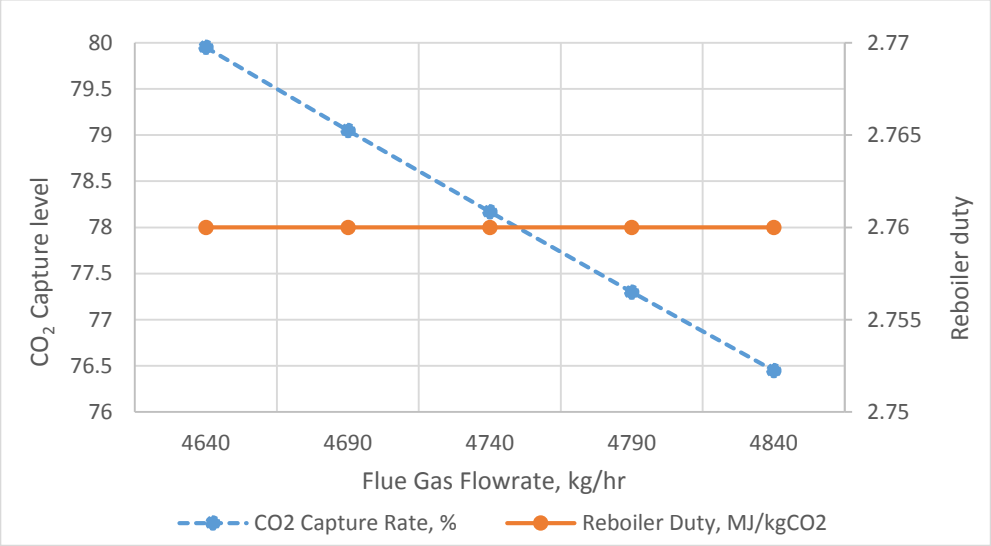

Figure 4.5. Effects of Flue gas flowrate on CO_2 capture level & Reboiler duty

It could, therefore, be concluded that changes in the flue gas flowrate only affect the carbon capture efficiency of the system. This makes this parameter one of the most important parameters in the system. It could be observed that the carbon removal capability of the K_2CO_3 plant is very sensitive to changes in the flue gas flowrate. The lowest capture efficiency of 76.45% was obtained at the highest flue gas flowrate of 4840 kg/hr, while the highest capture rate of 79.95% was attained at the lowest flue gas flowrate of 4640 kg/hr. This result could be explained to have occurred due to the changes in the liquid to gas ratio that corresponds to the changes in the flue gas flowrate. When the flue gas flowrate is increased, the liquid (lean solvent flowrate) to gas (flue gas flowrate) ratio decreases. At lower liquid to gas ratio (L/G), the mass transfer rate of the absorption process is slow, yielding lower carbon capture efficiency in the system. On the other hand, as the flue gas flowrate decreases at constant lean solvent flowrate, the L/G value increases. The higher L/G value improves the mass transfer rate of the system as there is a relatively higher lean solvent stream entering the absorber column. This increased absorption rate ultimately improves the decarbonisation capacity of the capture process. As an optimisation strategy, the flue

gas flowrate could be decreased if higher carbon removal is desired at constant reboiler heat duty.

4.11.5 Effect of Lean Solvent Concentration

In this parametric analysis, the concentration of K_2CO_3 in the lean solvent stream was changed over the range of 25 wt% to 45 wt% (in steps of 5) to test the sensitivity of the system performance to this parameter. Since the carbon capture by the K_2CO_3 absorption process takes place at a higher temperature, it is believed that the solvent concentration could be increased a little beyond 40 wt% without any operational issues. This is also believed to be so due to the high stability of the potassium carbonate solvent, which drastically minimises the volatility of the chemical. To ascertain the validity of this assertion and to investigate the response of the decarbonising level and stripper energy duty to changes in this process parameter, the parametric analysis involving the K_2CO_3 concentration was carried out in this study. The outcomes of the analysis are summarised in Figure 4.6 below.

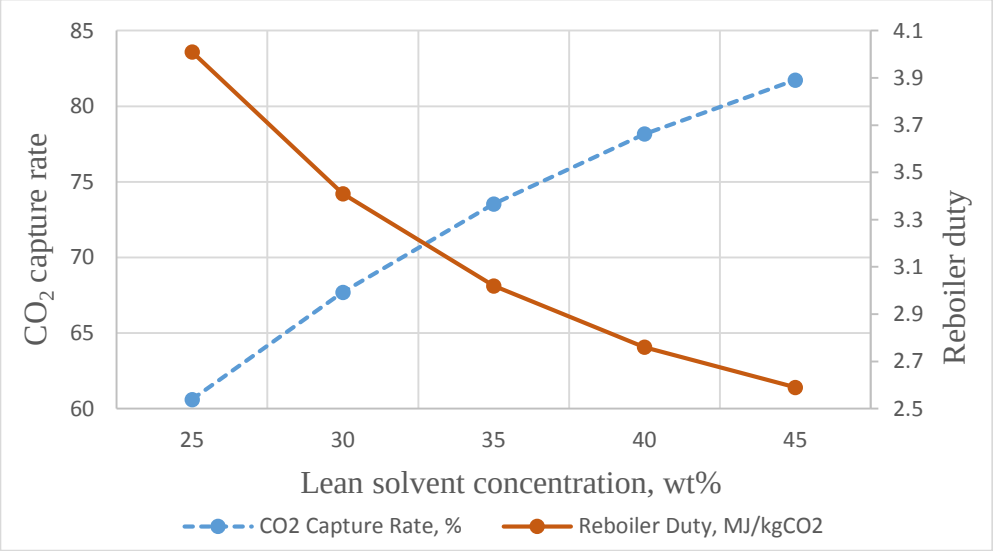

Figure 4.6. Effects of lean solvent concentration on CO_2 capture and reboiler duty

Figure 4.6 shows that the performance of the HPC capture process is quite sensitive to the concentration of the lean solvent stream fed to the absorber. This is obvious in how the specific reboiler heat requirement and the carbon removal efficiency of the process varies significantly with changes in the weight of K_2CO_3 dosed into the lean solvent stream. At higher lean solvent concentration, the capture rate of the process is observed to soar with corresponding low reboiler heat consumption. On the other hand, when

the concentration of K_2CO_3 in the lean solvent stream is low, it results in a lower carbon capture level at a higher reboiler duty. The reason for this observation could be that, at lower lean solvent concentration, the stream is less effective in absorbing the CO_2 molecules as the chemical absorbent is less. However, when the concentration of the absorbent in the stream increases, the lean solvent becomes more effective and is able to absorb more CO_2, yielding a higher capture level. The resulting high rich solvent stream is easier to regenerate in the stripper column, explaining why the reboiler duty decreases alongside the increased decarbonisation level. For optimisation purposes, it could be concluded that increasing the lean solvent concentration is an effective way to improve the performance of the HPC process. Nevertheless, since increasing the concentration of the carbonate in the system could result in increased salt precipitation which could interfere with the smooth operation of the process, further studies such as pilot plant tests are necessary to find out the optimum value of the weight of K_2CO_3 in the lean solvent stream.

4.11.6 Effect of Lean Solvent Temperature

To examine the system response to changes in the lean solvent temperature, the value was varied from 60 °C to 100 °C in step changes of 10. The influence of these changes on the carbon removal efficiency and the regeneration energy usage of the hot potassium carbonate process was recorded and summarised in Figure 4.7.

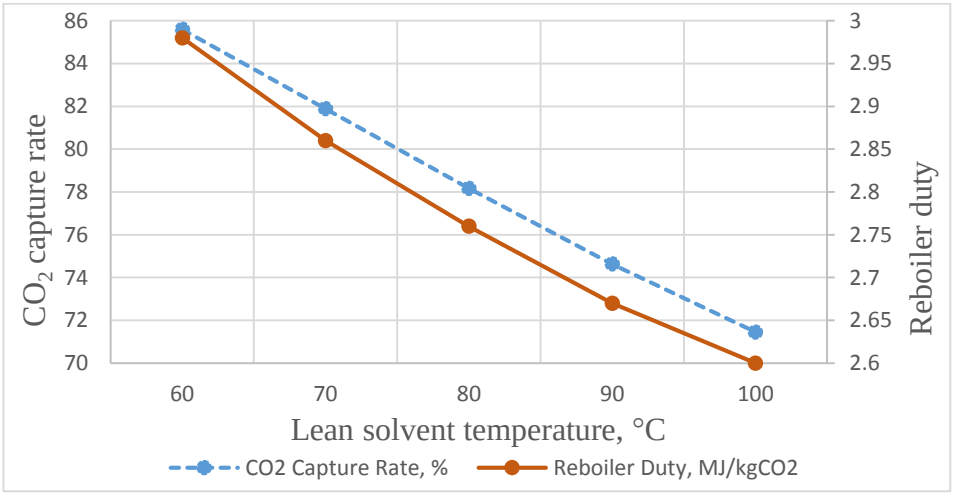

Figure 4.7. Effects of lean solvent temperature on CO_2 capture and reboiler duty

Inferring from the results in Figure 4.7, increasing the lean solvent temperature appears to positively impact the regeneration energy duty and hence the specific reboiler duty.

The same direction of change in the lean solvent stream temperature, however, adversely affects the carbon capture efficiency of the system. On the other hand, when the lean solvent temperature reached its lowest value of 60 °C, the carbon recovery of the process was seen to soar to as high as 85.6%. The corresponding reboiler duty recorded at this capture level was 2.98 MJ/kgCO_2. These observations could be linked to the effect of temperature changes on the driving force of the absorption process. As the lean solvent temperature decreases, the heightening temperature from the exothermic CO_2 absorption process is controlled. This improves the thermodynamic driving force in the absorber column and increases the mass transfer of CO_2 molecules into the absorbent stream. However, since the CO_2 rich solvent stream exits at a lower temperature and is fed to the stripper column at the same low temperature, more heat is required to recover the CO_2 in the stripping process. This accounts for the high carbon capture level at an increased specific reboiler duty. On the other hand, when the lean solvent temperature increases, the absorption process becomes more exothermic. As more heat is released, the absorption of CO_2 is negatively interfered with due to the diminishing thermodynamic driving force that occurs at higher temperatures. This accounts for the low carbon capture that results from this scenario. But since the rich solvent stream entering the stripper column is at a higher temperature, less heat is required in the column to regenerate the solvent. This is the reason why the stripper specific reboiler duty appears to decrease with increasing lean solvent stream temperature. Besides these observations, it could be seen that the HPC capture process appears to be very sensitive to the temperature of the lean solvent stream. This implies that the optimal value of this parameter is capable of yielding an improved capture system.

4.11.7 Effect of Flue Gas Temperature

The parametric analysis involving the flue gas temperature is completed in the same manner as in the previous section regarding the lean solvent temperature. The temperature of the gas stream was varied over the range of 80 to 120 in degree centigrade, using the step change of 10. Figure 4.8 depicts the result obtained from this analysis.

The results show that the effects of temperature changes in the flue gas stream on the HPC absorption process is quite pronounced on the reboiler duty. Although a similar

impact is observed on the carbon capture rate, it appears the lean solvent temperature has a more pronounced impact on the capture efficiency than the flue gas temperature. Nonetheless, similar patterns are observed in this analysis as were the cases in the analysis involving the lean solvent stream temperature. At higher temperatures of the flue gas stream, it is observed that the specific reboiler duty decreases substantially. There is also an associated decrease in the carbon removal level at high temperatures as well. This indicates that the mass transfer rate in the absorber column is negatively impacted as a result of the increased temperature. At the lowest temperature of 80 °C, the carbon recovery level climbed to its greatest percentage of 85.66.

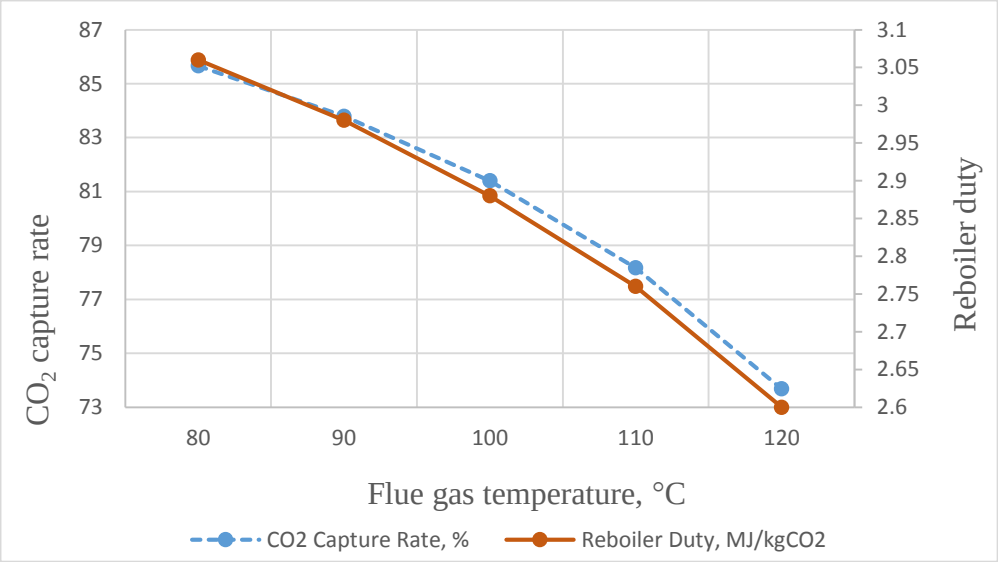

Figure 4.8. Effects of flue gas temperature on CO_2 capture and reboiler duty

The results from Figure 4.8 demonstrate that at the same temperature, the reboiler duty recorded its highest figure of 3.06 MJ/kgCO_2. This implies that decreasing the temperature of the flue gas stream also affects the thermodynamic driving force during the absorption process in a positive regard. This improves the carbon capture efficiency of the plant. But since the temperature of the rich solvent stream fed to the regenerator is at a lower level, higher heat requirement is incurred during the regeneration process, resulting in higher specific reboiler duty.

4.11.8 Effect of Absorber Operating Pressure

As discussed earlier, Zhao et al. 2013 observed that operating the absorber at high pressures from 10 to 20 bars could help to improve the performance of the hot potassium carbonate capture process. To investigate the validity of this information

and equally find out how the absorber operating pressure impacts the carbon recovery level and the regeneration energy usage of the HPC process, various pressures of 5, 10, 15, 20, 25 (in atmospheric unit, atm) were analysed. The summary of the results obtained is presented in Figure 4.9 below.

As depicted in Figure 4.9, the decarbonisation rate is seen to respond sensitively to changes in the absorber operating pressure. As the absorber operating pressure rises, the carbon capture level is observed to rise accordingly. This could be as a result of the intensified absorption rate which occurs in the absorber column as the pressure increases. As the absorption rate increases, the CO_2 loading in the rich solvent stream increases, resulting in a higher decarbonisation efficiency.

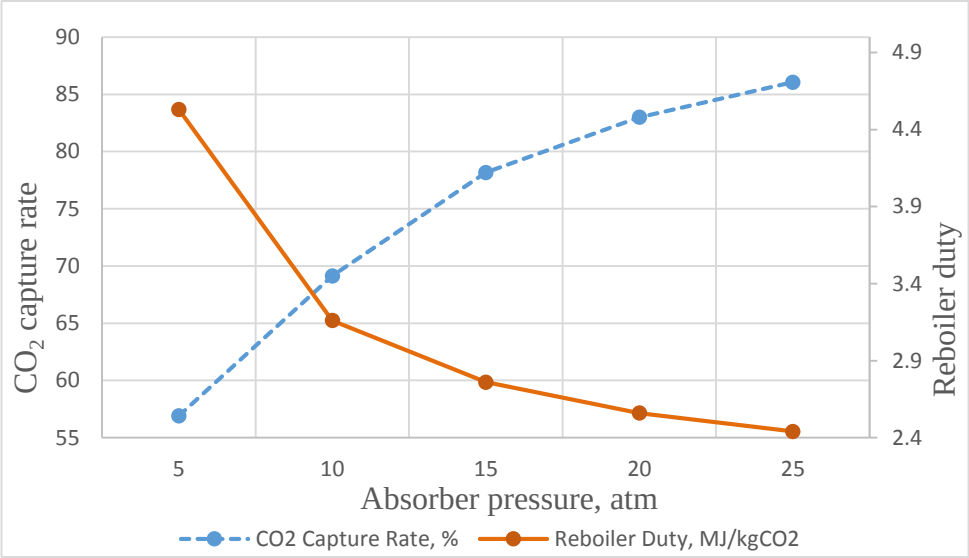

Figure 4.9. Effects of absorber operating pressure on CO_2 capture and reboiler duty

The higher pressure swing across the absorber and the stripper column also improves desorption during the regeneration process, resulting in a higher carbon capture level at declining specific reboiler duty. On the other hand, decreasing the absorber operating pressure lowers the mass transfer rate in the absorber column and reduces the pressure swing across the absorber and the stripper columns. The resulting less rich solvent stream at lower pressure requires more sensible heat in the regenerator, causing poor carbon capture efficiency and increased reboiler duty requirement. The sharp reboiler increase from 3.16 to 4.53 MJ/kgCO_2 which occurs when the absorber operating pressure decreases from 10 to 5 atm is quite profound. This indicates that operating the absorber below 10 atm in a hot potassium carbonate capture process might not be a good idea. However, since the quality, hence the cost of the absorber

column increases depending on the operating pressure, it is vital to conduct techno-economic analyses on the HPC system to ascertain the optimum value of this parameter.

4.12 OPTIMISED K_2CO_3 CAPTURE SYSTEM THROUGH SENSITIVITY ANALYSIS

The main objective of the optimisation is to increase carbon capture efficiency at reduced specific reboiler duty. The related optimisation equation, given as a function of the process energy duty and the rate of captured CO_2 is presented in Appendix C. To design the optimised HPC capture process, it was necessary to take a critical look at the results from the parametric analyses presented earlier. The system parameters that seem to yield the most sensitive results in the system performance were chosen for the optimisation process. As shown in Table 4.9, the packing type that demonstrated the best system performance, yielding the highest carbon capture efficiency at the lowest reboiler duty, is the Flexipac Koch Metal 1Y. For this reason, this packing material is selected for the optimised HPC capture process. Even though increasing the reflux ratio was able to enhance the carbon removal rate as displayed in Figure 4.3, the specific reboiler duty equally increases concurrently. On the other hand, when the reflux ratio was decreased, it was observed to negatively impact the carbon capture efficiency while reducing the reboiler duty. It was therefore decided to maintain the original reflux ratio as in the base case scenario. As shown in Figure 4.4, the performance of the HPC system appears to be sensitive to changes in the lean solvent flowrate. Increasing this parameter demonstrated improvements in both the carbon capture rate and the reboiler duty. As the flowrate was increased from 11,170 kg/hr to 11,270 kg/hr, the reboiler duty attained its lowest value. At the same rate, the carbon capture rate increased to its highest value. This led to the selection of 11,270 kg/hr as the optimum lean solvent flowrate. Regarding the flue gas flowrate, changes in this parameter did not appear to have any significant impact on the reboiler duty although it appears to influence the capture efficiency. Since the main focus of this optimisation is to consider parameters that positively impact both the carbon removal efficiency and the stripper reboiler duty, it was decided to maintain the original value of the flue gas flowrate. This same reason explains why the lean solvent temperature and the flue gas temperature were maintained at their original values. Increasing the

lean solvent concentration, however, affected both the decarbonisation rate and stripper reboiler duty positively. At the highest value of 45 wt%, which was chosen as the optimal value, the system yielded the highest carbon removal efficiency at the lowest reboiler duty. As displayed in Figure 4.9, changes in the absorber operating pressure also affected the system performance in the same manner. Nonetheless, since increasing the absorber operating pressure will demand higher pressure for the feed streams to the absorber, imposing higher compressor energy consumption, it was decided to increase the absorber pressure from 15 atm to a moderate value of 20 atm only. This would also ensure the equipment cost of the high-pressure absorber does not increase exorbitantly due to a very high operating pressure. A comparison of the optimised values which were used in the optimised model and the original figures in the non-optimised system are presented in Table 4.10. This is to clarify which values have been altered and to what degree. The optimisation function used is fully explained and solved in the Appendix.

Table 4.10: Comparison of Original and Optimised Parameters for HPC System

Parameters	Original	Optimised
Packing type	Raschig Norton Metal-32	Flexipac Koch Metal 1Y
Lean solvent concentration, wt%	40	45
Lean solvent flowrate, kg/hr	11,170	11,270
Absorber operating pressure, atm	15	20

4.12.1 Results for Optimised K_2CO_3 Capture Process

The results obtained from the optimised HPC capture model simulations are compared to the base case simulation results for K_2CO_3 and MEA in Table 4.11.

Table 4.11: Comparison of results for optimised K_2CO_3 to base case K_2CO_3 and MEA capture processes

System performance	Optimised K_2CO_3	K_2CO_3 Base Case	Deviation (%)	MEA Base Case	Deviation (%)
CO_2 capture level, %	88.03	78.17	12.61	85.96	2.41
Reboiler duty, MJ/kgCO_2	2.35	2.76	14.86	3.98	40.95
Condenser duty, MJ/kgCO_2	1.12	1.22	8.20	0.815	37.42
Cooling duty, MJ/kgCO_2	1.06	1.17	9.40	1.495	29.10

Heat Exchanger duty, $MJ/kgCO_2$	-	-	-	2.32	-
Total duty, $MJ/kgCO_2$	4.53	5.15	12.04	8.61	47.39

The results presented in Table 4.11 show the high performance of the optimised HPC capture model. Higher carbon capture rates, as well as reduced energy duties, are observed in the optimised process over the base case results for K_2CO_3 and MEA capture plants. This shows that at higher absorber operating pressure and at higher lean solvent concentration, the carbon removal capacity of the potassium carbonate capture process could compare closely with the high efficiency of the amine-based model. As presented in Table 4.11, it is interesting to see the optimised process performing better than the MEA base case scenario, with a percentage improvement of 2.41% in decarbonisation efficiency. The same observation is made for the base case HPC process, where the optimised process shows a superior carbon removal capacity of 12.61% increase. The most striking advantage of the optimised process examined in this study over the base case scenarios, however, is the high energy efficiency. Comparing the results of the base case K_2CO_3 process and that of the optimised K_2CO_3 process, it could be seen that the optimisation is able to attain reboiler duty minimisation of 14.86%. Equally, the total energy usage in the optimised absorption process is noticed to have experienced a substantial scale-down in the magnitude of 12.04% over the non-optimised K_2CO_3 process. In the case of the optimised HPC process and the base case model of the amine capture system, the differences in the system performances are even more pronounced. As seen from the table, a remarkable drop in reboiler heat duty in the magnitude of 40.95% is observed. Although the condenser cooling duty in the current optimised model experienced a soaring of 37.42% over the duty in the base case MEA model, the overall energy usage of the optimised process proved to have almost a half slash in value by the 47.39% reduction witnessed. The high energy minimisation observed in the optimised K_2CO_3 model is a good indication that the high-concentrated HPC absorption process is a more energy-efficient post-combustion carbon capture technology than its counterpart amine-based capture technology.

4.13 SUMMARY OF CHAPTER 4

Chapter 4 opens with a disclosure on the main software packages involved in the simulations and continues to give descriptions of the equilibrium-based modelling, rate-based modelling, dynamic modelling and the control system design completed in this study. The base case modelling and simulation for MEA-based and K_2CO_3-based capture processes are performed in this chapter. Complete validations of these processes are presented, and the comparison of the system performances between the two processes is discussed. The major constraints considered, as well as the simulation design and objectives, are also outlined. Finally, parametric analyses and optimisation are performed for the K_2CO_3-based capture process. It could be concluded from the parametric analyses that absorber pressure is very paramount in K_2CO_3-based capture process. To obtain good system performances, the absorber needs to be operated above 10 atmospheric pressure. The thesis objective #1 is partially achieved and research question #1 is answered in this chapter, as insights into the energy-efficiency of the HPC capture process are established. The main conclusion drawn from this chapter is that the K_2CO_3-based capture system is more energy-efficient than the conventional MEA-based absorption process.

CHAPTER 5

PROMOTED MEA AND K_2CO_3 CAPTURE SYSTEMS

This section describes the catalysis of the MEA system using piperazine (PZ) and the promotion of the HPC system with boric acid (H_3BO_3). The main reason for adding these promoters to the two solvents are different. Whereas the blending of MEA with PZ is for the purpose of reducing the energy usage in the system, the H_3BO_3 inclusion in the K_2CO_3 system is for the purpose of increasing the carbon capture efficiency.

5.1 PZ PROMOTED MEA CAPTURE PROCESS

After successful validation of the MEA base case simulation, the solvent was catalysed by adding aqueous piperazine (PZ) solution. This cyclic polyamine is known to have the catalytic quality of reducing the solvent degradation rate in the MEA capture system, improve capture efficiency and simultaneously decrease the regeneration energy requirement. Even though many recent works have used higher concentrations of the chemical in blended solutions, due to its low solubility in water, PZ is typically used in minimal quantities of 0.5 to 2.5 molality (Freeman et al. 2010; Yarveicy et al. 2018; Lu et al. 2017). The experimental study of 7 m MEA (30 wt%)/2 m PZ (10 wt%) system by Dugas revealed that the CO_2 partial pressure in the blended solvent is lower than that in the unpromoted MEA solution, indicating that the PZ promoted solvent has superior carbon dioxide absorption performance (Dugas 2009). Oyenekan et al. 2007 also completed an earlier simulation study using 7m MEA/2 m PZ and reported that the blended solution is able to achieve energy savings of 10.3% over the baseline value. In a recent quantum mechanics and molecular dynamics studies carried out by Narimani et al. 2017, where they investigated the diffusivity of CO_2 in MEA, PZ and their blend, the authors considered the addition of 5 wt% PZ to 25 wt% MEA as the most effective solution for CO_2 absorption. No work has however considered into detail how the PZ promoted MEA process compares to the unpromoted MEA in terms of total heat duty requirements of the two systems. This study, therefore, examines the blended solutions of 5 wt% PZ/25 wt% MEA and 7 wt% PZ/23 wt% MEA and compares the carbon capture efficiency and total energy consumption to the 28.5 wt% MEA baseline process.

5.1.1 PZ/MEA Model Reaction Equations (Plus[d] et al. 2008)

The following equilibrium and kinetic reactions were included in the PZ/MEA model development, as adapted from Plus[d] et al. 2008.

1. Equilibrium $2H_2O \rightleftharpoons H_3O^+ + OH^-$
2. Equilibrium $CO_2 + 2H_2O \rightleftharpoons H_3O^+ + HCO_3^-$
3. Equilibrium $HCO_3^- + H_2O \rightleftharpoons H_3O^+ + CO_3^{2-}$
4. Equilibrium $PZH^+ + H_2O \rightleftharpoons PZ + H_3O^+$
5. Equilibrium $PZ + HCO_3^- \rightleftharpoons PZCOO^- + H_2O$
6. Equilibrium $HPZCOO + H_2O \rightleftharpoons PZCOO^- + H_3O^+$
7. Equilibrium $PZCOO^- + HCO_3^- \rightleftharpoons PZ(COO^-)_2 + H_2O$
8. Equilibrium $MEAH^+ + H_2O \rightleftharpoons \text{MEA} + H_3O^+$
9. Equilibrium $MEACOO^- + H_2O \rightleftharpoons \text{MEA} + HCO_3^-$
10. Kinetic $CO_2 + OH^- \rightarrow HCO_3^-$
11. Kinetic $HCO_3^- \rightarrow CO_2 + OH^-$
12. Kinetic $\text{PZ} + H_2O + CO_2 \rightarrow PZCOO^- + H_3O^+$
13. Kinetic $PZCOO^- + H_3O^+ \rightarrow \text{PZ} + H_2O + CO_2$
14. Kinetic $PZCOO^- + H_2O + CO_2 \rightarrow PZ(COO^-)_2 + H_3O^+$
15. Kinetic $PZ(COO^-)_2 + H_3O^+ \rightarrow PZCOO^- + H_2O + CO_2$
16. Kinetic $\text{MEA} + H_2O + CO_2 \rightarrow MEACOO^- + H_3O^+$
17. Kinetic $MEACOO^- + H_3O^+ \rightarrow \text{MEA} + H_2O + CO_2$

5.1.2 Relations for Equilibrium and Kinetic Constants (Plus[d] et al. 2008)

The equilibrium constants for reactions 1-9 were determined using the Aspen Plus built-in equation:

$In(Keq) = A + \frac{B}{T} + C * In(T) + D * T$, where A, B, C and D are temperature-dependent coefficients and T is the temperature in Kelvin units.

The kinetic constants for reactions 10-17 were obtained using the Aspen Plus built-in reduced power-law expression: $r = k\exp\left(-\frac{E}{RT}\right)$, where k is a pre-exponential factor, E is activation energy, R is universal gas constant and T is the temperature in Kelvin units.

Table 5.1: Equilibrium constants for MEA-PZ-CO_2-H_2O system (Plus[d] et al. 2008)

Reaction No.	A	B	C	D
1	132.899	-13445.9	-22.4773	0
2	231.465	-12092.1	-36.7816	0
3	216.049	-12431.7	-35.4819	0
4	-4.0762	-7773.2	0	0
5	-4.6185	3616.1	0	0
6	-14.042	-3443.1	0	0
7	0.3615	1322.3	0	0
8	-3.038325	-7008.357	0	-0.00313489
9	-0.52135	-2545.53	0	0

Table 5.2: Kinetic constants for MEA-PZ-CO_2-H_2O system (Plus[d] et al. 2008)

Reaction No.	k	E (cal/mol)
10	4.32×10^{13}	13249
11	2.38×10^{17}	29451
12	4.14×10^{10}	8038.3
13	9.47×10^{20}	15333
14	3.62×10^{10}	8038.3
15	3.46×10^{20}	17958
16	9.77×10^{10}	9855.8
17	2.80×10^{20}	17230

5.1.3 PZ/MEA Results

The results from the PZ/MEA are compared to the baseline MEA results in Table 5.3 below.

Table 5.3: Comparison of Results for MEA and PZ/MEA

Base case performance	28.5 wt% MEA	5 wt% PZ/25 wt% MEA	Deviation (%)	7 wt% PZ/23 wt% MEA	Deviation (%)
CO_2 capture level, %	85.96	87.11	1.34	87.19	1.43
CO_2 product purity, vol%	99.99	97.89	2.10	97.98	2.01
Reboiler temp, ^oC	121.2	121.5	0.2	121.5	0.2

Reboiler duty, MJ/kgCO_2	3.98	3.91	1.76	3.93	1.26
Condenser duty, MJ/kgCO_2	0.815	0.578	29.08	0.579	28.96
Cooling duty, MJ/kgCO_2	1.495	1.847	23.54	1.920	28.43
Heat Exchanger duty, MJ/kgCO_2	2.32	2.08	10.34	2.06	11.21
Total duty, MJ/kgCO_2	8.61	8.42	2.21	8.45	1.86

The results from the current study, as shown in Table 5.3, illustrate that PZ promoted MEA systems are able to achieve energy savings on the condenser duty as well as on the reboiler heat duty. In the case of the 5 wt% PZ/25 wt% MEA system, the blended solution is able to save reboiler duty by 3.91%, while cutting down the condenser duty with 29.08% over the unpromoted MEA base case. This blended solution is equally able to achieve a carbon capture efficiency of 1.34% over the base case. Similar improvements are also observed for the 7 wt% PZ/23 wt% MEA system. It is however observed that the product purity level in the PZ promoted system is not as high as in the base case scenario, indicating that if high product purity is desired, then optimisations need to be applied to the blended solution processes to achieve the desired purity. The cooling duties in the promoted systems were also observed to have higher values that of the uncatalysed system. This may be as a result of the higher reboiler temperatures attained in the PZ/MEA systems. Despite these downsides of the catalysed system, it is worth noting that the promoted systems attained total energy savings of 2.21% and 1.86% in the 5 wt% PZ/25 wt% MEA and 7 wt% PZ/23 wt% MEA systems respectively. Also, the 5 wt% PZ/25 wt% MEA blended solution appears to be a better option in terms of improvements in carbon capture efficiency whereas the 7 wt% PZ/23 wt% MEA system appears to have higher potentials in heat duty savings.

5.2 H_3BO_3 PROMOTED K_2CO_3 CAPTURE SYSTEM

This section discusses the base case absorption process of potassium carbonate with in situ boric acid solution. This blended solution is recently noted to have superior absorption performance over the uncatalysed K_2CO_3 system. Despite many works reporting the improvements in the form of increased mass transfer rate as a result of adding small amounts of boric acid to the K_2CO_3 system, no work has yet reported on the full impact of this solvent promotion in a full-scale plant study. The investigation of how the addition of boric acid affects other energy sectors of the hot potassium

carbonate capture process, including the impacts on cooling duties and other heat duties aside from the reboiler energy consumption, are explored in this section. The various blended solutions that were simulated are 2 wt% H_3BO_3/40 wt% K_2CO_3, 4 wt% H_3BO_3/40 wt% K_2CO_3, 6 wt% H_3BO_3/40 wt% K_2CO_3.

5.2.1 Equilibrium and Kinetic Equations for the H_3BO_3/K_2CO_3 System

The additional equilibrium and kinetic equations and their constants as included in the HPC process model as a result of the addition of boric acid are presented in Table 5.4. These additional equations and the constant values were obtained from the works of Smith et al. 2012.

Table 5.4: Equilibrium/Kinetic equations and constants for K_2CO_3-H_3BO_3-CO_2-H_2O system (Smith et al. 2012)

	A	B	C	k	E_a (J/mol)
Equilibrium equation					
$B(OH)_3.H_2O \rightleftharpoons B(OH)_4^- + H^+$	177.6	-10266.5	-28.9	-	-
Kinetic equation					
$B(OH)_4^- + CO_2 \rightleftharpoons B(OH)_3 + HCO_3^-$	30.7	8106	0	2.195×10^{13}	67.393

The other equations are the same as what was used for the unassisted potassium carbonate model.

5.2.2 Results for H_3BO_3/K_2CO_3 Model Simulations

The results from the simulated boric acid promoted potassium carbonate capture process are presented in Table 5.5 below. The comparison of the various catalysed systems and the base case K_2CO_3 system are included on the same table.

Table 5.5: Results for K_2CO_3- H_3BO_3-CO_2-H_2O system

System performance	40wt% K_2CO_3	40wt% K_2CO_3/2wt % H_3BO_3	40wt% K_2CO_3/4wt % H_3BO_3	40wt% K_2CO_3/6wt % H_3BO_3
CO_2 capture level, %	78.17	78.70	78.88	79.14
Reboiler duty, MJ/kgCO_2	2.76	2.75	2.75	2.75
Condenser duty, MJ/kgCO_2	1.22	1.22	1.22	1.21
Cooling duty, MJ/kgCO_2	1.17	1.17	1.18	1.18
Total duty, MJ/kgCO_2	5.15	5.14	5.15	5.14

The results from the catalysis of the hot potassium carbonate absorption process using boric acid, as summarised in Table 5.5, proves that although the mass transfer rate of the HPC process is enhanced as a result of the addition of small amounts of boric acid, the reboiler duty and the overall energy consumption of the process remains almost the same. This could be observed in almost all the cases of the promoted system where almost all the heat and cooling duties remain approximately the same, with only the 40 wt% K_2CO_3/2 wt% H_3BO_3 system and 40 wt% K_2CO_3/6 wt% H_3BO_3 system demonstrating slight total energy reduction of 0.01 MJ/kgCO_2. Another observation that could be made from the same table is that the improvement in the carbon capture efficiency of the HPC process increases with increasing amount of boric acid, with the 40 wt% K_2CO_3/6 wt% H_3BO_3 blended solution yielding the highest improvement of 0.97%. It is, however, worth noting that piperazine appears to have a higher impact on the system performance in the MEA carbon capture process than the performance of boric acid in the K_2CO_3 system. As displayed earlier in Table 5.3, the addition of 5 wt% PZ is able to increase the decarbonisation efficiency in the MEA system by 1.34% and simultaneously reduce the total energy usage by 2.21%. In the case of the 7 wt% PZ/23 wt% MEA, these figures are 1.43% and 1.86% respectively. Comparing these results to the performance of boric acid as a promoter in the K_2CO_3 system, one could conclude that PZ is a better promoter than H_3BO_3. The reason for this poor performance of the blended solution in the latter system could be as a result of the high temperature at which the system is operated. This conclusion could be drawn based on the findings from Gosh et al. 2009, which observed that boric acid only functions as an effective promoter in the K_2CO_3-based capture system at temperatures of 50 to 80 °C. Using the results obtained here and the results from the parametric analyses presented earlier in this section optimised systems for the boric acid assisted HPC were proposed. The model of this optimised HPC system is explored in the next section.

5.3 OPTIMISED H_3BO_3/K_2CO_3 CAPTURE SYSTEM THROUGH SENSITIVITY ANALYSIS

To design the optimised H_3BO_3/K_2CO_3 system, 6 wt% boric acid was added to the optimised K_2CO_3 system. A comparison of the optimised values which were used in the optimised model and the original figures in the non-optimised system are presented in Table 5.6.

Table 5.6: Comparison of Original and Optimised H_3BO_3/K_2CO_3 Parameters

Parameters	Original	Optimised
Packing type	Raschig Norton Metal-32	Flexipac Koch Metal 1Y
Lean solvent concentration, wt%	40	45
Boric acid concentration, wt%	-	6
Lean solvent flowrate, kg/hr	11,170	11,270
Absorber operating pressure, atm	15	20

5.3.1 Results for Optimised H_3BO_3/K_2CO_3 Capture Process

The results obtained from the optimised H_3BO_3/K_2CO_3 capture model simulation is compared to the base case simulation results for K_2CO_3 and MEA on Tables 5.7.

Table 5.7: Comparison of results for optimised H_3BO_3/K_2CO_3 to base case K_2CO_3 and MEA capture processes

System performance	Optimised H_3BO_3/K_2CO_3	K_2CO_3 Base Case	Deviation (%)	MEA Base Case	Deviation (%)
CO_2 capture level, %	90.01	78.17	15.15	85.96	4.71
Reboiler duty, MJ/kgCO_2	2.40	2.76	13.04	3.98	39.70
Condenser duty, MJ/kgCO_2	1.13	1.22	7.38	0.815	38.65
Cooling duty, MJ/kgCO_2	1.07	1.17	8.55	1.495	28.43
Heat Exchanger duty, MJ/kgCO_2	-	-	-	2.32	-
Total duty, MJ/kgCO_2	4.60	5.15	10.68	8.61	46.57

The results presented in Table 5.7 show the high performances of the optimised H_3BO_3/K_2CO_3 capture model. In the results for optimised H_3BO_3/K_2CO_3 model, the improvement in decarbonisation efficiency is even more interesting than in the optimised K_2CO_3 (which was previously discussed in Chapter 4), as the optimised process attained 4.71% rise over the base case result for MEA and 15.15% increase over the base case result for K_2CO_3. Compared to the optimised K_2CO_3-based capture process, the optimised H_3BO_3/K_2CO_3 capture process has a superior capture in the magnitude of 2.25%. In the case of the lean solvent stream cooling duty, the current system equally demonstrates better performance over the un-optimised base case scenarios in the K_2CO_3 and MEA systems. Even though the reboiler duty and total energy requirement of the optimised H_3BO_3/K_2CO_3 are slightly higher than that

observed earlier in the optimised K_2CO_3 system, the energy usage here is still much lower than the requirement in the un-optimised K_2CO_3 and MEA systems. This demonstrates that the optimised boric acid promoted HPC capture process is equally a highly energy-efficient carbon capture technology.

5.4 SUMMARY OF CHAPTER 5

The simulation objectives of this chapter are to understand the system performances of PZ promoted MEA capture process and H_3BO_3 assisted K_2CO_3 absorption system. The effectiveness of PZ and H_3BO_3 as promoters is discussed. Moreover, various blended solutions of boric acid and potassium carbonate are studied to investigate the sensitivity of the system performance to variations in boric acid concentration. A similar study is performed for various blended solutions of PZ and MEA. Based on these analyses, it is shown that PZ demonstrates higher promotion efficacy in the MEA-based capture process than the performance of H_3BO_3 in the K_2CO_3-based capture process. An optimised H_3BO_3/K_2CO_3 capture process is proposed to increase the carbon capture level by approximately 2% over the optimised K_2CO_3 capture system. However, it is concluded in this chapter that the optimised K_2CO_3 absorption process is slightly more energy-efficient than the optimised H_3BO_3/K_2CO_3 capture process. The major achievement in this chapter is the demonstration of the performance of H_3BO_3 as a promoter in the HPC-based capture technology.

CHAPTER 6

MODIFIED PROCESS CONFIGURATIONS

This chapter investigates the impact of process modifications on the performance of the MEA and HPC capture processes.

6.1 MODIFIED CONFIGURATIONS FOR MEA CAPTURE PROCESS

Several modified configurations have been presented in many papers to have benefits of improving upon the performances of the MEA capture process. The literature reports are however limited in the fact that the modified processes are only disclosed to either have higher carbon capture efficiency or attain lower reboiler heat duty. Information on how these modified processes affect the condenser duty, the cooling duty, heat exchanger duty, and CO_2 product purity are scarce in literature. Also, data on the added energy requirement for added equipment such as compressors which are used in some modifications, are lacking in the literature. Thus, the purpose of conducting simulation on the majority of the modified processes in the current study is to close these research gaps.

6.1.1 Absorber Intercooling

The intercooled absorber modification, as presented in Figure 6.1, is a well-researched configuration which has been reported to have the tendency of enhancing the absorption process in the absorber column. Since the CO_2 absorption process is exothermic by nature, the temperature in the absorber column increases as the reaction progresses, limiting the mass transfer efficiency of the chemical solvent. When a portion of the liquid mixture in the absorber system is withdrawn at the side of the column, cooled down and reinjected into the column at a lower temperature, the system is able to maintain the column internal temperature at a moderate value. This moderate column temperature is able to enhance the mass transfer efficiency of the overall CO_2 absorption process. Many researchers have reported that absorber intercooling has the capability of increasing the carbon capture efficiency of the process, decreasing the absorber column height required to attain a particular plant performance and also

reduces the lean solvent flowrate in some cases. Some researchers also indicated that since the CO_2 loading of the rich solvent stream increases upon the modification, the overall energy requirement during regeneration also decreases. Rezazadeh et al. 2017 however reported that the absorber intercooling modification is most effective only with the lean solvent loading of 0.30 to 0.34 (mol CO_2/mol MEA). To study the performance of this modification in the current work, 100 kg/hr of liquid mixture was withdrawn from stage 3 of the absorber column (stream S1), cooled down from 72.5 °C to 35 °C (in COOLER) and reinjected into the 2nd stage of the column (stream S2). The CO_2 loading in the lean solvent stream was calculated to be 0.303 mol CO_2/mol MEA, which is within the good for absorber intercooling as declared by Rezazadeh et al. 2017.

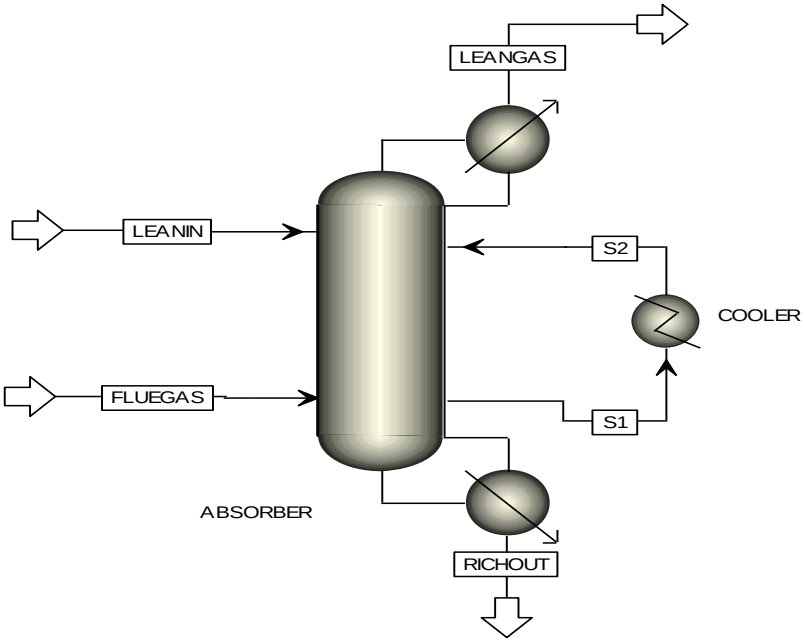

Figure 6.1. Intercooled Absorber

6.1.1.1 Intercooled Absorber Results

The results from the intercooled absorber simulation are compared to the conventional MEA baseline results in Table 6.1 below.

Table 6.1: Comparison of Results for MEA and Intercooled Absorber

System performance	Conventional MEA base case	Intercooled Absorber	Deviation (%)
CO_2 capture level, %	85.96	91.01	5.87
CO_2 product purity, vol%	99.99	99.99	0
Reboiler temp, ^oC	121.2	122.9	1.4

Reboiler duty, MJ/kgCO_2	3.98	3.86	3.02
Condenser duty, MJ/kgCO_2	0.815	0.771	5.40
Cooling duty, MJ/kgCO_2	1.495	1.426	4.62
Heat Exchanger duty, MJ/kgCO_2	2.32	2.09	9.91
Total duty, MJ/kgCO_2	8.61	8.15	5.34

The results from the intercooled absorber, as shown in Table 6.1, demonstrates that this modification has the capability to achieve improvements in almost all aspects of heat duty and cooling duty in the capture system. Applying the intercooled absorber modification has proven to increase the carbon capture efficiency by 5.87% at a lower heat duty (3.02% less) as compared to the values in the conventional system without the intercooler. The condenser duty and cooling duty in all the cooler systems in the modified process have shown to require less energy than is needed in the unmodified process. The high energy saving of 9.91% heat duty achieved in the lean/rich solvent cross heat exchanger might probably be as a result of the higher reboiler temperature in the modified process. Since the reboiler temperature is higher, the lean solvent exiting the stripper system is also at a higher temperature, contributing to a higher heating effect in the cross heat exchanger, and requiring less heat from an external source. The total energy saving of 5.34% over the conventional configuration is a much higher value than attained in the PZ promoted system. This indicates that if the capital and operational cost of adding an extra cooling system is negligible, then the intercooled absorber modification might be a preferred improvement strategy over the catalysis with piperazine in an MEA-based capture process.

6.1.2 Flue Gas Precooling

The flue gas precooling configuration works similar to the intercooled absorber modification. It is believed by some researchers that cooling the flue gas to a moderate temperature, below what is attainable in the direct contact cooler before feeding into the absorber is capable of improving the thermodynamics of the mass transfer rate and enhance the overall absorption level. To investigate the full impact of this modification on the MEA-based capture system, the flue gas was precooled from its initial temperature of 57.9 °C to 40 °C. All other parameters in the model, aside from the flue gas temperature, were maintained at their initial value during this analysis.

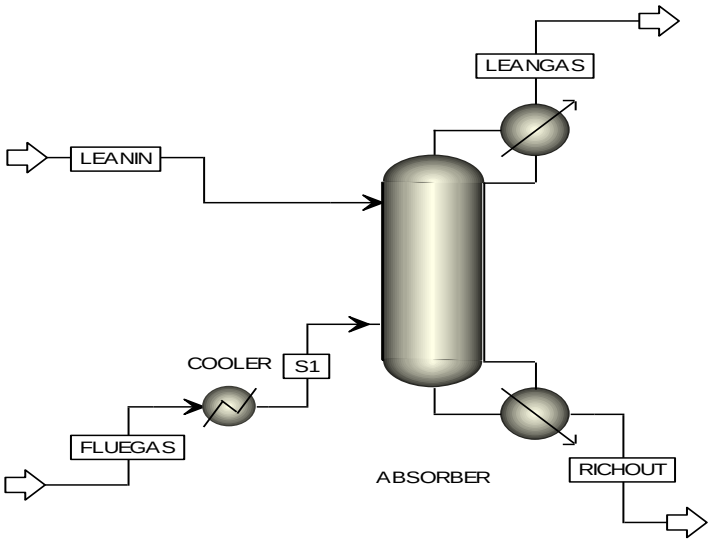

Figure 6.2. Flue Gas Precooling

6.1.2.1 Flue Gas Precooling Results

The results from the flue gas precooling simulation are compared to the conventional MEA baseline results in Table 6.2 below.

Table 6.2: Comparison of Results for MEA and Flue Gas Precooling

System performance	Conventional MEA base case	Flue Gas Precooling	Deviation (%)
CO_2 capture level, %	85.96	86.97	1.2
CO_2 product purity, vol%	99.99	99.99	0
Reboiler temp, ^oC	121.2	120.9	0.2
Reboiler duty, MJ/kgCO_2	3.98	3.98	0
Condenser duty, MJ/kgCO_2	0.815	0.800	1.8
Cooling duty, MJ/kgCO_2	1.495	1.578	5.6
Heat Exchanger duty, MJ/kgCO_2	2.32	2.38	2.6
Total duty, MJ/kgCO_2	8.61	8.74	1.5

The results from the flue gas precooling modification shows that this modification is not an energy-saving modification. The reason being that although the system is able to attain a slightly higher carbon capture efficiency, it has no impact on the reboiler duty requirement for the solvent regeneration. Even though there was a slight decrease in the condenser duty due to the flue gas precooling modification, the overall cooling

energy requirement in the modified process was higher by 5.6% over the conventional configuration. The lean/rich cross heat exchanger was seen to have also experienced a slight increase in heat duty, about 2.6% over the conventional configuration without the flue gas pre-cooling. Ultimately, the total energy requirement of the modified process is 1.5% higher than it is the case in the conventional process.

6.1.3 Flue Gas Split

The flue gas split configuration, shown in Figure 6.3, involves the insertion of the flue gas feed at multiple stages in the absorber column. This allows better control of the absorption stages in the column while assisting in the control of high temperatures that usually occur as the exothermic absorption process progresses (Oh et al. 2016). To fix the split streams at appropriate stages in the column, it is good to understand the temperature profile of the absorber column to find out the stages with the peak temperatures. Since the peak temperatures in the current study were discovered to be located on the middle stages of the absorber column, it was decided to split 15% of the flue gas stream (stream S1) into the 15^{th} stage of the column while the remaining 85% (stream S2) was injected on the last stage (stage 20).

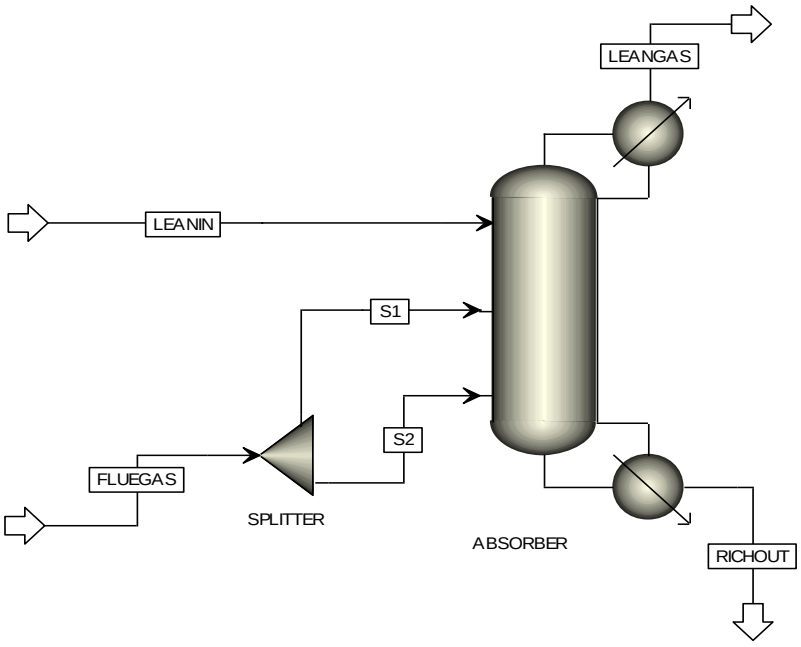

Figure 6.3. Flue Gas Split

6.1.3.1 Flue Gas Split Results

The results from the flue gas split simulation are compared to the conventional MEA baseline results in Table 6.3 below.

Table 6.3: Comparison of Results for MEA and Flue Gas Split

System performance	Conventional MEA base case	Flue Gas Split	Deviation (%)
CO_2 capture level, %	85.96	88.99	3.52
CO_2 product purity, vol%	99.99	99.99	0
Reboiler temp, ^oC	121.2	120.5	0.58
Reboiler duty, MJ/kgCO_2	3.98	3.86	3.02
Condenser duty, MJ/kgCO_2	0.815	0.724	11.17
Cooling duty, MJ/kgCO_2	1.495	1.410	5.69
Heat Exchanger duty, MJ/kgCO_2	2.32	2.04	12.07
Total duty, MJ/kgCO_2	8.61	8.03	6.74

When Oh et al. 2016 studied the same process configuration, the authors reported that the flue gas split modification is able to reduce the energy cost of the capture plant by 7.4% over the conventional configuration. The results of the current study, as presented in Table 6.3, shows similar improvement as the total energy requirement of the capture process decreases by a figure of 6.74% over the standard unmodified process. In addition to the energy-saving benefits of this modification, the results of the current study also demonstrate the capabilities of the flue gas split configuration in improving the carbon capture efficiency by a figure of 3.52% over the standard unmodified process. This figure appears to be greater than that observed in the flue gas pre-cooling, indicating that the flue gas split configuration is a preferable modification to be applied to the flue gas stream as compared to the pre-cooling system.

6.1.4 Stripper Inter-heating

The inter-heated stripper system, also commonly referred to as ‘stripper inter-heating configuration’ is shown in Figure 6.4 This modification is known to be an energy-saving modification, and is mostly applied to the stripper column.

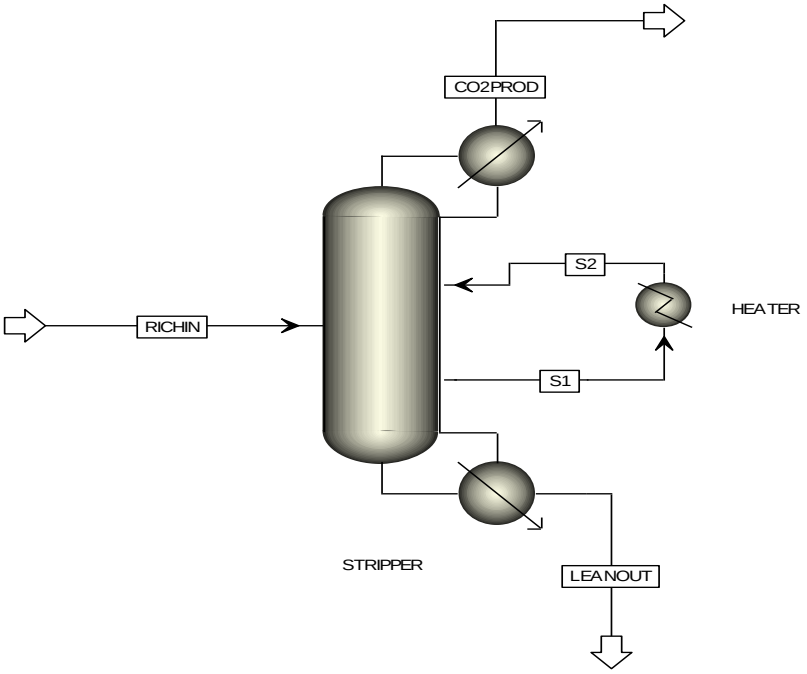

Figure 6.4. Inter-heated Stripper

The configuration is similar to the absorber intercooling, only, in this case, the liquid mixture withdrawn from the side of the stripper is heated up as opposed to cooling in the intercooled absorber system. Several researchers have reported the energy-saving benefits of this modification for MEA-based capture processes. Some recent works have also investigated the application of this modification in an aqueous ammonia system (Liu 2018; Li[d] et al. 2016). To access the impact of this modification on the total energy performance of the MEA-based capture process, 100 kg/hr of liquid mixture was withdrawn from the 5th stage (stream S1) of the stripper column, heated up from 87 °C to 115 °C (in HEATER), and reinjected into the 6th stage of the column (stream S2).

6.1.4.1 Inter-heated Stripper Results

The results from the inter-heated stripper simulation are compared to the conventional MEA baseline results in Table 6.4 below.

Table 6.4: Comparison of Results for MEA and Inter-Heated Stripper

System performance	Conventional MEA base case	Inter-heated Stripper	Deviation (%)
CO_2 capture level, %	85.96	90.00	4.70
CO_2 product purity, vol%	99.99	99.99	0
Reboiler temp, ^oC	121.2	122.7	1.24
Reboiler duty, MJ/kgCO_2	3.98	3.73	6.28
Condenser duty, MJ/kgCO_2	0.815	1.204	47.73
Cooling duty, MJ/kgCO_2	1.495	1.470	1.67
Heat Exchanger, MJ/kgCO_2	2.32	1.99	14.22
Heater duty, MJ/kgCO_2	-	0.65	-
Total duty, MJ/kgCO_2	8.61	9.04	4.99

The results of the performance of the MEA capture process under the inter-heated stripper configuration as seen in Table 6.4 confirm that this modification has high reboiler duty saving advantages. The carbon capture efficiency is also noted to have increased from 85.96% to 90%. The improvements in these two aspects of the capture system are the highest obtained so far for all the modifications. Nevertheless, the condenser cooling duty is observed to have experienced an increase of 47.73% over the standard case. This high cooling duty could be as a result of the higher temperature of the overhead vapour, which might have been caused by the inter-heating process. Since the inter-heating is carried out at the top half of the column, the vapour entering the condenser is expected to have higher temperatures in this scenario, requiring higher cooling duty. The additional heat duty required for the added heater equipment in the system also requires extra energy of 0.65 MJ per every CO_2 captured. This has ultimately resulted in the modified process requiring an extra 4.99 % energy over the conventional system. This observation indicates that although inter-heated stripper has very high potentials of decreasing the required energy in the reboiler duty, it is unlikely that the same modification is able to reduce the total energy requirement in a typical MEA-based capture process.

6.1.5 Rich Solvent Split

The rich solvent split is another well-known modification which is applicable in many solvent-based post-combustion carbon capture processes. The flowsheet of this modification is shown in Figure 6.5. As presented on the flowsheet, the principle is to split the CO_2 rich solvent stream into two or more streams (usually two) and inject them at different stages of the stripper column. One split stream is heated up in the rich/lean solvent cross heat exchanger while the other is directly introduced into the stripper column without heating. In many of these modifications, the cold stream is introduced at a higher stage in the column than the heated stream. This allows the cold stream to benefit from the heat in the vapour generated at the base of the column, reducing the volume of solvent mixture that needs to be heated up in the reboiler system, and ultimate decreasing the heat duty of the regeneration process. Alternatively, the vapour stream travelling up the column has the chance to strip off CO_2 from the cold rich stream introduced at the top section, thereby increasing the whole desorption process.

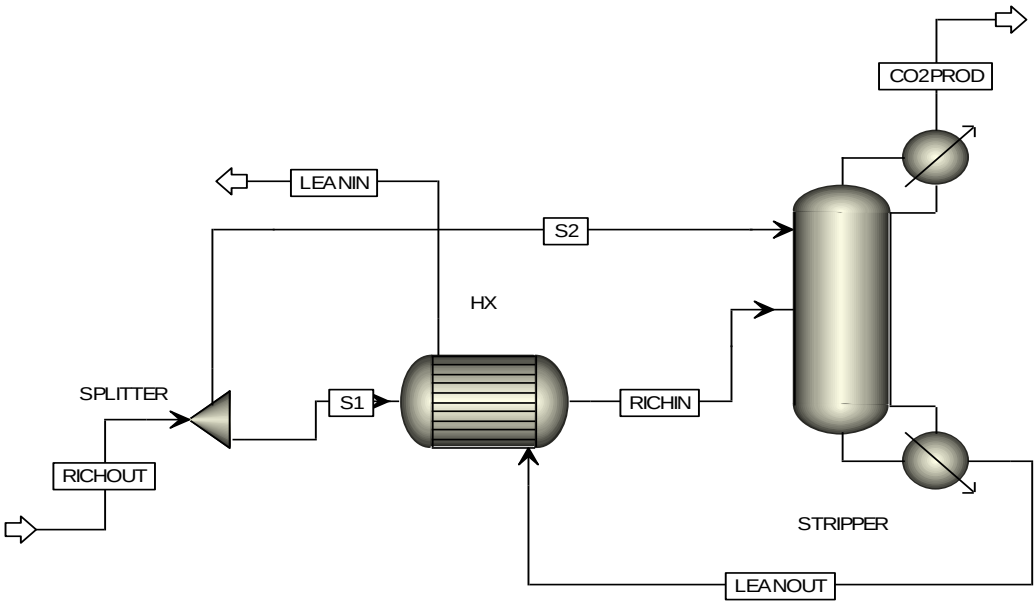

Figure 6.5. Rich Solvent Split

It is reported that this modification can achieve approximately 7 to 8% energy savings in the reboiler heat requirement as compared to the standard unmodified process (Xue et al. 2017; Li[b] et al, 2016). To ascertain the impact of this modification on all aspects of energy requirement in the MEA capture system, 10% of the rich solvent stream was split into the 2nd stage of the stripper column (stream S2) while the remaining 90% was

heated up in the cross heat exchanger before being introduced onto the 8th stage of the column (stream RICHIN).

6.1.5.1 Rich Solvent Split Results

The results from the rich solvent split simulation are compared to the conventional MEA baseline results in Table 6.5.

Table 6.5: Comparison of Results for MEA and Rich Solvent Split

System performance	Conventional MEA base case	Rich Solvent Split	Deviation (%)
CO_2 capture level, %	85.96	86.46	0.58
CO_2 product purity, vol%	99.99	99.99	0
Reboiler temp, ^oC	121.2	121.9	0.58
Reboiler duty, MJ/kgCO_2	3.98	3.75	5.78
Condenser duty, MJ/kgCO_2	0.815	0.441	45.89
Cooling duty, MJ/kgCO_2	1.495	1.522	1.81
Heat Exchanger duty, MJ/kgCO_2	2.32	1.98	14.66
Total duty, MJ/kgCO_2	8.61	7.69	10.69

Concluding from the performance of the MEA capture process obtained by splitting the rich solvent stream into two, as tabulated in Table 6.5, it is notable that the rich solvent stream has the highest improvement in decreasing the cooling duty demand in the stripper condenser. This could be as a result of the lower temperature of the vapour stream that enters the condenser system. Since the feed stream at the top of the stripper system is the cold stream, which strains heat from the rising vapour stream, the temperature of the vapour stream that eventually enters the condenser vessel is lesser than that it was in the standard unmodified process. This lower temperature demands less energy to achieve the required cooling in the condenser, thereby minimising the energy consumption. In the same vein, since the flowrate of the stream that is channelled through the cross heat exchanger is now lesser as a result of the splitting, less energy is required to heat up the rich solvent stream to the desired temperature. This explains why the splitting of the rich solvent stream also displays an added benefit of decreasing the energy consumption of the heat exchanger system. The reboiler heat duty also experienced a reduction of 5.78% over the conventional process, which is

quite close to the values reported in literature. The cooling duty in the lean solvent cooler, however, experienced a minimal increase in value which is approximately 1.81% over the standard value, because of the higher reboiler temperature attained in the modified process. Also, since there is less cooling work performed by the lean solvent stream in the cross heat exchanger because of the lesser flowrate of the rich solvent that was fed to the heat exchanger, the temperature of the lean solvent stream exiting the heat exchanger turns to be higher than it is in the standard configuration. This requires higher cooling energy to bring the lean solvent stream to the needed low temperature. That notwithstanding, the carbon capture efficiency was observed to attain a higher value by a small incremental percentage of 0.58%, and due to the high energy savings attained in many sections of the system, a total energy reduction of 10.69% was achieved in the modified process.

6.1.6 Lean Vapour Compression

The lean vapour compression also falls among the energy-saving modifications, although it is equally reported by some researchers to double as an improved-capture modification. As displayed on the diagram in Figure 6.6, the principle is to flash the lean solvent stream and retrieve the vapour for reuse in the stripper column. The vapour stream which is retrieved from the overhead of the flasher is compressed and reinjected into the stripper column. This reduces the steam demand from the reboiler system and ultimately results in minimising the regeneration energy consumption. The only drawback of this modification is the additional two or more extra equipment, which contributes to an increased capital cost. There is also the need to consider the energy consumption in this added equipment to ensure that the total energy demand is actually lower than the standard value. To discover the total effect of this modification on the MEA-based capture process, the lean vapour stream was flashed at approximately 1 bar to retrieve 5% (by mole) of the stream flowrate as vapour, containing 98.4% H_2O, 1.2% CO_2 and 0.4% MEA by mole. This stream was then compressed to a pressure of 2 atm and reinjected into stage 18 of the stripper column.

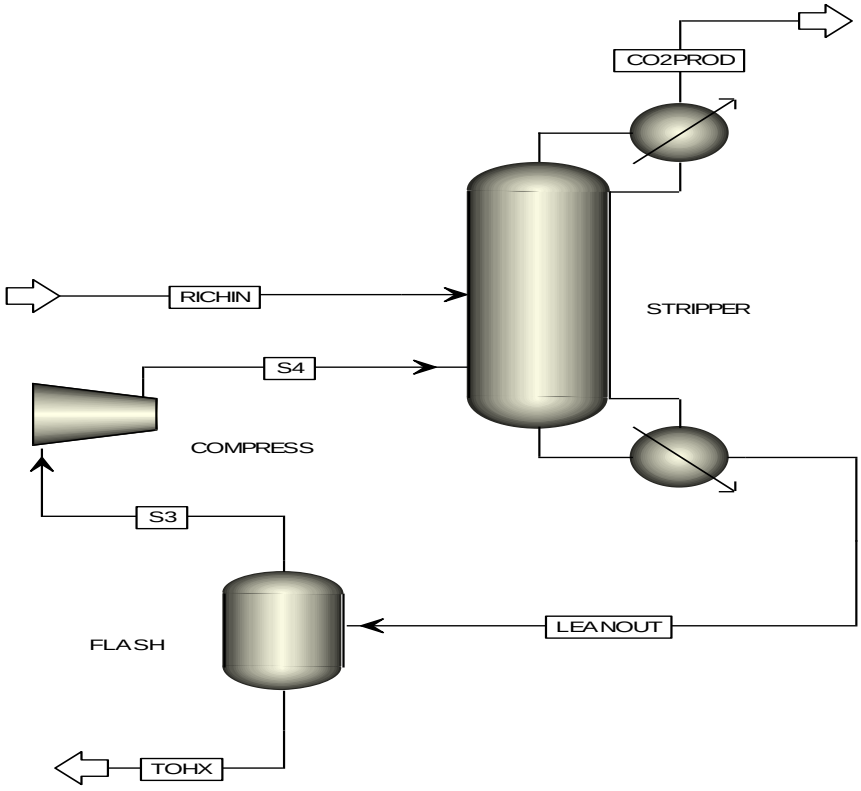

Figure 6.6. Lean Vapour Compression

6.1.6.1 Lean Vapour Compression Results

The results from the lean vapour compression simulation are compared to the conventional MEA baseline results in Table 6.6 below.

Table 6.6: Comparison of Results for MEA and Lean Vapour Compression

System performance	Conventional MEA base case	Lean Vapour Compression	Deviation (%)
CO_2 capture level, %	85.96	87.34	1.61
CO_2 product purity, vol%	99.99	99.27	0.72
Reboiler temp, ^oC	121.2	120.7	0.41
Reboiler duty, MJ/kgCO_2	3.98	2.76	30.65
Condenser duty, MJ/kgCO_2	0.815	0.707	13.25
Cooling duty, MJ/kgCO_2	1.495	0.802	46.35
Heat Exchanger duty, MJ/kgCO_2	2.32	2.24	3.45
Compressor duty, MJ/kgCO_2	-	0.082	-
Flasher duty, MJ/kgCO_2	-	0.335	-
Total duty, MJ/kgCO_2	8.61	6.93	19.51

The results from the lean vapour compression, as shown in Table 6.6, portrays this modification as one of the highest energy saving modifications. Apart from attaining very high reboiler duty minimisation, which is what this modified configuration is by

and large acknowledged for, it is also shown here that this modification equally reduces the cooling demand for the recycled lean solvent stream. This is possible because the lean solvent stream is completely liquid in this scenario as opposed to a mixture of liquid and vapour in the standard modification. For this reason, there is hardly any latent heat of condensation required to first convert any vapour portion of the lean solvent stream before cooling down to the desired low temperature. The high energy reduction of 46.35% in the cooling duty, 30.65% in the reboiler duty and 13.25% in the condenser duty has resulted in an overall energy scale-down of 19.51% over the standard configuration. The added advantage of 1.61% increased carbon capture efficiency demonstrates that if the added cost of the extra equipment and their maintenance has less relevance in the total cost of running this process, then the lean vapour compression is a very promising configuration for an improved absorption process.

6.1.7 Rich Solvent Preheating

As compared to stripper inter-heating and lean vapour compression, the rich-solvent preheating configuration in Figure 6.7 is a much less investigated heat integrated modification applied in solvent-based absorption processes. The principle of this modification is to preheat the rich solvent stream after it exits the rich/lean solvent heat exchanger before it is introduced into the stripper column.

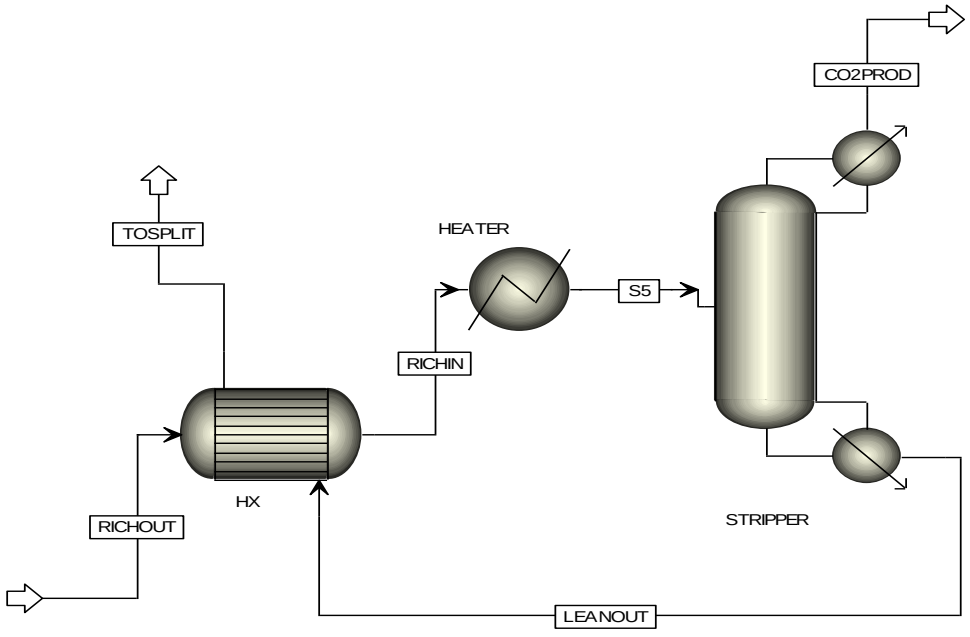

Figure 6.7. Rich Solvent Preheating

This preheating helps to attain a higher temperature in the cross heat exchanger. Since the rich solvent stream is already at a high temperature, the heat demand to attain a particular level of CO_2 desorption in the stripper system is less. This, in turn, reduces the steam demand by the reboiler system, and eventually lessens the reboiler duty. In a patent obtained by Gelowitz et al. in 2015, the authors proposed that the rich solvent stream could be preheated by the hot flue gas stream before it is cooled down in the direct contact cooler. This idea works effectively to redeem the heat from the flue gas stream, which would have been wasted in the direct contact cooler. It equally serves as a means of reducing the amount of cold water required to achieve a certain level of cooling in the direct contact cooler. The current study, therefore, assumes that the preheating is accomplished by using the hot flue gas stream. The heat duty of the heater used in the preheating is therefore ignored in calculating the total energy demand of the system. The impact of preheating the rich solvent stream from a temperature of 90 °C to 115 °C on an MEA-based capture process is demonstrated in this study.

6.1.7.1 Rich Solvent Pre-Heating Results

The results from the rich solvent pre-heating simulation are compared to the conventional MEA baseline results in Table 6.7 below.

Table 6.7: Comparison of Results for MEA and Rich Solvent Pre-Heating

System performance	Conventional MEA base case	Rich Solvent Pre-Heating	Deviation (%)
CO_2 capture level, %	85.96	86.97	1.17
CO_2 product purity, vol%	99.99	99.99	0
Reboiler temp, ^oC	121.2	121.1	0.08
Reboiler duty, MJ/kgCO_2	3.98	3.43	13.82
Condenser duty, MJ/kgCO_2	0.815	1.758	115.71
Cooling duty, MJ/kgCO_2	1.495	1.888	26.29
Heat Exchanger duty, MJ/kgCO_2	2.32	1.90	18.10
Total duty, MJ/kgCO_2	8.61	8.98	4.30

The results obtained from the rich solvent preheating modification on Table 6.7 indicates that this modification could be a good choice for scaling down the heat duty of the capture process, but not a good choice to minimise the total energy requirement

of the system. This is because, although the preheating contributes to decreasing the reboiler duty requirement and the heat exchanger heat duty by 13.82% and 18.10% respectively, the hike in the condenser duty and the cooling duty nullifies the improvement achieved by the modification. This could be as a result of the higher temperature of the whole capture system which comes along with the preheating. The more vapour produced in the rich solvent stream as a result of the preheating implies more vapour will be entering the condenser and cooler vessels. The extra latent heat of condensation required to convert the extra vapour into liquid contributes to the hiking of the overall cooling demand in the system. Despite the 1.17% improvement in carbon recovery efficiency obtained over the conventional configuration, the ultimate 4.30% rise in total energy requirement makes this modification generally unattractive as a heat integration configuration.

6.2 MODIFIED PROCESS CONFIGURATIONS FOR K_2CO_3 CAPTURE PROCESS

Literature information has disclosed several modified configurations geared towards the improvement upon the absorption efficiency or reduction in the energy usage in the post-combustion carbon capture systems. Whereas the configurations investigated are broad, the chemical absorbents covered are limited. The majority of these modifications are seen to be applied to amine-based capture processes, especially MEA, and ammonia-based capture technologies. Information on modified configurations for potassium carbonate-based capture processes are rare to find in literature. This study, therefore, endeavours to close this research gap by examining the application of these modified configurations in the HPC capture process. The optimised K_2CO_3 process is used in this investigation, and the configurations studied are the flue gas splitting, flue gas pre-cooling, absorber intercooling, rich solvent splitting, rich solvent pre-heating, inter-heated stripper, and lean vapour compression. The sections that follow discuss the listed modified configurations that have been studied in this work and how they impact the overall performance of the optimised K_2CO_3 absorption technology.

6.2.1 Results for Flue gas splitting

Splitting the flue gas in the case of MEA-based capture process was seen to have improved carbon capture efficiency and reduced the energy requirement of the system. The focus of the application of this modification in the HPC capture system is to determine how this configuration influences the performance of the process with regards to cooling and heat duties. To do this, 10% of the flue gas stream was split and fed into different stages of the absorber column while the remaining 90% was fed to stage 12, which is the last bottom stage of the column. The results obtained are summarised in Table 6.8.

Table 6.8: Comparison of results for optimised K_2CO_3 and flue gas split modification

System performance	Optimised K_2CO_3	Split stage			
		10	8	6	4
CO_2 capture level, %	88.03	88.03	88.04	88.04	88.04
Reboiler duty, MJ/kgCO_2	2.35	2.35	2.35	2.35	2.35
Condenser duty, MJ/kgCO_2	1.12	1.12	1.12	1.12	1.12
Cooling duty, MJ/kgCO_2	1.06	1.06	1.06	1.06	1.06
Total duty, MJ/kgCO_2	4.53	4.53	4.53	4.53	4.53

In all four cases of the flue gas split modified configurations shown in Table 6.8, it appears that the splitting has no significant influence on the performance of the hot potassium carbonate capture technology. Only a slight increase in carbon capture efficiency is seen in the cases for the split stage 8, 6 and 4. In the application of this modification to the MEA-based capture technology, it was believed that a relatively cold flue gas stream which is split and fed at a higher stage in the absorber column works perfectly just as the intercooled absorber by enhancing the thermodynamics of the absorption process and increasing mass transfer rates. These enhancements are translated into richer solvent stream fed to the stripper column, and ultimately higher carbon capture and lower heat duty. In the case of the HPC process, however, the flue gas stream is at a high temperature. Feeding a split section of the flue gas stream at a higher stage in the absorber column, therefore, achieves no cooling effect in the system. This could explain why the flue gas split modification hardly has any impact on the overall system performance in the K_2CO_3 capture technology.

6.2.2 Results for Flue Gas Precooling

The flue gas pre-cooling was performed by cooling the flue gas stream from 110 to 100 and 90 centigrade degrees to see how this modification could influence the decarbonisation efficiency and energy usage in the HPC-based capture system. The results obtained at the various temperatures are tabulated below.

Table 6.9: Comparison of results for optimised K_2CO_3 and flue gas precooling modification

System performance	Optimised K_2CO_3	Precooling temperature, °C			
		100	%Diff.	90	%Diff.
CO_2 capture level, %	88.03	90.87	3.23	93.06	5.71
Reboiler duty, MJ/kgCO_2	2.35	2.44	3.83	2.51	6.81
Condenser duty, MJ/kgCO_2	1.12	1.10	1.79	1.09	2.68
Cooling duty, MJ/kgCO_2	1.06	1.03	2.83	1.01	4.72
Total duty, MJ/kgCO_2	4.53	4.57	0.88	4.61	1.77

The results from the flue gas precooling, as shown in Table 6.9, demonstrates that the modification is very effective in the K_2CO_3 system. The improvements of 3.23% and 5.71% achieved in the decarbonisation efficiency for precooled temperatures of 100 °C and 90 °C respectively are higher than the 1.2% improvement obtained for the same modification in the MEA system. Similar to the effect of this modification in the MEA system, the improvements in the carbon capture efficiency comes along with increment in the total energy usage of the system. Unlike in the MEA system where the modification has no impact on the reboiler duty but rather results in increased heat exchanger duty and cooling duty, the case of the K_2CO_3 system appears to be different. The reboiler duty increases in similar percentage magnitude as the increments observed in the carbon capture efficiency. In the case of the precooled temperature of 100 °C, where the modification recorded a 3.23% increase in the carbon capture efficiency, the reboiler duty also increased by 3.83%. Similarly, the increase of 5.71% carbon capture rate for the 90 °C precooled temperature also comes along with a 6.81% increase in the reboiler duty. This ultimately results in an increase of 1.77% in the total energy usage over the base case scenario.

6.2.3 Results for Intercooled Absorber

To demonstrate how the intercooled absorber configuration influences the performance of the hot potassium carbonate capture system, 100 kg/hr of the liquid mixture in the absorber column was withdrawn from stage 10, cooled down from about 113 °C to 70 °C and reinjected into different stages of the column. The results obtained are shown in Table 6.10.

Table 6.10: Comparison of results for optimised K_2CO_3 and intercooled absorber modification

System performance	Optimised K_2CO_3	Reinjection stage			
		8	6	4	2
CO_2 capture level, %	88.03	88.24	88.23	88.24	88.22
Reboiler duty, MJ/kgCO_2	2.35	2.35	2.35	2.35	2.35
Condenser duty, MJ/kgCO_2	1.12	1.12	1.12	1.12	1.12
Cooling duty, MJ/kgCO_2	1.06	1.07	1.07	1.07	1.07
Total duty, MJ/kgCO_2	4.53	4.54	4.54	4.54	4.54

As showcased in Table 6.10, it appears the intercooled absorber has a slightly higher impact on the HPC capture technology than the flue gas splitting. Whereas the total energy requirement experienced a slight scale-up of 0.01 MJ/kgCO_2 in all four cases of the modified process configuration, the capture efficiency experienced an increase of about 0.238% over the base case configuration in all four scenarios investigated. The higher total energy duty could be ascribed to the additional cooling requirement in the added cooler system. It could be seen from the table of results that this extra cooling equipment increased the total cooling duty in all four cases of the modified configuration by the same factor of 0.01 MJ/kgCO_2, which translated into the increased total energy usage in the modified systems. The improved carbon capture in all four cases could be attributed to the slight improvement in the mass transfer rate in the absorber column as a result of the cooling effect. The impact of the modification in the case of the HPC process, however, does not seem to match up to its application in the benchmarking amine solvent. The reason could be that as the absorber column is operating at a very high temperature in the HPC process, the cold stream which is reinjected into the system quickly assumes the temperature of the column and has little effect on the absorption process. To achieve a higher impact of this modification in the

HPC process, it might be advisable to increase the flowrate of the side stream withdrawn and decrease the cooling temperature a little more. All these strategies will, however, contribute to extra cooling duty in the system. Hence, an optimisation analysis is very crucial in determining the best parameters needed to increase the impact of intercooled absorber on the system performance of the hot potassium carbonate capture technique.

6.2.4 Results for Rich Solvent Splitting

To demonstrate the impact of rich solvent split on the hot potassium carbonate capture technology, a portion of the rich solvent stream was split and introduced on stage 2 of the stripper column as the remainder is fed to stage 3. The results for splitting 5%, 10%, 15%, 25% and 90% of the rich solvent stream are presented in Table 6.11 below.

Table 6.11: Comparison of results for optimised K_2CO_3 and rich solvent split modification

System performance	Optimised K_2CO_3	Split portion				
		5%	10%	15%	25%	90%
CO_2 capture level, %	88.03	86.74	86.81	86.87	86.97	87.65
Reboiler duty, MJ/kgCO_2	2.35	2.39	2.39	2.39	2.39	2.36
Condenser duty, MJ/kgCO_2	1.12	1.12	1.12	1.12	1.12	1.12
Cooling duty, MJ/kgCO_2	1.06	1.07	1.07	1.07	1.07	1.06
Total duty, MJ/kgCO_2	4.53	4.58	4.58	4.58	4.58	4.54

The results presented in Table 6.11 is an indication that the rich solvent split is not quite a good modification for the HPC capture process. The configuration of this modification in amine-based capture processes involves splitting the CO_2 rich solvent stream into two parts. One part, which is usually the smaller portion, is fed to an upper stage of the stripper column without heating in the lean/rich heat exchanger as shown in Figure 6.8. The second part which is heated up in the cross heat exchanger is introduced into the stripper at a lower stage than the cold stream. This allows for the cold stream fed at the upper stage to benefit from heat in the vapour streams climbing up the column and decreases the work done by the reboiler system to supply enough heat for the regeneration system. As this heat exchange occurs between the vapour stream and the cold rich solvent stream, mass transfer of CO_2 from the cold liquid

stream to the hot vapour stream also occurs simultaneously. This works perfectly to reduce the reboiler duty, condenser duty and increase the carbon capture efficiency in the MEA-based capture scenario as presented in Table 6.5.

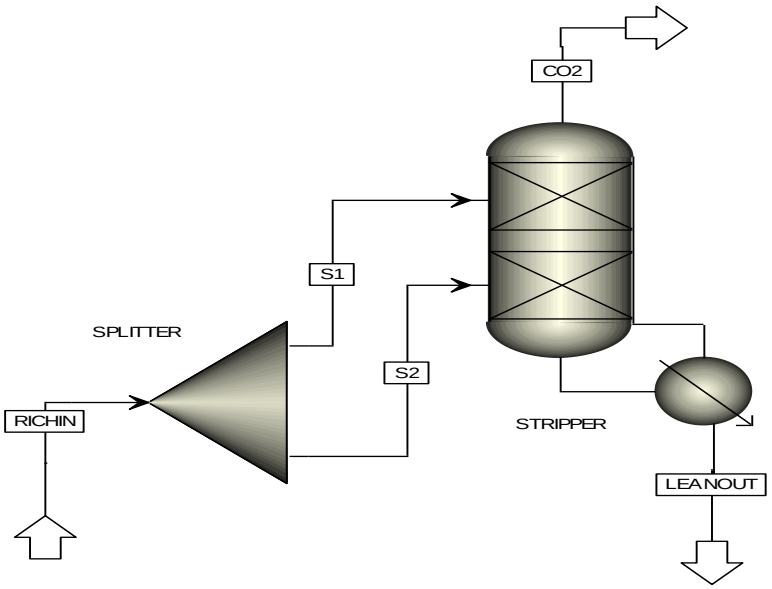

Figure 6.8. Rich Solvent Split in HPC Process

Unlike the rich solvent modification in the amine-based process, the modification in the hot K_2CO_3 capture process excludes the cross heat exchanger. This could be seen in Figure 6.8. The implication of this is that both split streams are hot and are only fed at two different stages of the stripper column. There is, therefore, no extra benefit of heat exchange and mass transfer between any cold liquid stream and hot vapour stream as a result of the modification as it is the case in the amine-based system. The larger portion of the stream is fed at a lower stage in the column and it only reduces the residence time of the stream in the stripper system. The contact time of vapour and liquid for mass transfer processes also decreases slightly. This results in a lower carbon capture rate in the HPC system, and ultimately, it adversely impacts the specific energy usage. However, as the portion of the rich solvent stream injected at the upper stage of the column increases however, the system performance improves. This is because an increased portion of the stream is now benefitting from longer residence time and mass transfer processes in the column. This is what accounts for the modified system nearly returning to normal operation performance when 90% of rich solvent split is fed at the upper stage of the column.

6.2.5 Results for Rich Solvent Preheating

To investigate the impact of this modification on the K_2CO_3 system, the rich solvent stream was heated up from 115 °C to 120 °C and 125 °C before feeding into the stripper column. The results obtained for the two different temperatures are shown in Table 6.12.

Table 6.12: Comparison of results for optimised K_2CO_3 and rich solvent pre-heating modification

System performance	Optimised K_2CO_3	Preheating temperature, °C			
		120	%Diff.	125	%Diff.
CO_2 capture level, %	88.03	86.18	2.10	83.86	4.74
Reboiler duty, MJ/kgCO_2	2.35	2.19	6.81	2.01	14.47
Condenser duty, MJ/kgCO_2	1.12	1.14	1.79	1.16	3.57
Cooling duty, MJ/kgCO_2	1.06	1.07	0.94	1.09	2.83
Pre-heating duty, MJ/kgCO_2	-	0.24	-	0.51	-
Total duty, MJ/kgCO_2	4.53	4.64	2.43	4.77	5.30

Concluding from the results presented in Table 6.12, the rich pre-heating configuration does not appear to be a good modification for the K_2CO_3 system. As compared to the performance of this modification in the MEA system, similar levels of reduction in the reboiler duty were attained. In the MEA system, the modification is able to reduce the reboiler duty by 13.82%, as shown in Table 6.7. In the case of the K_2CO_3 system, as displayed in Table 6.12, reductions of 6.81% and 14.47% were obtained for pre-heating the rich solvent stream to temperatures of 120 °C and 125 °C respectively. On the contrary, although this modification is able to yield improvement in the decarbonisation level in the MEA system, no such observation is made in the K_2CO_3 system. That notwithstanding, the two solvents experience similar hikes in total energy usage as a result of the modified configuration. An increase of 4.30% in total energy was observed in the MEA system while the highest value obtained in the K_2CO_3 system is 5.30%. These results further confirm that the hot K_2CO_3-based carbon capture technology performs better as a pressure swing absorption than a temperature swing absorption technique.

6.2.6 Results for Inter-Heated Stripper

To demonstrate the impact of the inter-heated stripper configuration on the system performance of the HPC process, 100 kg/hr of liquid solvent mixture was withdrawn from the 3rd stage of the stripper, heated up from approximately 102.5 °C to 115 °C and reinjected to different stages of the column. The results obtained for reinjection to these different stages are tabulated below.

Table 6.13: Comparison of results for optimised K_2CO_3 and inter-heated stripper modification

System performance	Optimised K_2CO_3	Reinjection stage number			
		4	5	6	7
CO_2 capture level, %	88.03	87.90	87.94	87.97	87.99
Reboiler duty, MJ/kgCO_2	2.35	2.31	2.31	2.31	2.31
Condenser duty, MJ/kgCO_2	1.12	1.12	1.12	1.12	1.12
Cooling duty, MJ/kgCO_2	1.06	1.06	1.06	1.06	1.06
Extra Heater duty, MJ/kgCO_2	-	0.04	0.04	0.04	0.04
Total duty, MJ/kgCO_2	4.53	4.53	4.53	4.53	4.53

Irrespective of the reinjection stage number, the inter-heated stripper appears not to have any significant impact on the system performance in the hot K_2CO_3 system. Unlike the MEA system, where the same configuration was able to improve the carbon capture efficiency by 4.7%, the HPC system experienced a slight decrease in the decarbonisation rate when the modification was introduced. Conversely, while the modification was observed to increase the total energy usage in the MEA system by 4.99% due to the extra heat duty requirement in the auxiliary heat exchanger, the total heat duty in the K_2CO_3 system remains the same for all reinjection stages. The results from Table 6.13 shows that the stripper inter-heating configuration has no meaningful influence on the system performance of the HPC-based carbon capture technology.

6.2.7 Results for Lean Vapour Compression

The lean vapour compression modification applied to the HPC capture process is the same modification applied to the MEA-based capture process in Figure 6.6. The hot lean solvent stream was flashed at a pressure of 1.05 atm to recover 5% of the stream in the vapour state. This overhead vapour stream, containing 89% water and 11% carbon dioxide, was compressed to 2 atm and reinjected to different stages of the

stripper column. The results obtained are displayed in Table 6.14 for the different reinjection column stages.

Table 6.14: Comparison of results for optimised K_2CO_3 and lean vapour compression modification

System performance	Optimised K_2CO_3	Reinjection stage number			
		7	6	5	4
CO_2 capture level, %	88.03	87.09	87.09	86.43	85.51
Reboiler duty, MJ/kgCO_2	2.35	1.46	1.47	1.49	1.51
Condenser duty, MJ/kgCO_2	1.12	1.12	1.13	1.13	1.14
Cooling duty, MJ/kgCO_2	1.06	1.00	1.01	1.01	1.02
Compressor duty, MJ/kgCO_2	-	0.06	0.06	0.06	0.06
Flasher duty, MJ/kgCO_2	-	0.79	0.79	0.80	0.82
Total duty, MJ/kgCO_2	4.53	4.43	4.46	4.49	4.55

The lean vapour compression has demonstrated to have a huge impact on the reboiler duty in the HPC capture system. This could be viewed in Table 6.14 as the modified configuration is able to scale down the heat duty in the reboiler system from 2.35 MJ/kgCO_2 to as low as 1.46 MJ/kgCO_2 in the case of compressed vapour reinjection to the 7^{th} stage of the stripper column. Similar energy minimisation effects were witnessed for the other reinjection stages as well. But a trend of poorer improvement in this regard is observed as the reinjection stage climbs up the stripper column, with the least improvement seen for reinjection stage 4. The reason for this phenomenon could be that as the compressed vapour stream is introduced at a higher stage in the stripper column, the stages below the reinjection stage do not benefit from the heat in the reinjected vapour stream. This puts a little bit more demand on the reboiler system and increases the duty eventually. The same reason is true for the poorer carbon capture efficiency experienced as the reinjection stage climbs up the column. As the reinjected vapour fails to have any vapour/liquid contact with the streams on the stages below the reinjection stage, the overall mass transfer in the stripper column decreases, forcing the desorption efficiency and ultimately the decarbonisation rate to lessen. The general observation made on the lower carbon capture level in the modified process over the standard configuration could be explained as a result of the lower pressure swing that exists between the compressed vapour stream and the stripper column. Due to the splitting of the lean vapour stream in the flash vessel, the rich solvent stream fed to the

stripper column eventually decreases. In this case, the rich solvent stream was seen to decrease from about 12696 kg/hr to 12368 kg/hr. The difference of 328 kg/hr is the compressed vapour stream which was recovered from the flash vessel. In the standard HPC configuration, the pressure swing between the rich solvent stream and the stripper column is 19 atm since the rich solvent is fed at 20 atm and the stripper operates at 1 atm. In the lean vapour compression configuration, however, the pressure swing between the compressed vapour stream and the stripper column is only 1 atm since the compression pressure is 2 atm. The lower pressure swing in the modified process decreases the overall desorption process in the stripper column. Therefore, since part of the rich solvent stream which could have benefitted from a higher pressure swing desorption in the standard configuration now experiences a lower pressure swing in the modified system, the overall carbon capture efficiency is affected negatively. This accounts for the lower carbon removal level seen in the lean vapour compression configuration over the standard HPC configuration. That been said, it is important to note that the modified configuration attains a good saving in total energy usage when the compressed vapour stream is fed at the lowest possible stage in the stripper column. This could be observed for the reinjection stage 7, where the total energy consumption slumped down from 4.53 MJ/kgCO_2 to 4.43 MJ/kgCO_2.

6.3 SUMMARY OF CHAPTER 6

This chapter concludes research objective #1 and fully address research question #2, which seeks to find out the impact of process modifications on the hot potassium carbonate-based capture process. The implementation of various modified process configurations for the MEA-based capture process and the K_2CO_3-based capture plant highlights the influence of the modifications on the latter process as compared to the former. The effect of the process modifications on the total heating and cooling duties, as well as the extra duties incurred due to the addition of auxiliary equipment, are discussed. The analyses performed in this chapter led to the following major conclusions:

1. The flue gas precooling modification is the best configuration to employ in enhancing the carbon capture level in the HPC absorption process as it is able to increase the capture efficiency from 88.03% to 93.06%, the greatest improvement recorded.

2. To reduce energy usage in the HPC-based capture plant, the lean vapour compression proves to be the first choice. Despite the auxiliary duties incurred as a result of adding extra equipment in this configuration, the modified process was able to scale down the total energy duty by 2.26%, which is the highest among all the modifications implemented for the HPC-based capture process.

CHAPTER 7

DYNAMIC SIMULATION AND CONTROL STUDY OF K_2CO_3 AND H_3BO_3/K_2CO_3-BASED CAPTURE PROCESS

The dynamic model was completed in the Aspen Plus Dynamics Modeller V10. The model was initially developed using the equilibrium-based thermodynamic modelling and exported to the dynamic platform upon the sizing of all the equipment and incorporating pressure controllers. The impact of changes in various manipulated variables (MVs) on the two controlled variables (CVs) over time were then analysed to generate data for the control system design. This data was used to generate the gain (K_p), time constant (τ_p) and dead time (θ_p) by employing the design analysis tool in Loop-Pro Trainer 5 using the First Order Plus Dead Time (FOPDT) model. The values obtained for the process gains, process time constants, and the process dead times were used to design single input single output (SISO) and multiple-input multiple-output (MIMO) step response control systems in MATLAB Simulink.

Table 7.1: Process Parameters for HPC Capture Plant

Controlled Variable	**Manipulated Variable**	**Control Objectives**
Carbon capture efficiency	Lean solvent flowrate	To observe the dynamic response of the carbon removal level to step ramps in the lean solvent flowrate
Stripper reboiler temperature	Stripper reboiler duty	To study the dynamic behaviour of the stripper reboiler temperature as a result of variations in the reboiler duty
Disturbance Variable		**Reason for Inclusion in Control Design**
CO_2 concentration in the flue gas stream		To demonstrate the unavoidable fluctuations of the carbon concentration in the flue gas produced from a real power plant
Flue gas flowrate		To test the control system behaviour in situations where the flue gas feed to the capture plant is not under strict control
Lean solvent concentration		To observe the dynamic behaviour of a closed-loop capture plant which

	practically demonstrates some fluctuations in the lean solvent concentration as a result of changes in the concentration of chemical absorbent in the recycled stream
Concentration of boric acid	To understand how the system dynamically responds to sudden fluctuations in the promoter concentration in the lean solvent stream

The relative gain array (RGA) analyses were performed in MATLAB to determine the appropriate pairing of the control variables and the manipulated variables. The RGA analysis results were used to select the carbon capture efficiency and the stripper reboiler temperature as the CVs, while the lean solvent flowrate and stripper reboiler duty were set as the MVs. The CO_2 concentration in the flue gas stream, the flue gas flowrate, the lean solvent concentration and the concentration of boric acid were set as measured disturbances. The controllers used were proportional integral derivative (PID) controllers. Table 7.1 shows the pairings for the MVs and the CVs alongside the control objectives. The reasons for introducing the measured disturbances are also presented in the same table. Figure 7.1 illustrates the process flowsheet in the Aspen Plus Dynamic platform. Detail descriptions of the full PID control structures are covered in the Appendix.

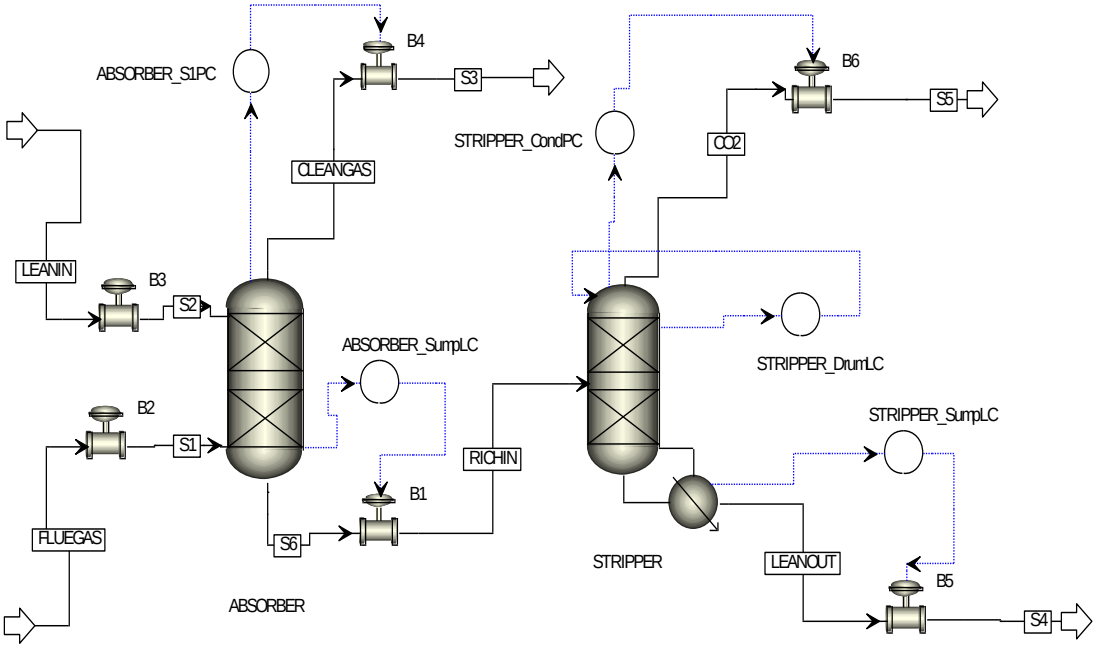

Figure 7.1. Dynamic process flowsheet for K_2CO_3 and H_3BO_3/K_2CO_3

For ease of the preliminary dynamic and control studies intended in this project, the flow-driven dynamic approach was adopted instead of the pressure-driven dynamic approach. The base case un-optimised HPC capture process with 40 wt% K_2CO_3 was used for the dynamic modelling, and in the H_3BO_3/K_2CO_3 dynamic system, 4 wt% of boric acid was used for the initial simulation. Also, in each dynamic simulation case, the steady-state simulation was run for at least 10 minutes before any disturbance was introduced. The disturbances were introduced in a magnitude of ±5% of the initial value.

7.1 DYNAMIC SENSITIVITY ANALYSES

The dynamic sensitivity analyses were required to suggest appropriate control loops for the HPC-based capture processes. These analyses involve step changes in the manipulated variables and their influences on the controlled variables over time. To obtain the steady-state gains (K_p), the processing time constants (τ_p, in hours) and the dead time (θ_p) for each MV-CV pairing, step changes of ±5% was introduced into the system for all the MVs. The resulting process parameters for both the K_2CO_3 and H_3BO_3/K_2CO_3 systems are tabulated in Table 7.2.

Table 7.2: Process Parameters for HPC Capture Plant

	F_{FG}			F_L			T_{FG}			T_L		
	K_p	τ_p	θ_p	K_p	τ_p	θ_p	K_p	τ_p	θ_p	K_p	τ_p	θ_p
K_2CO_3												
CC%	-0.00157	0.001	0	0.004273	0.7383	0.8761	-0.3365	0.4278	0.01132	-0.1712	2.601	1.365
T_{Reb}, °C	-0.000152	0.6367	0.4251	-0.000103	0.7706	-1.475	0.02954	0.7427	0	0.01888	1.182	1.439
H_3BO_3/K_2CO_3												
CC%	-0.01416	0.001	0.01013	0.004303	0.8056	0.7591	-0.06719	0.6804	0	-0.1347	4.589	0.9069
T_{Reb}, °C	-0.000161	0.627	0.3796	-0.000103	0.8268	1.464	0.006291	0.8216	0.06943	0.01808	0.9456	1.394
	C_{CO2}			**C_{K2CO3}**			**Q_{Reb}**			**C_{H3BO3}**		
	K_p	τ_p	θ_p	K_p	τ_p	θ_p	K_p	τ_p	θ_p	K_p	τ_p	θ_p
K_2CO_3												
CC%	-336.2	0.001	0	38.28	0.238	1.035	6.082	0.01125	0.01258	-	-	-
T_{Reb}, °C	-1.011	5.843	0.5543	61.24	0.8053	1.517	2.835	0.05707	0.001006	-	-	--
H_3BO_3/K_2CO_3												
CC%	-269.7	0.001	0	16.5	0.1622	0.869	4.933	0.01564	0.0107581	4.764	0.08141	0.696
T_{Reb}, °C	-1.053	1.971	0	69.85	0.7509	1.398	2.425	0.05484	0	50.24	0.7459	1.429

F_{FG}: Flowrate of flue gas; F_L: Flowrate of lean solvent; T_{FG}: Temperature of flue gas; T_L: Temperature of lean solvent stream; C_{CO2}: Concentration of CO_2 in flue gas stream (mole basis); C_{K2CO3}: Concentration of K_2CO_3 in lean solvent stream (weight basis); C_{H3BO3}: Concentration of H_3BO_3 in lean solvent stream (weight basis); Q_{Reb}: Specific reboiler duty; $CC_{\%}$: Percentage CO_2 capture rate; T_{Reb}: Temperature of stripper reboiler.

7.2 OPEN-LOOP ANALYSES

The open-loop system for both the unpromoted and promoted K_2CO_3 capture process was analysed for the response of decarbonisation level and stripper reboiler temperature to changes in system variables such as flue gas flowrate, lean solvent flowrate, flue gas temperature, lean solvent temperature, CO_2 concentration in the flue gas stream, K_2CO_3 concentration in the lean solvent stream, boric acid concentration and stripper reboiler duty. This section discusses the results from the open-loop analyses for both the uncatalysed and boric acid catalysed HPC dynamic system.

7.2.1 Results for ±5% Decrease and Increase in Flue Gas Flowrate

This section presents the open-loop transient responses of the carbon removal rate and stripper reboiler temperature for the K_2CO_3 and H_3BO_3/K_2CO_3 systems. Figures 7.2 to 7.5 summarise the response of these CVs as a result of the disturbances introduced in the flue gas flowrate.

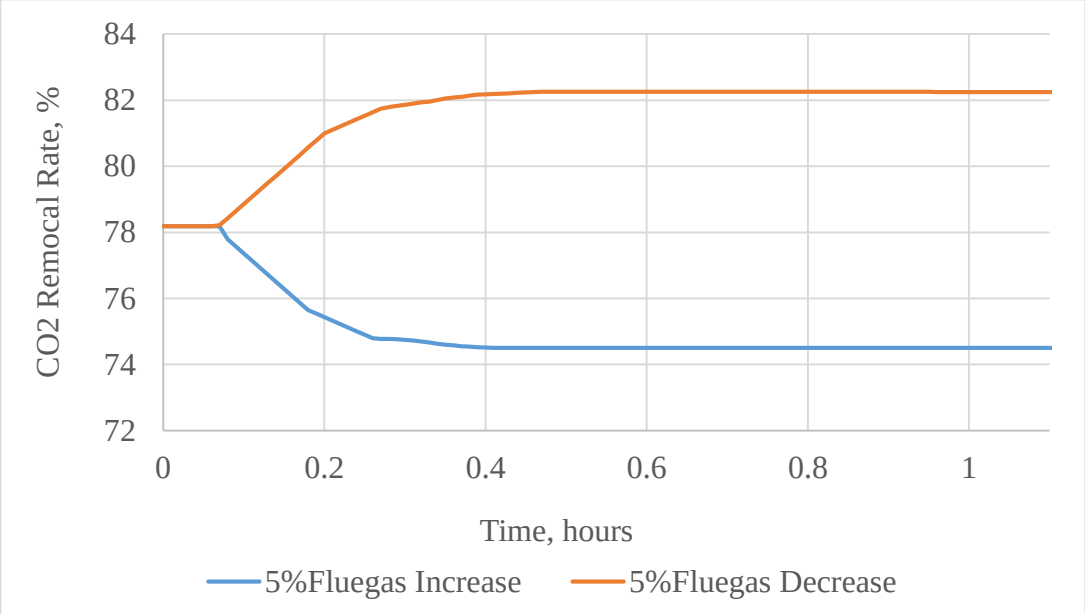

Figure 7.2. Transient response of CO_2 removal level to flue gas flowrate disturbance in K_2CO_3 system

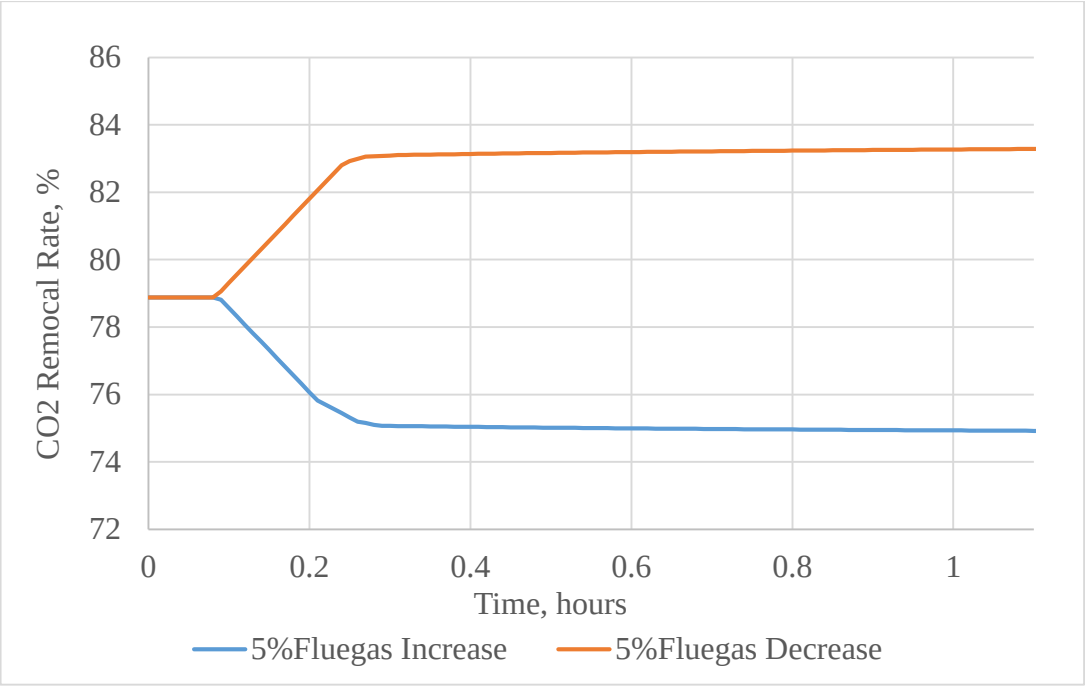

Figure 7.3. Transient response of CO_2 removal level to flue gas flowrate disturbance in H_3BO_3/K_2CO_3 system

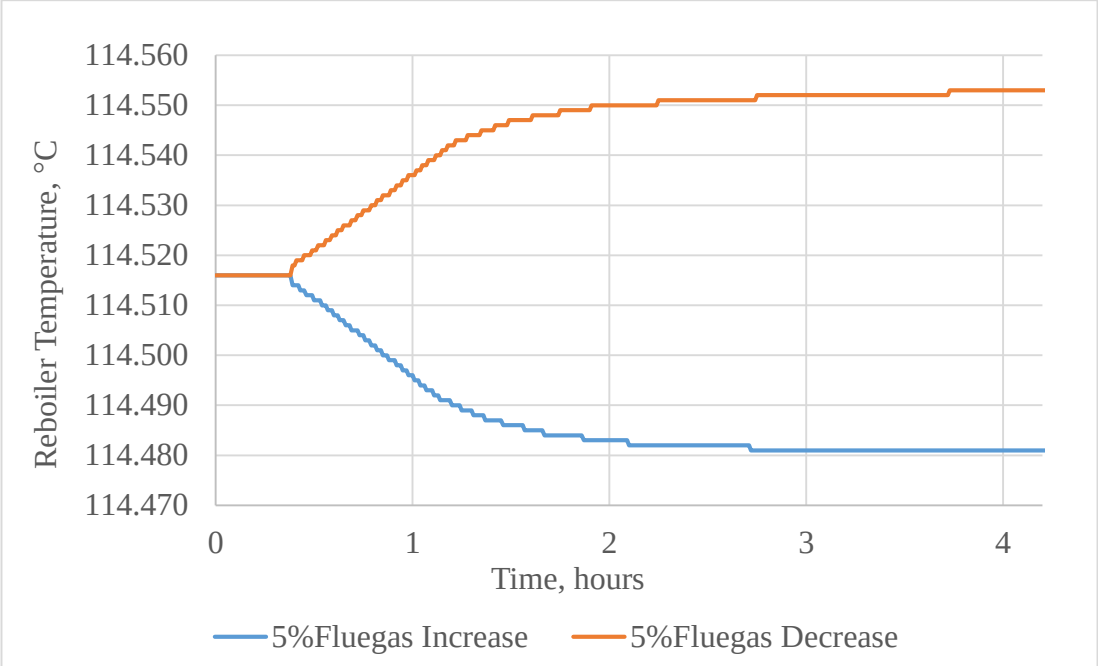

Figure 7.4. Transient response of reboiler temperature to flue gas flowrate disturbance in K_2CO_3 system

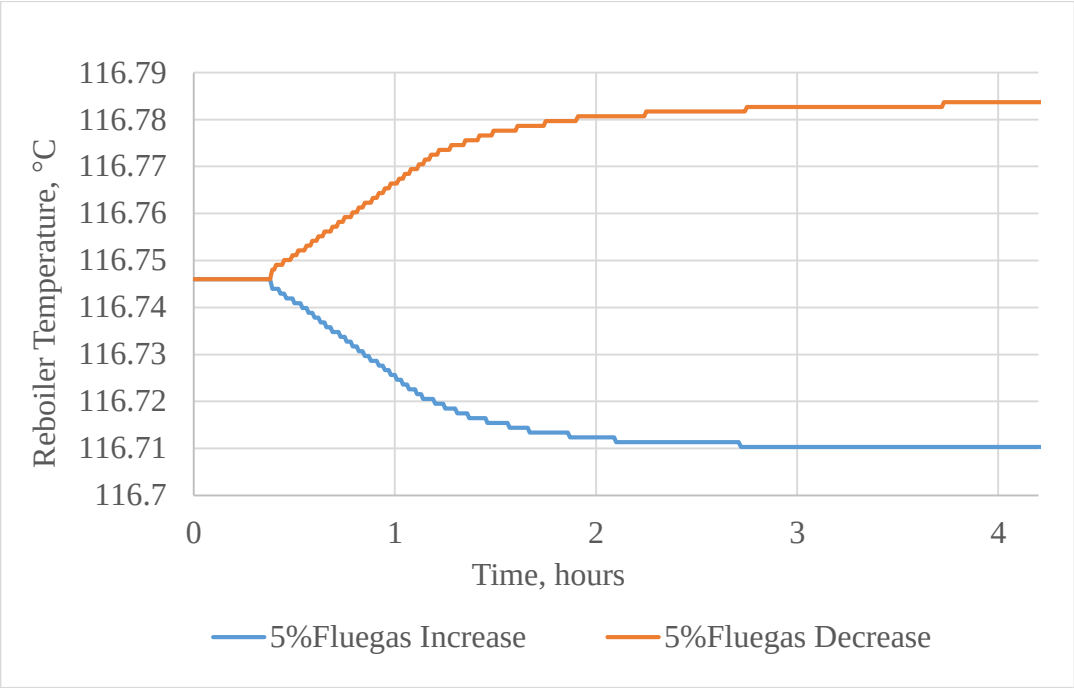

Figure 7.5. Transient response of reboiler temperature to flue gas flowrate disturbance in H_3BO_3/K_2CO_3 system

The transient response of the carbon removal rate due to changes in the flue gas flowrate appeares to be very quick. This could be observed in Figure 7.2 and Figure 7.3 where it took less than half a minute for the systems to attain a new steady state. This is possibly due to the sharp change in the total amount of CO_2 in the system, resulting in a sharp change in capture rate since the rate is a ratio of the stripped amount of CO_2 to the total amount of CO_2 in the flue gas. A sharp decrease in the denominator, therefore, causes an increase in the percentage value of the carbon removed, and vice versa. Both systems also demonstrate the same pattern of response to the disturbance. As the flue gas flowrate is decreased, the corresponding residence time of the vapour stream increases in the absorber column, causing the decarbonisation efficiency of the process to increase. Looking at the high influence of the step changes in the flue gas flowrate on the system performance, it would be advisable to employ higher gain controllers to maintain the HPC process at the set point. As the carbon removal rate rises at constant reboiler duty, the reboiler temperature is forced to increase. These scenarios could be observed in Figures 7.4 and 7.5. The response time for the reboiler temperature is however much longer, as the new steady-state values are only reached after about 3.5 hours in both the K_2CO_3 system and the blended H_3BO_3/K_2CO_3 system. The reverse is also true when the flue gas flowrate is increased.

7.2.2 Results for ±5% Decrease and Increase in Lean Solvent Flowrate

Figures 7.6 to 7.9 summarise the response of the CVs as a result of the disturbances introduced in the lean solvent flowrate.

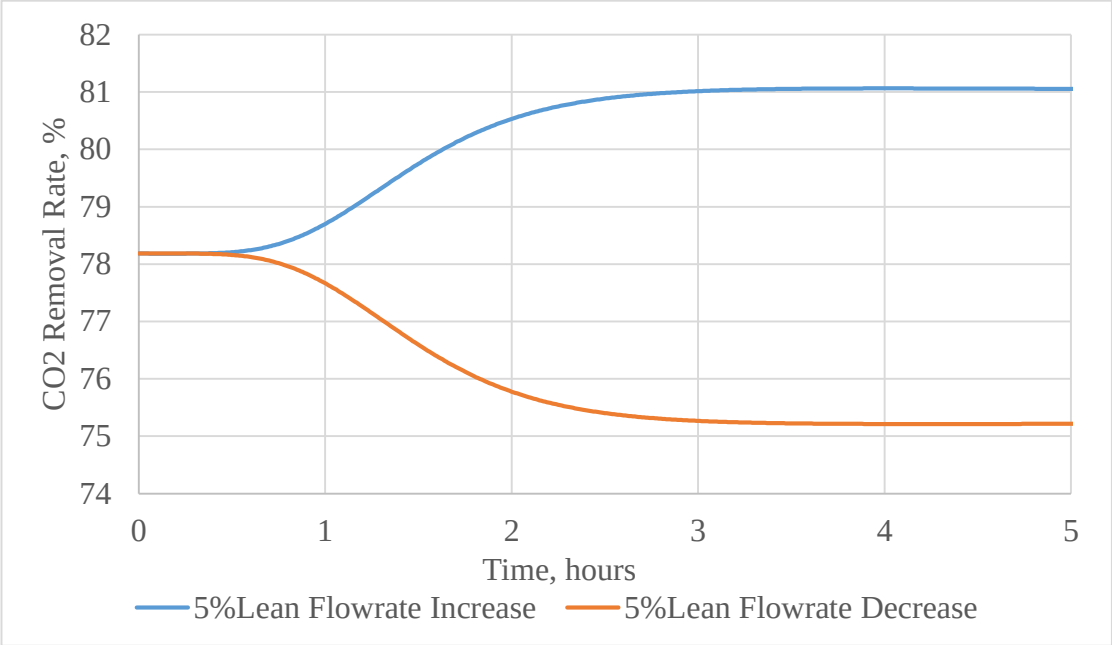

Figure 7.6. Transient response of CO_2 removal level to lean solvent flowrate disturbance in K_2CO_3 system

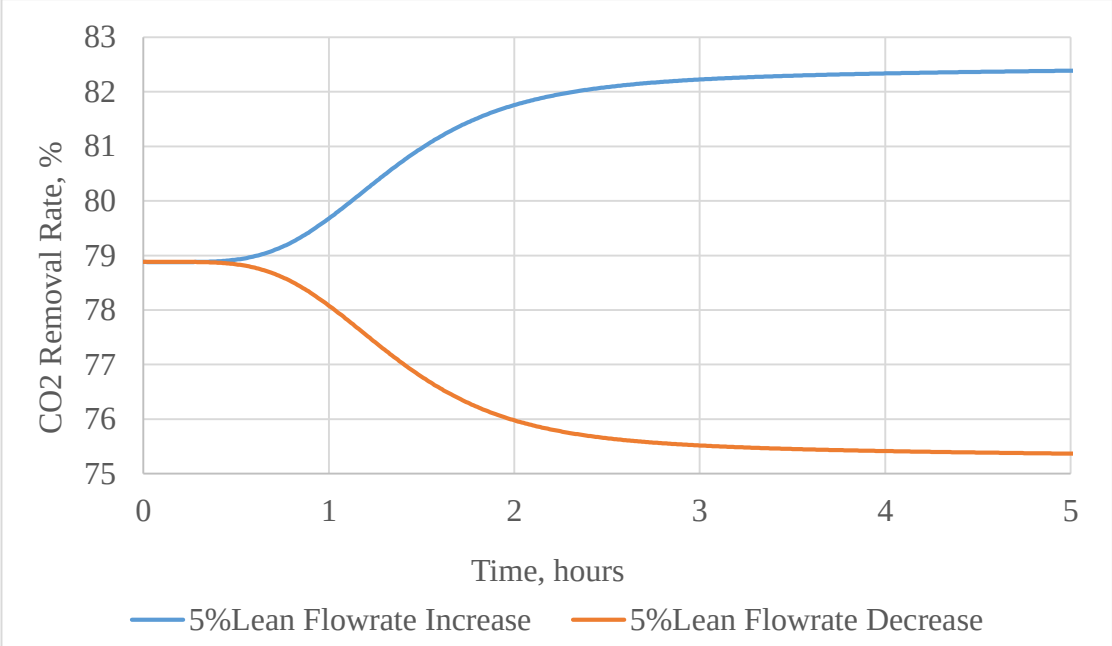

Figure 7.7. Transient response of CO_2 removal level to lean solvent flowrate disturbance in H_3BO_3/K_2CO_3 system

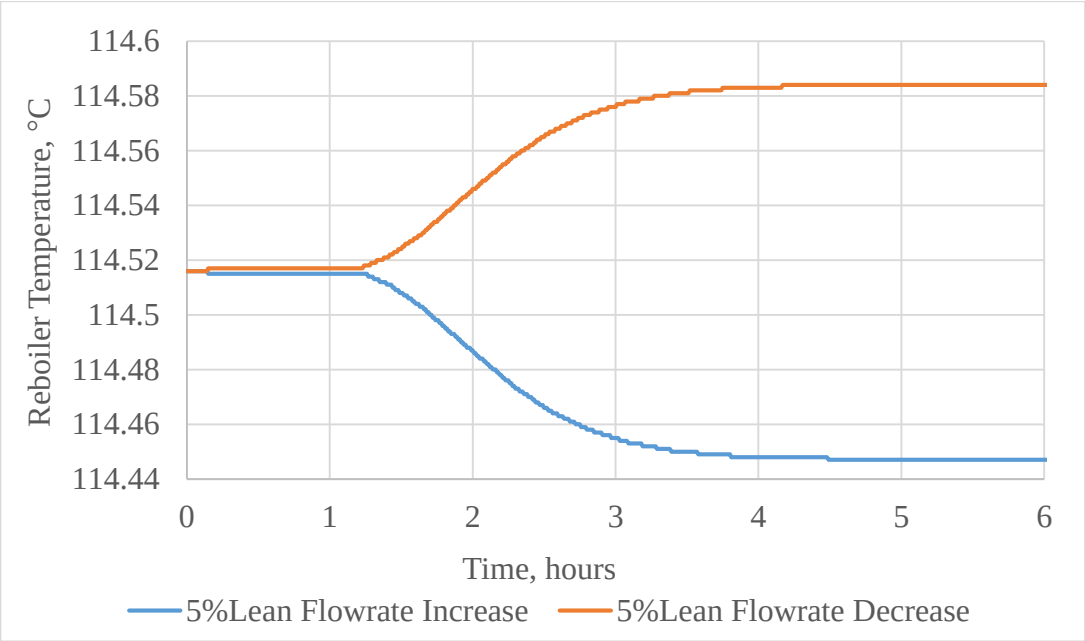

Figure 7.8. Transient response of reboiler temperature to lean solvent flowrate disturbance in K_2CO_3 system

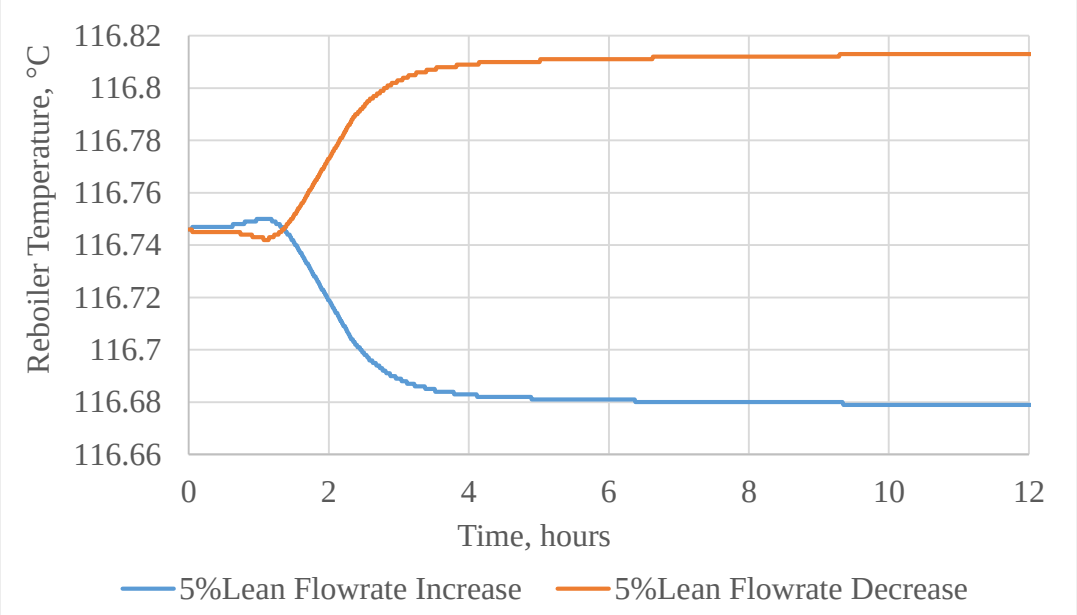

Figure 7.9. Transient response of reboiler temperature to lean solvent flowrate disturbance in H_3BO_3/K_2CO_3 system

In the case of step changes in the lean solvent flowrate, the response of the carbon capture rate is in the same direction as the direction of the change in the flowrate. As the lean solvent flowrate increases, the carbon removal efficiency increases as well. This could be due to the higher CO_2 loading that is attained in the absorber column as a result of the higher amount of lean solvent used. This higher loading results in a richer solvent stream that exits the absorber column and fed into the stripper column. This causes an ultimate increase in the carbon capture level in the whole system.

However, as the solvent flowrate increases the reboiler temperature decreases at a constant reboiler duty value. This is possibly due to the lesser sensible heat requirement in the stripper column as a result of the richer solvent stream introduced. When the lean solvent flowrate is reduced, the absorption capacity of the liquid stream in the absorber column decreases, and this results in lower CO_2 loading in the rich solvent stream introduced into the stripper column. This eventually leads to lower carbon capture efficiency in the system. The reboiler temperature also increases accordingly as the stripper reboiler duty is maintained at a constant value. Again, the overall transient response of the controlled variables to the disturbances took about an hour, and the new steady-state values are attained after 3.5 hours in all four scenarios.

7.2.3 Results for ±5% Decrease and Increase in Flue Gas Temperature

Figures 7.10 to 7.13 summarise the response of the CVs as a result of the disturbances introduced in the flue gas temperature.

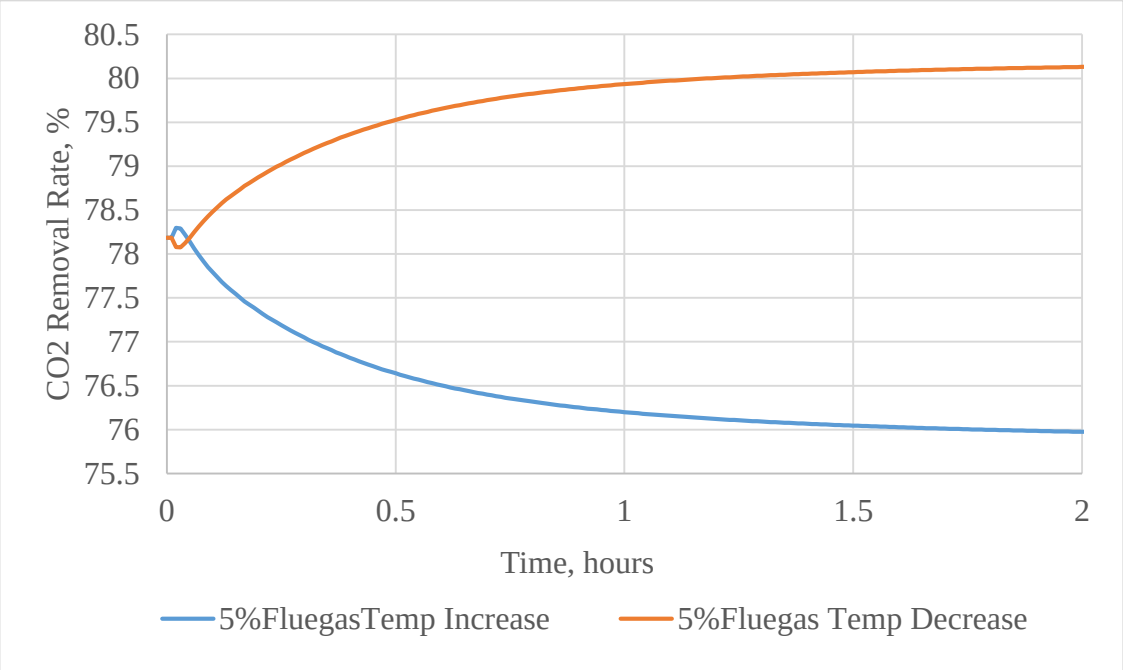

Figure 7.10. Transient response of CO_2 removal level to flue gas temperature disturbance in K_2CO_3 system

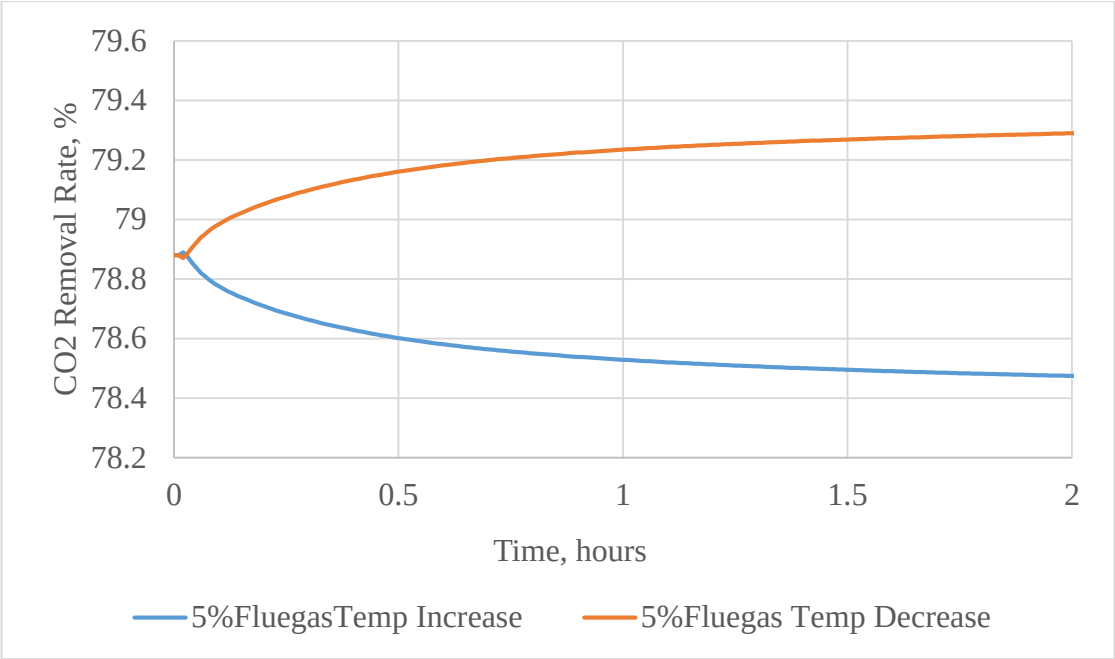

Figure 7.11. Transient response of CO_2 removal level to flue gas temperature disturbance in H_3BO_3/K_2CO_3 system

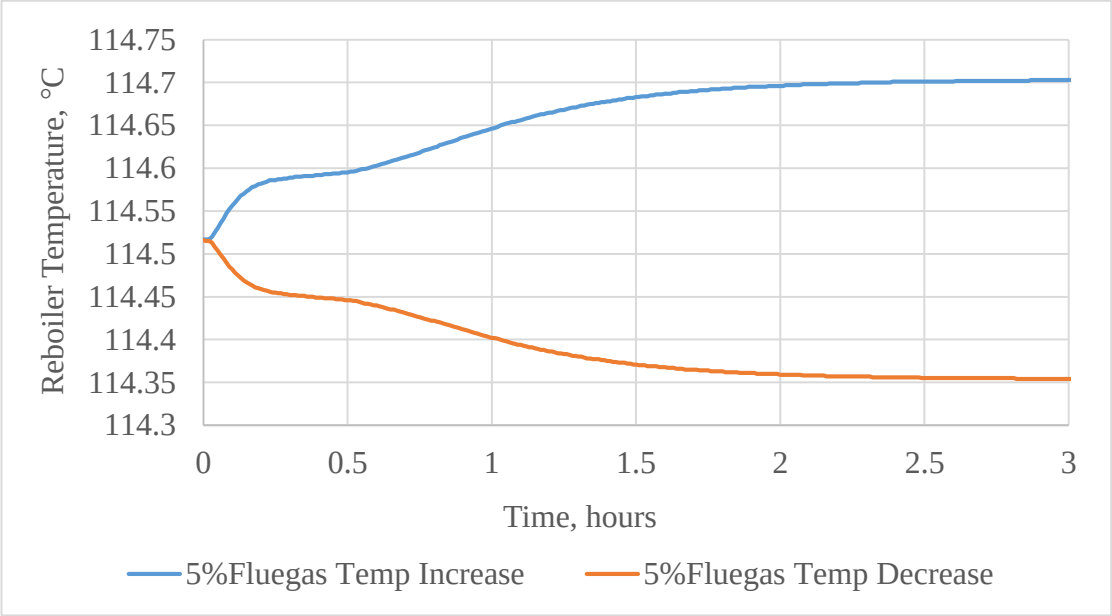

Figure 7.12. Transient response of reboiler temperature to flue gas temperature disturbance in K_2CO_3 system

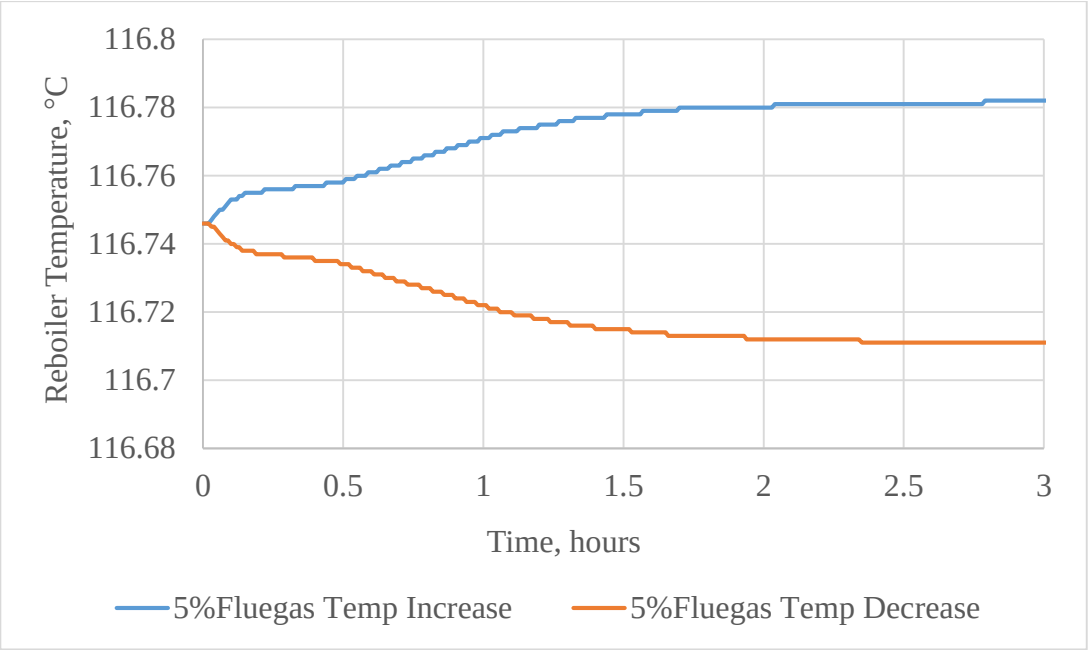

Figure 7.13. Transient response of reboiler temperature to flue gas temperature disturbance in H_3BO_3/K_2CO_3 system

In Figures 7.10 to 7.13, the decrease in flue gas temperature is observed to increase the carbon removal efficiency rate and reduces the reboiler temperature. This observation is at par with the steady-state parametric analysis that was discussed earlier in Chapter 4. The reduced flue gas temperature enables the exothermic absorption reaction in the absorber column to be controlled to some extent. This helps in increasing the mass transfer rate in the system and yields a higher carbon capture rate. As the carbon capture rate increases at constant reboiler duty, the reboiler temperature reduces. However, unlike in the previous cases of the feed flowrate disturbances, the overall transient response of the HPC process to changes in the flue gas temperature is seen to be faster. In the case of the carbon capture rate, the new steady state is reached in less than 2 hours, while the reboiler temperature attains its new steady state in less than 3 hours. Also observable on Figures 7.10 and 7.11 is the fact that the steady state gain is less for the promoted system as compared to the unpromoted system. Thi indicates that the system response is less sensitive for the H_3BO_3/K_2CO_3 system as compared to the unpromoted K_2CO_3 system. The inverse response shown in Figure 10 is likely due to the interaction between the sharp change in the temperature of the rich solvent stream and the decarbonisation efficiency of the system. For instance, when the flue gas temperature is decreased, it lowers the temperature of the rich solvent stream and the reboiler temperature as observed in Figures 7.12 and 7.13. This instantaneous decrease in reboiler temperature causes the carbon capture level to

decrease slightly. However, as the lower flue gas temperature enhances the carbon absorption efficiency of the absorber system, the carbon capture efficiency eventually increases again as it is the case in Figures 7.10 and 7.11. On the other hand, when the flue gas temperature increases, the rich solvent temperature also rises, and the reboiler temperature increases. This sharp increase in the reboiler temperature enhances the carbon capture level at first. However, as the higher flue gas temperature affects the thermodynamics of the mass transfer process in the absorber column, the carbon capture level eventually decreases.

7.2.4 Results for ±5% Decrease and Increase in Lean Solvent Temperature

Figures 7.14 to 7.17 summarise the response of the CVs as a result of the disturbances introduced in the lean solvent temperature.

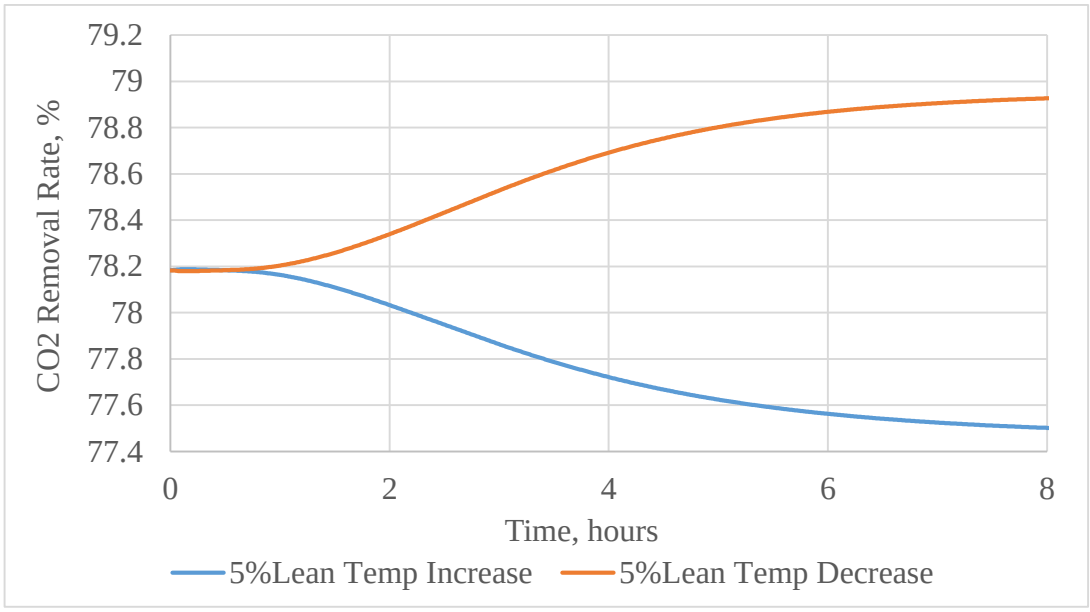

Figure 7.14. Transient response of CO_2 removal level to lean solvent temperature disturbance in K_2CO_3 system

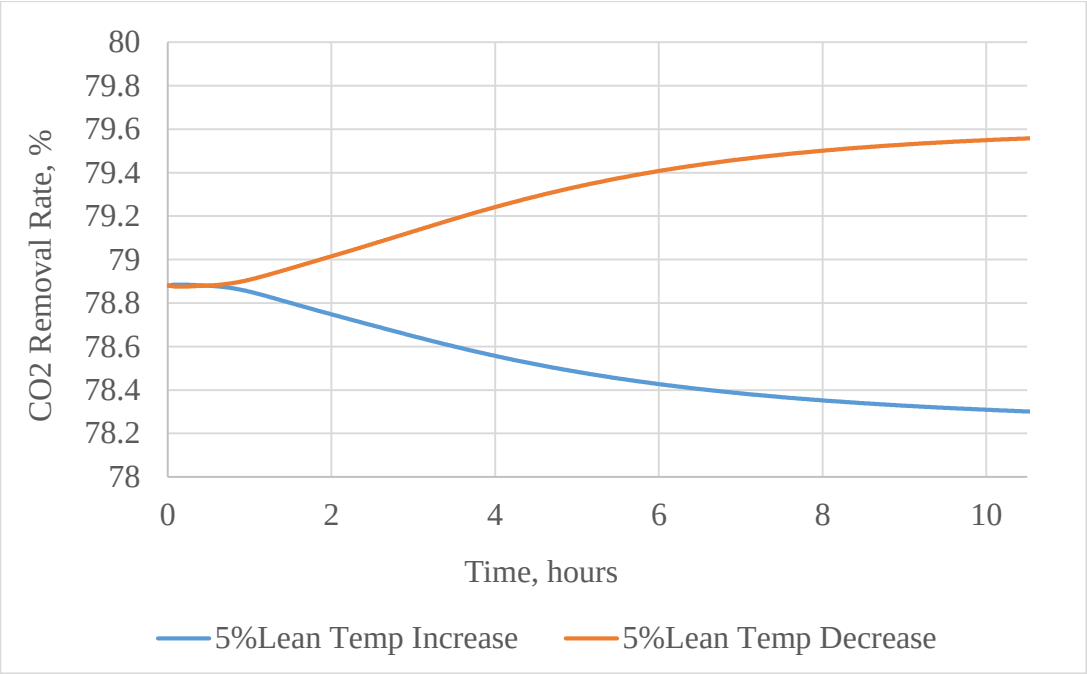

Figure 7.15. Transient response of CO_2 removal level to lean solvent temperature disturbance in H_3BO_3/K_2CO_3 system

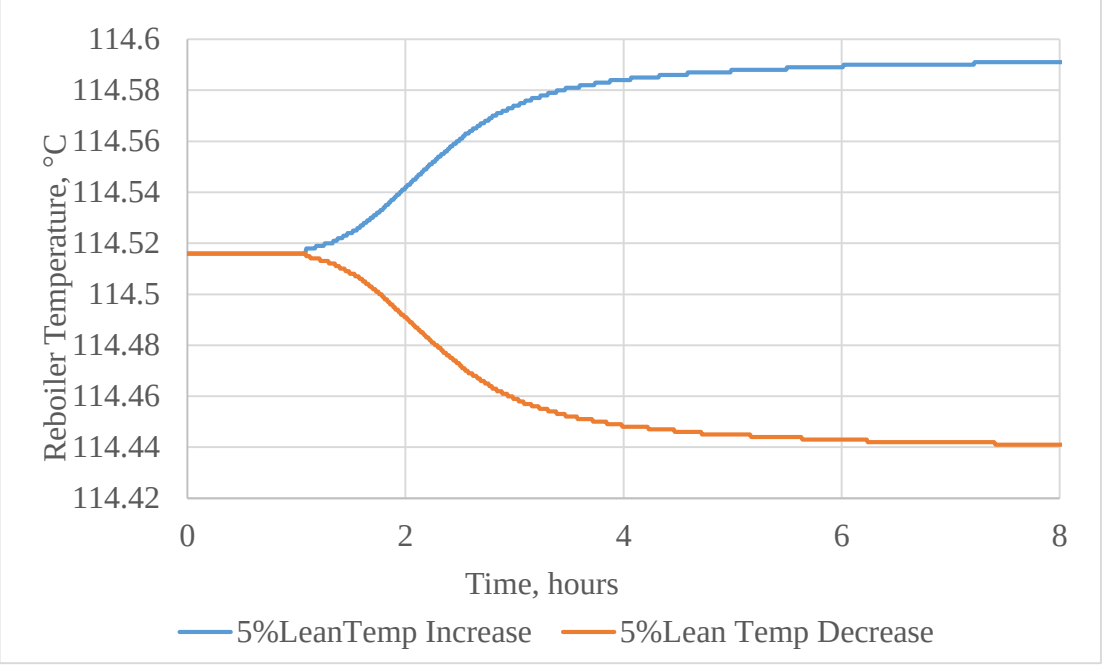

Figure 7.16. Transient response of reboiler temperature to lean solvent temperature disturbance in K_2CO_3 system

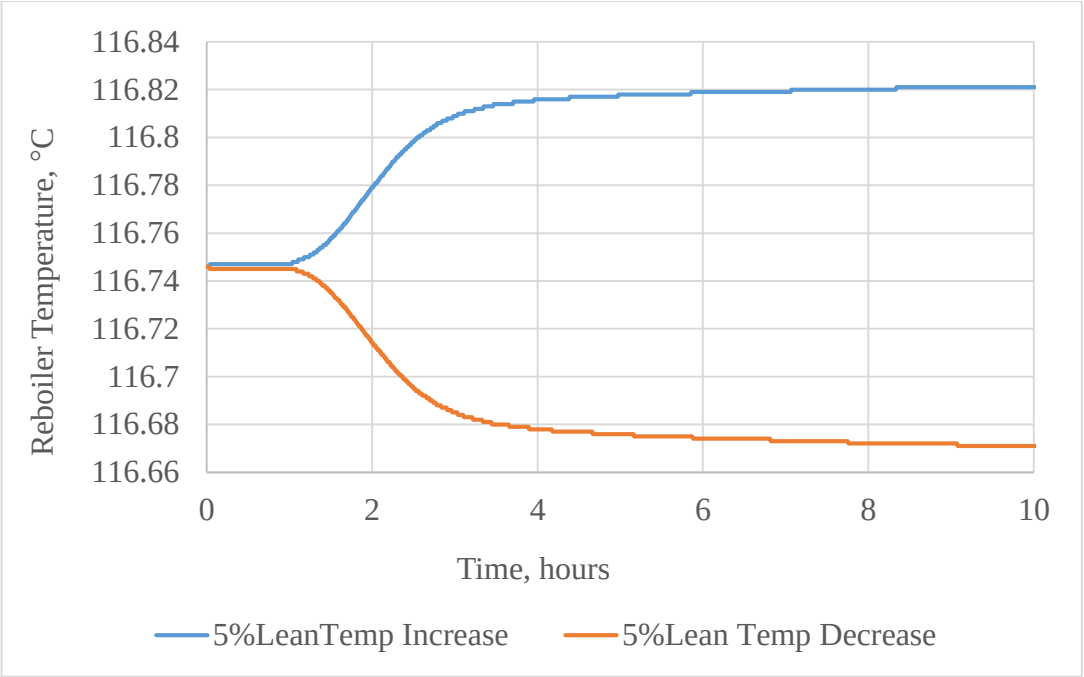

Figure 7.17. Transient response of reboiler temperature to lean solvent temperature disturbance in H_3BO_3/K_2CO_3 system

The transient response patterns demonstrated by the carbon removal efficiency and reboiler temperature due to disturbances introduced in the lean solvent temperature is similar to the cases described for the flue gas temperature variation. But in the case of the lean solvent temperature variations, the system response is seen to be much slower as it takes approximately 10 hours for the new steady-state value to arrive at for the carbon capture rate. The reboiler temperature also takes roughly 8 hours to arrive at the new steady-state value. This demonstrates that the dynamic response of the HPC capture process to disturbances in lean solvent temperature could be very slow, and requires a robust control system to make the system respond faster.

7.2.5 Results for ±5% Decrease and Increase in CO_2 Concentration

Figures 7.18 to 7.21 summarise the response of these CVs as a result of the disturbances introduced in the CO_2 concentration in the flue gas stream.

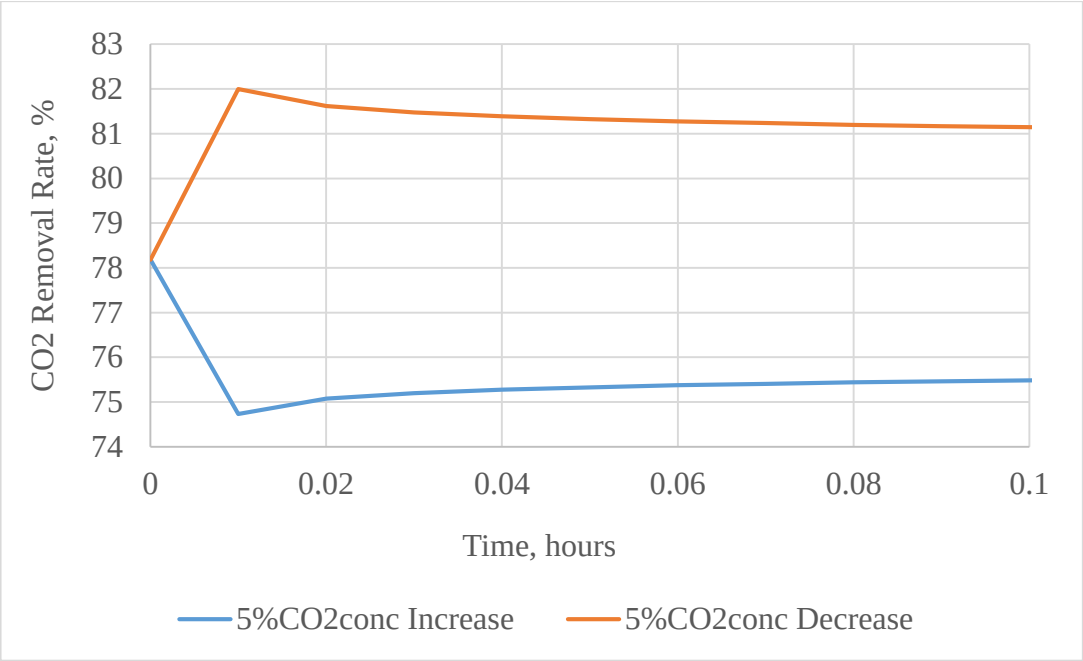

Figure 7.18. Transient response of CO_2 removal level to CO_2 concentration disturbance in K_2CO_3 system

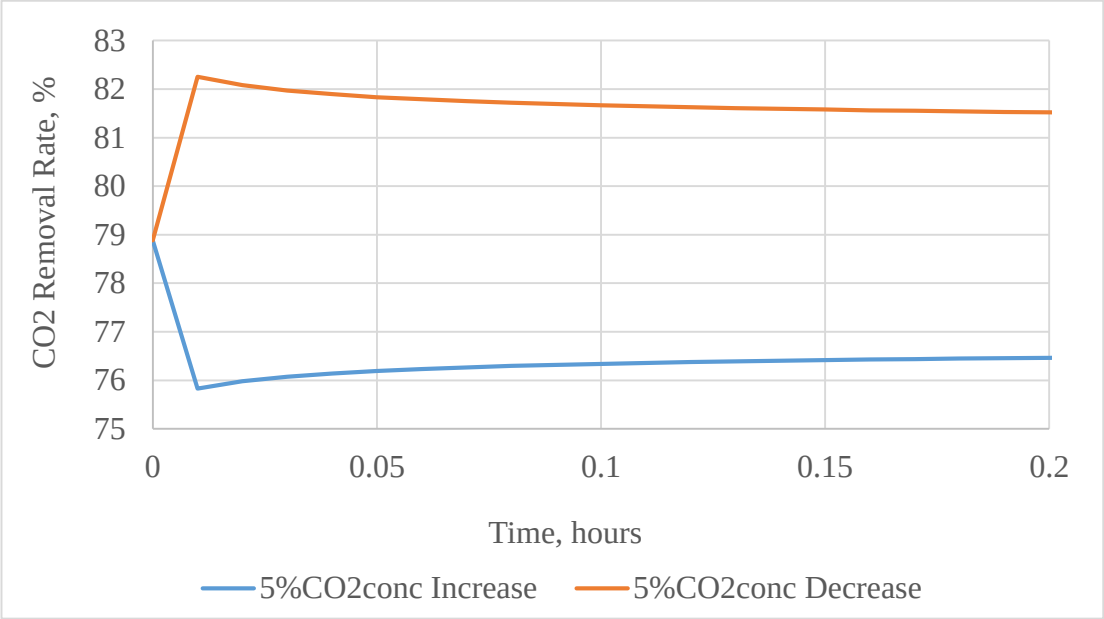

Figure 7.19. Transient response of CO_2 removal level to CO_2 concentration disturbance in H_3BO_3/K_2CO_3 system

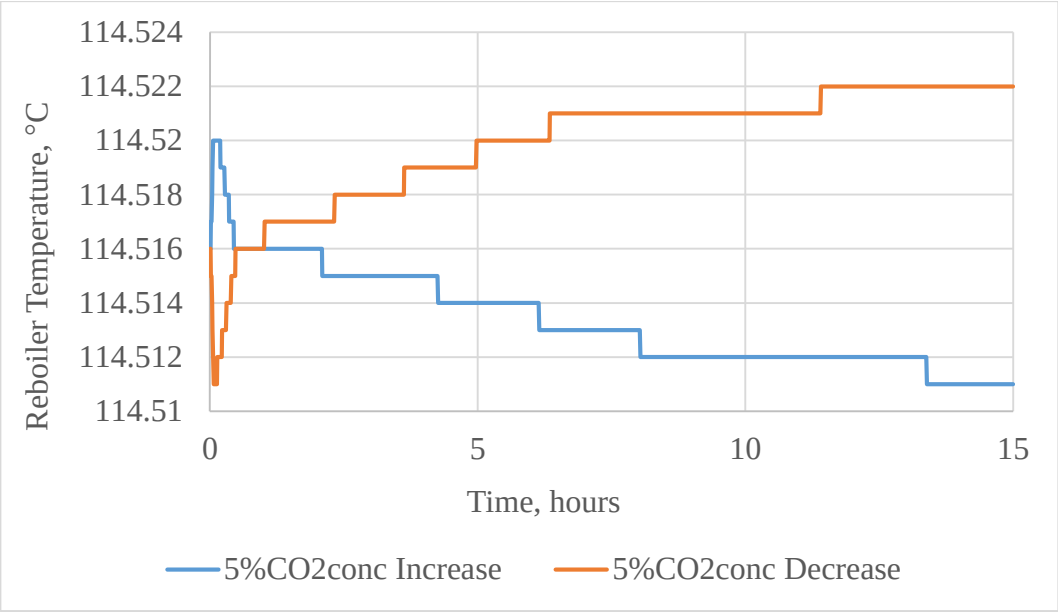

Figure 7.20. Transient response of reboiler temperature to CO_2 concentration disturbance in K_2CO_3 system

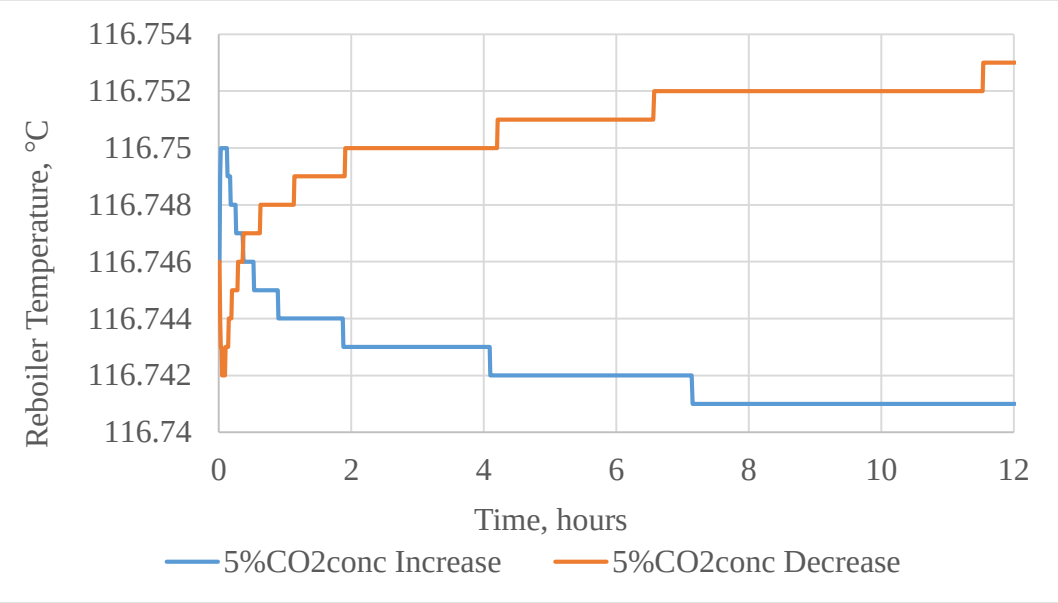

Figure 7.21. Transient response of reboiler temperature to CO_2 concentration disturbance in H_3BO_3/K_2CO_3 system

As shown in the graphs in Figures 7.18 to 7.21, disturbances introduced in the CO_2 concentration (by mole basis) are seen to have similar influences on the carbon capture rate of the hot potassium carbonate capture process in similar manner as the influences imposed by disturbances in flue gas flowrate. The sharp change in the CO_2 flowrate in the flue gas stream ultimately affects the percentage of CO_2 removal from the stripper overhead. As the carbon flowrate increases and the lean solvent flowrate remains

constant, the absorption capacity of the absorbent decreases. This results in lower carbon content in the rich solvent stream and eventually decreases the carbon removal rates from the stripper. These scenarios could be observed in Figure 7.18 and Figure 7.19. Conversely, when the flowrate of the CO_2 in the flue gas stream is reduced, the absorption capacity of the lean solvent increases. This results in higher carbon loading in the solvent stream channelled to the stripper column and results in greater carbon removal rate from the system. Since the stripper reboiler duty is fixed at a constant magnitude, the increasing carbon capture is associated with increasing reboiler temperature. The higher temperature allows the possible desorption rate to be attained in the stripper column. The transient response of the reboiler temperature is very interesting. Unlike any of the graphs described earlier, the temperature seems to fluctuate in the opposite direction at the beginning before finally taking the right course to attain a steady-state. Also, the temperature appears to respond in a gradual manner. This could be observed from the graphs in Figure 7.20 and Figure 7.21. It could be seen from these Figures that the reboiler temperature maintains a constant value for a few minutes to hours before progressing to the new value. The same pattern is true for both the unpromoted and promoted HPC capture processes. Because of this gradual progression, it takes quite a long time for the system to eventually attain a new steady-state value. The inverse responses demonstrated in these figures also indicate that the transient responses have two competing gains. Although the initial responses seem faster, they have smaller gains compared to the latter responses. The approximate time taken by both the K_2CO_3 and H_3BO_3/K_2CO_3 systems to achieve their new steady-state values is 14 hours and 12 hours respectively. Due to this high response time, it might be advisable to introduce any disturbances in the flue gas carbon concentration in small quantities to allow the system to perform dynamically better and faster. Equally, the high settling times experienced by the system show that controllers with short time integrals would be recommended to keep the process within a meaningful short closed-loop control.

7.2.6 Results for ±5% Decrease and Increase K_2CO_3 Concentration

Figures 7.22 to 7.25 summarise the response of the CVs as a result of the disturbances introduced in the K_2CO_3 concentration.

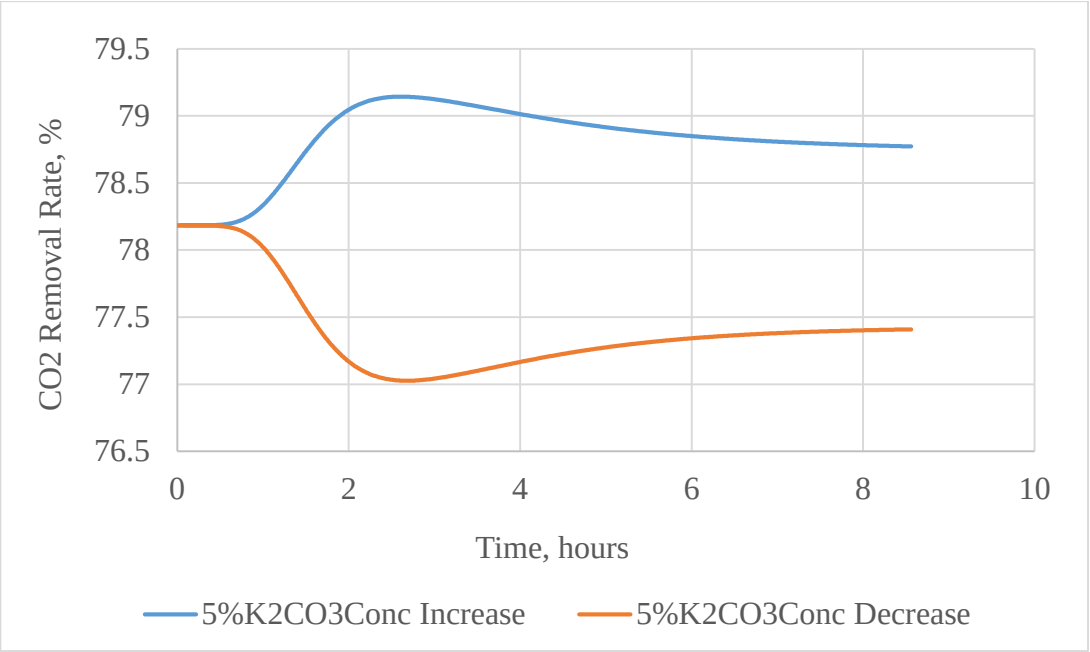

Figure 7.22. Transient response of CO_2 removal level to K_2CO_3 concentration disturbance in K_2CO_3 system

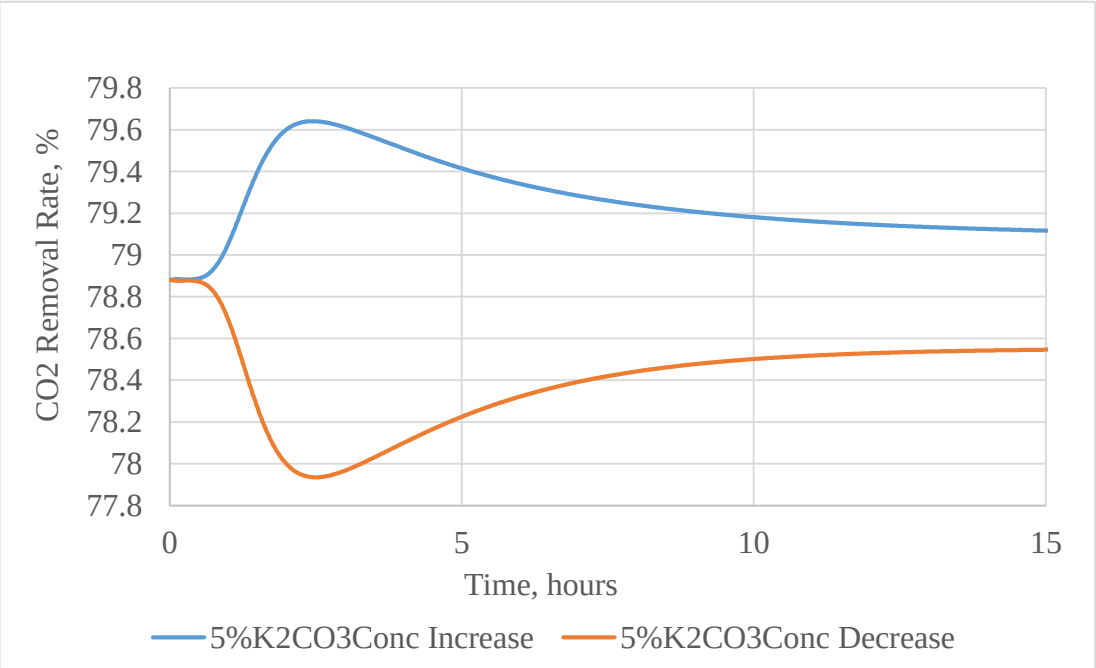

Figure 7.23. Transient response of CO_2 removal level to K_2CO_3 concentration disturbance in H_3BO_3/K_2CO_3 system

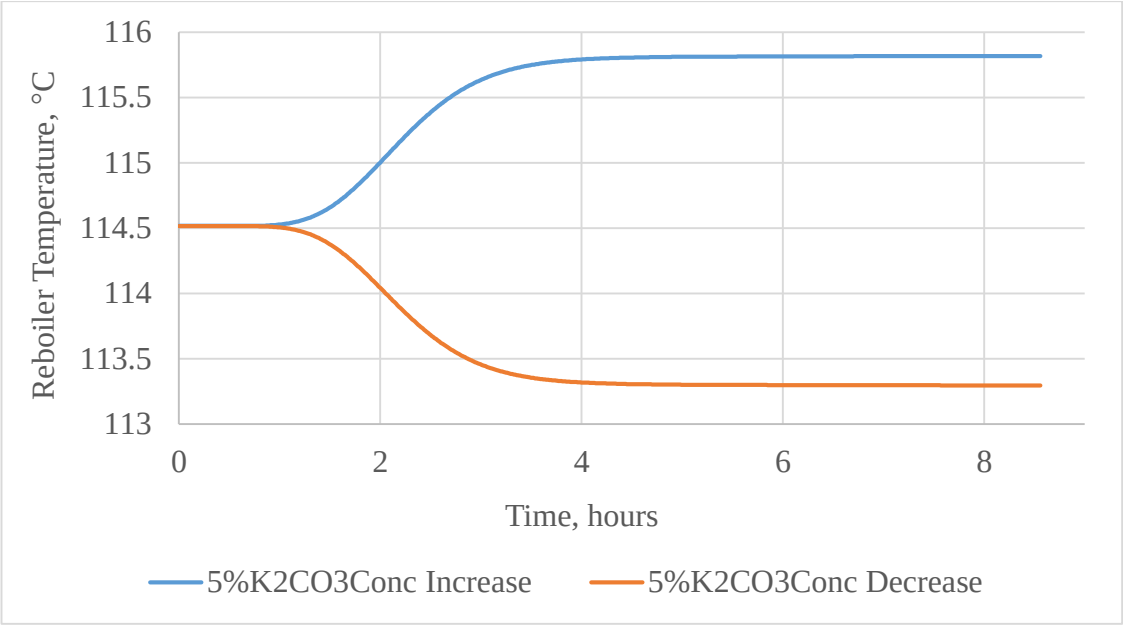

Figure 7.24. Transient response of reboiler temperature to K_2CO_3 concentration disturbance in K_2CO_3 system

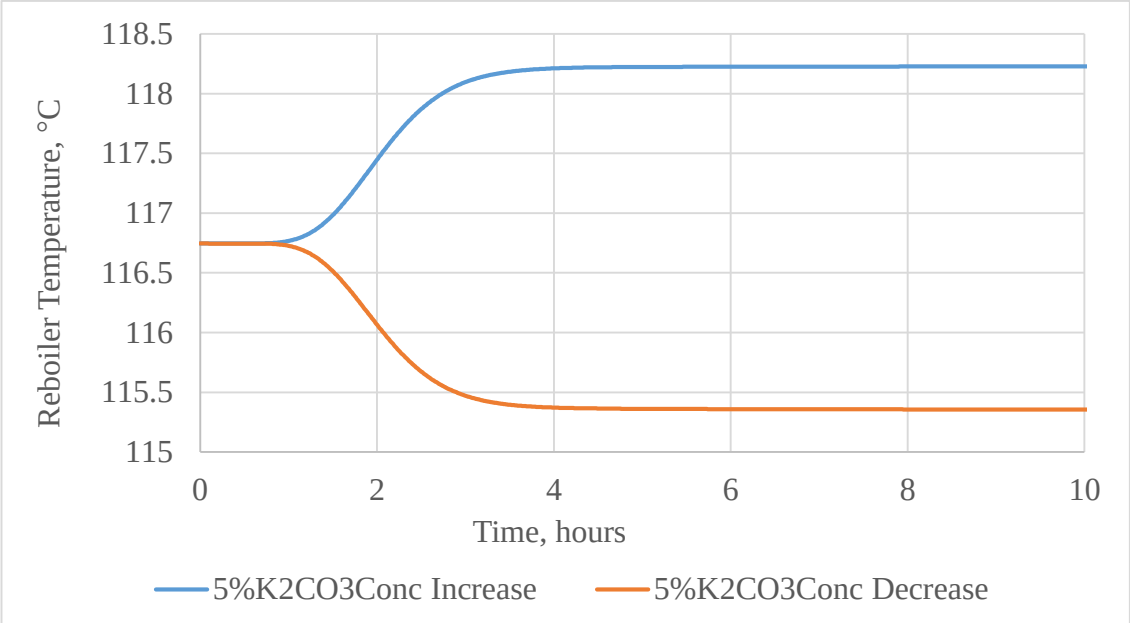

Figure 7.25. Transient response of reboiler temperature to K_2CO_3 concentration disturbance in H_3BO_3/K_2CO_3 system

Figures 7.22 and 7.23 display the transient response of carbon removal efficiency to disturbances in the lean solvent concentration. At the initial stage of introducing the disturbance, the CO_2 removal rates were observed to fluctuate beyond the new steady-state before gradually narrowing down to a flat value. After about 8 hours in the K_2CO_3 system and about 14 hours in the H_3BO_3/K_2CO_3 system, the new steady-state values

are observed to be close to the original set point. This could be as a result of maintaining the reboiler duty at a constant value. As the lean solvent concentration increases, the solvent is able to absorb more CO_2 in the absorber column, yielding a richer solvent stream for regeneration in the stripper column. Nonetheless, as the process proceeds, the richer stream would require a higher reboiler duty to recover all the CO_2 in the stripper column. As the magnitude of this duty is fixed, the desorption efficiency of the process is affected negatively. This causes the carbon removal rate to lower again. The new steady-state value is however higher than the original set point. The reverse phenomenon is also true for decreasing the lean solvent concentration. On the other hand, the reboiler temperature is observed to attain a new steady-state value at a shorter time than the carbon capture efficiency. This could be observed in Figures 7.24 and 7.25, where the new steady-state value is reached in about 4 hours for both the catalysed and uncatalysed K_2CO_3 capture processes.

7.2.7 Results for ±5% Decrease and Increase in Stripper Reboiler Duty

Figures 7.26 to 7.29 summarise the response of the CVs as a result of the disturbances introduced in the stripper reboiler duty.

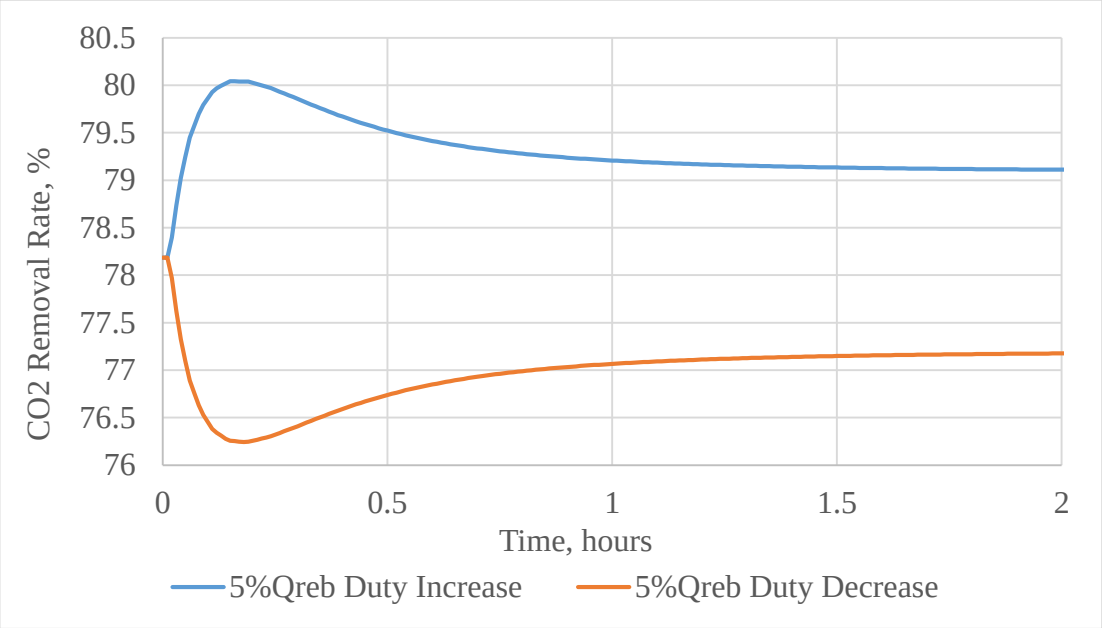

Figure 7.26. Transient response of CO_2 removal level to stripper reboiler duty disturbance in K_2CO_3 system

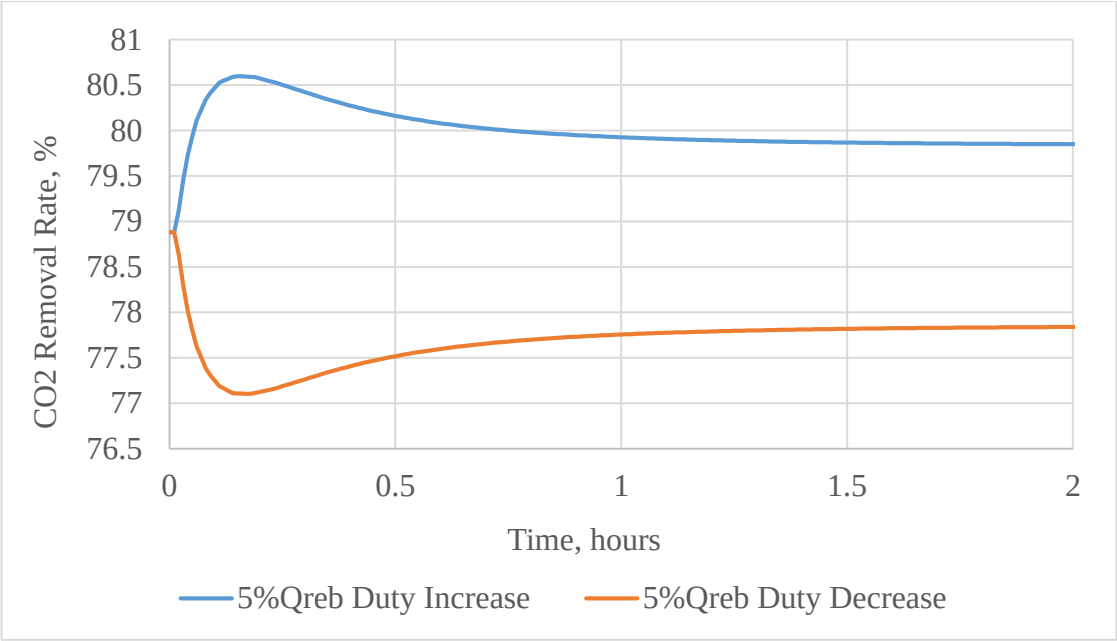

Figure 7.27. Transient response of CO_2 removal level to stripper reboiler duty disturbance in H_3BO_3/K_2CO_3 system

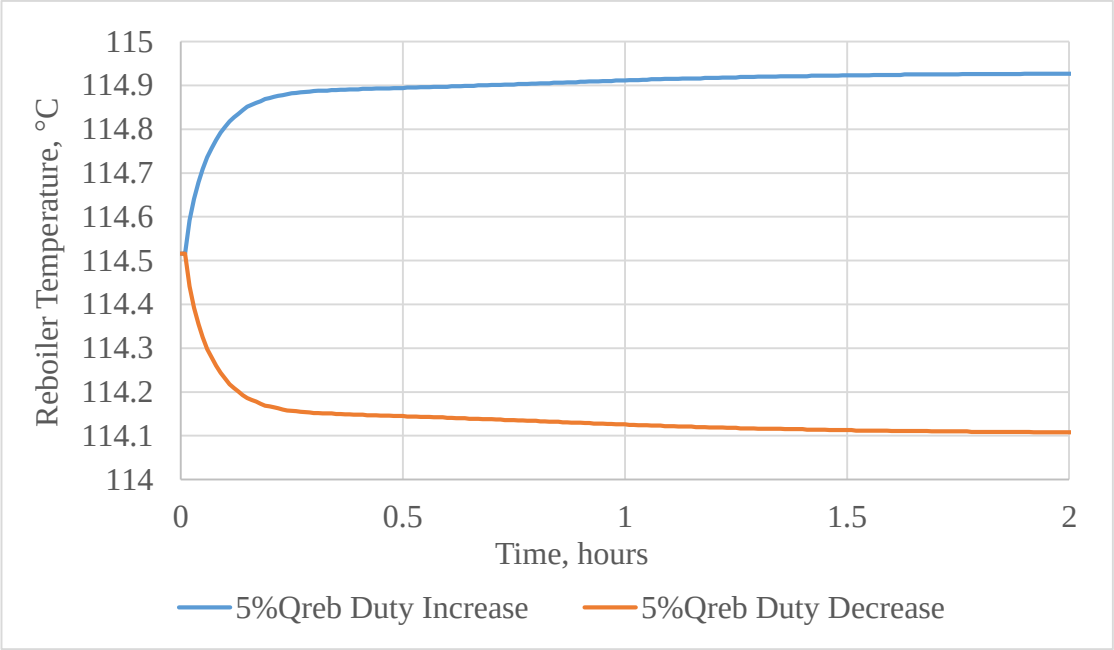

Figure 7.28. Transient response of reboiler temperature to stripper reboiler duty disturbance in K_2CO_3 system

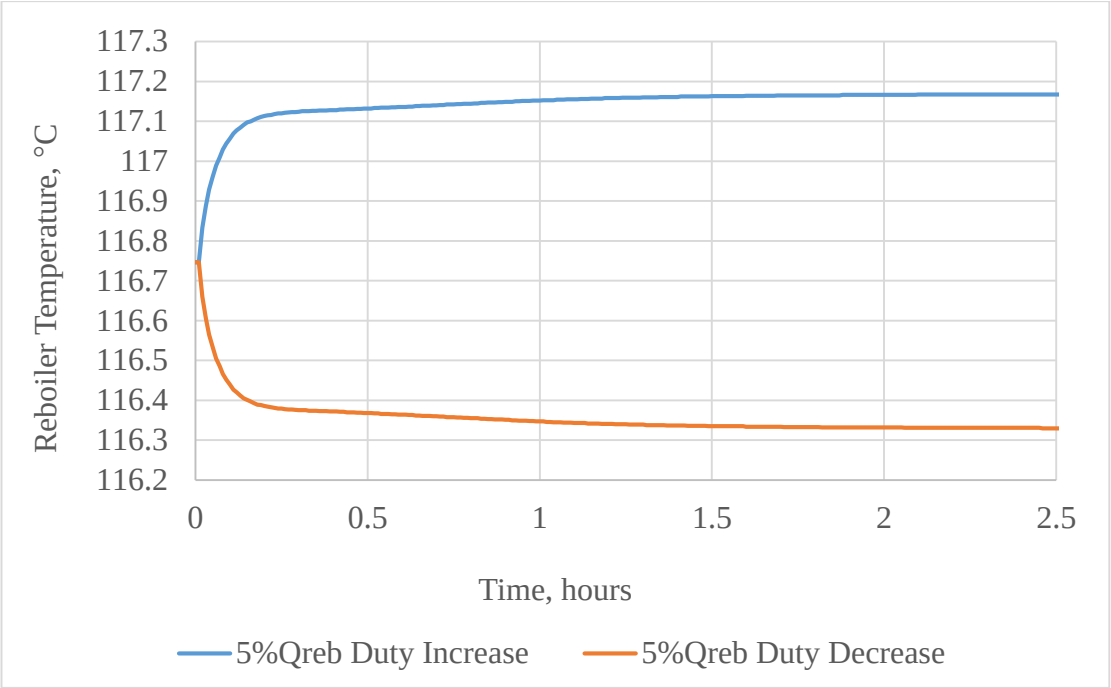

Figure 7.29. Transient response of reboiler temperature to stripper reboiler duty disturbance in H_3BO_3/K_2CO_3 system

From the graphs in Figures 7.26 to 7.29, it could be observed that the HPC process takes a shorter time on the average to respond to changes in the stripper reboiler duty than it takes to respond to the changes in other process parameters. In all four cases presented, the new steady-state values in the carbon capture rate and reboiler temperature are attained within 1–2 hours. As the reboiler duty increases, the carbon capture efficiency is seen to experience a sharp incremental response and gradually lowers to settle on the new steady-state value. This increase is simply due to the higher desorption efficiency that is caused by the higher reboiler duty in the stripper column. Similarly, as the reboiler duty increases along with the increasing carbon removal rate, the reboiler temperature also experiences a slight increase. Decreasing the reboiler duty yields the reverse result. These results, as shown on all four graphs, show the strong interactions between the carbon capture efficiency, stripper reboiler temperature and the reboiler duty.

7.2.8 Results for ±5% Decrease and Increase in H_3BO_3 Concentration

Figures 7.30 to 7.31 summarise the response of the CVs as a result of the disturbances introduced in the H_3BO_3 concentration.

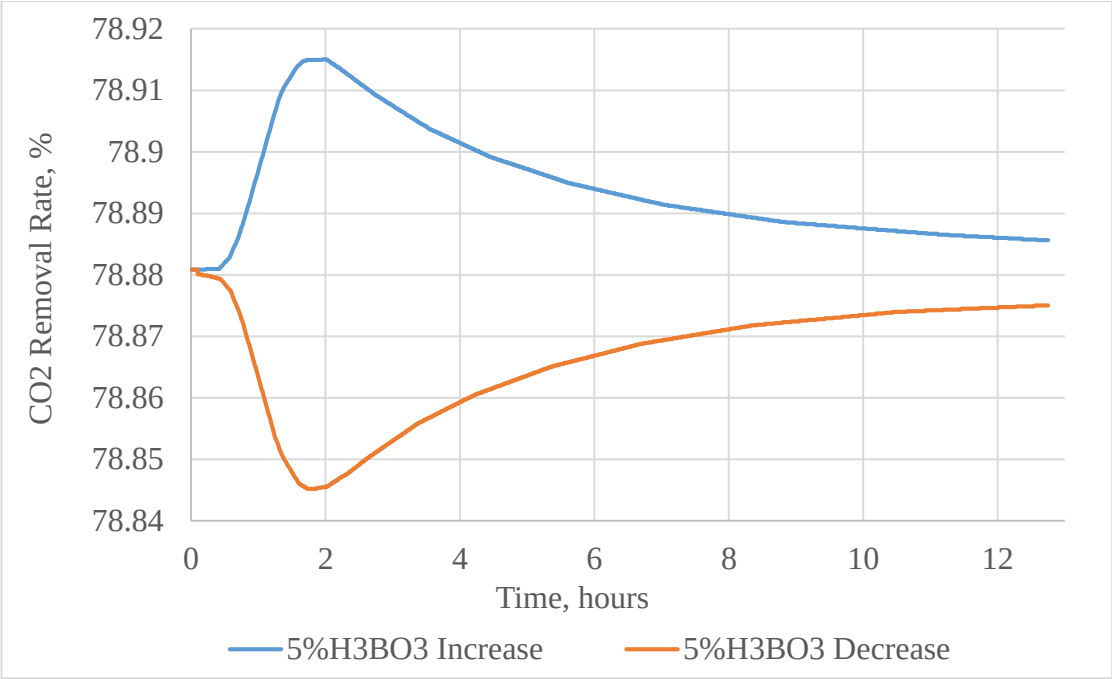

Figure 7.30. Transient response of CO_2 removal level to H_3BO_3 concentration disturbance in H_3BO_3/K_2CO_3 system

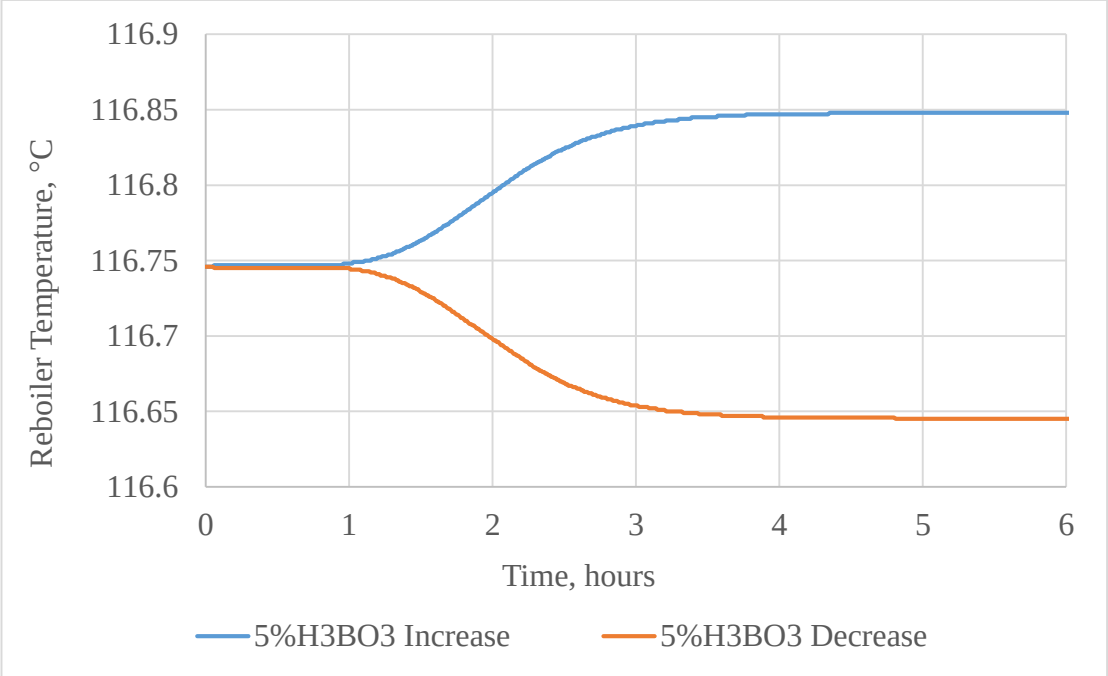

Figure 7.31. Transient response of reboiler temperature to H_3BO_3 concentration disturbance in H_3BO_3/K_2CO_3 system

The dynamic interactions between the carbon capture efficiency, stripper reboiler temperature, and boric acid concentration are displayed in Figures 7.30 and 7.31. Decreasing the boric acid concentration causes a sharp decline in the carbon capture

efficiency as observed in Figure 7.30. This decline is however only in a small magnitude as the maximum deviation is less 0.04 from the original set point. As the process continues, the system begins to return to the original carbon capture rate. The final steady-state value is, however, lesser than the original value. Although the carbon absorption efficiency in the absorber column reduces slightly due to the decrease in boric acid concentration, which in turn results in lower carbon removal rate at the initial stage, the constant reboiler duty forces a higher stripping effect of the rich solvent stream in the stripper column. This explains why the carbon capture rate increases gradually again to a value close to the original set point. It takes a large amount of time for the system to attain the new steady state. The reboiler temperature is seen to achieve a new steady-state in a much shorter time, but it took a long time to respond to the disturbance at the initial stage.

7.3 RGA ANALYSES

To design the feedback control loop for the HPC processes, the relative gain array (RGA) analyses are performed to properly pair the manipulated variables to their respective controlled variables. The chosen MVs used in these analyses are the lean solvent flowrate (F_L) and the stripper reboiler duty (Q_{Reb}). The controlled variables are the CO_2 capture rate ($CC_{\%}$) and the stripper reboiler temperature ($T_{Reb,°C}$). The RGA matrix, Λ_{RGA}, is defined as follows:

$$\Lambda_{RGA} = G \otimes (G^{-1})^T \quad \ldots\ldots\ldots\ldots\ldots\ldots\ldots\ldots\ldots 7.1$$

where G is the process steady-state gain matrix. The steady-state gains indicated in Table 7.1 and 7.2 were substituted into Equation 7.1 to generate RGA matrices for the K_2CO_3 and H_3BO_3/K_2CO_3 systems below:

$$\Lambda_{RGA}^{K2CO3} = \begin{matrix} \\ CC_{\%} \\ T_{Reb,°C} \end{matrix} \begin{bmatrix} F_L & Q_{Reb} \\ 0.9508 & 0.0492 \\ 0.0492 & 0.9508 \end{bmatrix} \ldots\ldots\ldots\ldots 7.2$$

$$\Lambda_{RGA}^{H3BO3/K2CO3} = \begin{matrix} \\ CC_{\%} \\ T_{Reb,°C} \end{matrix} \begin{bmatrix} F_L & Q_{Reb} \\ 0.9536 & 0.0464 \\ 0.0464 & 0.9536 \end{bmatrix} \ldots\ldots\ldots\ldots 7.3$$

As the RGA analyses portrayed in Equations 7.2 and 7.3, it is clear that the lean solvent flowrate could be paired with the carbon capture rate, whiles the stripper reboiler duty pairs perfectly with the reboiler temperature. These MV-CV pairings are true for both

the K_2CO_3 and H_3BO_3/K_2CO_3 capture processes. Considering that this is a preliminary control study, and there are no negative values in the static RGA matrix (Tung et al. 1981), the dynamic RGA (DRGA) was not considered in this study. This is however recommended for further studies in the same research area.

7.4 CLOSED-LOOP SISO ANALYSES

After the correct pairing of the MVs and CVs were determined using the RGA analysis, the single input single output (SISO) control analyses were performed. A feedback closed-loop control system with PID controllers were used for these analyses. The tuning parameters for the controllers are presented in Table 7.3. All tunings were completed using MATLAB auto tunning function, and optimized using the Genetic algorithm toolbox, which is one of the widely used natural selection for solving difficult problems. The integral time absolute error (ITAE) values after optimization are also included in the Table.

Table 7.3: Tuning Parameters for Controllers in HPC CO_2 capture plant for SISO control model

CV	MV	P	I	D	ITAE
K_2CO_3 CAPTURE SYSTEM					
CC%	F_L	110	127	16	109.3
T_{REB}	Q_{Reb}	0.68	16.48	-0.0008	1.4
H_3BO_3/K_2CO_3 CAPTURE SYSTEM					
CC%	F_L	146	166	25	93.2
T_{REB}	Q_{Reb}	0.85	20.15	-0.00109	1.5

The design included disturbances in the flue gas flowrate, lean solvent concentration and CO_2 concentration in the flue gas stream for the K_2CO_3 system. In the model for the H_3BO_3/K_2CO_3 system, the boric acid concentration is considered as an additional disturbance.

7.4.1 Results of the SISO analyses

The results obtained for the SISO analyses are presented in Figures 7.32 to 7.35.

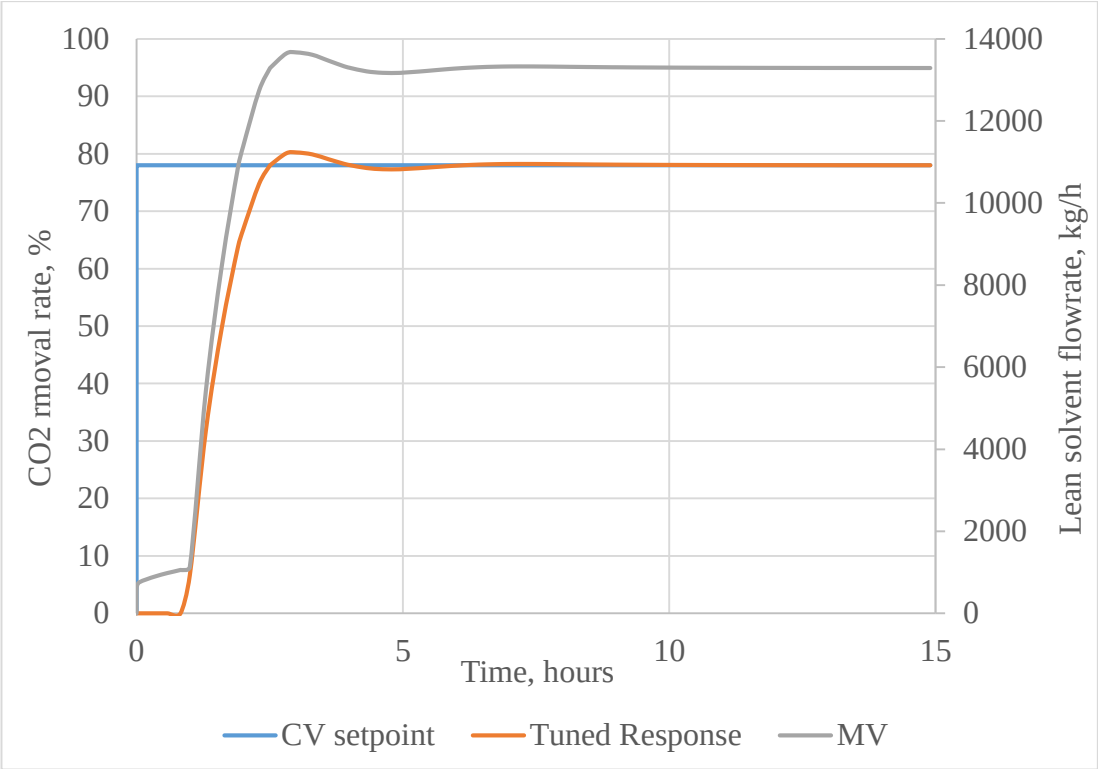

Figure 7.32. PID control signal of carbon capture rate in K_2CO_3 system

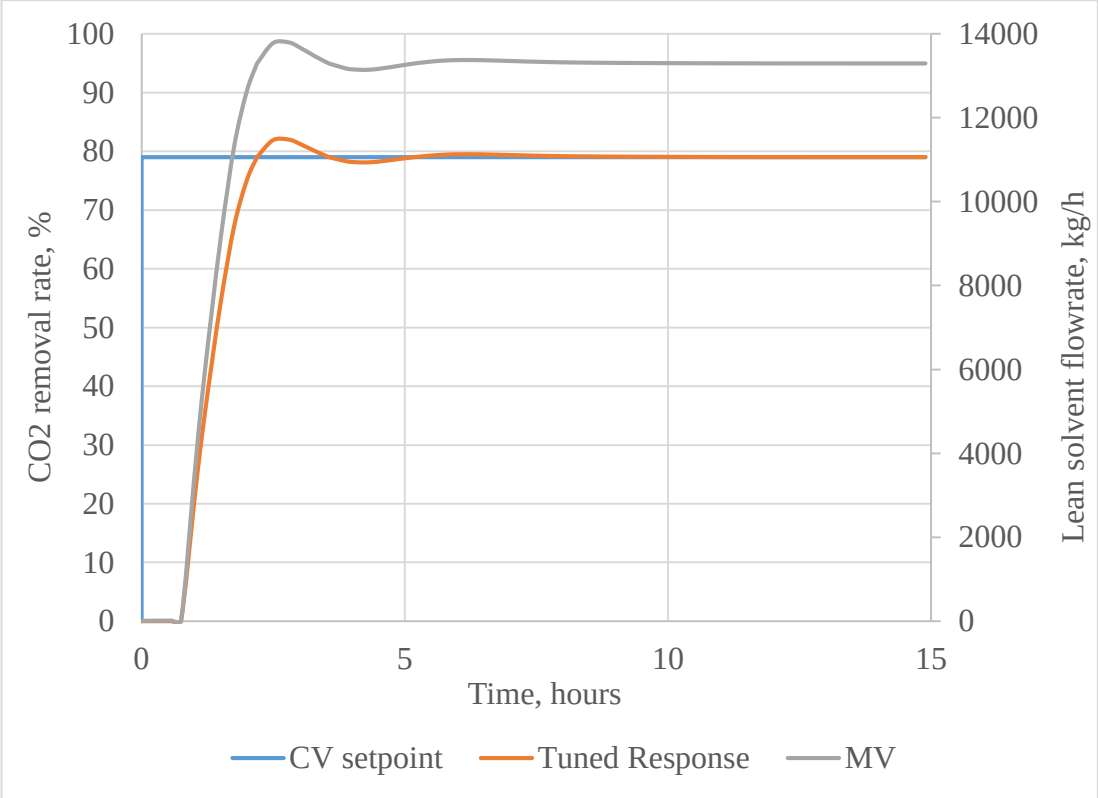

Figure 7.33. PID control signal of carbon capture rate in H_3BO_3/K_2CO_3 system

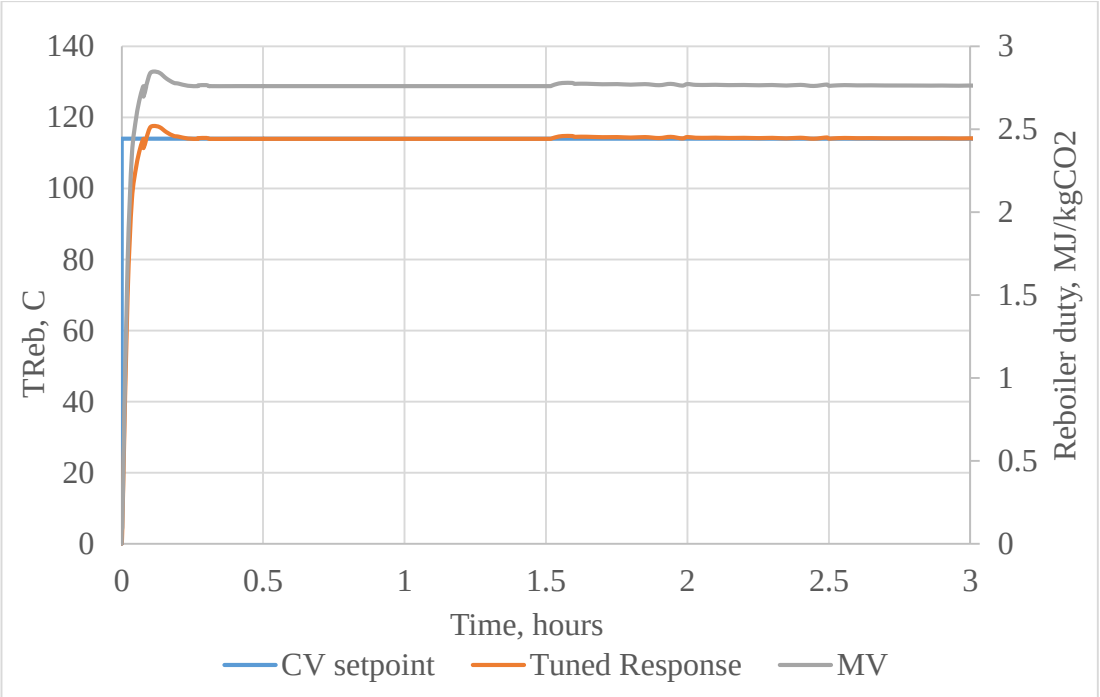

Figure 7.34. PID control signal of reboiler temperature in K_2CO_3 system

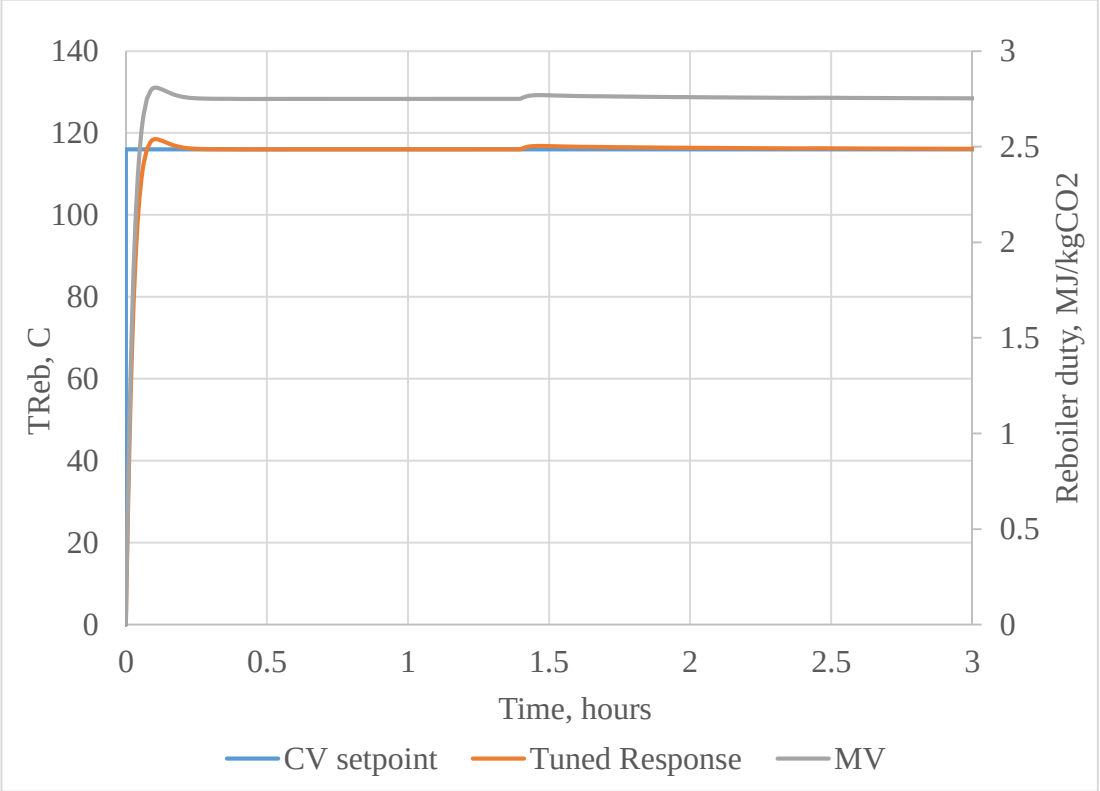

Figure 7.35. PID control signal of reboiler temperature in H_3BO_3/K_2CO_3 system

In all four cases of the SISO analyses presented in Figures 7.32 to 7.35, it appears that the PID controllers are able to bring the HPC capture operations to the setpoint by manipulating the appropriate MVs. But it takes quite a long time for the plant to arrive

at the setpoint for the carbon capture level. For instance, in the case of the boric acid promoted process, the plant is only able to reach the study state condition after 7 hours, with some noticeable noise still lingering beyond 15 hours. Even though no noticeable noise is observed in the unpromoted HPC system after 10 hours, this system also takes approximately 7 hours to arrive at the setpoint. This explains why the controller gains for the carbon capture rate are quite high in Table 7.3.

The reboiler temperature, however, takes a much shorter time to attain the setpoint value. This time is less than an hour for both plants as shown in Figures 7.34 and 7.35. That notwithstanding, the system appears to experience another mild fluctuation after an hour of reaching a steady state. This fluctuation appears to reoccur ocassionally and remain beyond an hour before diminishing again. Apart from these observations, it is quite obvious that the additional disturbance in the boric acid promoted system does not seem to have any significant effects on the controllers' performance in tuning the plant to attain desired setpoints.

7.5 CLOSED-LOOP MIMO ANALYSES

Since the carbon capture rate and the stripper reboiler temperature have interactions in a real carbon capture process, it is decided to explore the multiple input multiple output control analyses to see how the interaction affects the controller performances. The respective controller tuning parameters for these analyses are presented in Table 7.4. The integral time absolute error (ITAE) values after optimization using Genetic algorithm are also included in the Table.

Table 7.4: Tuning Parameters for Controllers in HPC CO_2 capture plant for MIMO control model

CV	MV	P	I	D	ITAE
K_2CO_3 CAPTURE SYSTEM					
CC%	F_L	109	125	15	108.8
T_{REB}	Q_{Reb}	0.69	16.49	-0.0008	1.4
H_3BO_3/K_2CO_3 CAPTURE SYSTEM					
CC%	F_L	146.5	165	26	91.8
T_{REB}	Q_{Reb}	0.95	22.5	-0.0011	1.3

7.5.1 Results of the MIMO analyses

The PID signal plots for the MIMO system are presented in Figures 7.36 to 7.39 below.

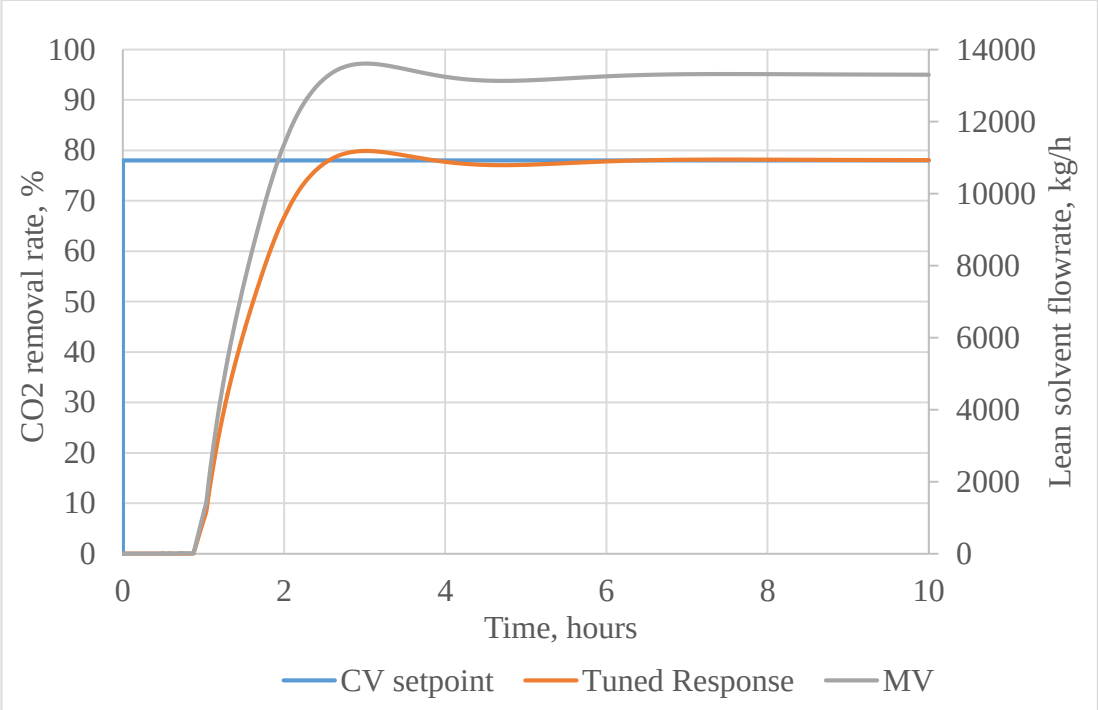

Figure 7.36. PID control signal of carbon capture rate in K_2CO_3 system for MIMO model

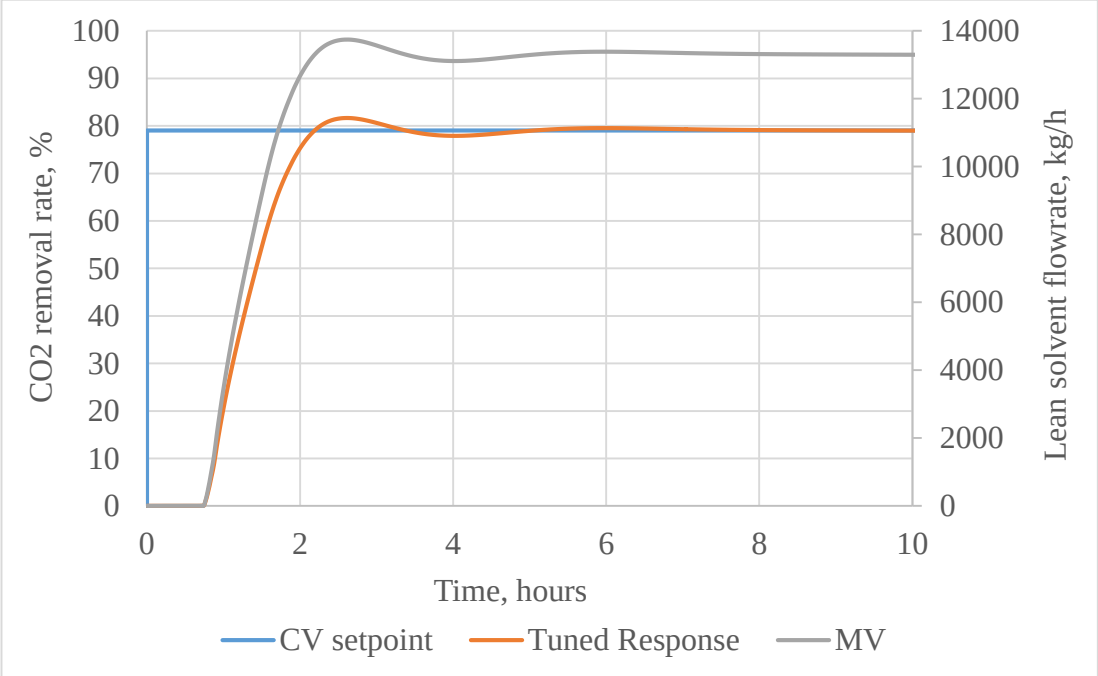

Figure 7.37. PID control signal of carbon capture rate in H_3BO_3/K_2CO_3 system for MIMO model

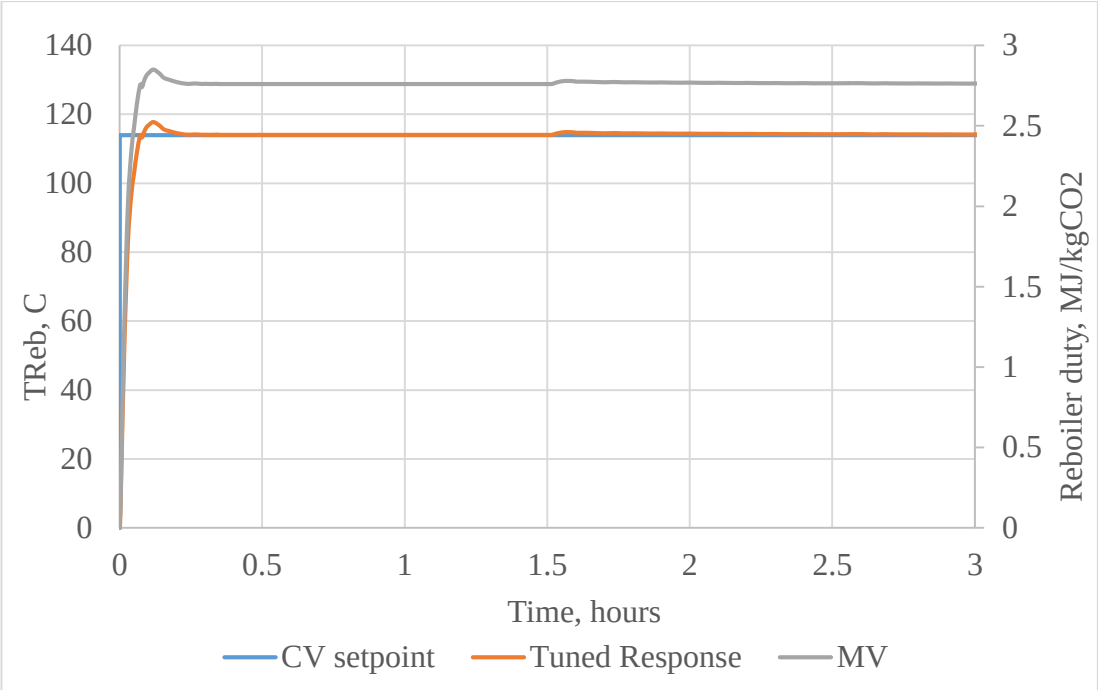

Figure 7.38. PID control signal of reboiler temperature in K_2CO_3 system for MIMO model

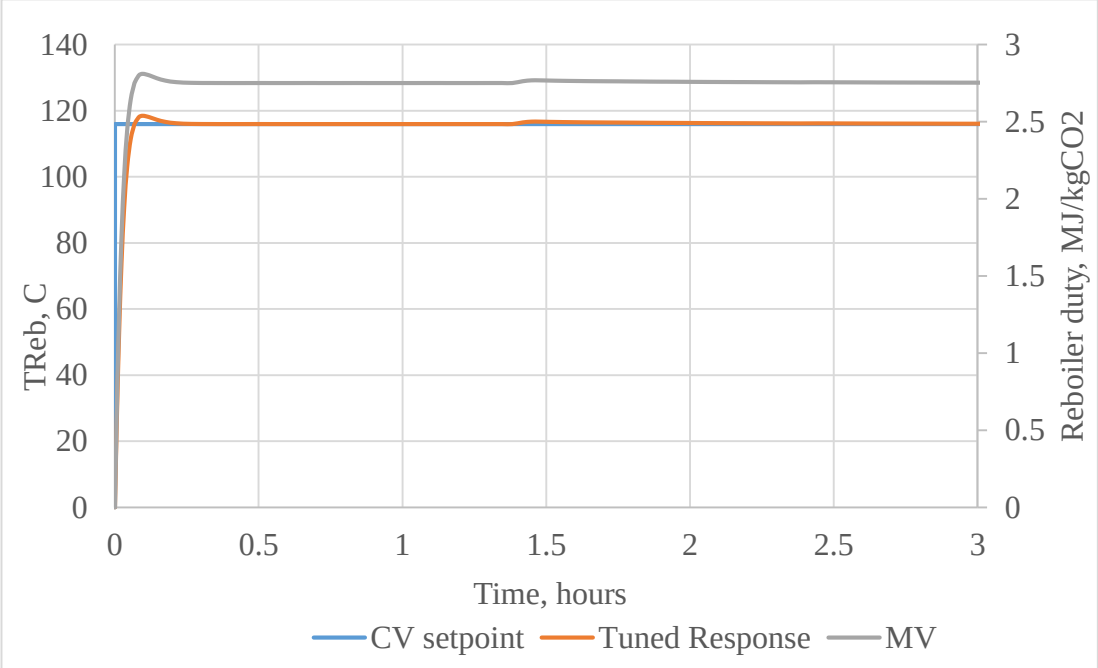

Figure 7.39. PID control signal of reboiler temperature in H_3BO_3/K_2CO_3 system for MIMO model

The overall responses in the MIMO models, as shown on all four graphs in Figures 7.36 to 7.39, demonstrate that the interaction effect does not negatively impact the performance of the PID controllers. For this reason, decouplers were not included in the MIMO control system design. In the case of the carbon capture level, no significant differences are observed for the time taken for the plant to attain the setpoint in the

MIMO system as compared to the SISO model. Whereas it was not the case in the SISO scenario, the performance of the carbon capture rate in the MIMO model indicates that minor fluctuations remain beyond 10 hours in the unpromoted HPC process as shown in Figure 7.36. The time taken to achieve steady-state condition for the reboiler temperature also appears to be similar in both the MIMO and SISO models. These observations confirm that there are no significant negative interaction effects in the MIMO control models.

7.6 LIMITATIONS OF PID CONTROLLERS

It has been acknowledged by many researchers that PID algorithms perform poorly when used alone in closed-loop control systems. These limitations of the PID controllers are particularly noted for higher order systems, and processes with resonances and unstable plant transfer functions (Onat 2019; Zheng et al. 2019; Ezema et al. 2014; Sung et al. 1996). This section briefly discusses some of the limitations of the PID control algorithms.

PID controllers pose difficulties in controlling both disturbance rejection processes and set-point tracking. If the controller performs well for the step set-point change or step output disturbance rejection process, it commonly shows a poor performance for the usual disturbance rejection process, because the step input disturbance is more frequent than the step output disturbance. Even though the dynamics of the algorithm is usually slower than that of the process, most often than not, the algorithm is designed to respond to the fast disturbance dynamics. So it usually responds sluggishly to slow disturbances. Alternatively, if it is designed to guarantee a good control performance for the step input disturbance, it usually shows too aggressive control action for the step set-point change. Also, since the PID controller only has one integrator, it usually have difficulties in manipulating ramptype set-point disturbances.

Further, the PID control algorithm usually have difficulties in controlling high order processes, and models with large time delays. In general, the control action is intended to guarantee a faster closed-loop response than the open-loop response in first order systems. However, if the time delay is much larger than the time constant of the process, this time delay term plays as a bottleneck for the fast closed-loop response. In recent years, the PID control systems are increasingly designed with a hierarchy

structure in order to allow the upper level controllers to control higher order processes efficiently.

Specific to the study completed in this thesis, the use of static RGA has the possibility of overshawing the true dynamic interactions between the manipulated and controlled varibles studied in this report. This could particularly limit the performance of the closed-loop control system if there are negative values present in the RGA. For such systems, it could be predicted that inverse responses are likely in the closed-loop control system, and as such requires the implementation of the dynamic RGA.

7.7 SUMMARY OF CHAPTER 7

In this chapter, research question #3 and thesis objectives #2 and #3 are addressed. The chapter covers the dynamic simulation and control study for the unpromoted and H_3BO_3 promoted HPC absorption process. Further details on how the dynamic simulations and control design are performed is explained here. The controlled variables, manipulated variables, and control objectives are discussed. Open-loop dynamic analyses and closed-loop control analyses are done. The major observations made in this chapter are as follows:

1. The HPC capture systems require a long settling time to attain new setpoints when disturbances in the lean solvent concentrations and CO_2 concentration in the flue gas stream are introduced.
2. Generally, the H_3BO_3 promoted HPC capture system has a slower dynamic response to variations in the lean solvent flowrate than the unpromoted HPC capture process. Both systems, however, showed a similar response rate to disturbances in the CO_2 concentration in the flue gas stream.
3. Manipulating the lean solvent flowrate is able to control the carbon capture efficiency as anticipated, indicating a strong relationship between the two variables.
4. The stripper reboiler temperature can also be controlled effectively by manipulating stripper reboiler duty, indicating a strong relationship between the two variables.
5. From the PID control analyses, the MIMO control system appears to be able to bring the system back to steady-state at a faster pace than the SISO system.

CHAPTER 8

CONCLUSIONS AND RECOMMENDATIONS

This section details the major conclusions made from this study. A comparison of the benchmarking absorbent for post-combustion carbon capture technologies, MEA, and hot potassium carbonate (HPC) are presented on their basis of carbon capture efficiency and energy efficiency. Conclusions on the most energy-efficient modified configurations studied in this work are also presented along with the most recommended modification for higher decarbonisation rate. Furthermore, the major conclusions drawn from the dynamic simulations and control study for HPC are mentioned. Finally, recommendations for future works on K_2CO_3 and H_3BO_3/K_2CO_3 carbon capture processes are highlighted.

8.1 CONCLUSIONS ON ENERGY EFFICIENCY OF MEA AND HPC

Steady-state rate-based analyses of the performances the benchmarking chemical solvent employed in the post-combustion carbon capture techniques are performed in this study. Rigorous efforts are taken to determine the complete energy requirements of both the MEA and HPC capture processes. Unlike many other research works that look into the reboiler duty and carbon capture efficiencies only as the basis of comparing these two solvents, this study disclosed the total cooling duty, heating duty and energy usage of major equipment such as heat exchangers, compressors and flash vessels. The considerations of these various energy duties confirmed the holistic approach taken in this work to ensure a fair comparison of the two solvents.

The results from the analyses conducted in this project show that hot potassium carbonate is a more energy-efficient chemical absorbent than the benchmarking solvent, MEA. In the amine carbon capture plant simulation, the specific reboiler duty is estimated to be 3.98 MJ/kgCO_2, along with a total cooling duty of 2.31 MJ/kgCO_2 (comprising condenser duty and lean solvent cooler duty) and heat exchanger energy requirement of 2.32 MJ/kgCO_2. These summed up to a total energy usage of 8.61 MJ/kgCO_2 for the amine carbon capture plant. In the piperazine promoted MEA capture process, the least total energy requirement is obtained for 5 wt% PZ/25 wt%

MEA. The total duty for this system is estimated to be 8.42 MJ/kgCO_2, which is roughly 2.21% energy savings over the unpromoted amine process. The unpromoted hot potassium carbonate capture plant however required 5.15 MJ/kgCO_2 as the total energy duty. This could be broken down into the reboiler duty of 2.76 MJ/kgCO_2 and total cooling duty of 2.39 MJ/kgCO_2. These results show that the HPC-based post-combustion carbon capture plant is able to save 30.65% of the reboiler duty in the amine-based capture plant, and attain a total energy slash down of 40.19% over the unpromoted MEA carbon capture system. The addition of boric acid is not found to significantly reduce the energy duty in the K_2CO_3 system. However, the promoted system is able to attain a 79.14% decarbonisation rate as compared to 78.17% in the unpromoted system. Due to the little improvement observed for the boric acid assisted HPC process, an optimised process for the unpromoted solvent is developed based on the results from the parametric analyses conducted. The optimisation entails increasing the lean solvent concentration from 40 wt% to 45 wt%, increasing the lean solvent flowrate by approximately 0.9% and increasing the absorber operating pressure from 15 atm to 20 atm. Instead of the Raschig Norton Metal-32 packing used in the base case study, the optimised process utilised Flexipac Koch Metal 1Y. This optimised process was able to enhance the carbon capture efficiency of the HPC process from 78.17% to 88.03%. This is calculated to be an improvement of 12.61% over the un-optimised K_2CO_3 process and 2.41% improvement over the unpromoted MEA-based process. The total energy consumption in this optimised K_2CO_3 process is also obtained to be 4.53 MJ/kgCO_2, which is 12.04% less than the requirement in the un-optimised K_2CO_3 process and 47.39% lesser than the usage in the unpromoted MEA process.

Following the detailed results above, it could be confidently confirmed that the hot potassium carbonate capture process utilises less energy than the benchmarking amine absorbent. K_2CO_3-based carbon capture technology in the post-combustion capture route, therefore, proves to be more energy-efficient than the MEA-based carbon capture technology. Even with optimisation of the K_2CO_3 process, the carbon capture rate is closely comparable to that obtained in the MEA-based capture process, with a slight improvement of 2.41% witnessed in the optimised process. Many other research works have however reported higher carbon capture rates for the MEA-based carbon capture process. For that reason, the slight improvement in the carbon capture rate of

the optimised K_2CO_3 over the benchmarking solvent reported in this study is not a proof of the superiority of the current solvent over the amine absorbent in terms of their decarbonisation capabilities.

8.2 CONCLUSIONS ON MODIFIED PROCESS CONFIGURATIONS

A total of seven different standalone process modifications were investigated for the MEA-based carbon capture system. The purpose of these investigations was to ascertain the total impact of the modified configurations on the performance of the MEA process. The impact of the modifications on the total heating and cooling duties, as well as the extra duties incurred due to the addition of auxiliary equipment, were reported. Based on the results of these analyses, intercooled absorber modification is the best configuration to employ for the enhancement of the decarbonisation level in the amine-based capture process. This modification was able to increase the carbon removal level from 85.96% in the base case process to 91.01%, equalling a rise of 5.87%. Despite the auxiliary duties incurred in the lean vapour compression modification, it was observed that this modification has the highest energy-saving capabilities. The analysis in this study proved that this modified configuration is able to scale down the total energy requirement of the amine process by 19.51%, reducing the magnitude from 8.61 MJ to 6.93 MJ per kilogramme of CO_2 captured.

In the hot potassium carbonate capture process, a total of seven standalone modified configurations were examined as well to ascertain their full influences on the system performance of the capture plant. The impacts of these modifications on the HPC process were not as profound as was the case in the amine process. The results singled out the flue gas precooling as the best modification for improving the capture rate in the HPC process. This modification was able to increase the decarbonisation level of the optimised HPC process from 88.03% to 93.06% when the flue gas temperature was reduced from 110 °C to 90 °C. Again, the choicest energy-saving configuration is the lean vapour compression. This modification was able to reduce the total energy requirement of the optimised HPC process from 4.53 MJ/kgCO_2 to 4.43 MJ/kgCO_2. However, the 2.26% improvement observed here is not comparable to 19.51% observed in the amine-based capture system. This is due to the higher auxiliary duties encountered in the HPC process.

The overall results of these analyses, however, demonstrate that the best energy-saving configuration in both MEA-based post-combustion carbon capture process and the HPC-based carbon capture process is the lean vapour compression. When looking at improving the carbon capture rate in the two solvents, the intercooled absorber configuration proves to be the most capable for the MEA-based capture process while the flue gas precooling appears to be the best for the hot potassium carbonate system.

8.3 CONCLUSIONS ON DYNAMIC SIMULATION AND CONTROL SYSTEM

The transient response of the carbon capture rate and the stripper reboiler duty to changes in diverse system parameters was investigated in this study. These analyses were completed for both the uncatalysed K_2CO_3 process and the H_3BO_3/K_2CO_3 systems. It is observed that the capture systems require a long settling time to attain new setpoints when disturbances in the lean solvent concentrations and CO_2 concentration in the flue gas stream were introduced. In the case of the uncatalysed K_2CO_3 system, the carbon capture rate was only able to attain a new set point after about 7 hours when ±5% disturbance in the lean solvent concentration was introduced. The H_3BO_3/K_2CO_3 process was only able to attain the new set point after about 14 hours. This shows that the catalysed HPC process is slower to respond to changes in the lean solvent concentration. When disturbances in the CO_2 concentration were introduced, both systems took approximately 12 hours to attain new setpoints for the stripper reboiler temperature. These results indicate the overall slow dynamic behaviour of the hot potassium carbonate capture process.

Using the lean solvent flowrate and the reboiler duty as the respective manipulated variables for controlling the carbon capture rate and the stripper reboiler temperature, PID control systems were designed for the HPC process. These CV-MV pairings were concluded after RGA analyses were performed. The flue gas flowrate, CO_2 concentration in the flue gas stream, lean solvent concentration and boric acid concentration were selected as disturbance variables. It was observed that the capture plants take longer time to attain the carbon capture level setpoints, whereas it takes a much shorter time to reach the steady state values for the reboiler temperature. Additionally, no significant negative interaction effects were observed in the MIMO

control system. This signifies that the SISO controller tuning parameters can perform adequately well in a MIMO scenario.

8.4 NOVEL SCIENTIFIC CONTRIBUTIONS FROM THIS RESEARCH

The following contributions are believed to be the major new additions made by this research work to the existing body of knowledge in the science of carbon capture and storage:

1. Modified process configurations have been implemented for hot K_2CO_3-based post-combustion carbon capture technology.
2. Optimised H_3BO_3 promoted hot K_2CO_3-based post-combustion carbon capture system is proposed and proven to be more energy-efficient as compared to the conventional MEA-based absorption process.
3. Dynamic simulations are performed for unpromoted and H_3BO_3 promoted hot K_2CO_3-based carbon capture plant.
4. Preliminary PID control analyses are completed for unpromoted and H_3BO_3 promoted hot K_2CO_3-based carbon capture plant.

8.5 ANSWERS TO THE RESEARCH QUESTIONS FOR THIS STUDY

1. As far as energy efficiency is concerned, the major insight that could be obtained from this research work is that unpromoted and H_3BO_3 promoted K_2CO_3-based absorption processes are promising energy-efficient post-combustion carbon capture technologies.
2. Regarding process modifications, it is discovered in this research work that flue gas pre-cooling could have a significant positive impact on the carbon capture efficiency of the HPC-based capture process. The lean vapour compression is also revealed to minimise the total energy usage in the said process. The rest of the modified processes analysed in this study only had marginal impacts on the system performance of the K_2CO_3-based capture plant.
3. To advance the commercial application of the HPC capture technology in post-combustion carbon capture plants, a robust control system is required to improve the flexibility of this technology and speed up the dynamic response of the controlled variables to variations in the manipulated variables.

8.6 RECOMMENDATIONS FOR FUTURE WORK

- As the first recommendation for future works that may want to investigate the performance of the HPC capture process, the author would suggest lab-scale studies and/or pilot plant studies of the H_3BO_3/K_2CO_3 system to gain a better understanding of the performance of this blended solvent. This would serve to confirm the true potentials of boric acid in improving the system performance of the HPC process. Nonetheless, other promoters with higher catalytic efficiency than boric acid could also be explored for the enhancement of the HPC capture rate.
- Additionally, rigorous techno-economic analyses of the HPC process in a lab-scale and/or pilot plant setting would be beneficial to further confirm the results obtained in the simulation-based study of this work. These techno-economic studies would enhance the understanding of how the unpromoted and promoted HPC capture systems, which have been studied in this work, perform in a real commercial-scale setting both technically and economically. These understandings are required to advance the application of this technology on a large scale.
- Further, as the dynamics studies completed in this work only considers disturbances of ±5% only, it is recommended for future works to consider higher changes such as ±10%, ±15%, ±20% and higher. This would further shed lights on how the system responds in transient scenarios when the disturbances change in higher magnitudes.
- Also, as the relative gain array implemented in the current study is the static one, the dynamic relative gain array is recommended for future works. This dynamic RGA could be particularly useful in tackling difficulties with inverse responses in the closed-loop system, which is highly likely for a static RGA with negative values.
- To improve upon the controllability of the HPC process, model predictive controllers (MPC) could be utilised to establish their superior performance over the conventional PID controllers. Also, the PI-PD control systems which are increasingly adopted as improved control algorithms over the conventional PID controllers could also be studied to investigate their performance for the HPC capture system.

- Finally, the PID, PI-PD and MPC control analyses could be implemented for promising modified process configurations such as intercooled absorber, rich solvent split, and lean vapour compression to understand their dynamic behaviour. As these modified configurations are generally acknowledged to enhance the performances of carbon capture systems, it is imperative to understand their dynamic behaviours before their applications could be advanced on a commercial scale.

REFERENCES

Ahmadi, M., V. G. Gomes, and K. Ngian. "Advanced modelling in performance optimization for reactive separation in industrial CO_2 removal." *Separation and Purification Technology* 63, no. 1 (2008): 107-115.

Alexanda Petrovic, Ben, and Salman Masoudi Soltani. "Optimization of Post Combustion CO_2 Capture from a Combined-Cycle Gas Turbine Power Plant via Taguchi Design of Experiment." *Processes* 7, no. 6 (2019): 364.

Ali, Usman, Elvis O. Agbonghae, Kevin J. Hughes, Derek B. Ingham, Lin Ma, and Mohamed Pourkashanian. "Techno-economic process design of a commercial-scale amine-based CO_2 capture system for natural gas combined cycle power plant with exhaust gas recirculation." *Applied Thermal Engineering* 103 (2016): 747-758.

Augustsson, Ola, Barath Baburao, Sanjay Dube, Steve Bedell, Peter Strunz, Michael Balfe, and Olaf Stallmann. "Chilled ammonia process scale-up and lessons learned." Energy Procedia 114 (2017): 5593-5615.

Bak, Chul-U., Muhammad Asif, and Woo-Seung Kim. "Experimental study on CO_2 capture by chilled ammonia process." Chemical Engineering Journal 265 (2015): 1-8.

Barchas, R., and R. Davis. "The Kerr-McGee/ABB Lummus Crest technology for the recovery of CO_2 from stack gases." *Energy Conversion and Management* 33, no. 5-8 (1992): 333-340.

Baxter, Larry, Andrew Baxter, and Stephanie Burt. "Cryogenic CO_2 capture as a cost-effective CO_2 capture process." In *International Pittsburgh Coal Conference*. 2009.

Behr, P., A. Maun, K. Deutgen, A. Tunnat, G. Oeljeklaus, and K. Görner. "Kinetic study on promoted potassium carbonate solutions for CO_2 capture from flue gas." *Energy Procedia* 4 (2011): 85-92.

Benson, H. E., J. H. Field, and R. M. Jimeson. "CO/sub 2/absorption: employing hot potassium carbonate solutions." *Chem. Eng. Prog.;(United States)* 50, no. 7 (1954).

Bi, Wentao, Tao Zhu, Dong Wha Park, and Kyung Ho Row. "Sorption of carbon dioxide by ionic liquid- based sorbents." *Asia- Pacific Journal of Chemical Engineering* 7, no. 1 (2012): 86-92.

Birkelund, Even Solnes. "CO_2 Absorption and Desorption Simulation with Aspen HYSYS." Master's thesis, Universitetet i Tromsø, 2013.

Black, Sean, Richard Rhudy. "Chilled Ammonia – Pilot Testing at the We Energies Pleasant Praire Power Plant." *12th IEA Post-combustion Meeting*. Regina, Saskatchewan. 30th September 2009.

Bohloul, M. R., M. Arab Sadeghabadi, S. M. Peyghambarzadeh, and M. R. Dehghani. "CO_2 absorption using aqueous solution of potassium carbonate: Experimental measurement and thermodynamic modeling." Fluid Phase Equilibria 447 (2017): 132-141.

Borhani, Tohid N., Eni Oko, and Meihong Wang. "Process modelling and analysis of intensified CO_2 capture using monoethanolamine (MEA) in rotating packed bed absorber." *Journal of cleaner production* 204 (2018): 1124-1142.

Borhani, Tohid Nejad Ghaffar, Abbas Azarpour, Vahid Akbari, Sharifah Rafidah Wan Alwi, and Zainuddin Abdul Manan. "CO_2 capture with potassium carbonate solutions: A state-of-the-art review." *International Journal of Greenhouse Gas Control* 41 (2015): 142-162.

Bravo, Jose L. "Mass transfer in gauze packings." *Hydrocarbon processing* 64 (1985): 91-95.

Brief, Carbon. "Around the world in 22 carbon capture projects." *Fonte: Carbon Brief clear on climate: https://www. carbonbrief. org/around-the-world-in-22-carboncapture-projects* (2014).

Brunetti, Adele, Francesco Scura, Giuseppe Barbieri, and Enrico Drioli. "Membrane technologies for CO_2 separation." *Journal of Membrane Science* 359, no. 1-2 (2010): 115-125.

Canepa, Roberto, and Meihong Wang. "Techno-economic analysis of a CO_2 capture plant integrated with a commercial scale combined cycle gas turbine (CCGT) power plant." *Applied Thermal Engineering* 74 (2015): 10-19.

Chen, Feng- Feng, Kuan Huang, Jie- Ping Fan, and Duan- Jian Tao. "Chemical solvent in chemical solvent: A class of hybrid materials for effective capture of CO_2." *AIChE Journal* 64, no. 2 (2018): 632-639.

Cheng, Lijing, Kevin E. Trenberth, John Fasullo, Tim Boyer, John Abraham, and Jiang Zhu. "Improved estimates of ocean heat content from 1960 to 2015." *Science Advances* 3, no. 3 (2017): e1601545.

Chiesa, Paolo, and Stefano Consonni. "Shift reactors and physical absorption for low-CO_2 emission IGCCs." *Journal of Engineering for Gas Turbines and Power* 121, no. 2 (1999): 295-305.

Chinen, Anderson Soares, Joshua C. Morgan, Benjamin Omell, Debangsu Bhattacharyya, and David C. Miller. "Dynamic data reconciliation and validation of a dynamic model for solvent-based CO_2 capture using pilot-plant data." *Industrial & Engineering Chemistry Research* 58, no. 5 (2019): 1978-1993.

Choi, Seung Wan, Jialiang Tang, Vilas G. Pol, and Ki Bong Lee. "Pollen-derived porous carbon by KOH activation: Effect of physicochemical structure on CO_2 adsorption." *Journal of CO_2 Utilization* 29 (2019): 146-155.

Chowdhury, Firoz Alam, Hidetaka Yamada, Takayuki Higashii, Kazuya Goto, and Masami Onoda. "CO_2 capture by tertiary amine absorbents: a performance comparison study." *Industrial & engineering chemistry research* 52, no. 24 (2013): 8323-8331.

Cousins[a], Ashleigh, Leigh T. Wardhaugh, and Paul HM Feron. "Preliminary analysis of process flow sheet modifications for energy efficient CO_2 capture from flue gases using chemical absorption." *Chemical Engineering Research and Design* 89, no. 8 (2011): 1237-1251.

Cousins[b], Ashleigh, Leigh T. Wardhaugh, and Paul HM Feron. "Analysis of combined process flow sheet modifications for energy efficient CO_2 capture from flue gases using chemical absorption." *Energy Procedia* 4 (2011): 1331-1338.

Dai, Zhongde, Luca Ansaloni, and Liyuan Deng. "Recent advances in multi-layer composite polymeric membranes for CO_2 separation: A review." *Green Energy & Environment* 1, no. 2 (2016): 102-128.

Darde, Arthur, Rajeev Prabhakar, Jean-Pierre Tranier, and Nicolas Perrin. "Air separation and flue gas compression and purification units for oxy-coal combustion systems." *Energy Procedia* 1, no. 1 (2009): 527-534.

Darde, Victor, Willy JM van Well, Erling H. Stenby, and Kaj Thomsen. "CO_2 capture using aqueous ammonia: kinetic study and process simulation." *Energy Procedia* 4 (2011): 1443-1450.

Decardi-Nelson, Benjamin, Su Liu, and Jinfeng Liu. "Improving Flexibility and Energy Efficiency of Post-Combustion CO_2 Capture Plants Using Economic Model Predictive Control." *Processes* 6, no. 9 (2018): 135.

Dugas, Ross Edward. "Carbon dioxide absorption, desorption, and diffusion in aqueous piperazine and monoethanolamine." (2009).

Ebner, Armin D., and James A. Ritter. "State-of-the-art adsorption and membrane separation processes for carbon dioxide production from carbon dioxide emitting industries." *Separation Science and Technology* 44, no. 6 (2009): 1273-1421.

Echt, W., 2013. Technologies for Efficient Purification of Natural and Synthesis Gases-UOP Benfield™ Process. Available: https://www.uop.com/technologies-forefficient-purification-of-natural-and-synthesis-gases/. [Accessed July 17, 2019]

Eisenberg, Benjamin, and Russell R. Johnson. "Amine regeneration process." U.S. Patent 4,152,217, issued May 1, 1979.

Ezema, E. E., I. I. Eneh, and O. L. Daniya. "Improving structural limitations of PID controller for unstable processes." International Journal of Engineering Research & Applications 4, no. 9 (2014): 87-90.

Freeman, Stephanie A., Ross Dugas, David H. Van Wagener, Thu Nguyen, and Gary T. Rochelle. "Carbon dioxide capture with concentrated, aqueous piperazine." *International Journal of Greenhouse Gas Control* 4, no. 2 (2010): 119-124.

Furukawa, S. K., and R. K. Bartoo. "Improved Benfield process for ammonia plants." *Universal Oil Products, Des Plaines, USA* (1997).

Gaspar, Jozsef, John Bagterp Jorgensen, and Philip Loldrup Fosbol. "Control of a post-combustion CO_2 capture plant during process start-up and load variations." *IFAC-PapersOnLine* 48, no. 8 (2015): 580-585.

Gaspar, Jozsef, Philip Loldrup Fosbøl, John Bagterp Jørgensen, Kaj Thomsen, and Nicolas von Solms. "CO_2 Capture Dynamic and Steady-State Model Development, Optimization and Control: Applied to Piperazine and Enzyme Promoted MEA/MDEA." (2016).

Gaspar, Jozsef. "CO_2 Capture Dynamic and Steady-State Model Development, Optimization and Control: Applied to Piperazine and Enzyme Promoted MEA/MDEA." PhD diss., Technical University of Denmark (DTU). 2016. https://orbit.dtu.dk/files/128046202/611331_Jozsef_Gaspar_Thesis.pdf [Accessed August 7, 2019]

Gelowitz, Don, Paitoon Tontiwachwuthikul, and Raphael Idem. "Method and absorbent compositions for recovering a gaseous component from a gas stream." U.S. Patent 9,028,593, issued May 12, 2015.

Ghosh, Ujjal K., Sandra E. Kentish, and Geoff W. Stevens. "Absorption of carbon dioxide into aqueous potassium carbonate promoted by boric acid." *Energy Procedia* 1, no. 1 (2009): 1075-1081.

Ghosh, Ujjal K., Sandra E. Kentish, and Geoff W. Stevens. "Absorption of carbon dioxide into aqueous potassium carbonate promoted by boric acid." *Energy Procedia* 1, no. 1 (2009): 1075-1081.

Gielen, Dolf, Jacek Podkański, and Jacek Podkanski. *Prospects for CO_2 capture and storage*. Simon and Schuster, 2004.

Global Carbon Capture and Storage Institute's report on the global status of CCS in 2018. https://indd.adobe.com/view/2dab1be7-edd0-447d-b020-06242ea2cf3b [Access July 12, 2019]

Goto, Kazuya, Katsunori Yogo, and Takayuki Higashii. "A review of efficiency penalty in a coal-fired power plant with post-combustion CO_2 capture." *Applied Energy* 111 (2013): 710-720.

Grimekis, Dimitrios, Sotirios Giannoulidis, Konstantina Manou, Kyriakos D. Panopoulos, and Sotirios Karellas. "Experimental investigation of CO_2 solubility and its absorption rate into promoted aqueous potassium carbonate solutions at elevated temperatures." *International Journal of Greenhouse Gas Control* 81 (2019): 83-92.

Guo, Dongfang, Hendy Thee, Gabriel da Silva, Jian Chen, Weiyang Fei, Sandra Kentish, and Geoffrey W. Stevens. "Borate-catalyzed carbon dioxide hydration via the carbonic anhydrase mechanism." *Environmental science & technology* 45, no. 11 (2011): 4802-4807.

Habib, Mohamed A., Medhat A. Nemitallah, and Hassan M. Badr. *Oxyfuel Combustion for Clean Energy Applications*. Springer, 2019.

Harkin, Trent, Andrew Hoadley, and Barry Hooper. "Using multi-objective optimisation in the design of CO_2 capture systems for retrofit to coal power stations." Energy 41, no. 1 (2012): 228-235.

Harun, Noorlisa, Thanita Nittaya, Peter L. Douglas, Eric Croiset, and Luis A. Ricardez-Sandoval. "Dynamic simulation of MEA absorption process for CO_2 capture from power plants." *International Journal of Greenhouse Gas Control* 10 (2012): 295-309.

Hasan, MM Faruque, Eric L. First, and Christodoulos A. Floudas. "Cost-effective CO_2 capture based on in silico screening of zeolites and process optimization." *Physical Chemistry Chemical Physics* 15, no. 40 (2013): 17601-17618.

Hatmi, Khalid Al, As' ad Al Mashrafi, Sa'Ud Al Balushi, Haitham Al-Kalbani, Mundhir Al-Battashi, and Mohammed Shaikh. "Energy Savings of Amine Sweetening Process through Lean and Rich Vapor Compression Approaches." In Abu Dhabi International Petroleum Exhibition & Conference. Society of Petroleum Engineers, 2018.

Hedin, Niklas, Linnéa Andersson, Lennart Bergström, and Jinyue Yan. "Adsorbents for the post-combustion capture of CO_2 using rapid temperature swing or vacuum swing adsorption." *Applied Energy* 104 (2013): 418-433.

Hemmati, Abbas, and Hamed Rashidi. "Optimization of industrial intercooled post-combustion CO_2 absorber by applying rate-base model and response surface

methodology (RSM)." *Process Safety and Environmental Protection* 121 (2019): 77-86.

Herrin, J. Pearman. "Process sequencing for amine regeneration." U.S. Patent 4,798,910, issued January 17, 1989.

Ho, Minh T., Enrique Garcia-Calvo Conde, Stefania Moioli, and Dianne E. Wiley. "The effect of different process configurations on the performance and cost of potassium taurate solvent absorption." International Journal of Greenhouse Gas Control 81 (2019): 1-10.

http://apett.net/aem/co2-removal-using-lo-heat-benfield-process-2/ [Accessed July 17, 2019]

https://climate.nasa.gov/evidence/ [Accessed June 7th 2019]

https://netl.doe.gov/sites/default/files/event-proceedings/2016/C0$_2$%20cap%20review/2-Tuesday/D-Muraskin-GE-Alstom-Chilled-Ammonia-Large-Pilot.pdf [Access July 15, 2019]

https://www.alstom.com/press-releases-news/2010/12/alstom-chilled-ammonia-process-selected-for-leading-CO_2-capture-plant-in-romania [Access July 15, 2019]

https://www.esrl.noaa.gov/gmd/ccgg/trends/ [Accessed March 6, 2019]

https://www.ge.com/power/steam/CO_2-capture/post-combustion-cap [Access July 15, 2019]

https://www.grandviewresearch.com/blog/worlds-largest-carbon-capture-plant-to-open-soon [Access July 12, 2019]

https://www.iea.org/statistics/CO_2emissions/ [Accessed June 26th 2019]

https://www.nasa.gov/press-release/2018-fourth-warmest-year-in-continued-warming-trend-according-to-nasa-noaa [Accessed June 6th 2019]

https://www.uop.com/technologies-for-efficient-purification-of-natural-and-synthesis-gases/ [Accessed July 17, 2019]

Hu, Guoping, Kathryn H. Smith, Yue Wu, Sandra E. Kentish, and Geoff W. Stevens. "Screening amino acid salts as rate promoters in potassium carbonate solvent for carbon dioxide absorption." *Energy & Fuels* 31, no. 4 (2017): 4280-4286.

Hu, Guoping, Nathan J. Nicholas, Kathryn H. Smith, Kathryn A. Mumford, Sandra E. Kentish, and Geoffrey W. Stevens. "Carbon dioxide absorption into promoted potassium carbonate solutions: A review." *International Journal of Greenhouse Gas Control* 53 (2016): 28-40.

Hu[a], Yue, Gang Xu, Cheng Xu, and Yongping Yang. "Thermodynamic analysis and techno-economic evaluation of an integrated natural gas combined cycle (NGCC) power plant with post-combustion CO_2 capture." *Applied Thermal Engineering* 111 (2017): 308-316.

Jang, Eunji, Seung Wan Choi, Seok-Min Hong, Sangcheol Shin, and Ki Bong Lee. "Development of a cost-effective CO_2 adsorbent from petroleum coke via KOH activation." *Applied Surface Science* 429 (2018): 62-71.

Jansen, Daniel, Matteo Gazzani, Giampaolo Manzolini, Eric van Dijk, and Michiel Carbo. "Pre-combustion CO_2 capture." *International Journal of Greenhouse Gas Control* 40 (2015): 167-187.

Jassim, Majeed S., and Gary T. Rochelle. "Innovative absorber/stripper configurations for CO_2 capture by aqueous monoethanolamine." *Industrial & engineering chemistry research* 45, no. 8 (2006): 2465-2472.

Jeong, Yeong Su, Jaeheum Jung, Ung Lee, Changryung Yang, and Chonghun Han. "Techno-economic analysis of mechanical vapor recompression for process integration of post-combustion CO_2 capture with downstream compression." *Chemical Engineering Research and Design* 104 (2015): 247-255.

Ji, Guozhao, and Ming Zhao. "Membrane separation technology in carbon capture." *Recent Advances in Carbon Capture and Storage; Yun, Y., Ed* (2017): 59-90.

Jiang, Kaiqi, Kangkang Li, Hai Yu, and Paul HM Feron. "Piperazine-promoted aqueous-ammonia-based CO_2 capture: Process optimisation and modification." Chemical Engineering Journal 347 (2018): 334-342.

Kamijo, T. I. M. M., Masaki Iijima, Tomio Mimura, and Yasuyuki Yagi. "Apparatus and method for CO_2 recovery." *Mitsubishi Heavy Industries, Kansai Electric Company. EP1695756* (2006).

Karimi, Mehdi, Magne Hillestad, and Hallvard F. Svendsen. "Capital costs and energy considerations of different alternative stripper configurations for post combustion CO_2 capture." *Chemical engineering research and design* 89, no. 8 (2011): 1229-1236.

Kaur, Balpreet, Raj Kumar Gupta, and Haripada Bhunia. "Chemically activated nanoporous carbon adsorbents from waste plastic for CO_2 capture: Breakthrough adsorption study." *Microporous and Mesoporous Materials* 282 (2019): 146-158.

Keller, Laura, Theresa Lohaus, Lorenz Abduly, Greta Hadler, and Matthias Wessling. "Electrical swing adsorption on functionalized hollow fibers." *Chemical Engineering Journal*371 (2019): 107-117.

Khanna, Yogya, Shivam Puri, Prakhar Verma, Dasaradhi Putta, and Preeti Joshi. "Separation of Nitrogen from Combustion Using Pressure Swing Adsorption (PSA) Technique and Incorporating Zeolites." In *Advances in Interdisciplinary Engineering*, pp. 131-140. Springer, Singapore, 2019.

Kothandaraman, Anusha. Carbon dioxide capture by chemical absorption: a solvent comparison study. Vol. 72, no. 01. 2010.

Kozak, Fred, Arlyn Petig, Ed Morris, Richard Rhudy, and David Thimsen. "Chilled ammonia process for CO_2 capture." *Energy Procedia* 1, no. 1 (2009): 1419-1426.

Lawal, Adekola, Meihong Wang, Peter Stephenson, and Hoi Yeung. "Dynamic modeling and simulation of CO_2 chemical absorption process for coal-fired power plants." In *Computer Aided Chemical Engineering*, vol. 27, pp. 1725-1730. Elsevier, 2009.

Lawal, Adekola, Meihong Wang, Peter Stephenson, and Okwose Obi. "Demonstrating full-scale post-combustion CO_2 capture for coal-fired power plants through dynamic modelling and simulation." *Fuel* 101 (2012): 115-128.

Le Moullec, Yann, Thibaut Neveux, Adam Al Azki, Actor Chikukwa, and Karl Anders Hoff. "Process modifications for solvent-based post-combustion CO_2 capture." *International Journal of Greenhouse Gas Control* 31 (2014): 96-112.

Lecomte, Fabrice, Paul Broutin, and Étienne Lebas. *CO_2 capture: technologies to reduce greenhouse gas emissions*. Editions Technip, 2010.

Lee, Ji Hyun, No Sang Kwak, In Young Lee, Kyung Ryoung Jang, Dong Woog Lee, Se Gyu Jang, Byung Kook Kim, and Jae-Goo Shim. "Performance and economic analysis of commercial-scale coal-fired power plant with post-combustion CO_2 capture." *Korean Journal of Chemical Engineering* 32, no. 5 (2015): 800-807.

Lemaire, Eric, Pierre Antoine Bouillon, and Kader Lettat. "Development of HiCapt+ TM Process for CO_2 Capture from Lab to Industrial Pilot Plant." *Oil & Gas Science and Technology–Revue d'IFP Energies nouvelles* 69, no. 6 (2014): 1069-1080.

Leung, Dennis YC, Giorgio Caramanna, and M. Mercedes Maroto-Valer. "An overview of current status of carbon dioxide capture and storage technologies." *Renewable and Sustainable Energy Reviews* 39 (2014): 426-443.

Levitus, S.; Antonov, J.; Boyer, T.; Baranova, O.; Garcia, H.; Locarnini, R.; Mishonov, A.; Reagan, J.; Seidov, D.; Yarosh, E.; Zweng, M. (2017). NCEI ocean heat content, temperature anomalies, salinity anomalies, thermosteric sea level anomalies, halosteric sea level anomalies, and total steric sea level anomalies from 1955 to present calculated from in situ oceanographic subsurface profile data (NCEI Accession 0164586). Version 4.4. NOAA National Centres for Environmental Information. Dataset. doi:10.7289/V53F4MVP [Accessed June 7th 2019]

Li, Dawei, Jiaojiao Zhou, Yu Wang, Yuanyu Tian, Ling Wei, Zongbo Zhang, Yingyun Qiao, and Junhua Li. "Effects of activation temperature on densities and volumetric CO_2 adsorption performance of alkali-activated carbons." *Fuel* 238 (2019): 232-239.

Li, Xiaofei, Shujuan Wang, and Changhe Chen. "Experimental and rate- based modeling study of CO_2 capture by aqueous monoethanolamine." *Greenhouse Gases: Science and Technology* 4, no. 4 (2014): 495-508.

Li, Yifu, Li'ao Wang, Zhongchao Tan, Zhien Zhang, and Xinyue Hu. "Experimental studies on carbon dioxide absorption using potassium carbonate solutions with amino acid salts." *Separation and Purification Technology* 219 (2019): 47-54.

Li, Yingjie, Changsui Zhao, Huichao Chen, Qiangqiang Ren, and Lunbo Duan. "CO_2 capture efficiency and energy requirement analysis of power plant using modified calcium-based sorbent looping cycle." *Energy* 36, no. 3 (2011): 1590-1598.

Li[a], Kangkang. "Experimental and modelling study of advanced aqueous ammonia based post combustion capture process." PhD dissertation, Curtin University, 2016.

Liang, Haiwen, Zhigao Xu, and Fengqi Si. "Economic analysis of amine based carbon dioxide capture system with bi-pressure stripper in supercritical coal-fired power plant." *International journal of greenhouse gas control* 5, no. 4 (2011): 702-709.

Li[b], Kangkang, Wardhaugh Leigh, Paul Feron, Hai Yu, and Moses Tade. "Systematic study of aqueous monoethanolamine (MEA)-based CO_2 capture process: techno-economic assessment of the MEA process and its improvements." *Applied energy* 165 (2016): 648-659.

Li[c], Kangkang, Ashleigh Cousins, Hai Yu, Paul Feron, Moses Tade, Weiliang Luo, and Jian Chen. "Systematic study of aqueous monoethanolamine- based CO_2 capture process: model development and process improvement." *Energy Science & Engineering* 4, no. 1 (2016): 23-39.

Li[d], Kangkang, Hai Yu, Paul Feron, Leigh Wardhaugh, and Moses Tade. "Techno-economic assessment of stripping modifications in an ammonia-based post-combustion capture process." *International Journal of Greenhouse Gas Control* 53 (2016): 319-327.

Ling, Hao, Sen Liu, Hongxia Gao, and Zhiwu Liang. "Effect of heat-stable salts on absorption/desorption performance of aqueous monoethanolamine (MEA) solution during carbon dioxide capture process." *Separation and Purification Technology* 212 (2019): 822-833.

Littel, R. J., G. F. Versteeg, and Willibrordus Petrus Maria Van Swaaij. "Physical absorption of CO_2 and propene into toluene/water emulsions." *AIChE journal* 40, no. 10 (1994): 1629-1638.

Liu, Jialin. "Investigation of Energy-Saving Designs for an Aqueous Ammonia-Based Carbon Capture Process." *Industrial & Engineering Chemistry Research* 57, no. 45 (2018): 15460-15472.

Liu, Liangxu, Jun Zhao, Shuai Deng, and Qingsong An. "A technical and economic study on solar-assisted ammonia-based post-combustion CO_2 capture of power plant." *Applied Thermal Engineering* 102 (2016): 412-422.

Lombardo, Gerard, Ritesh Agarwal, and Jalal Askander. "Chilled ammonia process at technology center mongstad–first results." *Energy Procedia* 51 (2014): 31-39.

Lu, Ruize, Kangkang Li, Jian Chen, Hai Yu, and Moses Tade. "CO_2 capture using piperazine-promoted, aqueous ammonia solution: Rate-based modelling and process simulation." *International Journal of Greenhouse Gas Control* 65 (2017): 65-75.

Luis, Patricia. "Use of monoethanolamine (MEA) for CO_2 capture in a global scenario: Consequences and alternatives." *Desalination* 380 (2016): 93-99.

Mac Dowell, N., and N. Shah. "Optimisation of post-combustion CO_2 capture for flexible operation." *Energy Procedia* 63 (2014): 1525-1535.

Majoumerd, Mohammad Mansouri, and Mohsen Assadi. "Techno-economic assessment of fossil fuel power plants with CO_2 capture–Results of EU H2-IGCC project." *International Journal of Hydrogen Energy* 39, no. 30 (2014): 16771-16784.

Makino, Takashi, Katsuhiko Tsunashima, and Mitsuhiro Kanakubo. "CO_2 absorption and physical properties of tributyloctylphosphonium benzotriazolate." *Fluid Phase Equilibria* 494 (2019): 1-7.

Manaf, Norhuda Abdul, Ashleigh Cousins, Paul Feron, and Ali Abbas. "Dynamic modelling, identification and preliminary control analysis of an amine-based post-combustion CO_2 capture pilot plant." *Journal of Cleaner Production* 113 (2016): 635-653.

Mechleri, Evgenia, Adekola Lawal, Alfredo Ramos, John Davison, and Niall Mac Dowell. "Process control strategies for flexible operation of post-combustion CO_2 capture plants." *International Journal of Greenhouse Gas Control* 57 (2017): 14-25.

Mimura, T., Yagi, Y., Iijima, M., 2006. System and method for recovering CO_2. Patent No. CA 2557454 A1, The Kansai Electric Power Co. Inc., Mitsubishi Heavy Industries Ltd.

Mohanty, Kaustubha, and Mihir K. Purkait. *Membrane technologies and applications*. CRC press, 2011.

Mohsin, Hanan Mohamed, Azmi Mohd Shariff, and Khairiraihanna Johari. "Glycine (GLY) Mixed with 3-Dimethylamino-1-Propylamine (DMAPA) as a Potential Absorbent for Carbon Dioxide Capture and Subsequent Utilization." *Separation and Purification Technology* (2019).

Molina, Carol Toro, and Chakib Bouallou. "Assessment of different methods of CO_2 capture in post-combustion using ammonia as solvent." *Journal of Cleaner Production* 103 (2015): 463-468.

Mondino, Giorgia, Carlos A. Grande, Richard Blom, and Lars O. Nord. "Moving bed temperature swing adsorption for CO_2 capture from a natural gas combined cycle power plant." *International Journal of Greenhouse Gas Control* 85 (2019): 58-70.

Mukherjee, Alivia, Jude A. Okolie, Amira Abdelrasoul, Catherine Niu, and Ajay K. Dalai. "Review of post-combustion carbon dioxide capture technologies using activated carbon." *Journal of Environmental Sciences* (2019).

Mumford, Kathryn A., Kathryn H. Smith, Clare J. Anderson, Shufeng Shen, Wendy Tao, Yohanes A. Suryaputradinata, Abdul Qader et al. "Post-combustion capture of CO_2: results from the solvent absorption capture plant at Hazelwood power station using potassium carbonate solvent." *Energy & fuels*26, no. 1 (2011): 138-146.

Nakagaki, Takao, Ryutaro Yamabe, Yukio Furukawa, Hiroshi Sato, and Yasuro Yamanaka. "Experimental evaluation of temperature and concentration effects on heat of dissociation of CO_2-loaded MEA solution in strippers." *Energy Procedia* 114 (2017): 1910-1918.

Nandi, Shyamapada, Phil De Luna, Thomas D. Daff, Jens Rother, Ming Liu, William Buchanan, Ayman I. Hawari, Tom K. Woo, and Ramanathan Vaidhyanathan. "A single-ligand ultra-microporous MOF for precombustion CO_2 capture and hydrogen purification." *Science Advances* 1, no. 11 (2015): e1500421.

Narimani, Milad, Sepideh Amjad-Iranagh, and Hamid Modarress. "CO_2 absorption into aqueous solutions of monoethanolamine, piperazine and their blends: Quantum mechanics and molecular dynamics studies." *Journal of Molecular Liquids* 233 (2017): 173-183.

Nerem, Robert S., Brian D. Beckley, John T. Fasullo, Benjamin D. Hamlington, Dallas Masters, and Gary T. Mitchum. "Climate-change–driven accelerated sea-level rise detected in the altimeter era." *Proceedings of the National Academy of Sciences* 115, no. 9 (2018): 2022-2025.

Nittaya, Thanita, Peter L. Douglas, Eric Croiset, and Luis A. Ricardez-Sandoval. "Dynamic modelling and controllability studies of a commercial-scale MEA absorption processes for CO_2 capture from coal-fired power plants." *Energy Procedia*63 (2014): 1595-1600.

Nogalska, Adrianna, Adrianna Zukowska, and Ricard Garcia-Valls. "Atmospheric CO_2 capture for the artificial photosynthetic system." *Science of the Total Environment*621 (2018): 186-192.

Nwokedi, Ikenna C., and Philomena K. Igbokwe. "Chemical Process Absorption Column Design for CO_2 Sequestration." *Journal of Engineering Research and Reports* (2019): 1-14.

Obek, Christine Ann, Foster Kofi Ayittey, and Agus Saptoro. "Improved process modifications of aqueous ammonia-based CO_2 capture system." In MATEC Web of Conferences, vol. 268, p. 02004. EDP Sciences, 2019.

Oh, Se-Young, Michael Binns, Habin Cho, and Jin-Kuk Kim. "Energy minimization of MEA-based CO_2 capture process." *Applied energy* 169 (2016): 353-362.

Oh, Tick Hui. "Carbon capture and storage potential in coal-fired plant in Malaysia—A review." *Renewable and Sustainable Energy Reviews* 14, no. 9 (2010): 2697-2709.

Oko, Eni, Meihong Wang, and Atuman S. Joel. "Current status and future development of solvent-based carbon capture." *International Journal of Coal Science & Technology* 4, no. 1 (2017): 5-14.

Oko, Eni, Toluleke E. Akinola, Chin-Hung Cheng, Meihong Wang, Jian Chen, and Colin Ramshaw. "Experimental study of CO_2 solubility in high concentration MEA solution for intensified solvent-based carbon capture." In *MATEC Web of Conferences*, vol. 272, p. 01004. EDP Sciences, 2019.

Omidfar, Narges, Ali Mohamadalizadeh, and Seyed Hamed Mousavi. "Carbon dioxide adsorption by modified carbon nanotubes." *Asia‐Pacific Journal of Chemical Engineering* 10, no. 6 (2015): 885-892.

Onat, Cem. "A new design method for PI–PD control of unstable processes with dead time." ISA transactions 84 (2019): 69-81.

Othman, M. R., R. Zakaria, and W. J. N. Fernando. "Strategic planning on carbon capture from coal fired plants in Malaysia and Indonesia: A review." *Energy Policy* 37, no. 5 (2009): 1718-1735.

Oyenekan, Babatunde A., and Gary T. Rochelle. "Alternative stripper configurations for CO_2 capture by aqueous amines." *AIChE Journal* 53, no. 12 (2007): 3144-3154.

Oyenekan, Babatunde A., and Gary T. Rochelle. "Energy performance of stripper configurations for CO_2 capture by aqueous amines." *Industrial & Engineering Chemistry Research* 45, no. 8 (2006): 2457-2464.

Palomar, Jose, Maria Gonzalez-Miquel, Alicia Polo, and Francisco Rodriguez. "Understanding the physical absorption of CO_2 in ionic liquids using the COSMO-RS method." *Industrial & Engineering Chemistry Research* 50, no. 6 (2011): 3452-3463.

Parker, Larry, and Peter Folger. "Capturing CO_2 from Coal-Fired Power Plants: Challenges for a Comprehensive Strategy." (2010).

Pérez-Calvo, José-Francisco, Daniel Sutter, Matteo Gazzani, and Marco Mazzotti. "Application of a chilled ammonia-based process for CO_2 capture to cement plants." Energy Procedia 114 (2017): 6197-6205.

Plaza, M. G., and F. Rubiera. "Evaluation of a novel multibed heat-integrated vacuum and temperature swing adsorption post-combustion CO_2 capture process." *Applied Energy* 250 (2019): 916-925.

Plus[a], Aspen. "Rate Based model of the CO_2 capture process by MEA using Aspen Plus." *Aspen Technology Inc, Cambridge, MA, USA* (2008).

Plus[b], Aspen. "Rate Based model of the CO_2 capture process by NH_3 using Aspen Plus." *Aspen Technology Inc, Cambridge, MA, USA* (2008).

Plus[c], Aspen. "Rate Based model of the CO_2 capture process by K_2CO_3 using Aspen Plus." *Aspen Technology Inc, Cambridge, MA, USA* (2008).

Plus[d], Aspen. "Rate Based model of the CO_2 capture process by mixed PZ and MEA using Aspen Plus." *Aspen Technology Inc, Cambridge, MA, USA* (2008).

Posch, Sebastian, and Markus Haider. "Dynamic modeling of CO_2 absorption from coal-fired power plants into an aqueous monoethanolamine solution." *Chemical engineering research and design* 91, no. 6 (2013): 977-987.

Prasad, Babul, Ratul Mitra Thakur, Bishnupada Mandal, and Baowei Su. "Enhanced CO_2 separation membrane prepared from waste by-product of silk fibroin." *Journal of Membrane Science* (2019): 117170.

Qadir, Abdul, Lucy Carter, Tony Wood, and Ali Abbas. "Economic and policy evaluation of SPCC (solar-assisted post-combustion carbon capture) in Australia." *Energy* 93 (2015): 294-308.

Quyn, Dimple, Aravind V. Rayer, Jeffri Gouw, Indrawan Indrawan, Kathryn A. Mumford, Clare J. Anderson, Barry Hooper, and Geoffrey W. Stevens. "Results from a pilot plant using un-promoted potassium carbonate for carbon capture." *Energy Procedia* 37 (2013): 448-454.

Quyn, Dimple, Aravind V. Rayer, Jeffri Gouw, Indrawan Indrawan, Kathryn A. Mumford, Clare J. Anderson, Barry Hooper, and Geoffrey W. Stevens. "Results from a pilot plant using un-promoted potassium carbonate for carbon capture." *Energy Procedia* 37 (2013): 448-454.

Rackley, Stephen A. "Carbon capture and storage. Stephen A. Rackley." (2010).

Rao, Anand B., and Edward S. Rubin. "A technical, economic, and environmental assessment of amine-based CO_2 capture technology for power plant greenhouse gas control." *Environmental science & technology* 36, no. 20 (2002): 4467-4475.

Razi, Neda, Hallvard F. Svendsen, and Olav Bolland. "Validation of mass transfer correlations for CO_2 absorption with MEA using pilot data." *International Journal of Greenhouse Gas Control* 19 (2013): 478-491.

Reddy, Satish, John Gillmartin, and Valerie Francuz. "Integrated compressor/stripper configurations and methods." U.S. Patent Application 12/095,788, filed August 20, 2009.

Rezazadeh, Fatemeh, William F. Gale, Gary T. Rochelle, and Darshan Sachde. "Effectiveness of absorber intercooling for CO_2 absorption from natural gas fired flue gases using monoethanolamine solvent." *International Journal of Greenhouse Gas Control* 58 (2017): 246-255.

Rochelle, Gary T., G. Goff, Tim Cullinane, and Stefano Freguia. "Research results for CO_2 capture from flue gas by aqueous absorption/stripping." In *Proceedings of the Laurance Reid Gas Conditioning Conference*, no. 1, pp. 131-152. 2002.

Roussanaly, Simon, Chao Fu, Mari Voldsund, Rahul Anantharaman, Maurizio Spinelli, and Matteo Romano. "Techno-economic analysis of MEA CO_2 capture from a cement kiln–impact of steam supply scenario." *Energy Procedia* 114 (2017): 6229-6239.

Sander, Matthew T., and Carl L. Mariz. "The Fluor Daniel® econamine FG process: Past experience and present day focus." *Energy Conversion and management* 33, no. 5-8 (1992): 341-348.

Schach, Marc-Oliver, Rüdiger Schneider, Henning Schramm, and Jens-Uwe Repke. "Techno-economic analysis of postcombustion processes for the capture of carbon dioxide from power plant flue gas." *Industrial & Engineering Chemistry Research* 49, no. 5 (2010): 2363-2370.

Shafie, SMTMI Mahlia, Teuku Meurah Indra Mahlia, Haji Hassan Masjuki, and Andri Andriyana. "Current energy usage and sustainable energy in Malaysia: a review." *Renewable and Sustainable Energy Reviews* 15, no. 9 (2011): 4370-4377.

Shakerian, Farid, Ki-Hyun Kim, Jan E. Szulejko, and Jae-Woo Park. "A comparative review between amines and ammonia as sorptive media for post-combustion CO_2 capture." *Applied Energy* 148 (2015): 10-22.

Shakerian, Farid, Ki-Hyun Kim, Jan E. Szulejko, and Jae-Woo Park. "A comparative review between amines and ammonia as sorptive media for post-combustion CO_2 capture." *Applied Energy* 148 (2015): 10-22.

Sharifzadeh, Mahdi, and Nilay Shah. "MEA-based CO_2 capture integrated with natural gas combined cycle or pulverized coal power plants: Operability and controllability through integrated design and control." *Journal of cleaner production* 207 (2019): 271-283.

Sharma, Manish, Abdul Qadir, Rajab Khalilpour, and Ali Abbas. "Modeling and analysis of process configurations for solvent- based post- combustion carbon capture." *Asia‐Pacific Journal of Chemical Engineering* 10, no. 5 (2015): 764-780.

Sharma, Manish, Abdul Qadir, Rajab Khalilpour, and Ali Abbas. "Modeling and analysis of process configurations for solvent- based post- combustion carbon capture." *Asia‐Pacific Journal of Chemical Engineering* 10, no. 5 (2015): 764-780.

Shekarchian, M., Mahmoud Moghavvemi, T. M. I. Mahlia, and A. Mazandarani. "A review on the pattern of electricity generation and emission in Malaysia from 1976 to 2008." *Renewable and sustainable energy reviews* 15, no. 6 (2011): 2629-2642.

Shen, Shufeng, Xiaoxia Feng, Ruihong Zhao, Ujjal Kumar Ghosh, and Aibing Chen. "Kinetic study of carbon dioxide absorption with aqueous potassium carbonate promoted by arginine." *Chemical engineering journal* 222 (2013): 478-487.

Shen, Shufeng, Yanan Yang, and Shaofeng Ren. "CO_2 absorption by borate-promoted carbonate solution: Promotion mechanism and vapor liquid equilibrium." *Fluid Phase Equilibria* 367 (2014): 38-44.

Sherrick, Brian, Mike Hammond, Gary Spitznogle, David Muraskin, S. Black, and M. Cage. "CCS with Alstom's Chilled Ammonia Process at AEP's Mountaineer plant." In *proceedings of MEGA Conference, Baltimore, Maryland, USA*. 2008.

Sherrick, Brian, Mike Hammond, Gary Spitznogle, David Muraskin, Sean Black, Matt Cage, and F. Kozak. "CCS with Alstom's Chilled Ammonia Process at AEP's Mountaineer Plant. Alstom Power." (2009).

Sieminski, Adam. "International energy outlook 2013." *US Energy Information Administration (EIA) Report Number: DOE/EIA-0484* (2013).

Smith, Kathryn H., Clare J. Anderson, Wendy Tao, Kohei Endo, Kathryn A. Mumford, Sandra E. Kentish, Abdul Qader, Barry Hooper, and Geoff W. Stevens. "Pre-combustion capture of CO_2—Results from solvent absorption pilot plant trials using 30 wt% potassium carbonate and boric acid promoted potassium carbonate solvent." *International Journal of Greenhouse Gas Control* 10 (2012): 64-73.

Smith, Kathryn, Gongkui Xiao, Kathryn Mumford, Jeffri Gouw, Indrawan Indrawan, Navin Thanumurthy, Dimple Quyn et al. "Demonstration of a concentrated potassium carbonate process for CO_2 capture." Energy & fuels 28, no. 1 (2013): 299-306.

Smith, Kathryn, Ujjal Ghosh, Ash Khan, Michael Simioni, Kohei Endo, Xinglei Zhao, Sandra Kentish, Abdul Qader, Barry Hooper, and Geoff Stevens. "Recent developments in solvent absorption technologies at the CO2CRC in Australia." *Energy Procedia* 1, no. 1 (2009): 1549-1555.

Song, Chunfeng, Qingling Liu, Shuai Deng, Hailong Li, and Yutaka Kitamura. "Cryogenic-based CO_2 capture technologies: State-of-the-art developments and current challenges." Renewable and Sustainable Energy Reviews 101 (2019): 265-278.

Staton, James Stephen. *Performance and modeling of a hot potassium carbonate acid gas removal system in treating coal gas*. North Carolina State Univ., Raleigh (USA), 1985.

Stec, M., A. Tatarczuk, L. Więcław- Solny, A. Krótki, T. Spietz, and A. Wilk. "Process development unit experimental studies of a split- flow modification for the post- combustion CO_2 capture process." *Asia- Pacific Journal of Chemical Engineering* 12, no. 2 (2017): 283-291.

Styring, Peter, Elsje Alessandra Quadrelli, and Katy Armstrong, eds. *Carbon dioxide utilisation: closing the carbon cycle*. Elsevier, 2014.

Sung, Su Whan, and In-Beum Lee. "Limitations and countermeasures of PID controllers." Industrial & engineering chemistry research 35, no. 8 (1996): 2596-2610.

Surovtseva, Daria, Robert Amin, and Ahmed Barifcani. "Design and operation of pilot plant for CO_2 capture from IGCC flue gases by combined cryogenic and hydrate method." *chemical engineering research and design* 89, no. 9 (2011): 1752-1757.

Surovtseva, Daria. "CO_2 separation by cryogenic and hydrate." PhD dissertation, Curtin University, 2010.

Tantikhajorngosol, Puttipong, Navadol Laosiripojana, Ratana Jiraratananon, and Suttichai Assabumrungrat. "Physical absorption of CO_2 and H_2S from synthetic biogas at elevated pressures using hollow fiber membrane contactors: The effects of Henry's constants and gas diffusivities." *International Journal of Heat and Mass Transfer* 128 (2019): 1136-1148.

Tao, Lefu, Penny Xiao, Abdul Qader, and Paul A. Webley. "CO_2 capture from high concentration CO_2 natural gas by pressure swing adsorption at the CO2CRC Otway site, Australia." *International Journal of Greenhouse Gas Control*83 (2019): 1-10.

Telikapalli, Vauhini, Fred Kozak, Jean Francois, Brian Sherrick, Jody Black, Dave Muraskin, Matt Cage, Mike Hammond, and Gary Spitznogle. "CCS with the Alstom chilled ammonia process development program–Field pilot results." *Energy Procedia* 4 (2011): 273-281.

Thee, Hendy, Kathryn H. Smith, Gabriel da Silva, Sandra E. Kentish, and Geoffrey W. Stevens. "Carbon dioxide absorption into unpromoted and borate-catalyzed potassium carbonate solutions." *Chemical Engineering Journal* 181 (2012): 694-701.

Thee, Hendy, Nathan Johann Nicholas, Kathryn H. Smith, Gabriel da Silva, Sandra E. Kentish, and Geoffrey W. Stevens. "A kinetic study of CO_2 capture with potassium carbonate solutions promoted with various amino acids: Glycine, sarcosine and proline." *International Journal of Greenhouse Gas Control* 20 (2014): 212-222.

Thee, Hendy. "Reactive absorption of carbon dioxide into promoted potassium carbonate solvents." PhD dissertation, 2013.

Toftegaard, Maja B., Jacob Brix, Peter A. Jensen, Peter Glarborg, and Anker D. Jensen. "Oxy-fuel combustion of solid fuels." *Progress in energy and combustion science* 36, no. 5 (2010): 581-625.

Tonziello, Jacopo, and Michela Vellini. "Oxygen production technologies for IGCC power plants with CO_2 capture." *Energy Procedia* 4 (2011): 637-644.

Tranier, Jean-Pierre, Richard Dubettier, Arthur Darde, and Nicolas Perrin. "Air Separation, flue gas compression and purification units for oxy-coal combustion systems." *Energy Procedia* 4 (2011): 966-971.

Tung, L. S., and T. F. Edgar. "Analysis of control-output interactions in dynamic systems." *AIChE Journal* 27, no. 4 (1981): 690-693.

Unit, I. E. A. C. C. S. "Carbon Capture and Storage: The solution for deep emissions reductions." IEA, 2015.

Walters[a], Matthew S., Joshua O. Osuofa, Yu-Jeng Lin, Thomas F. Edgar, and Gary T. Rochelle. "Process control of the advanced flash stripper for CO_2 solvent regeneration." *Chemical Engineering and Processing: Process Intensification*107 (2016): 21-28.

Walters[b], Matthew S., Thomas F. Edgar, and Gary T. Rochelle. "Dynamic modeling and control of an intercooled absorber for post-combustion CO_2 capture." *Chemical Engineering and Processing: Process Intensification* 107 (2016): 1-10.

Wang, Meihong, Adekola Lawal, Peter Stephenson, J. Sidders, and C. Ramshaw. "Post-combustion CO_2 capture with chemical absorption: a state-of-the-art review." *Chemical engineering research and design* 89, no. 9 (2011): 1609-1624.

Wang, Meihong, Atuman S. Joel, Colin Ramshaw, Dag Eimer, and Nuhu M. Musa. "Process intensification for post-combustion CO_2 capture with chemical absorption: a critical review." *Applied Energy* 158 (2015): 275-291.

Wang, Yibing, Jitong Wang, Cheng Ma, Wenming Qiao, and Licheng Ling. "Fabrication of hierarchical carbon nanosheet-based networks for physical and chemical adsorption of CO_2." *Journal of colloid and interface science* 534 (2019): 72-80.

Warudkar, Sumedh S., Kenneth R. Cox, Michael S. Wong, and George J. Hirasaki. "Influence of stripper operating parameters on the performance of amine absorption systems for post-combustion carbon capture: Part I. High pressure strippers." *International Journal of Greenhouse Gas Control* 16 (2013): 342-350.

Warudkar, Sumedh S., Kenneth R. Cox, Michael S. Wong, and George J. Hirasaki. "Influence of stripper operating parameters on the performance of amine absorption systems for post-combustion carbon capture: Part I. High pressure strippers." *International Journal of Greenhouse Gas Control* 16 (2013): 342-350.

William, L. L., and L. I. Chien. "Design and control of distillation systems for separating azeotropes." *A John Wiley & Sons, Inc* (2010).

Wu, Xiao, Jiong Shen, Yiguo Li, Meihong Wang, Adekola Lawal, and Kwang Y. Lee. "Dynamic behavior investigations and disturbance rejection predictive control of solvent-based post-combustion CO_2 capture process." Fuel 242 (2019): 624-637.

Wu, Yue, Fan Wu, Guoping Hu, Nouman R. Mirza, Geoffrey W. Stevens, and Kathryn A. Mumford. "Modelling of a post-combustion carbon dioxide capture absorber using potassium carbonate solvent in Aspen Custom Modeller." Chinese Journal of Chemical Engineering 26, no. 11 (2018): 2327-2336.

Xue, Boyang, Yanmei Yu, Jian Chen, Xiaobo Luo, and Meihong Wang. "A comparative study of MEA and DEA for post-combustion CO_2 capture with different process configurations." *International Journal of Coal Science & Technology* 4, no. 1 (2017): 15-24.

Yarveicy, Hamidreza, Mohammad M. Ghiasi, and Amir H. Mohammadi. "Performance evaluation of the machine learning approaches in modeling of CO_2 equilibrium absorption in Piperazine aqueous solution." *Journal of Molecular Liquids*255 (2018): 375-383.

Ye, Xinhuai, and Yongqi Lu. "Kinetics of CO_2 absorption into uncatalysed potassium carbonate–bicarbonate solutions: effects of CO_2 loading and ionic strength in the solutions." Chemical Engineering Science 116 (2014): 657-667.

Yu, Hai, Guojie Qi, Shujuan Wang, Scott Morgan, Andrew Allport, Aaron Cottrell, Thong Do, James McGregor, Leigh Wardhaugh, and Paul Feron. "Results from trialling aqueous ammonia-based post-combustion capture in a pilot plant at Munmorah Power Station: Gas purity and solid precipitation in the stripper." *International Journal of Greenhouse Gas Control*10 (2012): 15-25.

Zahra, Mohammad RM Abu, Eva Sanchez Fernandez, and Earl LV Goetheer. "Guidelines for process development and future cost reduction of CO_2 post-combustion capture." *Energy Procedia* 4 (2011): 1051-1057.

Zhang, Minkai, and Yincheng Guo. "Analysis on regeneration energy of NH_3-based CO_2 capture with equilibrium-based simulation method." Energy Procedia 114 (2017): 1480-1487.

Zhang, Qiang. "Modeling and Control of Post-combustion CO_2 Capture Process Integrated with a 550mwe Supercritical Coal-fired Power Plant." PhD diss., West Virginia University, 2016.

Zhao, Ruikai, Longcheng Liu, Li Zhao, Shuai Deng, Shuangjun Li, Yue Zhang, and Hailong Li. "Techno-economic analysis of carbon capture from a coal-fired power plant integrating solar-assisted pressure-temperature swing adsorption (PTSA)." *Journal of cleaner production* 214 (2019): 440-451.

Zhao, Wenying, Gerald Sprachmann, Zhenshan Li, Ningsheng Cai, and Xiaohui Zhang. "Effect of $K_2CO_3 \cdot 1.5\ H_2O$ on the regeneration energy consumption of potassium-based sorbents for CO_2 capture." *Applied energy* 112 (2013): 381-387.

Zhao, Zhonglin, Xingyu Cui, Jinghong Ma, and Ruifeng Li. "Adsorption of carbon dioxide on alkali-modified zeolite 13X adsorbents." *International Journal of Greenhouse Gas Control*1, no. 3 (2007): 355-359.

Zheng, Min, Tao Huang, and Guangfeng Zhang. "A New Design Method for PI-PD Control of Unstable Fractional-Order System with Time Delay." Complexity 2019 (2019).

Zheng, Zhang, Zhiwei Ge, Haizhou Huang, Baozhong Zhou, and Wei Zhang. "Research on Processing Simulation and Energy Analysis of CO_2 Capture by Aqueous Ammonia in Power Plant." In IOP Conference Series: Earth and Environmental Science, vol. 219, no. 1, p. 012014. IOP Publishing, 2019.

APPENDIX

This section presents the detailed equations of mass and energy balance equations that are not included in the earlier chapters. The optimisation objective function adopted for the optimised K_2CO_3 and H_3BO_3/K_2CO_3 capture systems, along with the solutions, are also covered here. The complete PID control structures involved and the kinetic models of the absorber and stripper columns are equally discussed.

A. MASS AND ENERGY BALANCE EQUATIONS

This section covers the general mass and energy balance equations as adopted from the works of Harun et al. 2012 and Decardi-Nelson et al. 2018.

A1. Molar component balance for the liquid and gas phase

The following molar balance equations, indicating the change of component concentrations (C_i) over time (t), are written along the axial direction of the absorber and stripper columns. This axial length is divided into elements of height Δz, where z is assumed to be positive along the upwards direction in the column and negative along the downward direction. Since it is assumed that the liquid and gas phases are well mixed, it is believed that there are no changes in the concentrations of the components across the radial length of the columns. Subscripts l and g are used to denote component concentrations in the liquid and gas phases respectively.

$$-\frac{dC_{ig}}{dt} = u_g \frac{\partial C_{ig}}{\partial z} + a_{gl} N_i \quad \ldots\ldots\ldots\ldots\ldots\ldots\ldots\ldots 9.1$$

$$\frac{dC_{il}}{dt} = u_l \frac{\partial C_{il}}{\partial z} + a_{gl} N_i \ldots\ldots\ldots\ldots\ldots\ldots\ldots\ldots 9.2$$

$$u_g = \frac{4F_g}{\pi D^2} \ldots\ldots\ldots\ldots\ldots\ldots\ldots\ldots 9.3$$

$$u_l = \frac{4F_l}{\pi D^2} \ldots\ldots\ldots\ldots\ldots\ldots\ldots\ldots 9.4$$

$$i = CO_2, MEA, H_2O, K_2CO_3$$

C_{ig} and C_{il}, computed in units of mol/m^3, are the concentrations of component i in the gas and liquid phase respectively. u_g and u_l are the velocities, in m/s, of the gas stream and liquid stream respectively. a_{gl} is the gas-liquid interfacial area in m^2/m^3. N_i represents the molar flux (mol/m^{2}s), and accounts for the interfacial mass transfer rate in the column. This mass transport rate could be defined as the net loss of component i in the gas phase and the net gain of the same component in the liquid phase. F is the phase volumetric flow rate in m^3/s, and D is the cross-sectional diameter of the column in metre units. In the absorption unit, F_l is a manipulated variable to control the CO_2 capture level, whereas F_g is a disturbance variable from the power plant. To estimate the interfacial area and mass transfer coefficient in this study, the Brf-85 correlation developed by Bravo, Rocha and Fair was used (Bravo et al. 1985).

A2. Energy balance for the liquid and gas phase

The energy balance for the liquid and gas phases in the packed columns can be obtained by applying the differential volume element approach for a section Δz inside the column. Accordingly, the resulting energy balance phase equations are as follows:

$$\frac{dT_g}{dt} = -u_g \frac{\partial T_g}{\partial z} + \frac{Q_g a_{gl}}{\sum C_{ig} C_{pi}} \dots\dots\dots\dots\dots\dots\dots\dots 9.5$$

$$\frac{dT_l}{dt} = u_l \frac{\partial T_l}{\partial z} + \frac{Q_l a_{gl}}{\sum C_{il} C_{pi}} \dots\dots\dots\dots\dots\dots\dots\dots 9.6$$

$$Q_g = h_{gl}(T_l - T_g) \dots\dots\dots\dots\dots\dots\dots\dots 9.7$$

$$Q_l = h_{gl}(T_l - T_g) + \Delta H_{rxn} N_{CO_2} + \Delta H_{vap} N_{H_2O} - h_{out}(T_l - T_{amb}) \dots\dots\dots\dots 9.8$$

T (K) is the phase temperature, C_p (J/mol.K) is the specific heat capacity, Q (J/m^{3}s) is the interfacial heat transfer and h_{gl} (W/m^{2}K) is the heat transfer coefficient. This factor is calculated using the Chilton and Colburn analogy method. ΔH_{rxn} (J/mol) is the heat of reaction per mole of CO_2, ΔH_{vap} (J/mol) is the heat of vaporisation per mole of water, h_{out} (W/m^{2}K) is the column wall heat transfer coefficient and T_{amb} (K) is the surrounding ambient temperature.

A3. Equilibrium relation and rate equation

The equilibrium relations and mass transfer rate of H_2O, CO_2, MEA and K_2CO_3 at the interfacial liquid-gas phase in the packed columns is estimated using the standard two-film model equations below:

$$N_i = K_{gi}P_t(y_i - y_i^*) \ldots\ldots\ldots\ldots\ldots\ldots\ldots\ldots 9.9$$

$$i = CO_2, MEA, H_2O, K_2CO_3$$

$$y_i^* P_t = x_i \gamma_i P_i^v \ldots\ldots\ldots\ldots\ldots\ldots\ldots\ldots 9.10$$

$$i = MEA, H_2O, K_2CO_3$$

$$y_i^* P_t = He_i \gamma_i C_i^* \ldots\ldots\ldots\ldots\ldots\ldots\ldots\ldots 9.11$$

$$i = CO_2$$

K_{gi} is the overall mass transfer coefficient in mol/m^{3}Pa, P_t is the stage pressure in Pa, y_i and y_i^* are the respective bulk and equilibrium gas phase component mole fractions. x_i is the component mole fraction in the liquid phase, γ_i is the activity coefficient of component i, He_i is the Henry's constant, C_i^* is the concentration of free CO_2 in bulk liquid phase measured in units mol/m^3, and P_i^v is the saturated vapour pressure of component i in Pa. The definition of i in each of the equations is given under the equation.

B. CALCULATION OF CO_2 CAPTURE LEVEL AND REBOILER DUTY

The equations presented here are adopted according to data obtained from Warudkar et al. 2013, Mac et al. 2014, Harun et al. 2012 and Li[a] 2016. These equations were used in computing the CO_2 removal rate and specific reboiler duties for the various models.

$$\%CO_2\ Removal = 100\left(\frac{CO_2^{in} - CO_2^{out}}{CO_2^{in}}\right) \ldots\ldots\ldots\ldots\ldots\ldots\ldots\ldots 9.12$$

$$Specific\ Reboiler\ Duty\ (\frac{MJ}{kgCO_2}) = \frac{Q_{reb}}{CO_2^{in} - CO_2^{out}} \ldots\ldots\ldots\ldots\ldots\ldots\ldots\ldots 9.13$$

CO_2^{in} is the mass flowrate of CO_2 in the flue gas stream in kg/hr, CO_2^{in} is the mass flowrate of CO_2 in the vent gas from the absorber overhead in kg/hr, Q_{reb} is the energy consumption in the stripper column during the regeneration process in MJ/hr. This regeneration energy consists of three main components as shown below:

$$Q_{reb} = Q_{des} + Q_{sen} + Q_{vap} \ldots\ldots\ldots\ldots\ldots\ldots 9.14$$

where Q_{des} is the desorption energy required to break down the chemical bonds between the solvent and the CO_2 molecules, Q_{sen} is the sensible energy required to heat up the solvent feeds to the stripper to the column operating temperature, and Q_{vap} is the latent energy of vapourisation required to convert the liquids to gaseous state in the stripper column. The equations for these energy components are expressed below:

$$Q_{des} = \sum n_i H_i + n_{CO_2} H_{CO_2} \ldots\ldots\ldots\ldots\ldots\ldots 9.15$$

$$Q_{sen} = m_{solv} C_p (T_{in} - T_{out}) \ldots\ldots\ldots\ldots\ldots\ldots 9.16$$

$$Q_{vap} = \left(n_{vap}^{H_2O} \times H_{vap}^{H_2O}\right) + \left(n_{vap}^{solv} \times H_{vap}^{solv}\right) \ldots\ldots\ldots\ldots\ldots\ldots 9.17$$

n_i is the mole for all the species, mol; H_i is the molar enthalpies for all the species, MJ/mol; n_{CO_2} is the moles of CO_2 desorbed, mol; H_{CO_2} is the enthalpy per mole of CO_2 desorbed during the regeneration process. m_{solv} is the mass flowrate of solvent flowing through the stripper, kg/hr; C_p is specific heat capacity of the solvent, MJ/kg·K; $(T_{in} - T_{out})$ is the solvent temperature difference in and out of the stripper,

K. The lesser the solvent mass flowrate and temperature difference, the smaller the sensible heat required. $n_{vap}^{H_2O}$ is the moles of excess steam leaving the stripping column, mol; $H_{vap}^{H_2O}$ is the latent heat of steam generation; n_{vap}^{solv} is the moles of gaseous solvent leaving the stripping column, mol; and H_{vap}^{solv} is the latent heat of vaporisation for the solvent.

C. OBJECTIVE FUNCTION FOR OPTIMISATION

The main reason for the optimisation completed for the unpromoted and H_3BO_3 promoted K_2CO_3-based capture process is to render this technology more energy-efficient and improve the carbon capture level. The objective function considered for this optimisation is adopted from the works of Alexandra et al. 2019. The related equation, given as a function of the process energy duty and the captured CO_2, is presented below:

$$A\left(\frac{MJ}{kgCO_2}\right) = \frac{R + C + P}{F_{CO_2}} \ldots\ldots\ldots\ldots\ldots\ldots 9.18$$

A is the objective function in units of MJ/kgCO_2, R is the reboiler duty in units of MJ/hr, C is the stripper condenser duty in units of MJ/hr, P is the compression and pumping duty in units of MJ/hr, and F_{CO_2} is the mass flowrate of CO_2 in units of kg/hr. The smaller the magnitude of A, the better. To solve the objective function, the various parameters were computed from the simulation file and inputted into equation 9.18. The solutions are displayed below:

$$A\ (base\ case) = \frac{2074.7 + 919.753 + 0}{752.174} = 3.98$$

$$A\ (optimised\ K_2CO_3\ process) = \frac{1990.51 + 947.172 + (3.5987 + 191.578)}{847.069}$$

$$= 3.70$$

$$A\ (optimised\ H_3BO_3\ promoted\ K_2CO_3\ process)$$

$$= \frac{2081.74 + 978.012 + (3.5987 + 191.578)}{866.103} = 3.76$$

From the solutions above, it could be seen that the aim of the optimisation was achieved as the value of the optimisation function decreased after the optimisations were implemented. The solutions also indicate that the optimised K_2CO_3-based capture process is the most energy-efficient.

D. PID CONTROL STRUCTURE

This presents the complete control structures for the single-input single-output (SISO) and multiple-input multiple-output (MIMO) control structures developed in the MATLAB Simulink for the control analyses.

D1. SISO control structures

The SISO control structures designed for unpromoted and H_3BO_3 promoted K_2CO_3-based capture processes are shown in this section. The control structure depicts the designs for the carbon capture level (CV) vs lean solvent flowrate (MV), and the reboiler temperature (CV) vs reboiler duty (MV).

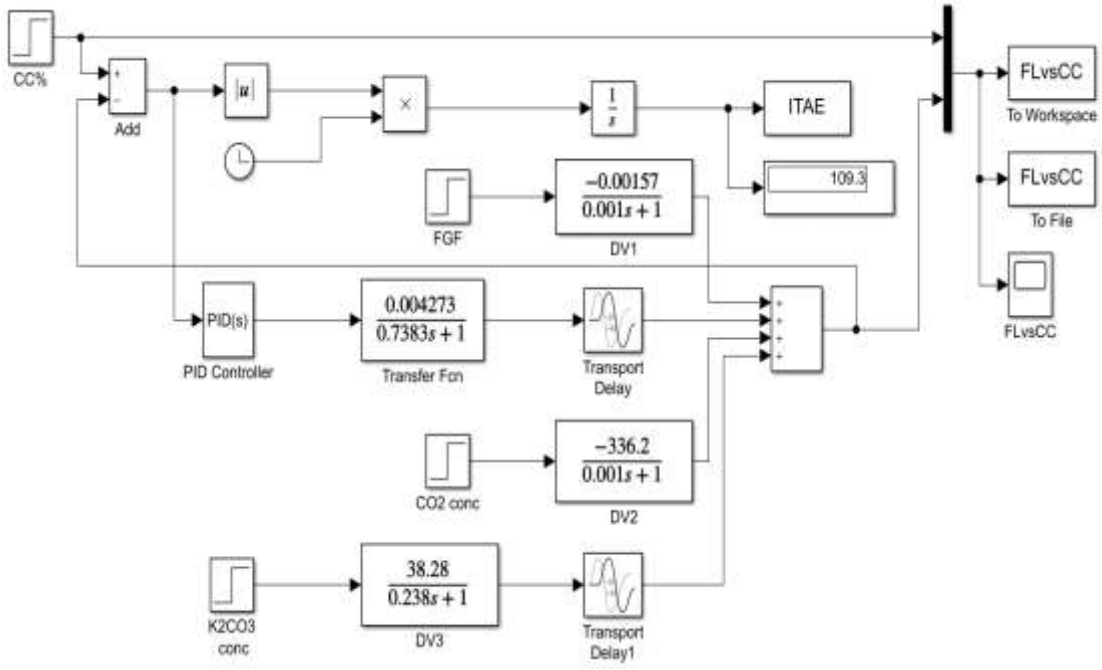

Figure 8.1. PID control structure for carbon capture level vs lean solvent flowrate in K_2CO_3 system

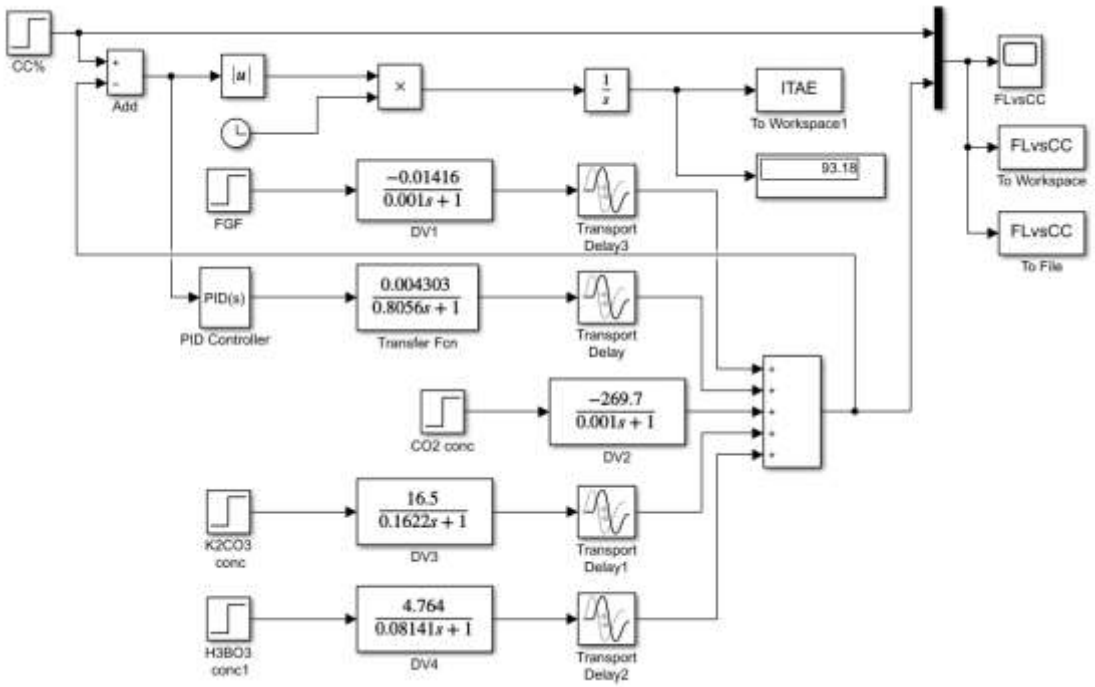

Figure 8.2. PID control structure for carbon capture level vs lean solvent flowrate in H_3BO_3/K_2CO_3 system

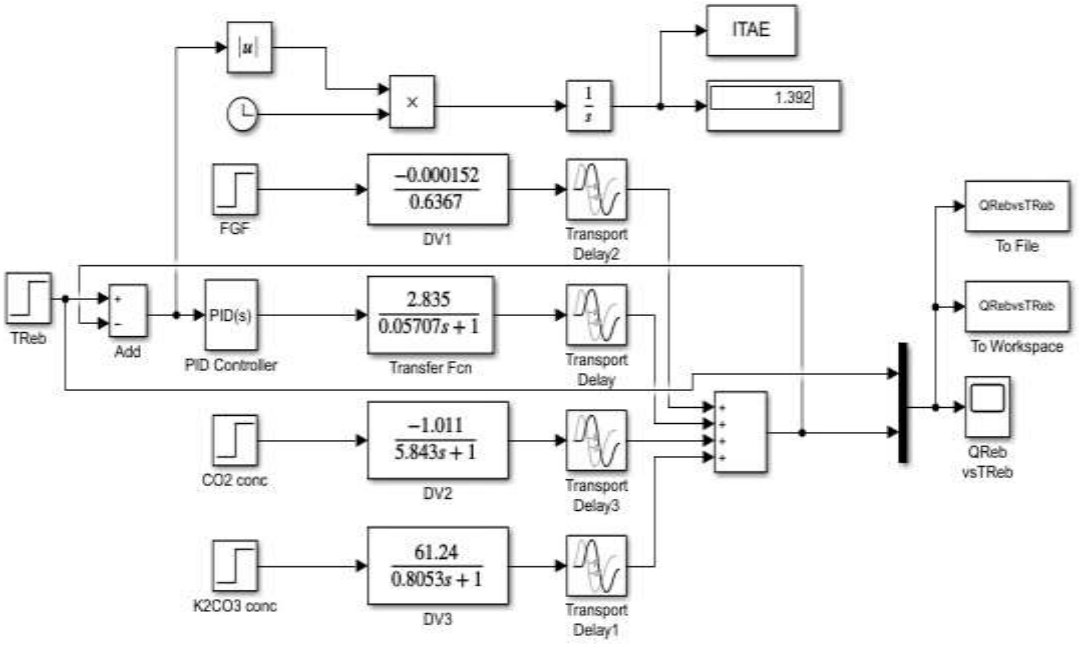

Figure 8.3. PID control structure for reboiler temperature vs reboiler duty in K_2CO_3 system

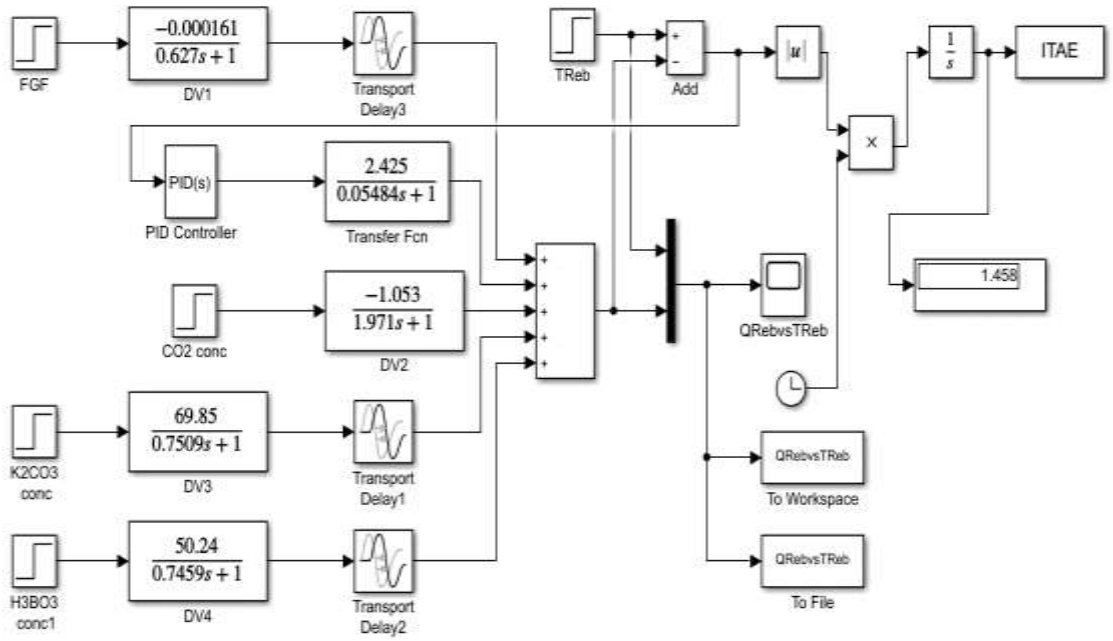

Figure 8.4. PID control structure for reboiler temperature vs reboiler duty in H_3BO_3/K_2CO_3 system

D2. MIMO control structures

The MIMO control structures for unpromoted and H_3BO_3 promoted K_2CO_3-based capture processes are shown in this section. The designs here show the interactions between the two controlled variables and the two manipulated variables. The transfer functions for the disturbance variables in the various systems are also shown on the control structures.

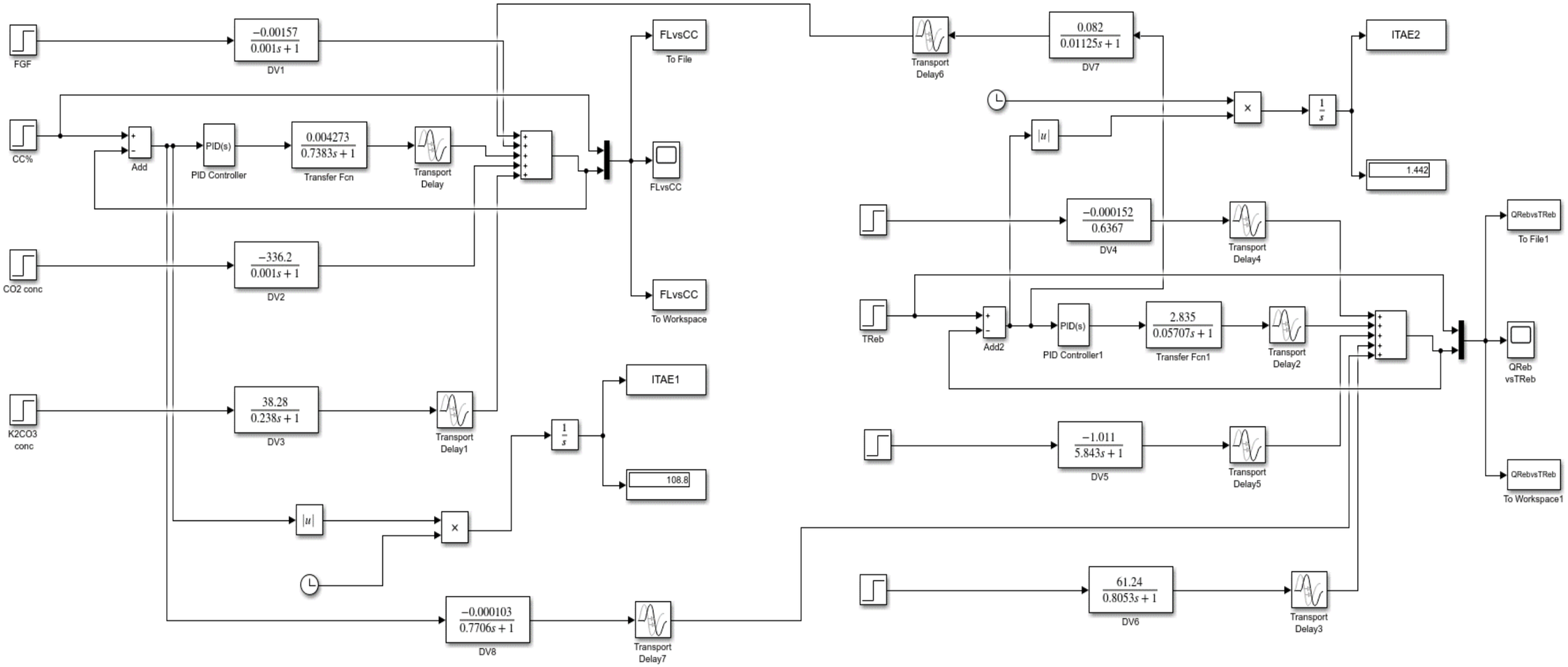

Figure 8.5. MIMO control structure for K_2CO_3 system

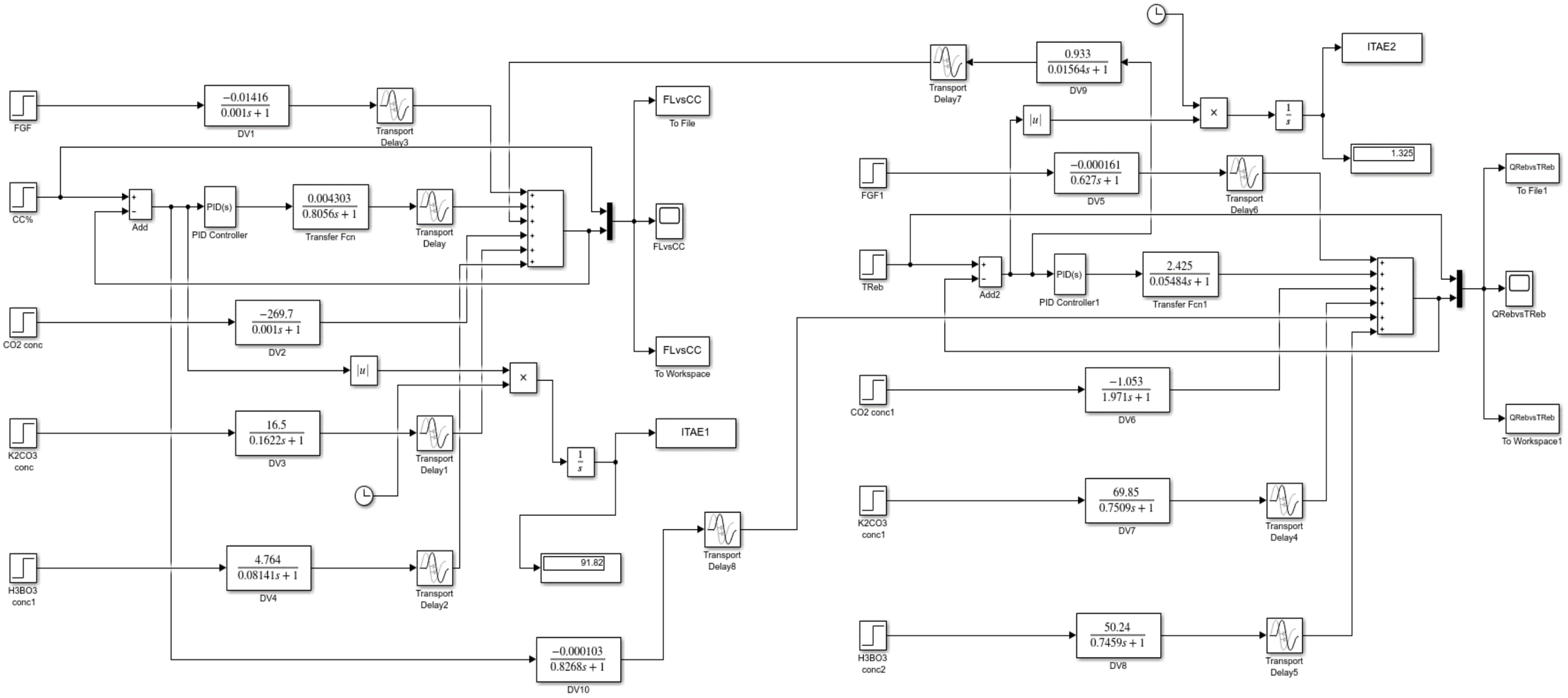

Figure 8.6. MIMO control structure for H_3BO_3/K_2CO_3 system